UNIVERSIDAD NACIONAL AUTÓNOMA DE MÉXICO

DOCTORADO EN CIENCIAS BIOMÉDICAS

INSTITUTO DE ECOLOGÍA

"MODELO DINÁMICO DE LA RED DE REGULACIÓN DEL CICLO CELULAR DE *Arabidopsis thaliana*"

TESIS

QUE PARA OPTAR POR EL GRADO DE:

DOCTORA EN CIENCIAS

PRESENTA:

ELIZABETH ORTIZ GUTIÉRREZ

TUTOR PRINCIPAL

DRA. MA. ELENA ÁLVAREZ-BUYLLA ROCES

INSTITUTO DE ECOLOGÍA, UNAM

COMITÉ TUTOR

DR. JOSEPH DUBROVSKY

INSTITUTO DE BIOTECNOLOGÍA, UNAM

DRA. MA. DE LA PAZ SÁNCHEZ JIMÉNEZ

INSTITUTO DE ECOLOGÍA, UNAM

CIUDAD UNIVERSITARIA, CD. MÉX., MAYO DE 2016.

Revisor 1: **Dr. Carlos Villarreal Luján**

Instituto de Física, UNAM

Revisor 2: **Dra. Alejandra Alicia Covarrubias Robles**

Instituto de Biotecnología, UNAM

Revisor 3: **Dra. Gladys Iliana Cassab López**

Instituto de Biotecnología, UNAM

Revisor 4: **Dr. Hernán Larralde Ridaura**

Instituto de Ciencias Físicas, UNAM

A mi pa y a mi ma.
Por su respaldo que me hace sentir segura
por donde sea que camine.

Agradecimientos

Este proyecto fue posible gracias a la participación de Elena, Maripaz, el Dr. Joseph, Eugenio y Karla. Estoy muy agradecida con ellos por su paciencia y porque siempre dedicaron tiempo a resolver mis dudas. Y con Eugenio también porque fue quien me invitó a colaborar en otros trabajos. Muchas gracias a Diana Romo, a Kahorik González y a Erika Rodríguez porque en varias ocasiones me sacaron de apuros y simplificaron el asunto de los trámites. Gracias también a quienes nos dieron clases y mostraron compromiso con mi formación académica y la de varios estudiantes más: Carlos Villarreal, Juan Carlos Martínez y Alberto Betancourt.

<div align="center">*</div>

A mis compañeros y amigos, Moni, Lesli, Libertad, Duhya, Ale Celeste, Vale, Checo, Euges, Juan López, Esther, Santiago, Karina Pichardo, Lalo, Luisa, mi comadre Citlalli, Are CereSon, Pablo Alvarado, los hermanos Cerezo, Lety Ton y Ross, muchas muchas gracias por su confianza, por la oportunidad de compartir tan buenos momentos y por dejarme aprender de ustedes. Y a las personas con las que tuve el gusto de vivir por algunos meses o varios años... Ale Celeste, Nancy, Liz, Juan, Jonathan, Claudia Camacho, Yuri y Tony, fue muy grato para mí compartir más que una casa o departamento, les agradezco mucho sus cuidados, los momentos inolvidables que compartimos, las comidas, las cenas, y hasta los ánimos que me daban mientras escribía estas páginas.

<div align="center">*</div>

Agradezco también a Maru, un ser humano del que tanto he aprendido, que ha caminado a mi lado y que ahora ocupa un lugar bien especial en mi vida. Y también gracias a Aime, por su energía y su alegría contagiosas, por contarme cuentos, y porque me visitó a pesar de que mi escuela estuviera muuuy lejos.

<div align="center">*</div>

Y por respetar y apoyar incondicionalmente mis decisiones, gracias a mis padres. Gracias por la confianza, por la protección y por su dedicación plena a la familia que han formado. Todo

lo que he aprendido lo debo a ustedes, y a lo que ustedes aprendieron de los abuelos; con sus consejos para la vida, una está lista para todo lo que venga. Gracias a Ross, a Daniel y a Lola por acompañarme durante tantos años y por varios caminos.

*

Gracias a la gente que con su trabajo hacen posible la ciencia y la educación pública en México.

*

Resumen

La sucesión cíclica de duplicación del ADN y segregación de una copia a las células hijas durante la división celular es dictada por la red de regulación del ciclo celular. En cada una de las fases del ciclo celular se expresan diferentes conjuntos de genes y están activas diferentes proteínas, interconectados en una red regulatoria dinámica. La división celular es esencial para el crecimiento y morfogénesis de los organismos multicelulares y, a su vez, también depende del programa de desarrollo. El objetivo de este trabajo fue proponer un modelo Booleano con las interacciones reportadas entre reguladores del ciclo celular de *Arabidopsis*, y que subyace la emergencia de su comportamiento cíclico. Cuando no había datos experimentales para plantas, consideramos referencias de levaduras y animales, puesto que muchos de sus componentes están conservados. La red resultante convergió a un único patrón cíclico de actividad o transcripción que se asemeja al comportamiento periódico de los componentes moleculares clave del ciclo celular. Para validar el modelo, simulamos mutaciones en los componentes de la red y las comparamos con el fenotipo correspondiente. Descartamos artefactos metodológicos obteniendo la aproximación continua del modelo Booleano, y mostramos que el modelo del ciclo celular es robusto a alteraciones transitorias. La validación y estos análisis sugieren que el patrón cíclico recuperado de presencia de los reguladores del ciclo celular, es una consecuencia emergente de la lógica de regulación propuesta. En conclusión, el modelo es una explicación sistémica de la progresión del ciclo celular, además de una herramienta con la que inferimos nuevas interacciones críticas para la regulación del ciclo celular de *Arabidopsis*.

Abstract

The cyclic succession of DNA replication and segregation of a copy to daughter cells, during cell division, is governed by the regulatory network of cell cycle progression. In each cell cycle phase, different sets of genes are expressed and different proteins are activated, interconnected in a dynamic regulatory network. Cell division is fundamental for growth and morphogenesis of multicellular organisms, and at the same time, it depends on developmental program. The main aim of this work was to propose a Boolean model with the interactions previously described between regulators of the *Arabidopsis* cell cycle, and which underlies the emergence of its cyclic behavior. When there were no experimental data from plants, we considered some references from yeast and animals since many of their cell cycle components are conserved. The proposed network converged to a unique cyclic pattern of activity or gene expression and, which is similar to the periodic behavior of the key molecular components of cell cycle. In order to validate our model, we simulated mutations in network components and then we compared them with the corresponding phenotype. To discard methodological artifacts, we obtained the continuous version of the Boolean model, and then we showed that the cell cycle model is robust to transient alterations. Together with the validation, these analyses suggest that the recovered cyclic pattern of presence of cell cycle regulators, is an emergent consequence from the regulatory logic proposed. In conclusion, the model is a systemic explanation for the cell cycle progression, and in addition, a tool with which we inferred new critical interactions for the cell cycle regulation in *Arabidopsis*.

Contenido

1

INTRODUCCIÓN

La homeostasis de órganos y tejidos que depende del equilibrio entre proliferación y diferenciación es necesaria para mantener la morfogénesis normal de un órgano multicelular [1]. Aunque la proliferación y la diferenciación celular se consideraron en algún momento como procesos distintos y espacialmente segregados, ahora sabemos que a nivel molecular existe una estrecha coordinación [2, 3], sugiriendo mecanismos sistémicos multiestables subyacentes que aún no comprendemos bien. Esta coordinación se vuelve evidente, por ejemplo, frente a alteraciones genéticas que conllevan a una reducción en el número de células sin afectar el patrón de desarrollo, debido a que éste se restablece por un incremento en la cantidad y el tamaño de células en diferenciación [4]. Dicho mecanismo de compensación involucra reguladores del Ciclo Celular (CC), el proceso por el que las células como unidades de la morfogénesis responden a señales globales del desarrollo, al mismo tiempo que su producción influye al crecimiento y al propio desarrollo [5, 6].

El CC se define como el proceso por el cual una célula da origen a dos células hijas [1]. Durante el CC la célula crece, duplica su material genético y lo segrega en las células hijas que comenzarán de nuevo el ciclo. Si estas células hijas son idénticas y además tienen el mismo destino, la división se conoce como 'proliferativa', ésta es la división que más contribuye al crecimiento de la planta. En cambio, cuando la división da origen a células con diferente destino celular, entonces la división es asimétrica o 'generativa', ya que es una forma de mantener la población de células troncales y a la vez permitir la diferenciación [7]. En la escala molecular, el CC es un proceso conservado entre plantas, animales y hongos. Proteínas como las Cinasas dependientes de ciclinas (CDK por sus iniciales en inglés) y las ciclinas forman heterodímeros que regulan la progresión del CC. Éstas y otras proteínas involucradas directamente en la regulación del CC están evolutivamente conservadas y algunas de ellas son lo suficientemente similares

que pueden complementar la pérdida de función de los ortólogos[1] en otras especies [8–12]. A diferencia de otros organismos, el número de componentes del CC es mucho mayor en plantas, como sucede en el caso de *Arabidopsis thaliana* (*Arabidopsis*) [13]. Inicialmente se propuso que su genoma codifica cerca de 61 genes involucrados en el control del CC [8], sin embargo esta cifra no incluye subunidades de los complejos que regulan la degradación específica de proteínas ni de factores transcripcionales (FTs) importantes para la división propiamente.

A pesar de las diferencias entre plantas y animales, en ambos organismos pluricelulares, la regulación del CC es fundamental para mantener el balance entre proliferación y diferenciación celular. Por ello, resulta fundamental entender a cabalidad los procesos complejos que subyacen a la regulación del CC. Los sistemas modelo experimentales más usados para el estudio de los componentes moleculares y sus interacciones en la regulación del CC han sido la levadura [14–16], la rana [17] y el ratón [18, 19]. En plantas se han descrito una parte importante de los mismos componentes, y aspectos muy importantes de la regulación del CC parecen estar conservados entre todos los eucariontes. Más aún, el entendimiento de cómo emerge el CC y por qué es robusto y resiliente ante una gran cantidad de señales intra- y extra-organísmicas, es aún parcial. Para poder estudiar este proceso, es indispensable contar con un modelo dinámico de la red de interacciones que regulan o que generan, como resultado de su dinámica, el CC. No existen estudios sistémicos formales y dinámicos que recuperen el comportamiento cíclico de transición de una célula en las distintas fases estereotípicas que caracterizan al CC de todos los eucariontes. Sólo existen algunos trabajos que han comenzado a enfrentar este reto [19,20]. Por ello, integramos los datos descritos en la planta experimental modelo, *Arabidopsis*, y con ellos propusimos un modelo de las interacciones entre los componentes moleculares capaz de recuperar el comportamiento cíclico de la célula. Para ello usamos formalismos de redes dinámicas discretas y contínuas, análisis de robustez, y validamos el modelo con el comportamiento observado en plantas silvestres y mutantes. El estudio resumido en esta tesis constituye una base formal para plantear nuevas hipótesis acerca de componentes del CC y de cómo éste puede interactuar con vías de transducción de señales o redes de regulación transcripcional. También puede servir de base para plantear nuevas hipótesis acerca de los procesos regulatorios que subyacen al CC de animales y levaduras.

Los análisis comparativos son un apoyo para identificar reguladores importantes, ya que a pesar de la enorme cantidad de información disponible, aún quedan preguntas sin resolver por la falta de integración de esos datos. A continuación se describen brevemente las interacciones que conforman la red de regulación del CC en *Arabidopsis* y una comparación general con el CC de otros organismos.

---

[1]Genes homólogos originados por un evento de especiación

1.1 Regulación del ciclo celular en eucariontes

La replicación del ADN y la mitosis definen las fases por las cuales transita una célula antes de dividirse. La célula crece en la fase G1, y si hay nutrientes suficientes, pasa a la fase S (de Síntesis) donde replica su ADN y, en seguida a la G2, donde verifica que el ADN no tenga daño y la disponibilidad de nutrientes. Si se cumplen estas condiciones y las señales intracelulares lo propician, la célula entra en fase M, donde segrega el material genético y ocurren la mitosis y la citocinesis[2]. En plantas es común encontrar ciclos con varias rondas de replicación de ADN sin mitosis, produciendo así células poliploides [21]. Este fenómeno se conoce como *endorreduplicación* y también se presenta en animales [22]. La transición entre fases demanda una coordinación muy precisa entre eventos [23]; por ejemplo, no se segrega el ADN antes de concluir su replicación. Dicha coordinación recae en Cinasas Dependientes de Ciclinas (CDKs) y, las ciclinas a las que se unen para formar complejos activos. Las ciclinas deben su nombre al perfil de trancripción oscilante que presentan a lo largo del CC. Además de la regulación transcripcional, hay otras tres formas de regulación molecular que se distinguen en la red del CC: interacciones físicas entre proteínas, fosforilación y degradación mediada por ubiquitinación [24]. Sólo hasta que los complejos CDK-ciclina alcanzan cierto umbral de actividad es que promueven la transición a la siguiente fase [25]. En *Arabidopsis*, los complejos CDKA;1-CYCD3;1 y CDKA;1-CYCB1;1 son factores limitantes para la transición G1/S y G2/M, respectivamente. En levaduras y animales, la especificidad de sustrato la confiere principalmente la ciclina; en cambio en plantas, esa especificidad depende también de las CDKs [26, 27].

Tanto en plantas, como en hongos y animales, los principales puntos de control ocurren en la transición G1/S y en la G2/M. En la primera, varias proteínas, junto con sus ligandos están conservados, a diferencia de las responsables de la transición G2/M, que no se han preservado entre eucariontes (ver Tabla 1.1). Hay proteínas que son exclusivas de plantas o que han adquirido nuevas funciones y se regulan de forma diferente, pero que conforman motivos regulatorios con propiedades dinámicas equivalentes. En seguida se describen las interacciones regulatorias responsables de mantener estos puntos de control, y se hace una comparación general señalando las variaciones entre el control del CC en *Arabidopsis* y otros organismos.

---

[2]División de la membrana plasmática

Tabla 1.1. Proteínas homólogas (o *equivalentes funcionales) involucradas en el control del CC eucarionte.

Fase CC	*Arabidopsis*	*O. tauri*	*S.pombe*	*S.cerevisiae*	Mamífero
G1/S, G2/M	CDKA;1	CDKA	Cdc2	Cdc28	CDK1
G2/M	CDKB	CDKB	-	-	-
G1/S, S	CYCD	CYCD	Puc1	Cln1, Cln2, Cln3	CycE, CycD
G2/M	CYCA	CYCA	Cig1/2	Clb5,Clb6	CycA
G2/M, M	CYCB	CYCB	Cdc13	Clb1, Clb2	CycB
G1/S, S	SCF-SKP2	SCF-Skp2	SCF	SCF	SCF
G1/S, G2/M	KRP	CKI?	Rum1*	Sic1*	P27, P21
S	RBR	RBR	-	Whi5	Rb, p107, p130
S	E2Fa/b, DPa	E2F,DP	Cdc10/Res1/2	Swi4/Swi6/Mbp1*	E2F1-5
S	E2Fc, DPb	-	-	-	E2F6
G2	DEL1	DEL	-	-	E2F7
M	APC^{Cdc20}	APC^{Cdc20}	Slp1	APC^{Cdc20}	APC^{Cdc20}
M/G1	APC^{CCS52}	APC^{CCS52}	Ste9	APC^{Cdh1}	APC^{Cdh1}
G2/M	WEE1	WEE	Wee1	Swe1	Wee1
G2/M	Cdc25-like	Cdc25	Cdc25	Mih1	Cdc25
M	MYB3R1/4	-	-	Fkh1/2, Ndd1, Mcm1	A/B/C-Myb

1.2 Regulación de la expresión genética durante el ciclo celular

En varios organismos se han identificado patrones de expresión genética a lo largo del CC, siendo las transiciones G1/S y G2/M las de mayor actividad transcripcional. En levaduras y mamíferos, también hay un incremento en la actividad transcripcional justo antes de la salida de la mitosis. Este fenómeno se debe en parte a los FTs de la vía Retinoblastoma-E2F [28] y a FTs como B- y c-Myb [23, 29]. Estudios en fibroblastos de rata y en ganglioblastos de humano reportaron que B-Myb regula genes que participan en la transición G2/M. Los FTs B-Myb se regulan transcripcionalmente por los E2Fs desde la transición G1/S. A partir de estas observaciones, Zhu y colaboradores [30] han señalado que los FTs de la familia E2Fs conectan la regulación de la transición de G1/S con la transcripción de la G2/M. En *S. cerevisiae* y mamíferos, la regulación transcripcional es tal que los FTs que participan antes regulan a los que funcionan más adelante para formar un ciclo regulatorio completamente conectado. En células sincronizadas de *Arabidopsis* MM2d, se detectó, por medio de RT-PCR cuantitativo, la expresión periódica de 239 FTs [31]. Estudios previos en *S. cerevisiae* han demostrado que tal transcripción periódica se puede mantener incluso en la ausencia de ciclinas de la fase S y ciclinas mitóticas [32], lo cual destaca el papel del oscilador de la red de FTs para la correcta progresión del CC [33]. Se propone que el oscilador de la red de regulación transcripcional sería complementario al oscilador de las CDKs [34].

En *Arabidopsis*, la proteína RBR (RETINOBLASTOMA-RELATED PROTEIN 1) es el ortólogo de la proteína Retinoblastoma de mamíferos, que previo a la transición G1/S bloquea el dominio de transactivación y, por lo tanto, también la actividad transcripcional de los E2Fs canónicos

(E2Fa, E2Fb y E2Fc). Se sabe que los E2Fs (Adenovirus E2 promoter-binding protein) regulan la expresión de genes necesarios para la síntesis de ADN y, en algunos casos, también la de algunos genes necesarios para la fase M. Los FTs E2Fa, E2Fb and E2Fc necesitan formar heterodímeros con proteínas DIMERISATION PARTNER (DP) para poder unirse al ADN [35]. E2Fa y E2Fb forman complejos con DPa y se consideran activadores transcripcionales, mientras que E2Fc se une a DPb y parece ser un represor transcripcional homólogo a E2F6 de humano, ya que no tienen el dominio de transactivación [36]. En la fase G1 temprana, RBR se encuentra unido a los E2F y por lo tanto sus blancos están transcripcionalmente apagados. En la fase G1 tardía, se forma el complejo CDK-CYCD que llevará a la célula a la fase S, fosforilando a RBR e induciendo su separación de los factores E2F. Una vez que estos FTs se liberan, comienza la transcripción de los blancos de los E2Fs, entre ellos están MCM, CDC6, PNCA, RNR, CDT1, ASHR3 y su propio represor RBR [37–42]. Los FTs E2F regulan una amplia variedad de genes que se pueden clasificar en dos grupos principales, genes involucrados en la replicación del ADN y genes necesarios para la reparación del ADN [37]. En mamíferos, los E2F también promueven la transcripción de CycE [43] y, en *Arabidopsis*, CYCD3;1 tiene sitios de unión de E2F [44], por lo que es posible que exista una asa de retroalimentación positiva entre los niveles de CYCD3;1 y la actividad de E2F, similar a lo que se observa en mamíferos y levaduras [45]. Los dominios de unión a ADN de los E2Fs en *Arabidopsis* parecen estar bien conservados con respecto a los dominios de E2Fs en humano [44].
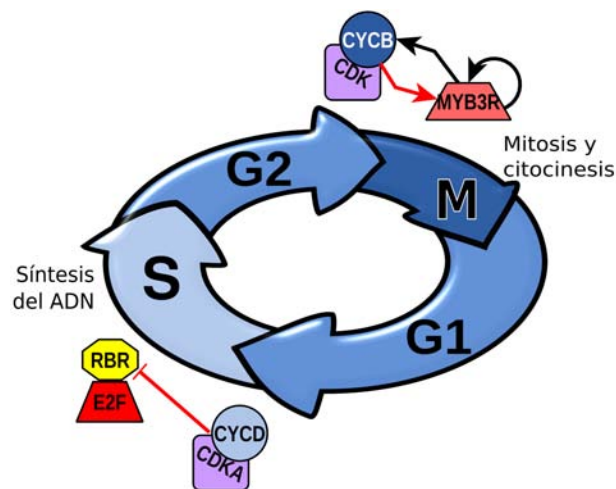
Fig. 1.1. CDK-Ciclina, elementos críticos para las transiciones G1/S y G2/M, y su efecto en la regulación transcripcional. Entre los blancos de los heterodímeros CDKA;1-CYCD se encuentra el represor de los FTs E2F, RBR. En la transición G2/M, el heterodímero CDK-CYCB fosforila a los FTs MYB3R1/4 para favorecer su actividad y estimular la producción de más CYCB y MYB3R1/4.

El segundo pico de actividad transcripcional observado en la transición G2/M se debe al motivo M-specific activator (MSA), el cual se reconoce por los FTs MYB, ampliamente conservados en plantas y vertebrados. En plantas, los FTs MYB con tres dominios de unión a ADN (R1R2R3-Myb) reconocen el motivo MSA [29]. Los vertebrados tienen tres miembros de esta familia, c-Myb, A-Myb and B-Myb, y algunos de ellos tienen una función en la transición G1/S [29]. El elemento MSA identificado inicialmente en tabaco se encuentra en las regiones regulatorias de genes específicos de la transición G2/M [29], entre los que están ciclinas del tipo B [46, 47], KNOLLE (proteína importante para la citocinesis) y algunas ciclinas de tipo A [29]. En humanos c-Myb regula la expresión de la ciclina B1 [48]. c-Myb es un protooncogen que se expresa principalmente en células hematopoyéticas y su pérdida de función es letal [48]. *Arabidopsis* tiene cinco FTs R1R2R3-Myb, de éstos MYB3R1 y MYB3R4 son estructuralmente similares entre ellos, y también son similares a NtmybA1 y NtmybA2 de tabaco. Un punto de regulación importante de estos FTs son las modificaciones postraduccionales. En tabaco, los complejos CDK-CYCB1, CDK-CYCA1 y CDK-CYCA2 fosforilan a NtmybA2 aumentando su actividad [29]. Asimismo, NtmybA1 y NtmybA2 contienen secuencias MSA en sus regiones promotoras y, por lo tanto, podrían autoregular su propia expresión [29]. *S. cerevisiae* no tiene ningún FT MYB pero presenta otros reguladores transcripcionales, tales como Fkh1/2, Ndd1 y Mcm1 [45, 49, 50], los cuales regulan la transición G2/M de forma similar a los MYBs de mamíferos.

Resulta notable que mientras la transición G2/M se promueve a sí misma a través de la regulación entre R1R2R3-Myb y ciclina tipo B, la regulación transcripcional G1/S, se inhibe a sí misma [51]. La retroalimentación negativa que se forma con la inducción de RBR por los E2Fs ayudaría a que el pico de transcripción de la fase G1/S no dure más de lo necesario (Ver Fig. 1.1).

1.3 La regulación de la replicación del ADN está conservada

Proteínas implicadas en la regulación del CC de mamíferos y la levadura *S. cerevisiae* comparten poca similitud en secuencia de aminoácidos, sólo algunos de sus dominios regulatorios son similares [52]. Probablemente, la transición G1/S y las proteínas involucradas en ella son las mejor conservadas entre animales y plantas, y comparten función con las proteínas de levaduras pero no origen. En levaduras, hay un punto entre la mitad y el final de la fase G1 en el que las células se comprometen a entrar al CC y dejan de responder a feromonas. Se le conoce como "INICIO" (*START*) y, en animales también ocurre algo similar con el punto R (Restricción), que es cuando las células ya no necesitan factores de crecimiento de suero [53]. Es posible que en *Arabidopsis* exista una regulación similar, hasta ahora desconocida. El control del paso a la fase S destaca

la importancia de las señales ambientales en el control del CC, ya que antes de este punto, las células tienen la opción de diferenciarse en lugar de dividirse.

En la fase G1, la célula verifica las condiciones internas y externas para mantenerse en G1 o para pasar a la fase S y replicar su material genético. En *Arabidopsis*, las principales proteínas responsables de esta transición son la CDKA;1 y las ciclinas de tipo D. La CDKA;1 es una cinasa bien conservada en diferentes eucariontes (ver Tabla 1.1). Aunque esta cinasa está presente durante todo el CC de células en proliferación, su actividad depende de diversos reguladores. Algunas ciclinas de tipo D tienen vidas medias cortas [52, 54, 55], la estabilidad de CYCD3;1 de *Arabidopsis*, Cln3 de levadura y CycD de mamíferos, por ejemplo, depende enormemente de las condiciones ambientales [54]. Si las condiciones son favorables, la CDKA;1 se une a la ciclina de tipo D y ésto desencadena la transición G1/S. Para que continue la progresión del CC después de esta transición, la regulación genética es clave [56], la cual está estrechamente acoplada a las redes de interacción de proteínas. En este caso, el blanco principal de los heterodímeros CDKA;1-CYCD es RBR que inhibe la actividad transcripcional de los FTs E2Fs. RBR es fosforilada por el heterodímero activo CDKA;1-ciclina D en la transición G1/S, y se mantiene así hasta la fase S media o tardía [36].

Se han encontrado homólogos de RBR en mamíferos (pRB), *Drosphila melanogaster* y *Caenorhabditis elegans* pero no en levaduras [57]. Sin embargo, en *S. cerevisiae*, la proteína Whi5 tiene funciones equivalentes a RBR, por ejemplo, cuando Whi5 se inhibe, los FTs SBF (Swi4-Swi6) y MBF (Mbp1-Swi6) quedan activos y comienzan la transcripción de sus blancos, entre ellos se encuentran las ciclinas Cln que inactivan completamente a Whi5 [52]. Los reguladores transcripcionales Swi4, Swi6 y Mbp1 tampoco parecen ser homólogos a E2F-DP [52]. De manera similar a plantas y levaduras, los complejos Cdk4/6-CycD, y después Cdk2-CycE, fosforilan a pRb en mamíferos [57, 58] liberando a los FTs E2F. Además de ocultar el dominio de transactivación de los FTs a los que se unen, pRB, Whi5 y RBR reclutan desacetilasas de histonas y factores remodeladores de la cromatina para reprimir la transcripción [52, 59–62].

En animales, la iniciación de la replicación se promueve por CycE y CycA [52], y por ciclinas de tipo B en levaduras [52]. En *Arabidopsis*, no está claro si es la CYCD3;1 la que participa en la activación de la replicación del ADN [53]. Componentes cruciales para la iniciación de la replicación del ADN como Cdc6 y Cdt1 se encuentran conservados entre levaduras, animales y *Arabidopsis* [41, 63].

Otro punto importante de regulación es la fosforilación del loop-T de CDKA;1 y Cdc28[3]. Esta acción se lleva a cabo por las cinasas activadoras de CDKs (CAK por sus siglas en inglés) que reconocen el residuo conservado Thr-161 [25]. Adicionalmente, los inhibidores estequiométricos

---

[3]Cinasa de *S. cerevisiae*, homóloga a CDKA;1

de CDKs como p16^{INK4}, p27^{KIP1} y p21 (también conocidos como KIP-RELATED PROTEIN, KRP, como *CDK inhibitory molecule*, CKI, o como *Inhibitor/Interactor of Cdc2 Kinase*, ICK) se unen a CDKs o a los dímeros CDK-ciclina y distorcionan el centro catalítico de unión a ATP de las CDKs [64]. En plantas, las proteínas KRPs son homólogas a p21/p27, y Sic1 tiene una función equivalente pero no parece tener un origen común, es decir, no es homólogo. La degradación específica de Sic1, Kip, y KRPs depende de SCF, pero para que este complejo pueda reconocerlos, necesitan ser fosforilados antes por CDKs [53]. El SCF participa principalmente en la transición G1/S [65].

1.4 Mecanismos de regulación de entrada y salida de la mitosis

A diferencia de la transición G1/S, para el inicio de la mitosis se requiere que la actividad de la CDK sea más alta. En animales, las ciclinas de tipo B en complejo con CDK actúan como factor promotor de mitosis (MPF) [66]. En plantas las ciclinas CYCA/B junto con la cinasa conservada CDKA;1, y las cinasas CDKB específicas de plantas, forman los complejos CDK-ciclina promotores de la mitosis [66–68]. En *Arabidopsis* las ciclinas de tipo A también podrían participan en la progresión de la fase S [69]. Los complejos mitóticos CDK-ciclina fosforilan y regulan histonas H1, proteínas de la lámina nuclear y reguladores transcripcionales como RBR y MYB3R1/4, entre otros [28, 70–72]. En ratón y en humano, la actividad de los factores B-Myb se promueve por CycA/E [29], mientras que en plantas, la actividad de los factores MYB homólogos se promueve por ciclinas de tipo B (ver detalles en la sección 1.2).

Antes del inicio de la mitosis, la célula necesita revisar la disponibilidad de nutrientes y la integridad del ADN. Las cinasas ATM (Ataxia-telangiectasia-mutated) y ATR (Ataxia-telangiectasia and Rad3-related) son proteínas clave involucradas en el punto de control de la integridad del daño en el ADN. ATM participa en la reparación del daño producido en el ADN y, ATR en estrés durante la replicación del ADN [7]. Estas proteínas están conservadas entre plantas y otros eucariontes, pero las cinasas Chk1 y Chk2, efectoras de ATM y ATR en animales, no están presentes en plantas [53]. Cuando la replicación del ADN no se ha completado o hay daño en esta molécula, la célula se detiene en G2 [54]. En mamíferos, este arresto del CC se debe a la cinasa Wee que fosforila e inhibe a la CDK, evitando la entrada a la fase M. Cuando se ha reparado el daño, la fosfatasa Cdc25 elimina la fosforilación inhibitora de CDK, y una vez activa, esta cinasa inhibe a Wee y aumenta la actividad de Cdc25 desencadenando la entrada irreversible a la mitosis [73].

En *Arabidopsis*, la falta de cualquier fenotipo obvio de las mutantes de pérdida de función de CDC25-like o WEE1 predicen que esos genes no están involucrados en la regulación de un

CC normal. CDC25-like tiene funciones de fosfatasa o de arsenato-reductasa dependiendo del sustrato, no recupera la función del Cdc25 endógeno en *S. pombe* y tampoco tiene el dominio regulatorio de estas fosfatasas [74]. La mutación Wee1$^{+/-}$ en embriones de ratón provoca inestabilidad genómica y los embriones no logran implantarse [75]. En *Arabidopsis* la mutación de esta cinasa no afecta ni la proliferación ni la endorreduplicación, y tampoco parece ser una proteína limitante para la progresión del CC [76]. *In vitro*, esta cinasa fosforila a la CDKA;1 [77] y funciona en respuesta al daño a ADN [74, 78], pero su blanco principal parece ser distinto a CDKA;1 [78]. En *Nicotiana tabacum*, WEE1 también inhibe la actividad de la CDK *in vitro* [79]. Por otro lado, WEE1 no parece tener un dominio de reconocimiento de CDKA;1 [80]. En conclusión, la retroalimentación positiva entre CDKA;1 y CDC25-like, así como el asa de retroalimentación mutuamente inhibitoria entre CDKA;1 y WEE1, parecen no estar conservados en *Arabidopsis*.

Boudolf y colaboradores han propuesto que las CDKs de tipo B, únicas en plantas, podrían tener una función equivalente a Cdc25 de humanos o levadura [81]. Se ha propuesto que las CDKs de tipo B junto con los inhibidores KRPs podrían estar regulando la actividad de los complejos mitóticos CDKA;1-CYCB1;1 [81], de forma similar a Wee y Cdc25 en mamíferos. Al igual que en las plantas, estas proteínas tampoco parecen ser esenciales en levaduras. Wee1 y Cdc25 monitorean el tamaño celular y son centrales en *S. pombe*, pero no en *S. cerevisiae* [53,82].

Otro punto de control relevante en la progresión del CC es la salida de la mitosis, no obstante la información al respecto es limitada en plantas. Para concluir la división celular, es preciso el decremento en la actividad de la CDK, principalmente controlada por el Anaphase-Promoting Complex/Cyclosome (APC/C), que junto con el SCF, es una ligasa de ubiquitina E3 que confiere especificidad de sustrato al proteosoma 26S durante el CC. Tanto los componentes moleculares del SCF como del APC/C están conservados [83]. En *S. pombe*, el APC/C ubiquitina a la ciclina B y a la securina, promoviendo la degradación de estas proteínas durante la anafase (penúltima etapa de la mitosis). La securina es una proteína que se une e inactiva a la separasa, otra proteína que cataliza la separación de las cromátidas hermanas después de que todos los cromosomas se han unido al huso [84]. La separasa y la securina, son proteínas conservadas en levaduras, *Drosophila* y vertebrados pero no se ha identificado una securina en *Arabidopsis* [85]. De la transición M/G1 a la G1/S, la actividad del APC/C se promueve por Cdh1 [52], del cual se han identificado tres homólogos en *Arabidopsis*: CCS52A1, CCS52A2 y CCS52B [86].

La citocinesis es el aspecto más divergente del CC eucariota. En plantas, la citocinesis es un proceso que implica la formación de una nueva pared celular que va a separar las dos células hijas, requiere de la regulación de la biogénesis de la membrana y de los componentes del citoesqueleto [1]. En levaduras y animales se contrae la membrana plasmática. En *S. pombe*,

la vía de regulación SIN (Septation Initiation Network) localiza proteínas para regular la contracción del anillo y la fusión de la membrana, y en *S. cerevisiae*, la vía MEN (Mitotic Exit Network) coordina el inicio de la formación del brote. Las vías de regulación SIN y MEN detectan los centros organizadores de los microtúbulos, inactivan indirectamente complejos CDK-ciclinas y promueven la citocinesis. Sólo algunos elementos de la vía SIN están conservados entre plantas y levaduras (spg1p/TEM1p y cdc7p/CDC15p) [11].

1.5   Endorreduplicación

Después de la división hay dos mecanismos de crecimiento celular que, con frecuencia, ocurren simultaneamente. Uno de ellos es por endorreduplicación, y el otro por expansión de la vacuola [87]. La endorreduplicación es más común en plantas que en otros eucariontes, y ocurre frecuentemente en células diferenciadas como pelos, células del xilema, y en células con alta actividad metabólica como el endospermo o el suspensor [38]. La endorreduplicación, como parte de la diferenciación, permite a las células adquirir nutrientes y proteínas necesarias para el desarrollo embrionario, aunque también se ha observado en células cancerosas [22]. Muchos de los componentes del CC también participan en el endociclo [22], por ejemplo la actividad de la CDKA;1 no sólo es necesaria para el CC sino también para la endorreduplicación, la diferencia es que la actividad de CDKs es mucho más alta para entrar a fase M que a fase S [88–90]. Otros reguladores del CC también importantes para la endorreduplicación en *Arabidopsis* son los KRPs, ciclinas mitóticas, APC/C^{CCS52A} y los FTs E2Fs [84]. Las proteínas KRP, que se unen a complejos CDK-ciclina e inhiben su actividad, inducen el arresto del CC o el retraso de la progresión en respuesta a señales intra- o extra-celulares [64]. KRP5, además de inhibir complejos CDK-ciclina, también se une a factores del complejo remodelador de la cromatina SWI/SNF para coordinar la endorreduplicación con la elongación celular en hoja [91]. La ligera sobre-expresión de KRP2 induce la transición a endociclo, *in vitro* este KRP solo se une a CDKA;1 pero no a CDKB1;1. La correlación inversa entre los niveles de KRP2 y la actividad de CDKB1;1, sugiere que la estabilidad de KRP2 es regulada por la fosforilación de CDKB1;1 [89].

Durante la endorreduplicación, uno de los pasos clave es la reactivación de la maquinaria de replicación del ADN, la cual se previene normalmente por los complejos CDK-ciclina que se unen al complejo de replicación durante las fases G2 y M. En *S. pombe*, la activación periódica del APC/C permite endociclos sucesivos, ya que al promover la degradación de la CycB, evita que esta ciclina se asocie a los orígenes de replicación permitiendo otra ronda de replicación [38]. Dependiendo de su concentración, CYCA2;3 también regula la transición a endociclo en *Arabidopsis* [92]. Boudolf y colegas [93] reportaron que la sobre-expresión de CYCA2;3 y CDKB1;1

provoca divisiones celulares ectópicas y disminución de la proporción de células en endorreduplicación. El APC/C^{CCS52A} regula la estabilidad de CYCA2;3 y, por lo tanto, afecta la actividad del complejo CDKB1;1-CYCA2;3 [93]. Se ha propuesto que un papel de CDKB1;1-CYCA2;3 al inhibir el endociclo podría ser a través de la regulación negativa de la reiniciación de la replicación del ADN [93].

Finalmente, en *Arabidopsis*, E2Fa-DPa tiene papel dual, se requiere para la mitosis y para la endorreduplicación [68]. E2Fb-DPa promueve mitosis y E2Fc-DPb la inhibe e induce endorreduplicación. E2Fb y E2Fc, además tienen sitios de unión a E2F en sus regiones promotoras [94] y parecen ser blancos de E2Fa. La activación de E2Fe/DEL1, un E2F atípico que reprime la expresión de CCS52A2 [95], depende de la presencia de E2Fb o de la falta de E2Fc [96]. Es posible que E2Fc sea parte de un proceso dinámico fínamente regulado que permite el control preciso del CC durante la fase S, eso es consistente con las observaciones de porqué E2Fc se expresa poco en células diferenciadas, las cuales ya no tienen potencial de división, y se expresa más en regiones meristemáticas, donde ocurre la proliferación celular [97]. El mecanismos del APC/C$^{Cdh1/CCS52}$ en la transición a endociclo está conservada, así como la participación del E2Fe represor y el E2Fc, o la regulación negativa del E2F7 humano sobre el Cdh1 [22]. Estas interacciones conservadas nos dan una idea de la importancia de coordinar la salida del estado proliferativo y la entrada a endociclo.

Aún desconocemos cómo se mantiene el endociclo antes de pasar a la diferenciación terminal, pero cada vez hay más evidencia de la estrecha relación entre salida del CC y el inicio de la diferenciación. En tricomas[4] por ejemplo, cuando SIAMESE, una proteína que reprime la actividad de los complejos CDK-ciclina, está mutada, las células reentran a la mitosis y algunos de esos tricomas pierden su identidad y revierten su fenotipo a células pavimentosas [3, 92, 98]. Otro ejemplo en la raíz involucraría a MYB36, un FT que promueve la transición de la elongación a la diferenciación en la epidermis, activa genes requeridos en la diferenciación y reprime genes involucrados en la proliferación celular [99]. Suprimir a la ciclina B también podría ser esencial para el endociclo, ya que su sobre-expresión en tricomas es suficiente para cambiar un endociclo a ciclo mitótico [67, 87].

1.6 La raíz de *Arabidopsis* como modelo para el estudio del desarrollo

En las plantas los patrones morfogenéticos parecen ser más robustos que en animales, mientras los animales presentan severos fenotipos cuando se alteran la producción celular, las plantas tol-

---

[4]Células grandes epidermales que dejaron de dividirse.

eran variaciones en su número de células [100]. Ejemplo de ello es que al sobre-expresar genes reguladores del CC, como la ciclina mitótica, se observan aumentos anormales en la cantidad de células de los meristemos pero no se producen deformaciones drásticas del meristemo de la raíz [101]. Un caso en donde las plantas presentan tumoraciones, sería por ejemplo los causados por infección de bacterias como *Agrobacterium tumefaciens* [102].

Se ha propuesto que esta plasticidad del desarrollo vegetal se ha adquirido como respuesta a distintas condiciones físicas y bióticas en las cuales crecen y se desarrollan las plantas [103]. Su morfología depende en gran medida de condiciones ambientales como la luz [96], estrés osmótico [104], estrés hídrico [7], interacciones con otros organismos [105], disponibilidad de nutrientes como sacarosa [65], e incluso de la etapa del desarrollo en que se encuentra la planta cuando se presentan esas condiciones. Debido a su desarrollo post-embrionario, estos organismos pueden seguir generando estructuras nuevas a lo largo de su ciclo de vida a partir de los meristemos, un grupo de células indiferenciadas que se encuentran en los extremos en crecimiento [7]. Las plantas tienen dos meristemos principales, uno de ellos se encuentra en la punta del tallo (meristemo apical del vástago aéreo) y otro en la punta de la raíz (meristemo apical de la raíz) [106]. La raíz es un sistema ideal para el estudio cuantitativo y en vivo del desarrollo de órganos y tejidos. En particular la raíz de *Arabidopsis*, es un órgano transparente, con pocos tipos celulares y de fácil acceso. Además de que *Arabidopsis* se ha empleado como organismo modelo por tener un ciclo de vida corto y un genoma relativamente pequeño y el primero en ser secuenciado. En la punta de su raíz se puede identificar un patrón morfológico bien definido. En el ápice se encuentra el nicho de células troncales (NCT, *sensu strictu*), seguido por el dominio de proliferación y de transición, y después las zonas de elongación y de diferenciación hacia el extremo basal. El NCT está formado por el organizador central (Centro Quiescente; CQ) y las células iniciales. Al igual que las células troncales en animales, las células del NCT de *Arabidopsis*, están indiferenciadas, son capaces de renovarse y, al mismo tiempo, dar origen a células con funciones especializadas. El meristemo apical de la raíz comprende al NCT, al dominio de proliferación celular y al de transición.

El balance entre proliferación y diferenciación celular es resultado de la regulación diferencial de la división celular a lo largo de la raíz. Las células del CQ pasan mucho tiempo en fase G1 y casi no se dividen [107], las células iniciales que rodean al CQ se dividen a tasas intermedias, y las células del dominio de proliferación tienen una probabilidad alta de dividirse; en el dominio de transición esa probabilidad es muy baja y en ambos dominios el crecimiento celular es lento. Después, en la zona de elongación, las células dejan de dividirse, sólo se alargan y endorreduplican; es decir, duplican su material genético sin pasar por la fase M por lo que su ploidía y su tamaño aumentan [5, 108]. En la raíz, la proliferación junto con la elongación (crecimiento

celular en una dirección), son los principales procesos que contribuyen al crecimiento [109]. El criterio más válido de la transición a la elongación es el incremento abrupto en la tasa de crecimiento relativo, ya que células en diferentes filas de la raíz pueden salir del CC en diferentes puntos del eje longitudinal [110]. Durante el CC se duplica la longitud de la célula, pero durante la elongación, la longitud de la célula incrementa de 15 a 20 veces, y en maíz el tiempo que toma la elongación es menor a la duración de un CC [109]. Es durante la elongación que la célula comienza a desarrollar funciones específicas [109].
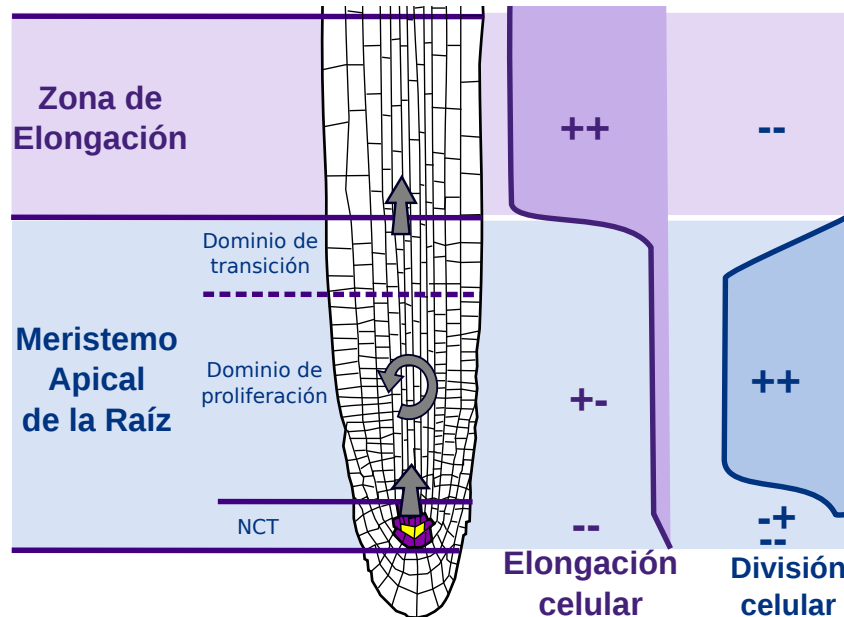
Fig. 1.2. La raíz de *Arabidopsis* y el balance entre proliferación y diferenciación celular [108, 109]. En el eje ápico-basal de la raíz se distingue el meristemo apical de la raíz conformado por el NCT, el dominio de proliferación y el de transición, y una zona de elongación donde las células comienzan a alargarse y a endorreduplicar. En el meristemo las células se dividen y no están diferenciadas, en la zona de elongación las células han dejado de dividirse y se comienzan a diferenciar. Las flechas representan la producción celular responsable de mantener el tamaño del meristemo de la raíz.

Es así que la homeostasis del meristemo de la raíz, depende de i) la tasa de entrada de las células desde el NCT al dominio de proliferación, ii) la tasa de división celular en el dominio de proliferación/transición y iii) la tasa de salida de las células del meristemo a la zona de elongación y diferenciación (ver Fig. 1.2). En la zona de diferenciación, las células adquieren un destino celular bien definido, en la epidermis por ejemplo se pueden apreciar los primeros pelos radicales. En general se considera que el ciclo de las células diferenciadas está detenido. La relación que mantienen los FTs que definen el destino celular y las hormonas, con el CC, ayudaría

a entender el comportamiento celular en el eje ápico-basal de la raíz, i.e. quiescencia, CC lento, CC y proliferación rápida, elongación y diferenciación. Un patrón morfogenético normal es resultado de la coordinación espacio-temporal adecuada de la detención del CC, la reactivación, la diferenciación celular, y la endorreduplicación. Una red común empleada en todos estos procesos, podría conectar las diferentes redes regulatorias de diferenciación celular o vías de transducción de señales y, así producir la emergencia de comportamientos celulares contrastantes en términos de división celular, entrada a endociclo o diferenciación, observados en la raíz de *Arabidopsis*.

Desde la perspectiva celular, en plantas el crecimiento de un órgano en estado estacionario está determinado por la longitud final de las células en la zona de elongación, y la tasa de producción celular en el meristemo [111]. Mientras la tasa de división celular indica qué tan rápido es el CC, la producción celular es la tasa a la que incrementa el número de células dentro de una población[5], la cual es función del número de células y de la duración de su CC. La duración del CC no es una función de la longitud de la célula *per se*, sino de la razón de la longitud de una célula después de la mitosis sobre la longitud de esa célula a la siguiente mitosis [110].

A diferencia de la tasa de producción celular, la tasa de división suele ser constante en el meristemo de la raíz [112], incluso cuando se sobre-expresa la ciclina B (sólo aumenta la cantidad de células meristemáticas) [101]. En este caso, la tasa de producción celular y el fenotipo se podrían deber a un número mayor de células en proliferación que se dividen a la misma tasa que las células silvestres [112]. Otro ejemplo es la sobre-expresión de una CDKB1;1 negativa dominante, que también tiene una tasa de proliferación celular igual que las células silvestres, ésto debido a que las células con la CDKB1;1 dominante negativa tienen una transición G2/M retrasada pero compensada por una fase G1 acelerada [113]. Entre diferentes ecotipos[6] de *Arabidopsis* se encontró que en aquéllos que tienen las mayores tasas de producción celular, hay una fuerte correlación entre la producción celular y la actividad de la CDKA;1 [111]. En conjunto, estas observaciones sugieren que la relación entre el crecimiento, la morfogénesis y la regulación del CC, no es simple, y que hay mecanismos de control, más que reguladores individuales, que aseguran que el CC sea un proceso robusto ante diferentes cambios en sus componentes.

1.7 Coordinación entre proliferación y diferenciación celular en la raíz de *Arabidopsis*

La división celular sin el control de la morfogénesis solo produciría tejidos callosos desorganizados [114]. Como hemos ejemplificado en las secciones previas, la morfogénesis requiere de la

---

[5]En el meristemo, la tasa de producción celular corresponde a las células que salen de él.

[6]Poblaciones locales que presentan variaciones genéticas

comunicación recíproca entre la división y la diferenciación celular, y del control espacial. Así mismo, los procesos de decisión del destino celular están asociados con modificaciones de la cromatina que ocurren en coordinación con eventos específicos del CC, como la replicación del ADN o la condensación de los cromosomas en la mitosis [115].

Los fenotipos de las mutantes de genes que regulan la progresión del CC en la raíz, son una evidencia del papel que tiene la red de regulación del CC no solo para la división celular, sino para el mantenimiento del estado quiescente o de la diferenciación celular. Pérdida de función de genes involucrados en la producción celular del NCT, o en la salida del meristemo a la zona de elongación, afectan la homeostasis del meristemo de la raíz, aún cuando se expresen muy poco o no se expresen en el meristemo. Esto se debe a la interdependencia entre las distintas zonas de la raíz. Un ejemplo serían las subunidades del complejo APC/C, CCS52A1 y CCS52A2, el primero de ellos se expresa en la zona de elongación, donde las células endorreduplican, y el segundo en el NCT, y con un perfil irregular, también en el meristemo [95]. Los fenotipos resultantes de la mutación de estas proteínas son opuestos: las raíces con pérdida de función de CCS52A1, proteína que participa en la transición de CC a endociclo, fueron un poco más largas que la silvestre, tienen meristemos más largos, más células en división y el índice de endorreduplicación (número medio de ciclos de replicación por núcleo) está reducido; con la pérdida de función de CCS52A2, que ayuda a mantener una proliferación reducida en el NCT, el crecimiento de la raíz está deteriorado, el meristemo es más pequeño, con menos células en división, pero con mitosis activa en el NCT. El ortólogo de CCS52A en mamíferos y en *Drosophila*, además participa en la degradación de reguladores transcripcionales [95], si esta función estuviera conservada en plantas, el APC/C establecería un vínculo adicional entre la proliferación y la división celular.

Alteraciones en los FT E2Fa y E2Fb, también ejemplifican cambios en el balance entre la proliferación y la diferenciación. Se ha propuesto que niveles altos de E2Fa escapan de la represión de RBR y así promueve mitosis y endorreduplicación dependiendo de la disponibilidad de factores específicos de tejidos. Con la expresión elevada de E2Fa hay meristemos más grandes [94] y su función parece depender de la etapa del desarrollo [116]. Las raíces de plantas que sobre-expresan al promotor de la división celular E2Fb, son aproximadamente 3 veces más cortas que las plantas control, y el tamaño de las células es menor, sugiriendo que la acumulación de E2Fb retrasa la diferenciación celular en la raíz [117]. Otros FTs que también regulan componentes del CC y que además participan en la regulación genética del meristemo apical de la raíz son SHORT ROOT (SHR), SCARECROW (SCR) y WOX5 (tema de la revisión [118]). RBR forma complejo con SHR y SCR para reprimir la división de las células troncales, y es fosforilado por CDKB1-CYCD6;1 [119]. WOX5 reprime la expresión de CYCD3;3, la mutación de

este regulador transcripcional incrementa el número de divisiones celulares en el CQ de raíces embriónicas [120].

Es importante señalar que no sólo el programa de diferenciación afecta a la maquinaria molecular del CC, sino que genes con función en la progresión del CC también regulan FTs implicados en la diferenciación celular. Esta otra relación entre proliferación y diferenciación se observa a nivel molecular con el FT GLABROUS1 (GL1 o MYB0), necesario para adquirir el fenotipo de tricomas, que es regulado por E2Fs [121]. Por último, la duración de las fases del CC también es relevante para el mantenimiento o la especificación y determinación del destino de las células troncales. La fase G1 de las células pluripontentes por ejemplo, son más cortas y las células con CC más rápidos expresan menos marcadores de diferenciación [122]. Recientemente se ha demostrado que también la regulación de la fase G2 es crítica para la diferenciación celular. La regulación epigenética como acetilación de histonas y remodelación de cromatina durante la fase S y G2 [115], son cruciales para la transición a la determinación. Esta propuesta nos lleva a pensar que mientras la especificación del destino celular ocurre durante la fase G1, el compromiso del destino celular y la pérdida de la pluripotencia se lleva a cabo en la G2 [123]; la ciclina responsable de la transición G2/M por ejemplo, promueve al estado pluripotente [124].

1.8 Regulación del ciclo celular por señales ambientales y hormonas vegetales

Mediante el CC, la morfogénesis vegetal responde y se ajusta al medio ambiente variable. Con frecuencia, la respuesta ante los cambios ambientales es mediada por hormonas vegetales. En plantas, las hormonas son morfógenos con influencia en el crecimiento y el desarrollo de la raíz, la mayoría tienen efectos en la proliferación y la expansión celular [125–127]. La interacción directa entre hormonas, lleva al comportamiento diferencial del CC en el eje logitudinal de la raíz [128]. Cuando hay estrés o se desencadena una respuesta inmune, el crecimiento de la planta se ve severamente afectado, eso de debe principalmente a una reconfiguración en el metabolismo y las vías de señalización de las hormonas [129]. A continuación se describen algunos ejemplos del efecto de las hormonas y señales ambientales sobre la progresión del CC.

Probablemente las ciclinas y las KRPs sean los integradores más importantes de las señales. Por ejemplo, la ciclina limitante para la transición G1/S CYCD3;1 [55], tiene una vida media de aproximadamente 7 minutos. Cuando se agota la sacarosa, los niveles de la CYCD3;1 disminuyen rápidamente y la célula se detiene en la fase G1. La expresión de la CYCD3;1 es inducida por hormonas como citocininas, brasinoesteroides, giberelinas y auxinas [9, 130, 131], mientras que el ácido abscisico y el ácido jasmónico causan una reducción en la cantidad del transcrito. La

regulación que ejercen estas hormonas sobre la progresión del CC es muy fina, por ejemplo cuando se altera la percepción de brasinoesteroides, decrementa la actividad mitótica, pero si las plantas son tratadas con brasinoesteroides, las células salen prematuramente del CC [132]. Además de CYCD3;1, los brasinoesteroides también inducen la expresión de CDKB1;1, aunque se desconoce si es una regulación directa [131]. La sinergia entre auxinas y citocininas por ejemplo, induce la expresión de CDKB1;1, CDKA;1 y CYCB1;1 [127]. Como las hormonas son un enlace entre las señales ambientales y las regulación del CC, las ciclinas de tipo D podrían haber evolucionado formas de regulación que permitan la integración de señales ambientales a la división celular y al desarrollo de la planta [133]. Por otro lado, la expresión de KRP2 y SIM es reducida por giberelinas [129], mientras que el nivel de la proteína KRP2 es regulado negativamente por auxinas [134].

Varios tipos de estrés, la temperatura y la luz son factores ambientales que modulan directamente la progresión del CC, esta última promueve la degradación de E2Fc y el incremento de la proteína E2Fb [69, 135]. Las bajas temperaturas, el estrés salino y el ácido abscisico inducen la transcripción del KRP1 [136, 137], influyendo negativamente en la progresión del CC. SMR5 y SMR7, otros inhibidores de la actividad de las CDKs, son activados por especies reactivas de oxígeno, deteniendo al CC ante el estrés provocado por exceso de fierro [138]. De modo similar, el estrés por sequía y el estrés osmótico inducido por manitol, reducen la división celular, este último además incrementa la expresión de SKP2A (subunidad del SCF; [139, 140]); en situaciones de estrés abiótico, el APC/C degrada al FT RSS1 (RICE SALT SENSITIVE 1), requerido para mantener el CC activo [65]. Y finalmente, el Ca^{2+}, necesario para la progresión del CC en mamíferos, se ha propuesto como otro señalizador de la regulación del CC en plantas [24] (referencia sugerida sobre regulación transcripcional y hormonal del desarrollo de la raíz [141]).

Cuando la sacarosa, principal fuente de carbono de las plantas, es deficiente, las proteínas involucradas en la transición G1/S como RBR y E2Fa se degradan vía proteosoma, quedando el CC detenido en la fase G1 [142, 143]. La ciclina del tipo P CYCP2;1, conservada también en *Drosophila* y *S. cerevisiae*, es el vínculo entre la disponibilidad de nutrientes y la progresión del CC. Su transcripción es activada por WOX9 (STIMPY; FT que activa el crecimiento del meristemo durante la germinación), por sacarosa, y posiblemente también por TOR1 [144, 145]. La cinasa conservada TOR1 (TARGET-OF-RAPAMYCIN1), activada por auxinas [129], integra información sobre la disponibilidad de nutrientes con la inducción de genes que participan en la glicólisis, el ciclo del ácido tricarboxílico y la síntesis de proteínas. TOR1 fosforila y activa a E2Fa cuando hay glucosa producto de la fotosíntesis, esta reacción induce la entrada a la fase S de células meristemáticas que previamente se encontraban en quiescencia [144, 146].

1.9 Modelos de la regulación del ciclo celular

El uso de enfoques sistémicos y dinámicos es esencial para entender el comportamiento colectivo de los componentes dentro de la red regulatoria del CC de *Arabidopsis*.

Tabla 1.2. Modelos propuestos sobre la regulación del CC en diferentes organismos.

Organismo	Aprox.	Descripción	Refs.
Rana	Continua	Regulación del heterodímero CDK-ciclina durante la mitosis. Una asa de retroalimentación negativa y un retraso de tiempo fueron suficientes para reproducir el comportamiento oscilatorio.	[17]
S. pombe	Continua	Destaca el papel de las asas de retroalimentación en la actividad biestable de los complejos CDK-ciclina durante la replicación del ADN.	[14]
S. pombe	Continua	Además de CDK-ciclina, incluye a otros reguladores para modelar las transiciones G1/S, G2/M y metafase/anafase. Análisis de fenotipos mutantes, se incluye el tamaño celular.	[147–150]
S. cerevisiae	Continua	Modelo que incluye regulación genética, fosforilación, degradación de proteínas e inhibición de la actividad de las CDKs por interacciones físicas. Se llevaron a cabo análisis de mutantes para describir la dinámica de las transiciones entre los estados estacionarios estables G1 y S/G2/M.	[16]
Genérico	Continuo	Se proponen módulos genéricos así como la lógica mínima para la regulación del CC eucarionte.	[151–153]
S. cerevisiae	Booleano (umbrales)	Toma en cuenta autodegradación para las proteínas que no tienen reguladores negativos. Incluye el tamaño de la célula como entrada del modelo. Recupera la secuencia de los eventos del CC en un atractor de punto fijo que corresponde a la fase G1, además de otros 6 atractores.	[15]
S. pombe	Booleano (umbrales)	Recupera 13 atractores en total, entre ellos uno de punto fijo que sería la fase G1. Despúes se validó simulando mutaciones y comparandolas con las correspondientes observaciones experimentales.	[82, 154]
S. cerevisiae	Booleano (reglas lógicas)	Para recuperar un atractor cíclico con todas las transiciones del CC, incluye retrasos de tiempo y nodos que definen eventos del CC (como la replicación del DNA, la formación del brote, la entrada a la fase M y la división celular).	[155]
S. cerevisiae	Booleano	Mejora en la robustez temporal especificando criterios en el orden de activación de los componentes. Usa 'model checking' para el análisis de la robustez temporal.	[156]
Mamíferos	Booleano (reglas lógicas)	Comparan aproximaciones sincrónica y asíncrona a partir de una propuesta en otro trabajo [18]. La ciclina CYCD es el nodo entrada del modelo (se autoregula). Se obtienen dos atractores, uno de punto fijo que representa la fase G0 y otro que es un atractor cíclico que recupera la dinámica del CC.	[19]
S. cerevisiae	Booleano (reglas lógicas)	Integra un modelo sobre la maquinaria central del control del CC, con otro modelo de la formación del brote y otro sobre la salida del CC. Además analiza el efecto que tienen algunas perturbaciones en el comportamiento global del CC.	[20]
Mamíferos	Híbrido	Incluye variables continuas y discretas que incorporan eventos aleatorios. La abundancia de ciclinas reportada por el modelo es congruente con la que se obtuvo por citrometría de flujo.	[157]
Arabidopsis	Continuo	Modelo sobre la regulación de la transición G1/S que confirma la conservación de este punto de control en eucariontes.	[158]
Solanum lycopersicum (jitomate)	Continuo	Se modela la transición a la endorreduplicación con ecuaciones diferenciales ordinarias, involucra regulación por auxinas. Se asume que los mecanismos descritos en *Arabidopsis* se conservan en jitomate.	[159]

En la Tabla 1.2 se presenta una muestra de los modelos que se han propuesto para la regulación del CC de diferentes organismos. Sin duda, esos trabajos han servido para analizar propiedades sistémicas, como la robustez del ciclo, la histeresis, la irreversibilidad y la biestabil-

idad [160–164], se recomienda la revisión [165] sobre algunos enfoques que se han empleado en el modelado del CC. Estas propiedades están estrechamente relacionadas, pues la base de todas ellas se encuentra en la coordinación de los circuitos regulatorios involucrados en la progresión del CC. La biestabilidad es la propiedad distintiva de la actividad de los heterodímeros CDK-ciclina, pues sólo tienen estados 'activo' o 'inactivo', pero no intermedios. La histeresis se refiere a que una vez que se ha inducido la transición a la siguiente fase, la célula tiende a mantenerse ahí, aun cuando la concentración de la ciclina que indujo la transición disminuya. Esas propiedades están involucradas en la progresión unidireccional y las transiciones irreversibles del CC, pues la célula debe asegurar que una vez iniciada la mitosis no se vuelva a replicar el ADN, y que los eventos que ocurren a lo largo del CC tengan un orden.

En contraste a otros eucariontes, en plantas se han hecho pocos intentos de integrar los datos experimentales sobre el CC para construir modelos computacionales dinámicos. Uno de estos trabajos modeló la transición a la endorreduplicación en jitomate [159], y otro implementó un modelo de la transición G1/S en *Arabidopsis* y otros organismos. Este último contribuyó a mostrar algunas características conservadas de este punto de control entre eucariontes [158]. Un modelo de la regulación del CC en *Arabidopsis*, sería necesario si queremos entender la homeostasis del meristemo de su raíz. Aunque hay varias similitudes en la red de regulación del CC de todos los eucariontes, también hay diferencias que se deben considerar cuando buscamos aproximarnos a las particularidades de las plantas.

Las principales diferencias entre la red de regulación del CC de *Arabidopsis* y la de otros eucariontes, tienen que ver con el número de parálogos[7] de algunos reguladores clave. *Arabidopsis*, tiene más de 10 copias de algunos de los genes que codifican para reguladores del CC (por ejemplo, familias de ciclinas o CDKs), mientras que en levaduras, mamíferos o el alga unicelular *Ostreococcus tauri*, hay muchos menos duplicados [8, 23, 40, 58]. La única excepción serían los homólogos de la proteína Retinoblastoma, de la cual hay tres miembros en humano y en ratón, y solo una copia en *Arabidopsis* [166].

Estas diferencias y las descritas en secciones previas, nos motivaron a proponer un modelo de la red de regulación del CC de *Arabidopsis* en particular. Elegimos los formalismos booleanos porque son simples y han demostrado ser útiles y de gran alcance para seguir los cambios cualitativos en la actividad de reguladores en diferentes organismos y procesos biológicos [167, 168]. Hemos planteado la siguiente hipótesis como la base de este proyecto:

---

[7]Genes homólogos originados por duplicación de secuencias

1.10 Hipótesis

Si incorporamos en un modelo dinámico los componentes mínimos (suficientes y necesarios) de la red de regulación del ciclo celular, entonces se puede recuperar el patrón cíclico de actividad o transcripción de las moléculas indicadoras de cada fase y transición del ciclo celular.

1.11 Objetivo general

Proponer un modelo booleano y su extensión continua de la red de regulación del ciclo celular que recupere en un atractor cíclico las fases y las transiciones de fase ordenadas del ciclo celular de *Arabidopsis*.

2

MODELO DINÁMICO DE LA RED DE REGULACIÓN DEL CICLO CELULAR DE *Arabidopsis*

Con frecuencia la regulación genética no guarda relaciones lineales, hay genes regulados por sus propios blancos o genes regulados por dos vías simultáneas. Al analizar fenotipos de dobles mutantes, puede pasar que el fenotipo de uno de esos genes sea enmascarado por el otro. Los modelos booleanos son instrumentos que facilitan la investigación los patrones de interacciones entre genes como las asas de retroalimentación (*feedback loops*) o las asas de alimentación hacia adelante (*feedforward loops*) [167]. Los modelos de redes booleanas también han demostrado ser de gran utilidad para inferir mecanismos de regulación a partir de datos experimentales; por ejemplo, de series de tiempo de expresión genética (más ejemplos en [168]). En este capítulo presentamos el modelo dinámico de la red de regulación del CC de *Arabidopsis*, la metodología que seguimos para su planteamiento, y los resultados obtenidos. El artículo derivado de este trabajo se encuentra en el ANEXO A [169].

2.1 Metodología

El carácter booleano de la red indica que para cada nodo X_i hay dos estados posibles (e.g., "prendido" o "apagado", "presente" o "ausente"), $X_i \in \{0, 1\}$. El estado de cada nodo puede cambiar con el tiempo de acuerdo a un conjunto de interacciones regulatorias que se representan por medio de funciones booleanas: $X_i(t+1) = F_i(X_{i_1}(t), X_{i_2}(t), \ldots, X_{i_k}(t))$, en donde $X_i(t+1)$ es el estado del nodo X_i un paso de tiempo después de t, y $X_{i_1}(t), X_{i_2}(t), ..., X_{i_k}(t)$ representa el estado de todos los reguladores de X_i al tiempo t. Dado que cada nodo tiene una función booleana asociada, es posible saber cómo cambia su estado a través del tiempo de acuerdo

al estado de sus reguladores. El conjunto de estados de los nodos de la red en un tiempo determinado es lo que define *la configuración de la red* en ese tiempo. Partiendo de todas las configuraciones posibles (2^n, donde n es el número total de nodos de la red), y aplicando las reglas lógicas a todos los nodos durante varias iteraciones, se puede seguir la dinámica de toda la red hasta que alcanza un estado estacionario: una configuración de red que ya no cambia, o un conjunto de configuraciones que son visitadas en una forma cíclica. Tal estado se llama *atractor*. Los atractores de punto fijo solo tienen una configuración de red, mientras que los atractores cíclicos con periodo s, tienen s configuraciones visitadas indefinidamente, siempre en el mismo orden.

2.1.1 Modelos Booleanos
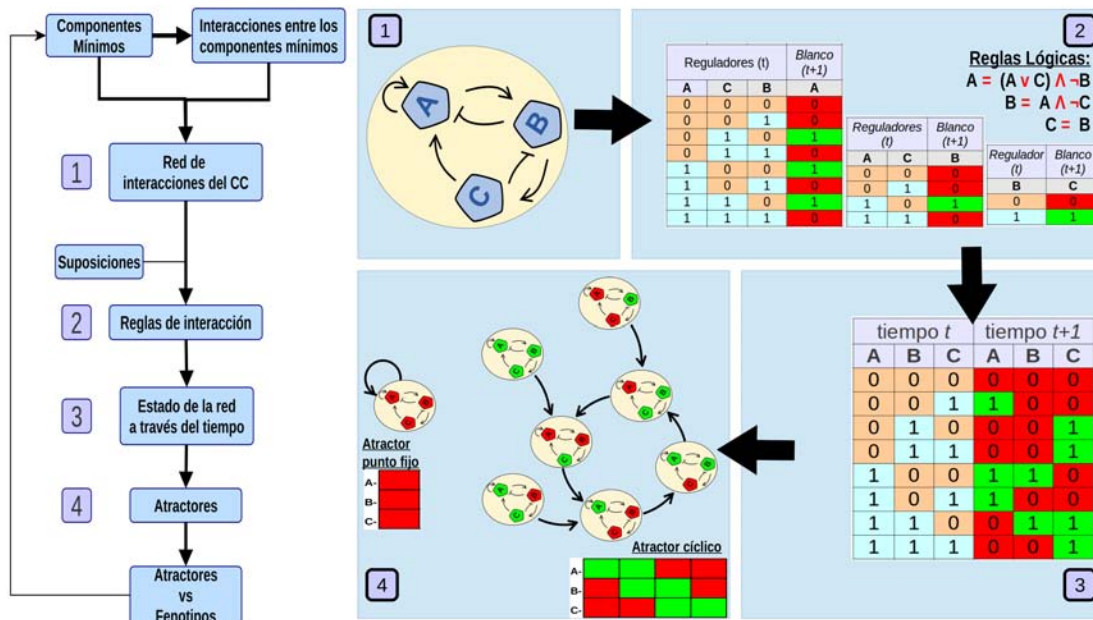
Fig. 2.1. Metodología. Después de construir la red (1) con las interacciones entre los componentes mínimos, se plantean las suposiciones que serán la base para el planteamiento de las reglas lógicas. Cada regla lógica (2) indica los estados de los reguladores que llevarán a una proteína a estar presente. Partiendo de todas las posibles configuraciones de la red y viendo cómo cambian con el tiempo (3), llegaremos eventualmente a estados estacionarios o atractores (4). Para validar si la construcción del modelo fue adecuada, se contrastan los resultados de simular mutaciones con los correspondientes fenotipos que se observan experimentalmente.

En la Fig. 2.1 se muestra un diagrama que resume las etapas de la construcción del modelo que hemos propuesto. El propósito de este modelo es entender el mecanismo de proliferación

celular a través de los patrones de presencia de las proteínas o complejos relevantes para cada fase, y responsables de la progresión del CC. Este punto es fundamental ya que la pregunta que se busca responder, o el objetivo con el que se construye el modelo, guían su construcción. Así, tomando en cuenta el propósito del modelo, para determinar los nodos que conformarán la red de regulación del CC, tomamos en cuenta nodos e interacciones que influyen directamente en la actividad de los heterodímeros CDK-ciclina, puesto que esa actividad es limitante para la progresión normal del CC.

2.1.2 Supuestos del Modelo

El procedimiento para la construcción del modelo requiere la especificación de suposiciones y una aplicación consistente de las mismas. Si los supuestos son apropiados ayudarán a obtener conclusiones después de una validación satisfactoria del modelo. Los supuestos del modelo Booleano del CC de *Arabidopsis* fueron los siguientes:

- Los nodos representan genes, proteínas o complejos de proteínas involucradas en las transiciones de fase del CC. El estado del nodo 1 representa presencia, y 0 ausencia; el último caso, también indica situaciones en las cuales un componente está presente pero inhabilitado por una modificación postraduccional, *e.g.* el estado del nodo RBR corresponde a 1 o presente cuando esta proteína está en su forma hipofosforilada.

- En las reglas lógicas, cuando no se especifica una CDK particular, una ciclina formaría complejo con CDKA;1, una cinasa que siempre está presente porque se expresa en tejidos en proliferación [170] y durante el todo el CC.

- E2Fa, E2Fb y E2Fc necesitan proteínas Dimerization Partner (DPa o DPb) para su unión a ADN. Dado que la expresión de DP no cambia drásticamente en el CC [171], asumimos que el estado del esos dímeros está dado solamente por la presencia de los factores E2F.

- La dinámica de la formación de complejos (tales como CDK-ciclina y KRP1, o RBR y los factores E2F) se especifica directamente en la función Booleana de sus genes blancos. Por ejemplo, la regla lógica de E2Fb es $E2Fa \ \& \ !RBR$, indicando que el estado de E2Fb es 1 cuando E2Fa lo activa transcripcionalmente porque RBR no está unido a E2Fa.

- El esquema de actualización para el estado de los nodos fue sincrónico.

Tabla 2.1. Interacciones demostradas mediante experimentos para la red del CC de *A. thaliana* y referencias.

Regulador		Blanco	Descripción de la interacción y referencias
CDKA;1-CYCD3;1	⊣	RBR	Diversos experimentos sugieren que esta interacción está conservada en *Arabidopsis*, de manera similar a como ocurre en mamíferos [40, 172], es decir, que la ciclina CYCD3;1 se une a CDKA;1 [27] y que los complejos CKDA;1-ciclinas tipo D se unen, fosforilan e inactivan a RBR [173, 174], su principal blanco [27].
CDKA;1-CYCD3;1	⊣	RBR–E2Fb	El complejo E2Fb–RBR disminuye cuando CYCD3;1 está sobre-expresada [94].
CDKA;1-CYCD3;1	⊣	E2Fc	El reconocimiento de E2Fc por la ligasa de ubiquitinas SCF requiere la fosforilación mediada por la cinasa CDKA;1 [69].
SCF	⊣	CYCD3;1	La ligasa de ubiquitinas SCF está involucrada en la ubiquitinación que dirige la degradación de la ciclina CYCD3;1 [54].
SCF	⊣	KRP1	La ubiquitinación de KRP1 por el SCF promueve la degradación de este inhibidor de CDKs [136, 175].
SCF	⊣	E2Fc	El FT E2Fc se acumula cuando la subunidad del SCF, SKP2A, está mutada, mientras que la sobre-expresión de esta subunidad reduce los niveles de E2Fc [69, 176].
RBR	⊣	E2Fa/b	RBR hipofosforilado se une a E2Fa/b y es un regulador negativo de su actividad transcripcional [44, 94].
E2Fa	→	E2Fb	La transcripción de E2Fb se induce en la línea sobre-expresora de E2Fa [39].
E2Fa	→	E2Fc	E2Fc tiene sitios de unión de los E2Fs [39] y su expresión está inducida en las líneas sobre-expresoras de E2Fa-DPa [117].
E2Fa	→	RBR	El control transcripcional de RBR está bajo la actividad transcripcional de E2Fa [116].
E2Fa	→	APC/C	CCS52A2, una subunidad del complejo APC/C, se induce cuando se sobre-expresa una forma de E2Fa que no se puede unir a RBR [94].
E2Fb	→	CYCB1;1	La expresión de CYCB1;1 está inducida cuando incrementa la concentración de una forma de E2Fb que no se puede unir a RBR; los blancos de E2Fb son genes necesarios para la transición G2/M [2, 94, 117].
E2Fb	→	CDKB1;1	La inducción de la expresión de E2Fb promueve la expresión de CDKB1;1 [2].
E2Fb	→	E2Fe	E2Fb induce la transcripción de E2Fe [96]
E2Fc	⊣	CDKB1;1	El efecto positivo de E2Fb puede ser contrarrestado por E2Fc; con la desestabilización de E2Fc, incrementan los niveles de CDKB1;1 [96, 135].
E2Fc	⊣	CYCB1;1	La expresión de CYCB1;1 incrementa con la reducción de la expresión de E2Fc; la sobre-expresión de E2Fc reduce los niveles de CYCB1;1 [177].
E2Fc	⊣	E2Fa	Los mensajeros de E2Fa incrementan con el silenciamiento de la expresión de E2Fc por RNA de interferencia [177].
E2Fc	⊣	E2Fe	E2Fc contrarresta el efecto positivo que tiene E2Fb en la expresión de E2Fe [96].
E2Fe	⊣	APC/C	La expresión de CCS52A, una subunidad del APC/C, es inhibida por E2Fe [178].
MYB3R1/4	→	CYCB1;1	MYB3R1/4 reconoce la secuencia AACGG requerida para la expresión de CYCB1;1; otros reguladores parecen dirigir su expresión específica de la transición G2/M [47, 179].
CDKB1;1	–	CYCA2;3	CYCA2;3 interactúa con CDKB1;1 para formar un complejo funcional [93, 180].
CDKB1;1-CYCA2;3	⊣	KRP1	En complejo con CYCA2;3, CDKB1;1 podría promover la proteólisis de KRP1 como promueve la proteólisis de KRP2; ambos KRPs podrían tener papeles similares en la entrada de la mitosis, puesto que ambos interactúan con CDKA;1 y se expresan en G2/M [89, 93, 181].
CDKB1;1, CDKA;1	–	CYCB1;1	Las ciclinas de tipo B interactúan con CDKs de tipo B y tipo A [71, 180].
CDKA;1-CYCB1;1	→	MYB3R1/4	La sobre-expresión de MYB3R4 duplica la actividad de su promotor blanco con respecto al silvestre, y la coexpresión de MYB3R4 y CYCB1;1 la cuadruplican [72]; CycB1 y otras ciclinas mitóticas incrementan la actividad de los factores NtmybA2 en tabaco [29, 182].
KRP1	⊣	CYCD3;1	KRP1 interactúa con CDKA;1 y CYCD3;1 en el sistema doble híbrido en levadura [4, 136, 183, 184].
KRP1	⊣	CYCB1;1	La unión de KRP1 a CDKA;1 inhibe la actividad de CDKA–CYCB1;1 [137,183].
APC/C	⊣	CYCB1;1	El complejo APC/C ubiquitina a CYCB1;1 para que sea degradada [86].
APC/C	⊣	CYCA2;3	CYCA2;3 se estabiliza con las mutaciones de pérdida de función en subunidades del APC/C, o con mutaciones en su caja D [92, 93].

Resumen de la evidencia experimental que sustenta las interacciones del modelo de la red de regulación del CC de *Arabidopsis*. ⊣ representa la regulación negativa, → es la regulación positiva y – representa la formación de complejos funcionales.

Tabla 2.2. Interacciones hipotéticas de la red del CC de *Arabidopsis*.

Regulador		Blanco(s)	Datos que apoyan la interacción propuesta y referencias
E2Fb	→	SCF	Skp2 es un proteína F-box que forma parte del complejo SCF; esta proteína es regulada transcripcionalmente por E2F1 en humano [185]. E2Fb es el ortólogo de E2F1 en *Arabidopsis*. Hasta ahora solo se ha reportado que los factores E2F regulan a la proteína F-box FBL17 en *Arabidopsis* [158]
E2Fb	→	MYB77	La regulación directa entre los factores E2F y MYB se ha reportado en mamíferos [30] y entre las proteínas funcionalmente equivalentes de *S. cerevisiae* [186], pero no en *Arabidopsis*. Consideramos que en plantas podría incluir al menos un intermediario, ya que la presencia de otras características como la regulación periódica, nos hace pensar que la regulación trancripcional es similar. Después de analizar las dos familias principales de FTs involucrados en la regulación del CC, TCP y MYB [56], nosotros proponemos a MYB77 como un mediador entre la regulación de E2F y MYB. En análisis de expresión dependiente del CC por microarreglos, se encontró que MYB77 presenta un pico de expresión en la fase M [187–189]. Este FT de la familia MYB tiene sitios de unión para E2F, y como el sitio consenso que reconoce ya se identificó, planteamos la posibilidad de que MYB77 regula a MYB3R1/4 y a otros genes de la red del CC de *Arabidopsis*.
MYB77	→	E2Fe, KRP1, MYB3R1/4, CYCB1;1, CYCA2;3, CDKB1;1, CCS52A2	La secuencia CNGTTR identificada como un sitio consenso reconocido por MYB77 [190, 191] se usó para encontrar sus posibles blancos entre los reguladores de la red del CC. Varios de ellos se expresan justo antes de la transición G2/M.
MYB3R1/4	→	SCF, RBR, CDKB1;1, CYCA2;3, APC/C, E2Fc, MYB3R1/4, KRP1	Con la metodología descrita en la Sección 2.1.4, el sitio consenso que reconoce MYB3R4, se encontró en SKP2A, RBR, CDKB1;1, CYCA2;3, CCS52A2, KRP1, E2Fc, MYB3R1/4 y CYCB1;1. En tabaco, los genes NtmybA1 y NtmybA2, ortólogos de MYB3R1/4, también tienen la secuencia MSA y pueden autorregularse [29]. MYB3R1/4 podría promover la expresión de KRP1, puesto que este inhibidor de CDKs tiene un pico de expresión en G2/M y tiene 8 elementos MSA putativos [181]. Adicionalmente, la regulación CYCB1;1 por los FTs MYB3R1/4 también tiene una referencia experimental (ver Tabla 2.1).
CDKB1;1-CYCA2;3	⊣	E2Fa	Se ha propuesto que los niveles bajos de E2Fa se podrían deber a su alta tasa de recambio como resultado de la fosforilación por la CDKB1;1. Este FT tiene sitios putativos de fosforilación por la CDK en su extremo N-terminal, y la actividad alta de cinasas CDK correlaciona inversamente con su habilidad de unión a ADN *in vitro* [2, 117]. Esta interacción está demostrada en células de mamíferos [93, 192].
APC/C	⊣	SCF	Se ha propuesto que las funciones del complejo APC/C y el SCF son excluyentes durante la progresión del CC [193]. En células en proliferación de mamíferos, el nivel de Skp2, una de las subunidades que conforman el SCF, oscila siguiendo el patrón de los sustratos del APC/C, y la subunidad del APC/C Cdh1 está involucrada en la degradación de Skp2 [194]. Los complejos SCF y APC/C de *Arabidopsis*, parecen tener las mismas funciones que sus contrapartes en animales y su regulación también parece estar conservada [175, 195]

Resumen de la información que nos llevó a considerar interacciones adicionales a las demostradas experimentalmente para la regulación del CC en *Arabidopsis*. ⊣ representa regulación negativa y → es regulación positiva.

2.1.3 Reglas lógicas del modelo

Este modelo Booleano integra datos experimentales de 29 interacciones involucradas en la progresión del CC de *Arabidopsis*. También incorpora tres interacciones descubiertas en animales

(E2Fb→SCF, CDKB1;1-CYCA2;3⊣E2Fa, APC/C⊣SCF), y 16 interacciones basadas en análisis bioin-formáticos.

En las Tablas 2.1 y 2.2 [169] se describen con detalle las interacciones del modelo y la integración de esos datos quedó formalizada en las siguientes reglas lógicas:

$\wedge$ es el operador Booleano "AND", $\vee$ es el operador "OR", y $\neg$ es la negación. Dado que las reglas lógicas indican cómo cambia el estado de un nodo a través del tiempo, una regla recibe el estado de los reguladores del nodo al tiempo t para producir el estado de ese nodo al tiempo $t+1$, es decir, un paso de tiempo después.

1. $\mathrm{CYCD3;1} = \neg \mathrm{SCF}$

   La ciclina CYCD3;1 está presente cuando la ligasa de ubiquitinas SCF no está para promover su degradación.

2. $\mathrm{SCF} = \neg \mathrm{APC/C} \wedge ((\mathrm{E2Fb} \wedge (\neg \mathrm{RBR} \vee (\neg \mathrm{KRP1} \wedge \mathrm{CYCD3;1}))) \vee \mathrm{MYB3R1/4}$

   La presencia del SCF requiere la ausencia del APC/C y la activación transcripcional por parte del E2Fb o el MYB3R1/4 (a través de su subunidad SKP2A). Para que E2Fb sea funcional, no debe estar presente RBR o debe estar hiperfosforilado por el complejo activo CDKA;1-CYCD3;1.

3. $\mathrm{RBR} = (\mathrm{KRP1} \vee \neg \mathrm{CYCD3;1}) \wedge ((\mathrm{E2Fa} \wedge \neg \mathrm{RBR}) \vee \mathrm{MYB3R1/4})$

   La presencia de la forma hipofosforilada de RBR requiere la ausencia o la inactividad de CDKA;1-CYCD3;1 y la activación transcripcional por E2Fa (libre de RBR) o por MYB3R1/4.

4. $\mathrm{E2Fa} = (\mathrm{E2Fa} \vee \neg \mathrm{E2Fc}) \wedge \neg (\mathrm{CDKB1;1} \wedge \mathrm{CYCA2;3})$

   La presencia de E2Fc no afecta la expresión de E2Fa, pero su ausencia incrementa la expresión de E2Fa, y la actividad de CDKB1;1-CYCA2;3 correlacionan con niveles bajos del FT E2Fa.

5. $\mathrm{E2Fb} = (\mathrm{E2Fa} \wedge \neg \mathrm{RBR})$

   Cuando RBR no está unido a E2Fa, este FT activa la expresión de E2Fb.

6. $\mathrm{E2Fc} = \neg (\mathrm{SCF} \wedge \neg \mathrm{KRP1} \wedge \mathrm{CYCD3;1}) \wedge ((\mathrm{E2Fa} \wedge \neg \mathrm{RBR}) \vee \mathrm{MYB3R1/4})$

   E2Fc está presente cuando E2Fa (libre de RBR) o MYB3R1/4 lo activan transcripcionalmente, y cuando el SCF no ubiquitina a la proteína para que sea degradada. El reconocimiento de E2Fc por parte del SCF depende de la actividad de CDKA;1-CYCD3;1.

7. $\mathrm{E2Fe} = (\neg \mathrm{E2Fc} \vee (\mathrm{E2Fb} \wedge (\neg \mathrm{RBR} \vee (\neg \mathrm{KRP1} \wedge \mathrm{CYCD3;1})))) \vee \mathrm{MYB77}$

   La presencia de E2Fe depende de su expresión genética dirigida por MYB77 o E2Fb. La

activación por E2Fb requiere que RBR no esté presente o que esté hiperfosforilado por CDKA;1-CYCD3;1. E2Fc se une al mismo sitio que E2Fb, y reduce la inducción por E2Fb; E2Fe se expresa un poco cuando se elimina el sitio que reconocen estos E2Fs.

8. $MYB77 = E2Fb \wedge (\neg RBR \vee (\neg KRP1 \wedge CYCD3;1))$

   La expresión de MYB77 es inducida por E2Fb cuando RBR no está o se encuentra hiperfosforilado.

9. $MYB3R1/4 = MYB77 \vee (MYB3R1/4 \wedge CYCB1;1 \wedge \neg KRP1)$

   MYB3R1/4 transcribe a su propio gen cuando la proteína es fosforilada por CDKA;1-CYCB1;1. Alternativamente, la expresión de este gen es promovida por MYB77.

10. $CYCB1;1 = \neg APC/C \wedge (MYB3R1/4 \vee MYB77 \vee ((\neg RBR \vee (\neg KRP1 \wedge CYCD3;1)) \wedge E2Fb \wedge \neg E2Fc))$

    Esta ciclina esta presente cuando es transcrita por MYB3R1/4, MYB77 o E2Fb, y el APC/C no está (ligasa de ubiquitinas E3 que induce su degradación). Si su transcripción esta a cargo de E2Fb, es necesario que RBR no inhiba su función y que E2Fc no esté, ya que este FT reduce el efecto de E2Fb.

11. $CDKB1;1 = ((\neg RBR \vee (\neg KRP1 \wedge CYCD3;1)) \wedge E2Fb \wedge \neg E2Fc) \vee MYB3R1/4 \vee MYB77$

    La presencia de esta cinasa depende de su transcripción promovida por E2Fb o MYB3R1/4 o MYB77. El efecto de E2Fb depende de la ausencia de E2Fc y de RBR hipofosforilado.

12. $CYCA2;3 = \neg APC/C \wedge (MYB3R1/4 \vee MYB77)$

    La presencia de esta ciclina requiere la activación transcripcional por alguno de los FT MYB y la ausencia de APC/C que media su degradación.

13. $KRP1 = (MYB77 \vee MYB3R1/4) \wedge \neg(CDKB1;1 \wedge CYCA2;3 \wedge SCF)$

    KRP1 está presente cuando su expresión es regulada por MYB77 o MYB3R1/4, y cuando no es modificada postraduccionalmente por SCF y CDKB1;1-CYCA2;3.

14. $APC/C = \neg E2Fe \wedge ((E2Fa \wedge \neg RBR) \vee MYB3R1/4 \vee MYB77)$

    Este complejo es funcional cuando la expresión de su subunidad CCS52A es promovida por E2Fa (libre de RBR) o alguno de los FT MYB, y cuando E2Fe no reprime esa expresión.

2.1.4 Expresión periódica y análisis de secuencias promotoras

Para la validación del modelo continuo, se obtuvieron perfiles de expresión periódica de los trabajos de Menges y colaboradores [187–189]. Para los análisis de las secuencias promotoras se usó el sitio consenso CNGTTR para MYB77 [190, 196], mientras que para MYB3R4 fue
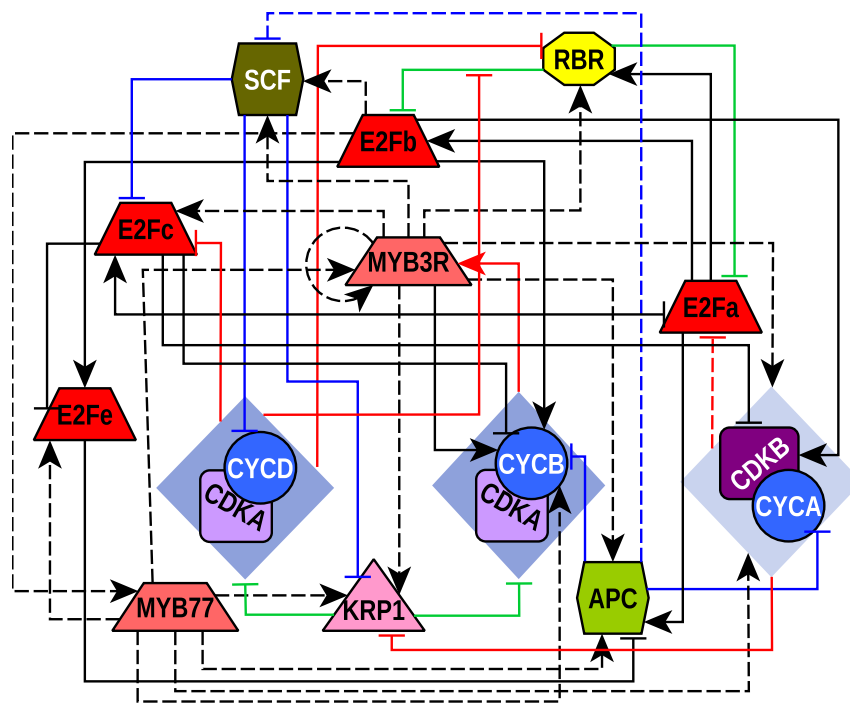
Fig. 2.2. Red de regulación del ciclo celular de *Arabidopsis*. Las líneas punteadas indican interacciones hipotéticas (Tabla 2.2), las líneas contínuas son interacciones demostradas (Tabla 2.1). Las interacciones negras son regulación transcripcional, las líneas verdes son interacciones físicas, las rojas son fosforilación y las azules ubiquitinación. Los complejos CDK-ciclina se representan por rombos, cuando una interacción llega al rombo es porque afecta tanto a la cinasa como a la ciclina. Los nodos rojos son FTs, los verdes son ligasas de ubiquitina E3, los azules son ciclinas, los lilas son cinasas y las proteínas que interactúan físicamente con otras son la amarilla y la rosa. Imagen tomada del artículo [169].

AACGG [179]. Esos motivos se buscaron en las secuencias regulatorias de todos los nodos de la red usando la herramienta Pathmatch[1] de TAIR. Usamos los dataset TAIR10 Loci Upstream Sequences-1000bp y TAIR10 5'UTRs como secuencias regulatorias.

2.1.5 Software para el análisis de robustez y simulación de mutantes

Para simular la dinámica de la red de regulación del CC y realizar los análisis de mutantes y de robustez usamos BoolNet[2] [198] y Atalia[3]. Para los análisis de robustez, las alteraciones sistemáticas en las funciones Booleanas se hicieron con Atalia, mientras que las perturbaciones estocásticas en redes aleatorias para evaluar la robustez del atractor se hicieron con BoolNet.

---

[1]http://arabidopsis.org/cgi-bin/patmatch/nph-patmatch.pl

[2]Librería del lenguaje R [197]

[3]Á. Chaos; http://web.ecologia.unam.mx/achaos/Atalia/atalia.htm

Aplicamos el método "bitflip" en las perturbaciones aleatorias hechas en las transiciones entre configuraciones de red o en las funciones Booleanas. Validamos el modelo simulando las mutaciones de pérdida y de ganancia de función con BoolNet, excluyendo su regla lógica y asignando el valor de "0" y "1", respectivamente.

2.1.6 Modelo Continuo

Para descartar posibles artefactos del modelo Booleano, debido a la naturaleza discreta y de su esquema de actualización sincrónico, comparamos los resultados del modelo Booleano con los resultados de su aproximación contínua. La versión continua del modelo la obtuvimos aplicando la metodología [199, 200] a la versión Booleana. En la versión contínua del modelo, el valor que toma cada nodo es su tasa de cambio representada por la siguiente ecuación diferencial:

$$\frac{dx_i}{dt} = \frac{-e^{0.5h_i} + e^{-h_i*(\omega_i)}}{(1 - e^{0.5h_i}) * (1 + e^{-h_i*(\omega_i - 0.5)})} - \gamma_i x_i$$

$$h_i \in \{1, 2, 5, 10, 15, 25, 35, 50, 75, 100\} \quad \text{y} \quad \gamma_i \in \{1, 1.1, 1.2, 1.3, 1.4, 1.5, 1.6, 1.7, 1.8, 2\}$$

El primer término corresponde a la tasa de producción y el segundo a la de decaimiento. ω_i es la forma continua de la tabla de verdad que se obtiene con lógica difusa:

$$
\begin{aligned}
x_i(t) \wedge x_j(t) &\mapsto \min(x_i(t), x_j(t)) \\
x_i(t) \vee x_j(t) &\mapsto \max(x_i(t), x_j(t)) \\
\neg x_i(t) &\mapsto 1 - x_i(t)
\end{aligned}
$$

h es el parámetro que indica qué tan parecida será la activación de un nodo a una función escalón; para $h = 1$ la activación será una línea recta con pendiente $=1$, y para h cercana a 100 o mayor, la curva se asemeja a una función escalón. γ_i es la tasa de decaimiento de cada nodo [199, 201]. El modelo continuo se evaluó inicialmente con valores por defecto para $h_i = 15$ y para $\gamma_i = 1$, y después probamos 10 valores diferentes para el parámetro h_i y 10 más para γ_i, para descartar que el comportamiento oscilatorio fuera dependiente de los parámetros. Mientras se evaluaba una h_i, se asignaban los valores por defecto al resto de los parámetros h y a las γ_i. A la inversa, cuando se evaluaba una γ_i, el resto de parámetros γ y las h_i tomaban los valores por defecto. De esta forma, probamos 28 parámetros, 2 por nodo, con 10 valores posibles. Siempre usamos la configuración de la fase G1 temprana como condición inicial (CYCD3;1=0, SCF=0, RBR=1, E2Fa=0, E2Fb=0, E2Fc=1, E2Fe=0, MYB77=0, MYB3R1/4=1, CYCB1;1=0, CDKB1;1=1, CYCA2;3=0, KRP1=0, APC/C=1).

2.2 Resultados

En el modelo propuesto integramos y sintetizamos datos publicados de las interacciones del CC de *Arabidopsis*, y algunos datos de otros organismos (mamíferos y levaduras) que proponemos como predicciones de la regulación en *Arabidopsis*. El conjunto completo de interacciones y nodos incluidos en el modelo se muestran en la Fig. 2.2. Se distinguen cuatro tipos de interacciones: (i) regulación transcriptional, (ii) ubiquitinación, (iii) fosforilación y (iv) interacciones físicas proteína-proteína. Adicionalmente, se llevó a cabo un análisis *in silico* de los FTs y promotores para sustentar 15 interacciones de la red (estas fueron: MYB77$\rightarrow$ E2Fe, MYB3R1/4, KRP1, CYCB1;1, CYCA2;3, CDKB1;1 y CCS52A2; MYB3R1/4 $\rightarrow$ SCF, RBR, CDKB1;1, CYCA2;3, APC/C, KRP1, E2Fc y MYB3R1/4).

2.2.1 El modelo propuesto recupera la dinámica de la regulación del ciclo celular de *Arabidopsis*

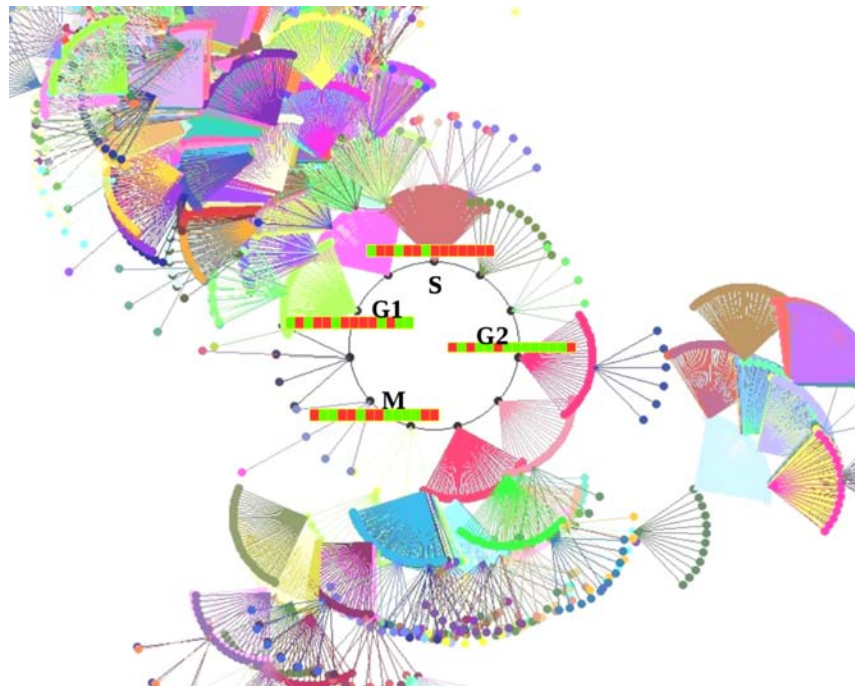**Fig. 2.3. Todas las configuraciones de red posibles convergen a un único atractor cíclico (acercamiento).** Cada punto representa una de las 2^{14} posibles configuraciones de red, y la línea indica la configuración a la que llega. En el centro se encuentra el atractor cíclico de 11 configuraciones (periodo 11).

Nuestros resultados muestran que los nodos considerados son necesarios y suficientes para

recuperar un único estado estacionario cíclico (Fig. 2.3), y así, el comportamiento cíclico robusto de los componentes considerados. Tal comportamiento es muy parecido a los patrones periódicos de las configuraciones de red observados durante la progresión real del CC (Fig. 2.4). Es importante aclarar que el atractor cíclico sólo indica la secuencia de cambios que ocurren durante el CC, pero no hay forma de conocer la duración real o relativa de un evento; por ejemplo no podemos saber el tiempo que pasa una célula en una fase a partir del número de configuraciones que la caracterizan.

Las primeras dos columnas del atractor o configuraciones de red de la Fig. 2.4, corresponden al estado G1, dado que durante la fase G1 temprana, el complejo CDKA;1-CYCD3;1 está ausente o inactivo por la presencia del KRP1 [54, 136, 174]. Como señalamos en los supuestos del modelo (Sección 2.1.2), el estado de CDKA;1-CYCD3;1 está dado solo por la presencia de CYCD3;1. Para facilitar la comprensión, se muestra el complejo CDKA;1-CYCD3;1 en lugar de solo CYCD3;1. La ausencia de ciclinas mitóticas (CYCA2;3 y CYCB1;1) en esta fase [47, 66], así como la presencia del APC/C hasta la fase G1 temprana, también coinciden con las observaciones experimentales [95, 178]. La presencia de la proteína RBR en la fase G1 implica que los E2F están transcripcionalmente inactivos, como se esperaría [60–62]. La tercer columna se asemeja a la transición G1/S, ya que la presencia del complejo CDKA;1-CYCD3;1 induciría la fosforilación de RBR y su inactivación [36]. En la cuarta configuración, la fase S está representada por la inactivación de RBR y la activación transcripcional de E2Fa/b [202]. En la quinta y la sexta configuración, E2Fc regresa al estado "presente" pero el estado de RBR se mantiene "ausente", lo cual indica que la transcripción dirigida por E2Fa/b aún puede estar ocurriendo. De hecho, el factor E2Fb aparece desde la quinta configuración y esto es consistente con su función de regulador de la expresión de los genes responsables de la transición G2/M. En la sexta configuración MYB77 está presente, aunque en experimentos de sincronización de células se ha observado que se transcribe desde el inicio de la mitosis [188]. Durante la fase G2 se expresan los FTs MYB y KRP1 [64, 136, 188], estos últimos mantendrían inactivos a los dímeros formados por CDKA;1 y las ciclinas mitóticas; en conjunto, estos datos son consistentes con lo que se observa en la séptima configuración del atractor del CC. En la octava columna, se pierde KRP1 porque CDKB1;1-CYCA2;3 lo fosforila, este heterodímero está activo en la transición G2/M y el inicio de la mitosis [93] La fosforilación de KRP1 lo lleva a su degradación y posterior activación de los complejos mitóticos tales como CDKA;1-CYCB1;1 que inician la mitosis [89, 181] (configuración 9 y 10 en la Fig. 2.4). La falta del APC/C al inicio de la mitosis es determinante para la acumulación de las ciclinas mitóticas, pero la presencia de este complejo es necesaria para la salida de la mitosis [203], la cual ocurre en la undécima configuración del atractor (Fig. 2.4). Así, nuestro modelo de regulación del CC recupera un único atractor cíclico de once configuraciones de red,

lo cual demuestra que el comportamiento cíclico de sus componentes es congruente con lo que se observa experimentalmente. Este resultado valida que el conjunto de restricciones propuestas convergen a un comportamiento cíclico que es independiente de las condiciones iniciales.
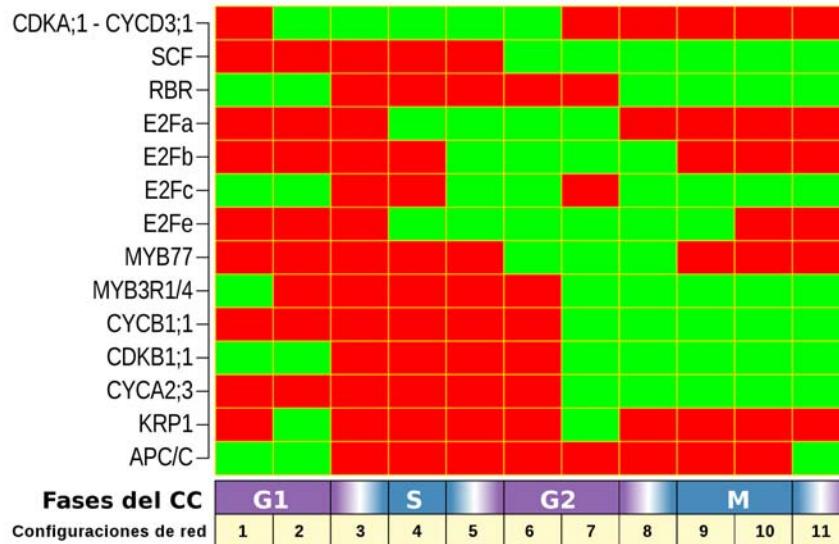
Fig. 2.4. Atractor del modelo de la regulación del ciclo celular de *Arabidopsis*. Las filas indican el cambio en el estado (presente/ausente) de los reguladores del CC. La presencia de los nodos está indicada en verde y la ausencia en rojo. Las columnas corresponden a la configuración de la red en cada fase o transición del CC, indicado con la barra horizontal inferior. Figura tomada del artículo [169].

2.2.2 Las mutantes de pérdida y de ganancia de función recuperan los patrones observados de un ciclo celular normal y del endociclo

Una validación adicional del modelo del CC de *Arabidopsis* implica simular mutaciones de pérdida y ganancia de función, y comparar los atractores recuperados con los perfiles de expresión documentados experimentalmente para cada mutante probada. Simulamos los mutantes fijando el nodo correspondiente en 0 para la pérdida de función, o en 1 para la ganancia. Los atractores de los mutantes simulados son coherentes con los datos experimentales en la mayoría de los casos. En la Tabla 2.3 se muestra una síntesis de los resultados de estas simulaciones, y en la Fig. 2.5 mostramos ejemplos de los atractores que recuperan los fenotipos esperados (indicados con **A** en la Tabla 2.3). Varios de estos atractores como la pérdida de función de la CDK de tipo B (Fig. 2.5 J), la ganancia de función de APC/C (Fig. 2.5 N) o el atractor con 8 configuraciones de la ganancia de función de E2Fa (Fig. 2.5 C), convergen a un atractor cíclico que corresponde a la configuración observada durante un ciclo de endorreduplicación.

Tabla 2.3. Resumen de los resultados de los análisis de mutaciones en los componentes de la red de regulación del CC

Nodo	+	Resultado de la ganancia de función	-	Resultado de la pérdida de función
CYCD3;1	PA	En las plantas con la pérdida de función de esta ciclina se inhibe la salida del CC, incrementa el tamaño de las zonas de división y las divisiones ectópicas. La duración de la fase G1 es menor y la de la G2 es mayor. Retraso en la expresión de los genes de la transición G2/M [55,174]. El atractor que se obtuvo con la simulación de esta mutante fue la fase G2 en punto fijo.	A	Cuando esta ciclina se elimina por la falta de sacarosa, las células se detienen en la fase G1; en hojas adultas, la triple mutante *cycd3;1-3* provoca la disminución del número de células [54, 204]. El atractor obtenido oscila entre la fase G1 y la transición G1/S.
SCF	NR	La ganancia de función de SKP2A estimula la proliferación celular, incrementa el número de células en G2/M y disminuye la ploidía [140, 205]. El modelo no recupera este fenotipo ya que éste oscila entre la fase G1 y S.	A	Las plantas con un nivel reducido de SKP2 no muestra un desarrollo afectado pero se acumula KRP1 [136].
RBR	A	En las células en donde RBR no es funcional el CC se detiene; en las células del meristemo de la raíz se pierde la expresión de CYCB1;1. En arroz decrementa el número de células que están sintetizando ADN [24, 172]. El atractor obtenido caracteriza la fase G1.	A	La proliferación se favorece y la diferenciación celular se afecta [166]; con la disminución de esta proteína en arroz se favorece el incremento de células que se encuentran en fase S [24].
E2Fa	A	La mitosis y la endorreduplicación se ven favorecidas [61,202]. Se obtuvieron dos atractores, uno de ellos, con el 40.48% de las condiciones iniciales, es el CC normal; el otro, con 59.52% de las condiciones iniciales, es similar a un endociclo pero la actividad del APC/C es menor.	PA	La expresión de E2Fb, RBR y otros reguladores del CC disminuye; hay más células en G1 y G2 con respecto a las plantas silvestres [94]. Se obtuvo un atractor de punto fijo que tiene E2Fe y CYCD3;1, sugiriendo que el CC se detiene en alguna fase G.
E2Fb	A	La alteración de este FT induce división celular y reduce endorreduplicación; la duración del CC y el tamaño de las células es menor; incrementa la cantidad de transcritos de fase S [2,117].	-	No hay información sobre el efecto de esta alteración en el CC. El atractor obtenido fue de punto fijo representando la transición G1/S.
E2Fc	PA	La sobre-expresión de una forma no degradable de E2Fc produce células más grandes o la falta de división. El atractor obtenido fue de punto fijo, congruente con un paro del CC donde solo E2Fc y CYCD3;1 estan presentes [69].	PA	Incrementa la expresión de proteínas mitóticas como CYCB1;1, la ploidía está reducida [176, 177]. El atractor obtenido caracteriza una detención en fase M.
E2Fe	PA	Esta alteración reduce los niveles de ploidía [178]. El CC se detiene en la fase M.	A	Aumenta la endorreduplicación [178].
MYB77	-	Las plantas son más cortas pero no se revisa el comportamiento del CC [196]. El atractor fue de punto fijo y corresponde a un CC detenido en un estado mitótico	-	No se caracterizó el comportamiento del CC de la mutante de MYB77 [196]. El atractor corresponde a un CC de 7 configuraciones.
MYB3R1/4	-	No hay datos disponibles acerca de las alteraciones en la división celular. Se obtuvieron dos atractores de punto fijo de paros del CC en la fase G1 temprana, la diferencia entre ellos fue el estado de E2Fa.	A	En el fondo mutante de MYB3R1/4 disminuyen los transcritos de los genes involucrados en la transición G2/M, la división celular no se completa [179]. Se obtuvo un atractor que parece tener comportamiento similar a un endociclo, y otro atractor con las configuraciones y transiciones del CC, solo que APC/C siempre está ausente.
CYCB1;1	A	Se acelera el crecimiento de la raíz y las células son ligeramente más pequeñas [101]. Se recuperó atractor representando al CC normal.	-	La ausencia de esta ciclina está asociada a la diferenciación [206]. El atractor parece corresponder a un endociclo aunque el APC/C nunca está presente.
CDKB1;1	A	No parece afectar el comportamiento del CC [207], el atractor que se obtuvo es un CC normal.	A	La sobre-expresión de un alelo negativo dominante favorece la endorreduplicación [68].
CYCA2;3	A	Esta alteración no es suficiente para producir tricomas multicelulares pero la proporción de células poliploides es menor [92].	PA	En mutantes nula de esta ciclina, la endorreduplicación se ve favorecida, los endociclos comienzan antes y son más rápidos que en las plantas silvestres [92].
KRP1	PA	Detención del CC e inhibición de la proliferación, la fase G2 es más larga; la sobre-expresión débil de KRP2 produce incremento en la ploidía [3, 89, 137]. El atractor oscila entre la fase G1 y la transición G1/S.	A	No hay efectos fenotípicos evidentes pero incrementa la actividad de la cinasa con respecto al silvestre [208].
APC/C	A	La ganancia de función de la subunidad del APC/C CCS52A2 favorece la entrada a la endorreduplicación; aumenta el número de células con mayor ploidía [178].	PA	La pérdida de función de la subunidad CCS52A2 de este complejo hay menos células meristemáticas en la raíz pero no se afecta el índice de endorreduplicación; las células de CQ se vuelven mitóticamente activas [95]. El atractor recuperado es de punto fijo, el CC se detiene previo a la salida de la mitosis.

Resumen de los fenotipos mutantes recuperados. **A** indica que el resultado es acorde con los datos disponibles, **PA** significa parcialmente de acuerdo con los datos experimentales, el resultado no fue completamente coherente con los datos experimentales. **NR** quiere decir que el fenotipo mutante no se recuperó en la simulación.

En tales atractores, los inductores de endorreduplicación, como APC/C, KRP1 y E2Fc [177, 181, 209] están presentes, al menos en algunas configuraciones de la red. Otra característica notable de estos atractores mutantes es que, aunque los complejos CDK-ciclina mitóticos podrían estar presentes, están inhibidos por KRP1, por lo tanto no hay ningún complejo CDK-ciclina activo que desencadene el inicio de la mitosis. Estos datos coinciden con la regulación reportada durante el inicio de la endorreduplicación [89]. En el atractor donde E2Fa coincide con estados alternantes de RBR, sugiere que la endorreduplicación podría ocurrir, debido a que el ciclo oscilaría en la fase S (atractor de 3 estados de la Fig. 2.5 D y H). Probablemente debido a la redundancia en las plantas, algunas mutaciones no tienen un fenotipo afectado obvio. Ese es el caso de la pérdida de función de KRP1, en el cual se recupera un atractor idéntico al original con la simulación (Fig. 2.5 M), como se esperaría, ya que tales mutantes no muestran un CC alterado evidente [136].

Es interesante que la simulación de un APC/C constitutivamente activo también converge a un único atractor cíclico, el cual corresponde a un ciclo de endorreduplicación, puesto que tiene fases G y S pero le falta una configuración de la fase M (Fig. 2.5 N). Esto coincide con la observación experimental de que la sobre-expresión de una de sus subunidades (CCS52A) promueve la entrada al endociclo [178]. Otro ejemplo notable es la mutación de la ganancia de función de E2Fa que produce dos atractores cíclicos, uno corresponde al CC normal y el otro al endociclo (Fig. 2.5 C). Ya se ha demostrado que este gen es necesario para ambos procesos [61] que aparentemente son excluyentes, puesto que en ambos procesos ocurre la replicación del ADN y entre los blancos del E2Fa hay genes necesarios para la fase S. Así, nuestro modelo sugiere que la regulación de E2Fa al final de la fase G2 es decisiva para la salida del CC y la transición a la endorreduplicación. En esta simulación de ganancia de función de E2Fa, encontramos una inconsistencia con APC/C porque se requiere esta ligasa de ubiquitina E3 para la endorreduplicación, mientras que en el atractor con 8 configuraciones de red sólo está presente en una de ellas. Tal comportamiento en este atractor de endorreduplicación lleva a una actividad inestable en el complejo CDK-ciclina, sugiriendo así que el incremento en el APC/C es necesario tanto al inicio de la endorreduplicación como en la progresión. En el atractor de la simulación de la ganancia de función del APC/C, el estado de los nodos CYCD3;1, SCF, y E2Fa es consistente durante todo el ciclo, a diferencia de los atractores de endorreduplicación de la pérdida de función de CDKB1;1 o ganancia de función de E2Fa (8 configuraciones), donde la presencia de CYCD3;1, SCF, E2Fb, E2Fc y los factores MYB alterna entre "presente" y "ausente". Es interesante que E2Fa en los 3 atractores de endorreduplicación está constitutivamente presente.

Consideramos que la simulación de la ganacia de función del APC/C proporciona un posible mecanismo de la acción de las hormonas vegetales sobre la maquinaria molecular del CC y cómo
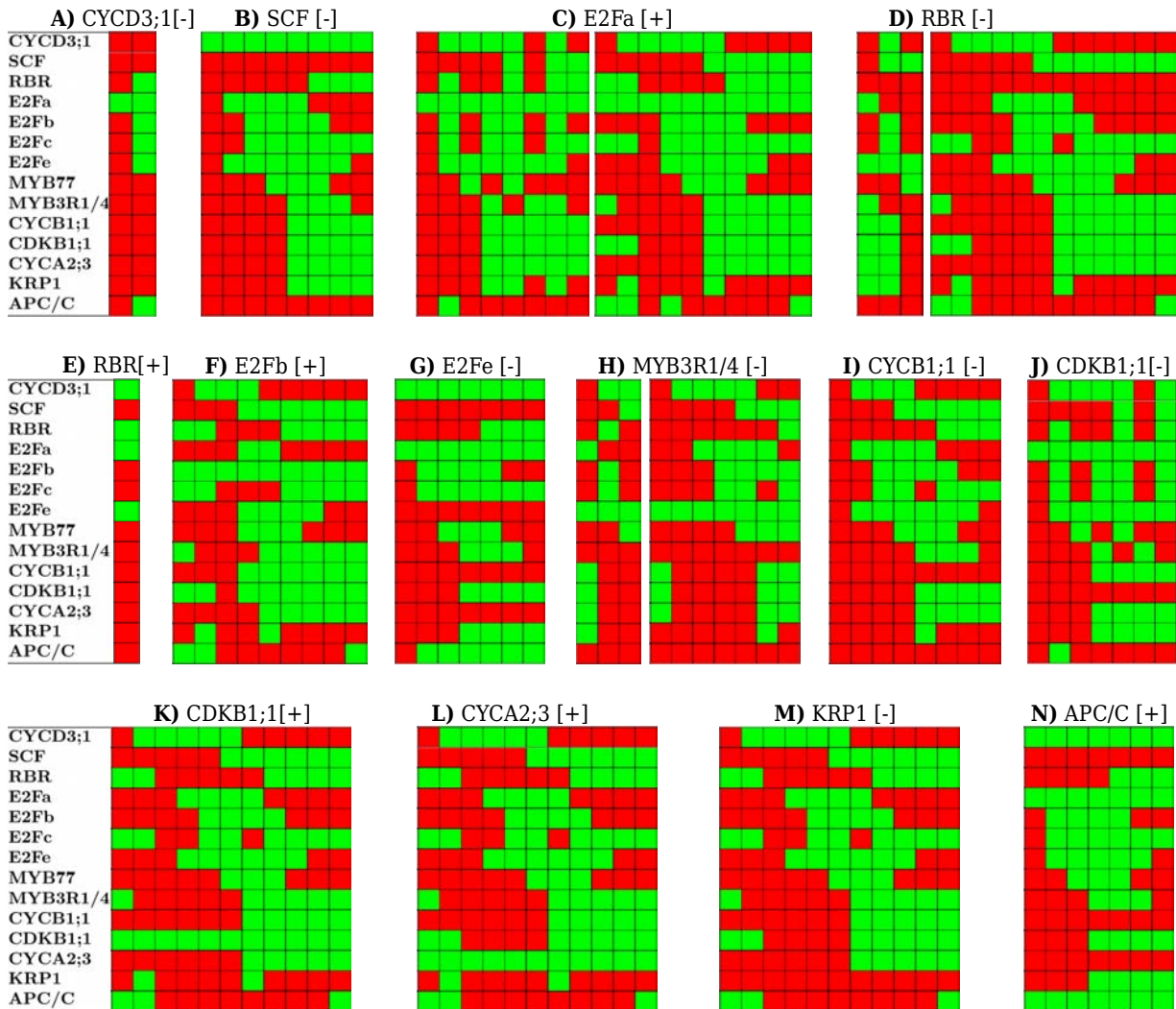
Fig. 2.5. Atractores obtenidos por el análisis de mutantes. Se muestran los atractores que recuperaron el comportamiento equivalente al fenotipo esperado. [-] significa pérdida de función y [+] es la ganancia. Los cuadros verdes indican que el componente molecular está presente, el rojo es de los que están ausentes. Para más detalles ver la Tabla 2.3.

tales morfógenos clave regulan patrones de proliferación celular. Recientemente, Takahashi y colaboradores reportaron una conexión directa entre citocininas y la maquinaria del CC en la raíz de *Arabidopsis* [210]. Los autores mostraron que en la transición a la zona de elongación, ARR2, un FT de la vía de señalización de las citocininas induce la expresión de la proteína CCS52A1, un activador del complejo APC/C. Nuestra simulación de ganancia de función del APC/C es congruente con esa observación, puesto que reproduce la configuración alcanzada por una célula que está entrando al endociclo cuando se promueve la actividad del APC/C,

de la misma forma como ocurre en la zona de elongación de la raíz de *Arabidopsis*. Por lo tanto, nuestro modelo es capaz de recuperar el atractor de los fenotipos mutantes de pérdida y de ganancia de función reportados experimentalmente, y de esta manera proporciona una explicación mecanicista de los patrones de expresión observados tanto en el CC normal como durante los ciclos de endorreduplicación o los endociclos.

2.2.3   El modelo Booleano del ciclo celular es robusto a perturbaciones aleatorias

Con la finalidad de proveer una validación más para la red regulatoria del CC propuesta, llevamos a cabo análisis de robustez del atractor ante tres tipos de alteraciones, en las funciones lógicas del modelo, en la transición entre configuraciones de red, o en redes aleatorias; estos análisis se encuentran resumidos en la Tabla 2.4. En plantas, el CC es bastante robusto a diversos tipos de perturbación; una manera de probar la red propuesta, es analizando qué tan robusto es el atractor cíclico recuperado. Primero, cambiamos cada uno de los bits de la salida de cada regla lógica (paso 2 de la Fig. 2.1), y obtuvimos los atractores a partir de esa nueva versión del modelo con la alteración. Encontramos que 87.47% de las redes perturbadas recuperaron el atractor original, mientras que 1.77% de las redes alteradas mantuvieron el atractor original y produjeron otros nuevos (descrito en el material Suplementario S3 del artículo [169]). En contraste, el 10.76% restante de las alteraciones redujo el número de configuraciones de la red del atractor original. En el segundo análisis de robustez, después de calcular la configuración de red a la que llega cada una de las posibles configuraciones iniciales (paso 3 de la Fig. 2.1), se elige aleatoriamente un bit (i.e. el estado de un nodo) de una configuración siguiente y se cambia su valor. Entonces, la red se reconstruye y de nuevo se obtienen sus atractores. Hicimos 100 perturbaciones y repetimos este procedimiento 100 veces, así encontramos que en 88.2±3.2 de las 100 perturbaciones (promedio ± desviación estándar) se vuelve a recuperar el atractor original. Estos resultados sugieren que la red de regulación propuesta para el CC de *Arabidopsis* es robusta ante alteraciones como se espera, y en concordancia como modelos previos de regulación propuestos para otros procesos del desarrollo [211, 212].

Para confirmar que la robustez recuperada en estos dos tipos de análisis es una propiedad específica de la red bajo estudio, llevamos a cabo análisis de robustez de redes generadas aleatoriamente y con estructura similar a la propuesta aquí para la regulación del CC de *Arabidopsis,* y comparamos los resultados del análisis de robustez de la red de *Arabidopsis* y los de esas redes aleatorias. Entonces, generamos 100 redes aleatorias, y 100 copias alteradas de cada red aleatoria y de la red original. En cada copia, se cambió aleatoriamente el valor de un bit en una regla lógica (para confirmar el primer análisis de robustez), o en una configuración de red siguiente (para el segundo análisis de robustez). Cuando se hicieron las perturbaciones en las

Tabla 2.4. Resumen de los análisis de robustez implementados para el modelo de la regulación del CC de *Arabidopsis*.

Análisis	Descripción	Resultado
1. Alteraciones en la salida de las reglas lógicas	Obtuvimos el atractor a partir de las tablas de verdad (construidas a partir de las reglas lógicas) con su salida alterada en un bit.	Se recupera el atractor de la red del CC en 87% de las redes con un cambio en sus tablas de verdad.
2. Cambios en la configuración de red a la que llega una configuración inicial	Obtuvimos el atractor a partir de una tabla de transiciones que tiene un cambio en el estado de un nodo de una siguiente configuración de red ($t + 1$).	En promedio, en 88.2% de las redes perturbadas se recupera el atractor de la red del CC.
3. Comparación de la red del CC con redes aleatorias	Se repite el análisis 1 y 2 para la red del CC y para 100 redes aleatorias con estructura similar a la del CC.	Cuando se repite: el análisis 1, el atractor original de la red del CC se recuperó en 68% de los casos, la mitad de las redes aleatorias recupera su atractor(es) original en 18.55% o menos de las modificaciones; el análisis 2, se recupera el atractor original en 88% de las perturbaciones de la red del CC, 50 de las redes aleatorias (la mitad) recuperan su atractor(es) original en 24.2% o menos de las alteraciones.

funciones lógicas, la red de regulación del CC de *Arabidopsis* recupera su atractor en 68% de las perturbaciones, mientras que la mediana de las copias alteradas que recupera el(los) atractor(es) original(es) de las redes aleatorias fue del 18.55% (promedio 19.12% $\pm$ 13.86 desviación estándar). La diferencia entre el 68% de este último análisis y el 87.47% del primer análisis de robustez se puede deber a un error de muestreo. Si se perturban las transiciones entre las configuraciones de red, la mediana de los atractores originales recuperados por las redes aleatorias fue de 24.2% (promedio 24.6%$\pm$18.2 desviación estándar) de las perturbaciones. En contraste, el atractor original de la red de regulación del CC de *Arabidopsis*, se encontró en 88% de las copias perturbadas que se obtuvieron a partir de la red sustentada en datos experimentales. Estos resultados confirman que la red de regulación propuesta aquí es mucho más robusta que redes con topología similar generadas aleatoriamente, y así sugiere que, además de la estructura, la dinámica también influye en la robustez.

2.2.4 Las oscilaciones se mantienen en la aproximación continua del modelo para diferentes valores de parámetros

Los modelos Booleanos pueden producir dinámicas cíclicas como un artefacto debido a su naturaleza discreta y tiempos de retardo implicados en su dinámica. Para abordar esta cuestión, aproximamos el modelo Booleano a un sistema continuo de ecuaciones diferenciales siguiendo [199, 200] y [213, 214]. Para recuperar los estados estacionarios de tal sistema continuo, la versión continua de la red de regulación se evaluó para 1000 condiciones iniciales diferentes elegidas aleatoriamente. En todos los casos e independientemente de la metodología (i.e. [199, 200]

o [213, 214]), recuperamos el atractor de ciclo límite. El atractor obtenido con la metodología implementada en Odefy se muestra en la Fig. 2.6. Una diferencia entre la metodología [199,200] y [213, 214], es que la primera produce una función que en ocasiones no es diferenciable y por lo tanto, en un futuro, no se podría analizar con métodos de ecuaciones diferenciales ordinarias [213]. En el modelo continuo, las ciclinas clave para las principales transiciones de fase, CYCD3;1 y CYCB1;1, tienen un comportamiento oscilatorio que no se atenúa con el tiempo. Variando γ_i, 13 de 140 modelos pierden las oscilaciones ($\gamma_{APC} = 2$, $\gamma_{CYCD3;1} = 2$, $\gamma_{E2Fa} \geq 1.4$, $\gamma_{E2Fb} = 2$, $\gamma_{E2Fc} \geq 1.4$, $\gamma_{MYB77} \geq 1.7$). Para los modelos donde variamos las h_i, solo 7 de 140 modelos perdieron las oscilaciones ($h_{E2Fc} = 1, 2$, $h_{KRP1} = 1, 2$, $h_{MYB3R1/4} = 1$, $h_{SCF} = 1, 2$). Hay una tendencia a perder las oscilaciones cuando las tasas de decaimiento son muy altas ($\gamma_i = 2$ o cercano a 2) y cuando el parametro h es muy pequeño ($h = 1, 2$). Es importante notar que el cíclo límite se recuperó en 92.86% de los casos, lo que sugiere que el comportamiento cíclico es robusto a cambios en los valores de los parámetros, en ese caso, de la tasas de decaimiento o del parámetro h (ver ejemplos en la Fig. 2.7).
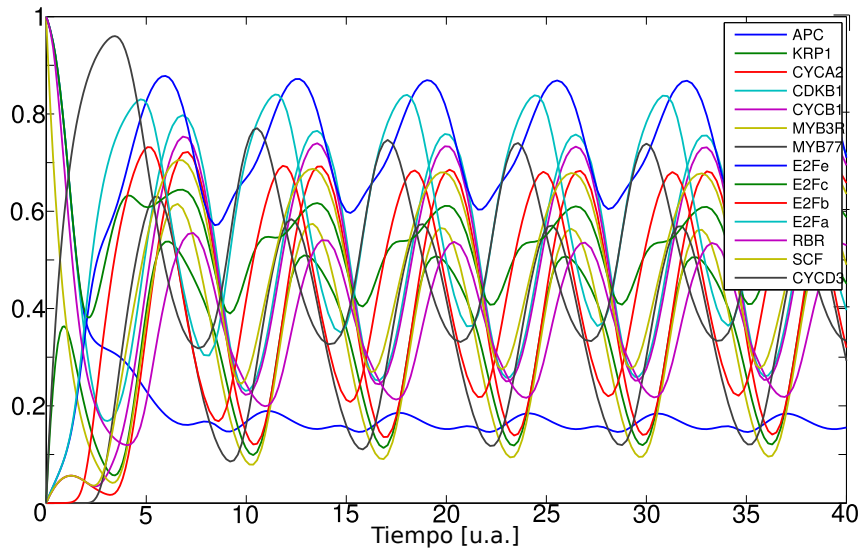
Fig. 2.6. Atractor cíclico obtenido con Odefy. Las oscilaciones del modelo continuo obtenido con la metodología [213] también se mantienen con el tiempo.

Los resultados del modelo continuo corroboran que el atractor del ciclo límite recuperado por la versión Booleana, no se debe a un artefacto asociado a la naturaleza discreta y sincrónica del modelo Booleano. Adicionalmente, recuperar el comportamiento cíclico del modelo continuo constituye una prueba de robustez adicional para el modelo Booleano. Con la finalidad de pulir los modelos del CC propuestos, trabajos previos han empleado esquemas de modelado con características diferentes al que hemos presentado, algunos por ejemplo, han utilizado actualización
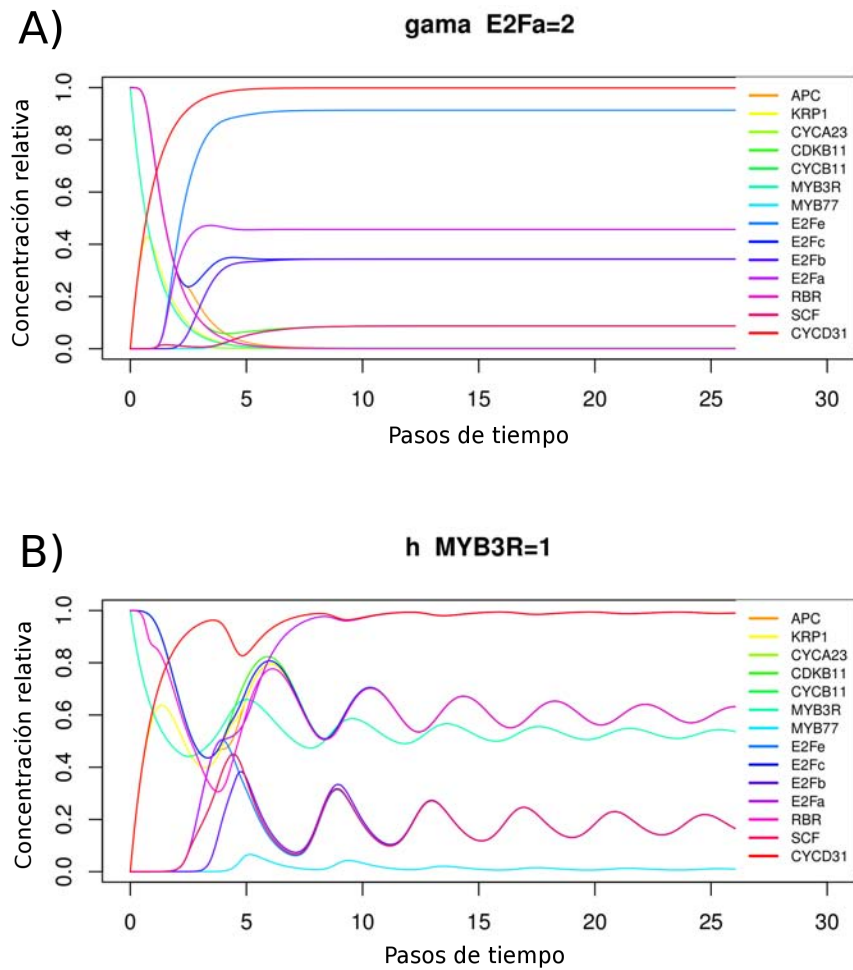
Fig. 2.7. Ejemplos de la pérdida de las oscilaciones del modelo continuo. A) Estado estacionario obtenido con valores para $\gamma_{E2Fa} \geq 1.4$. B) Las oscilaciones del atractor obtenido con $h_{MYB3R1/4} = 1$, se atenúan y desaparecen con el tiempo.

asíncrona con clases de prioridad que distinguen procesos rápidos y lentos [19]. Ese esquema de actualización en particular, se podría probar en nuestro modelo para refinar el atractor con un esquema plausible. En otros modelos también se han empleado tiempos de retardo en la actualización de los nodos, los cuales podrían estar involucrados en la progresión del CC pero no son suficientes para conferir propiedades como la irreversibilidad. La irreversibilidad o la progresión unidireccional del CC se ha propuesto como una consecuencia de la regulación a nivel de sistema [73, 163, 215], así que no dependerían de la herramienta empleada para su modelado; en este sentido hemos planteado la hipótesis de que las transiciones del CC de *Arabidopsis* son una propiedad emergente de la arquitectura de la red y de su dinámica.

Con esta versión continua del modelo evaluamos si la red de regulacion del CC recupera los

patrones de expresión periódica observados en experimentos de sincronización de los componentes moleculares del CC de *Arabidopsis*. A diferencia de otros nodos, el represor E2Fc y el KRP1 son reguladores que tienen dos lapsos cortos de expresión en el atractor recuperado en el modelo continuo, y experimentalmente ellos también mostraron dos picos de expresión cuando se sincronizaron con afidicolina[4] [189]. En tales experimentos de sincronización, la expresión de E2Fc incrementa desde finales de la fase S hasta como la mitad de la fase G2, pero después decrementa drásticamente al final de la fase G2. En el modelo, E2Fc aparece desde la fase S hasta la fase G2, y en seguida se observa un segundo incremento de la expresión de E2Fc en G2/M. La última correspondencia es otra validación del modelo de red de regulación que hemos propuesto. Adicionalmente, los experimentos de sincronización usando sacarosa han mostrado que KRP1 se expresa previo a la transición G1/S y antes de la mitosis [216], de forma similar a lo que ocurre en el modelo. Recientemente se ha propuesto que KRP1 tiene un papel durante las transiciones G1/S y G2/M [136]; lo último sería importante para el control de la endorreduplicación [181]. Una vez más, estos papeles y estos perfiles de expresión son consistentes con el estado de actividad de KRP1 recuperado en nuestro modelo.

En contraste con el comportamiento consistente de E2Fc y KRP1 recuperados en el modelo, los resultados de E2Fe no coinciden con las observaciones previas. En nuestro modelo este factor E2F presenta sólo un pico desde la fase S a la fase M temprana, pero de acuerdo con los experimentos de sincronización [171], E2Fe también tiene dos picos de expresión. Uno de sus picos se debe a la regulación por otros factores de la familia E2F durante la fase S, mientras que el pico G2/M podría deberse a elementos MSA. De hecho, cuando los motivos regulatorios reconocidos por los E2F se eliminan de E2Fe, todavía se puede expresar aunque a niveles bajos [96], sugiriendo que hay FTs adicionales regulando su expresión. Tales factores podrían pertenecer a la familia MYB, así como sugiere la red de regulación del CC propuesta aquí.

2.3 Discusión

El comportamiento cíclico canónico de las células eucariotas, desde la replicación del ADN hasta la citocinesis, sugiere la existencia de un mecanismo conservado que comparte componentes moleculares y/o una lógica de regulación entre todos los organismos eucariotas. Mientras que el CC de levaduras y animales ha sido ampliamente estudiado y modelado, el CC de plantas aún no tiene un modelo integrativo que compile la información relevante. En este estudio proponemos un modelo Booleano de la red de regulación del CC de *Arabidopsis*, y demostramos que

---

[4]Inhibidor reversible de la ADN polimerasa. Sin esta polimerasa no podría llevarse a cabo la replicación del ADN, y el CC quedaría detenido en fase S.

este modelo recupera un único atractor cíclico o estado estacionario con 11 configuraciones para los estados de activación de los componentes de la red. Tales configuraciones corresponden a aquéllas observadas experimentalmente para los componentes del CC incluidas aquí para cada fase del CC. Además, el orden temporal de las transiciones secuenciales que se recupera por el modelo propuesto también imita el patrón temporal observado de transiciones entre configuraciones a lo largo del CC de los eucariontes. El hecho de que las 16,384 condiciones iniciales del sistema propuesto converjan a este único atractor cíclico ya sugiere que la red conforma un módulo robusto a perturbaciones transitorias o condiciones iniciales. Esto sugiere que la red propuesta integra el conjunto de componentes moleculares necesarios y suficientes, así como sus interacciones, para recuperar las oscilaciones de las configuraciones de estados de activación de los componentes fundamentales durante el CC observadas experimentalmente. El modelo de red de regulación también es robusto a alteraciones genéticas, al igual que otros modelos publicados previamente para otros módulos de diferenciación celular o del desarrollo [211, 212, 217]. Más aún, los resultados del modelo se validaron recuperando configuraciones alteradas (de ganancia y de pérdida de función) del CC equivalentes al fenotipo de las mutaciones en la planta.

Con el modelo planteamos algunas hipótesis sustentadas en observaciones de otros organismos, y que hasta ahora no se han probado en plantas. También integramos las interacciones regulatorias entre KRP1, la CDK de tipo B específica de plantas y los FTs MYB para inferir la regulación alternativa de la transición G2/M en *Arabidopsis*. Además de recuperar el comportamiento observado para los componentes incluídos, para el caso de este sistema vegetal, se propone una lógica de regulación transcripcional a partir de la cual, emerge el comportamiento cíclico durante las transiciones celulares. Esto no se había propuesto en modelos previos del CC que fundamentalmente se enfocan en describir dicho comportamiento cíclico, más que entender los mecanismos sistémicos subyacentes a su emergencia.

En el modelo presentado aquí incluimos solamente componentes moleculares y evitamos usar asas de autodegradación artificial, las cuales se han usado por otros modelos para recuperar los atractores de ciclo límite. En el modelo que hemos propuesto, evitamos también la redundancia, aunque esta puede ser importante para la robustez del sistema. Por ejemplo, el nodo KRP1 representa a los miembros de la familia KRP que comparten varias de sus funciones. También la transición metafase-anafase se podría incluir en el modelo cuando haya más información acerca de la regulación del APC/C en plantas (e.g. de la asa de retroalimentación negativa que comprende a los complejos CDK-ciclina, o de la regulación de los homólogos de Cdc20). En nuestro modelo evitamos usar nodos que indiquen eventos del CC como la replicación del DNA, el inicio de la mitosis y el término de la división celular. En otros modelos se han ocupado esos

nodos para dirigir el orden en que ocurren las transiciones de fase en lugar de las interacciones moleculares entre las proteínas involucradas [155].

Algunas ciclinas tales como CYCD3;1 y CYCB1;1, componentes importantes para las transiciones G1/S y G2/M, muestran regulación mutuamente exclusiva, tal como ocurre en un sistema dinámico de depredador-presa Lotka-Volterra [218], incluso aunque ellas no interactúan directamente. Su exclusión mutua se logra gracias a la expresión genética coordinada con la degradación proteolítica específica: la regulación genética controlada por los FTs E2F-RBR en la fase S y los MYB en la entrada de la mitosis, y además la degradación específica de proteínas a cargo de las ligasas de ubiquitina E3 SCF y APC/C, actuando en la transición G1/S, y durante la salida de la mitosis, respectivamente.

Dos posibilidades alternativas podrían dirigir la progresión del CC en organismos actuales. La primera implicaría que las transiciones de un estado del CC al siguiente requeriría de señales externas, como el tamaño de la célula, por ejemplo. La posibilidad alternativa es que la progresión del CC y el patrón temporal de transiciones entre fases sea una consecuencia emergente de una red de regulación, y que no requiere señales externas, o que éstas solo refuerzan tal progresión temporal emergente de las interacciones regulatorias. Nuestro modelo de la red de regulación soporta la última posibilidad aunque las dos posibilidades no son excluyentes, sino que probablemente se complementan o promueven mutuamente. En la sección 1.8 se describe brevemente las señales fisiológicas y ambientales que intervienen en la progresión del CC y que podrían ser incluidas en el modelo como moduladores. Además de estas señales, fluctuaciones en algunos procesos moleculares asociados con concentraciones de componentes intracelulares (e.g. expresión genética o síntesis de proteínas), también pueden jugar un papel importante en la emergencia del patrón cíclico observado.

Otra diferencia con respecto a otros modelos del CC, es que el modelo del CC de *Arabidopsis* no incluye el tamaño de la célula, esto debido a que aún no hay un consenso sobre la relevancia del tamaño celular vegetal para la progresión del CC. En el meristemo de la raíz, por ejemplo, podría no haber un requerimiento absoluto para el tamaño, dado que las células en diferentes tejidos se dividen a muy diferentes tamaños promedio. Pero también es posible que el tamaño de las células tenga un papel regulando el CC. Por ejemplo, como las células raramente se dividen exactamente a la mitad, la mitosis de la célula más pequeña se retrasaría hasta llegar al tamaño promedio [110]. El crecimiento simplástico de la punta de la raíz, implicaría que la expansión de una célula mitótica debe continuar ininterrumpidamente, dirigida por el crecimiento de sus vecinas, mientras que en células en cultivo o células únicas, podrían crecer solo durante la interfase, y dejarían de expandirse cuando entran a la mitosis [110]. Es posible que en la raíz, el tamaño celular juegue un papel distinto al de las células en cultivo.

2.3.1 Predicciones novedosas para la regulación del ciclo celular de *Arabidopsis*

El modelo de red de regulación propuesto sugiere algunas predicciones con respecto a la regulación de ciertos componentes del CC de *Arabidopsis*. Tales predicciones se pueden clasificar en dos tipos. El primero pertenece a aquellas recuperadas por el análisis *in silico* de regiones promotoras. El segundo tipo se infirió de datos de otros eucariontes porque no se han observado en *Arabidopsis*, pero hay evidencias que sugieren que esas interacciones también son parte de la red de regulación de CC de esta planta. En el modelo hay tres interacciones que pertenecen al segundo tipo, E2Fb→SCF, CDKB1;1-CYCA2;3⊣E2Fa y APC/C⊣SCF. Aunque algunas observaciones previas soportan la idea de que esas interacciones podrían existir en *Arabidopsis*, faltaría examinarlas experimentalmente.

Adicionalmente, nuestro modelo provee una explicación dinámica del comportamiento cíclico de ciertos FTs y predice una interacción novedosa para los reguladores E2F y MYB en *Arabidopsis*; estos FTs conectan perfiles de expresión periódica que parecen ser clave para la emergencia del atractor de ciclo límite robusto que caracteriza el comportamiento del CC. Por la conexión directa que hay entre los FTs que regulan las transiciones en mamíferos y levaduras [30, 45], consideramos la posibilidad de que los MYB3R estuvieran directamente regulados por los E2Fs en *Arabidopsis*, pero ese no fue el caso y fue necesario incluir a MYB77. La interacción regulatoria entre los factores E2F y MYB (o entre sus reguladores equivalentes) podría estar conservada entre otros eucariotas (e.g. mamíferos y levaduras), pero no hay evidencia experimental que de soporte a eso en *Arabidopsis*. Después de buscar la misma evidencia directa en *Arabidopsis* y no encontrarla, consideramos un mecanismo regulatorio alternativo que consiste en FTs actuando entre E2F y MYB. Por lo tanto, decidimos analizar familias de FTs importantes para la regulación del CC, y conocidos hasta ahora, para averiguar si uno de sus miembros podrían estar mediando la regulación entre E2F y MYB. Se eligieron las familias TCP (Teosinte branched 1, Cycloidea, PCF) y MYB porque se ha reportado que están involucradas en la regulación del CC [56]. Con base en sus patrones de expresión genética y el análisis de secuencias promotoras, MYB77 fue nuestro mejor candidato: se expresa al inicio de la fase M, y podría ser regulado por E2F y también ser regulador de MYB (ver Tabla 2.2). Una segunda posibilidad podría ser que varios FTs específicos de tejidos estén involucrados en la regulación genética entre E2F y MYB (e.g. GL3, MYB88, SHR/SCR [65], MYB59 [219], incluso podrían estar involucrados miembros de la familia de genes MADS box). De hecho, recientemente documentaron en el laboratorio de Genética Molecular, Epigenética, Desarrollo y Evolución de Plantas (Instituto de Ecología, UNAM) que *XAL1*, un gen MADS-box, codifica para un FT que regula varios componentes del CC (García-Cruz et al., en preparación).

La red de regulación del CC de *Arabidopsis* no recuperó un atractor alternativo que corresponda al endociclo. Tenemos la hipótesis de que la misma red de regulación multiestable subyace ambos estados, y que componentes adicionales que se conecten a la red de regulación del CC tendrían que ser postulados para recuperar un segundo atractor cíclico más corto correspondiente al endociclo. En su forma actual, nuestro modelo sugiere que la función de CYCD3;1, la cual se ha asociado con el estado proliferativo [174] y con un retardo en el inicio del endociclo [204], es crítico para entrar al endociclo. Durante el CC, CYCD3;1 participa en la transición G1/S [55] y regula a la proteína RBR en la replicación del ADN [27], por lo que tendría sentido que el atractor de endorreduplicación obtenido en algunas de las simulaciones de mutantes apoye el papel de CYCD3;1 en la entrada al endociclo.

Previo a la división celular, la célula monitorea sus condiciones intracelulares y ambientales para arrestar o promover el progreso del CC. Tales señales afectan directamente a la maquinaria del CC, la cual no depende de un regulador maestro o central. El control del CC es el resultado de una red formada por asas de retroalimentación y de alimentación hacia adelante entre complejos de CDK-ciclinas y sus reguladores directos. No es intuitivo cómo procesos dinámicos complejos, como la progresión del CC, emergen de simples interacciones entre componentes actuando simultáneamente. La red de regulación del CC propuesta será útil para el estudio de cómo las decisiones de proliferación/diferenciación y su balance mantienen un control adecuado espacio-temporal del CC, durante el crecimiento y desarrollo vegetal, y posiblemente también contribuya a identificar interacciones fisiológicas o del desarrollo involucradas en la estrecha relación entre proliferación y diferenciación [1, 3, 95, 172, 174].

3

CONTRIBUCIÓN DEL MODELO DEL CICLO CELULAR EN *Arabidopsis*

Un aspecto distintivo de los seres vivos es la complejidad biológica que se manifiesta en cada uno de sus niveles de organización. Con frecuencia distinguimos y separamos variables para estudiar un sistema biológico, es decir, seguimos un enfoque analítico. En la medida de lo posible, se mantiene el entorno constante con el fin de garantizar la reproducibilidad de los resultados. En respuesta a este enfoque, surge el marco de pensamiento sistémico señalando que el organismo como un todo es más que la suma de sus partes (investigadas aisladamente), que no puede ser explicado por un enfoque puramente analítico, y que los elementos que lo constituyen interactúan dinámicamente. Además sostienen la existencia de una jerarquía de diversos niveles de complejidad y organización, los cuales cuentan con propiedades emergentes que no existen en un nivel inferior [220].

El pensamiento sistémico propone una forma diferente de estudiar sistemas biológicos, la cual, además, resulta complementaria a la metodología analítica. En este sentido, toda conclusión debe retomar las relaciones entre los componentes analizados, y tomar en cuenta las condiciones constantes bajo las cuales se realizaron los experimentos, puesto que la realidad es que los sistemas biógicos no se encuentran aislados ni en ambientes constantes. A diferencia de un modelo fenomenológico, los modelos dinámicos y sistémicos complementan los estudios experimentales y son un medio para identificar los mecanismos que llevan a la emergencia de nuevas propiedades y que no se descubrirían fácilmente solo con experimentos.

Los modelos del CC propuestos en otros organismos sugieren que la progresión unidireccional del CC, se logra a partir de módulos biestables que inducen irreversibilidad a nivel de sistema [163, 215]. Anteriormente se consideraba que la degradación de proteínas, eran el principal mecanismo que confería irreversibilidad a las transiciones de fase del CC. Sin embargo, la proteólisis podría ser contrarrestada por la transcripción periódica y síntesis de proteínas, por

eso Novak y Tyson han argumentado que la irreversibilidad es una propiedad emergente de las asas de retroalimentación que regulan la actividad de las CDKs [73]. En *S. cerevisiae*, por ejemplo, se ha demostrado experimentalmente que, el APC/C es suficiente para que el ciclo avance y la célula salga de la mitosis, pero no para asegurar la irreversibilidad, puesto que si el APC/C desaparece inmediatamente después de que se terminó de degradar la ciclina, ésta recupera sus niveles y entonces se reactiva el complejo CDK-ciclina mitótico, induciendo el regreso de la célula al estado mitótico. Sólo hasta que un inhibidor del complejo CDK-ciclina (Sic1) aparece, se asegura la irreversibilidad de la salida de la mitosis. Incluso, la inactivación del complejo CDK-ciclina sin la degradación de la ciclina, y por un periodo de tiempo suficientemente largo como para permitir la acumulación de Sic1, sugiere una salida irreversible de la mitosis. Esos experimentos demuestran que la irreversibilidad de las transiciones no se logra únicamente por la proteólisis, sino por la regulación a nivel de sistema que involucra una segunda vía de inactivación del complejo CDK-ciclina [73]. El trabajo de Tyson y Novak ha sido fundamental para entender el papel de los reguladores del complejo CDK-ciclina en la actividad biestable de este heterodímero durante las transiciones de fase del CC. Como mencionaba en la Sección 1.9, debido a la biestabilidad, los complejos CDK-ciclina presentan solo los estados, activo e inactivo, incluso aunque las ciclinas tengan concentraciones intermedias [164] (Fig. 3.1). Esta propiedad se ha probado experimentalmente en embriones de *X. leavis* [221], y durante la transición G1/S en *S. cerevisiae* [215] y en mamíferos [222].

Otra observación que destaca la importancia la red de regulación, son los resultados del análisis de los ecotipos de *Arabidopsis*, en los cuales se encontró que la concentración de la CDKA;1 solo explica el 32% de la variación observada en su actividad, posiblemente por el papel que tienen otros componentes moleculares en la actividad de esta cinasa [111]. Esto coincide con lo que otros autores han sugerido, que el CC se compone de diferentes osciladores que se conectan y regulan entre sí [165, 223, 224].

A continuación se presentan resultados de otras actividades relacionadas con el proyecto de la red de regulación del CC y que también realicé durante el posgrado. La primera fue una comparación de los perfiles de expresión cíclica de los reguladores del CC de *Arabidopsis* y de levadura. Después un modelo Booleano que integra a las auxinas en la regulación de la progresión del CC. Finalmente, se menciona brevemente dos proyectos donde pude colaborar; en el primero, se integra la dinámica de proliferación y el transporte de auxinas en un campo de fuerzas físicas; la segunda colaboración fue en un proyecto en donde se estudió la interacción entre los módulos funcionales de la proliferación y la diferenciación celular en *C. elegans*.
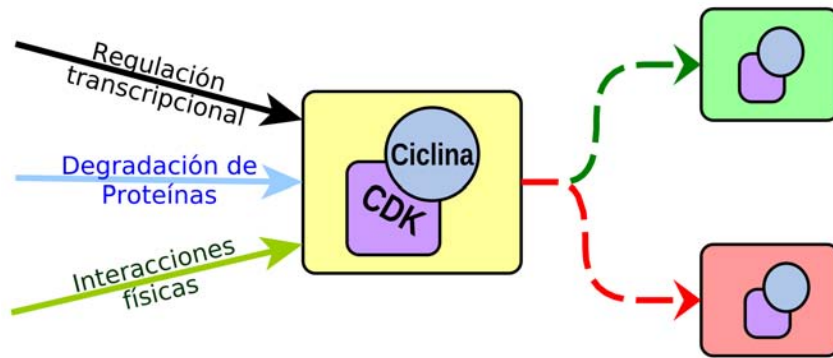
Fig. 3.1. Interacciones regulatorias de los heterodímeros CDK-ciclina responsables de su actividad biestable. La actividad de los heterodímeros CDK-ciclina está determinada por la integración de diferentes tipos de regulación, los cuales producen el comportamiento biestable (sin intermedios): activo o inactivo.

3.1 Perfiles de expresión cíclica en levadura y *Arabidopsis*

La división celular es crucial para el desarrollo de organismos multicelulares y para la continuación de la vida en general, en consecuencia no es de extrañar que se conserven elementos moleculares entre organismos tan diversos evolutivamente. Como señalabamos desde la Sección 1.2, la transcripción periódica dependiente del CC es una característica conservada en el CC de levaduras, vertebrados, *C. elegans* y plantas. Asumiendo que proteínas ortólogas (de genes con función generalmente conservada, que se originaron por un evento de especiación) o proteínas funcionalmente equivalentes entre el CC de *Arabidopsis* y el de *S. cerevisiae* están participando en las mismas fases del CC, examinamos si la red de regulación del CC recupera los patrones periódicos observados para componentes equivalentes en levadura. Para este análisis empleamos la versión continua del modelo del CC de *Arabidopsis*. De acuerdo a la Fig. 3.2, la expresión del homólogo de CYCB1;1 en levadura, CLB2, incrementa en la transición G2/M [225], comportamiento que también se observa en la versión continua del modelo del CC de *Arabidopsis*. En levaduras, CLN1 es homólogo de CYCD3;1 y está presente desde la transición G1/S, después su mensajero decrementa durante la fase S [226]. En el modelo continuo del CC de *Arabidopsis*, CYCD3;1 decrementan en la transición S/G2 (Fig. 3.2). Esta comparación indica que en *Arabidopsis* y levadura, el perfil de expresión de las ciclinas responsables de las transiciones G1/S y G2/M se encuentran cualitativamente conservados. Otros componentes, tales como los FTs E2F o sus reguladores equivalentes funcionales de la fase S en levaduras (Mbp1) [227], también muestran un comportamiento oscilatorio similar, desde la fase S a la G2, aunque con un patrón mas irregular que el de las ciclinas.
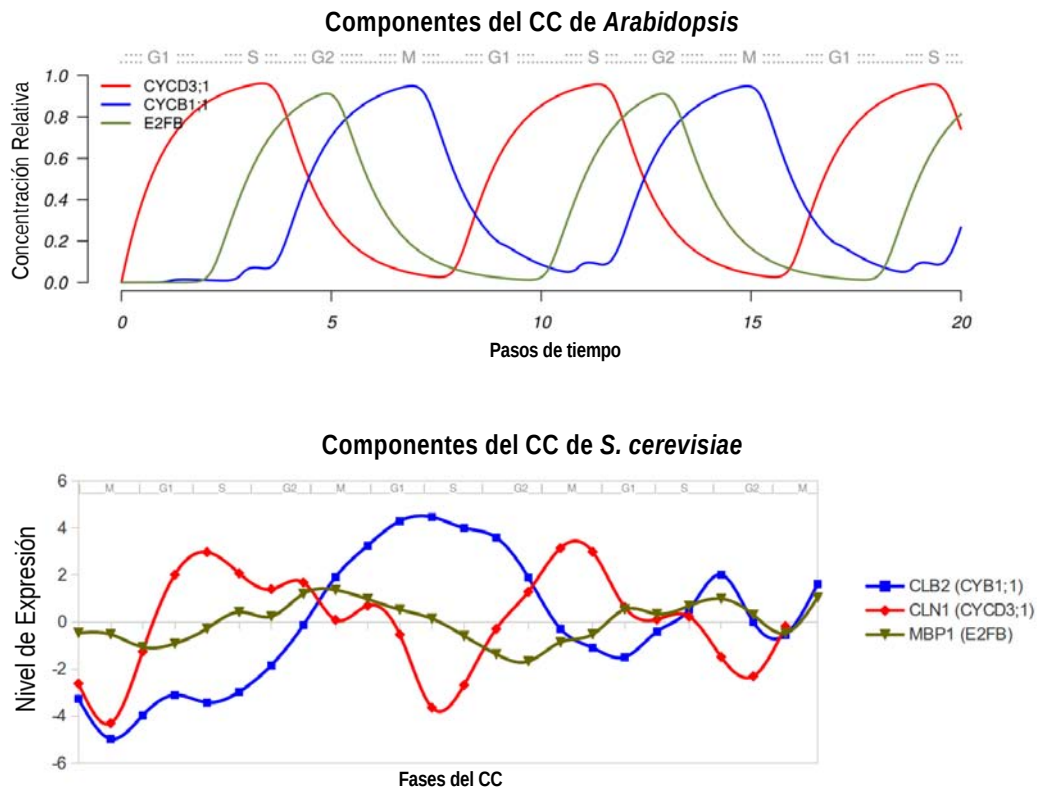
Fig. 3.2. Comparación entre el perfil de expresión de reguladores del CC de *S. cerevisiae* y la presencia de reguladores del CC de *Arabidopsis*. Los datos de expresión de los tres reguladores del CC de *S. cerevisiae* se obtuvieron de cyclebase.org [228] y los datos de microarreglo por sincronización Pramilla-alpha30 [229]. El nivel de expresión (eje vertical del perfil de *S. cerevisiae*) corresponde al $\log_2(\mathrm{S}_i/\mathrm{R}_i)$, donde S_i es la expresión en células sincronizadas y R_i es la expresión en una población de células no sincronizadas utilizadas como referencia. Las proteínas ortólogas o funcionalmente equivalentes se muestran en el mismo color.

Algunos autores han señalado que los numerosos patrones de expresión cíclica propuestos ocurren de manera continua, y entonces debería haber numerosos controles regulando esa expresión genética a través del CC [230, 231]. A diferencia de esta propuesta alternativa, las observaciones sobre la expresión periódica en diferentes organismos, es que ésta no es continua, sino que la mayoría de los genes con expresión dependiente del CC se estarían expresando poco después de la transición G1/S, G2/M y dependiendo de la especie, también al final de la mitosis. Incluso, en *Arabidopsis* se propone que no hay un único mecanismo de control transcripcional universal, puesto que no se encontró un motivo regulatorio particular en las secuencias rio arriba de genes que participan en el CC [232]. Los reguladores que se han propuesto para estos grupos

de genes serían los E2F-RBR y los FTs MYB. Como se ha demostrado para el CC de levaduras y mamíferos, y como proponemos para el de *Arabidopsis*, estos reguladores no son independientes, sino que están interconectados y ellos mismos influyen en sus propios inhibidores y activadores (e.g. RBR activado por E2Fs, o la ciclina mitótica que aumenta la actividad de los MYB3R1/4 además de ser su blanco), por lo tanto la regulación transcripcional periódica no necesita numerosos controles.

Cooper y colaboradores [230] analizaron la expresión dependiente del CC en células de ratón y encontraron que la expresión de 7 ciclinas es invariante durante el CC. Asimismo, otros trabajos han analizado la conservación de la expresión periódica dependiente del CC y concluyen que la tendencia de ortólogos a compartir sus perfiles de expresión es baja [233], estos mismos trabajos destacan la importancia de la regulación postraduccional. En el atractor, el estado de estos componentes regulados postraduccionalmente puede diferir de los perfiles de expresión documentados. Un ejemplo es la proteína RBR, ya que en el modelo, su nodo correspondiente muestra a la proteína RBR en un estado hipofosforilado, y cuando la proteína no se transcribe o está hiperfosforilada, aparece como ausente. Finalmente, otra observación que sustenta el fenómeno de la expresión periódica, sería el patrón de expresión irregular de genes reguladores del CC durante el desarrollo de *Arabidopsis*. Cuando se analiza *in situ* la expresión de reguladores del CC se ve que, en varios casos, es irregular en tejidos en proliferación [232], lo cual es congruente con la dinámica general de este modelo que señala que el estado de los reguladores depende de la fase en que se encuentra la célula.

En conclusión, aunque los componentes moleculares no estén conservados, la expresión periódica dependiente del CC sí ocurre en varios organismos. Es posible que por el vínculo entre la regulación del CC y las señales ambientales e intracelulares, dicha regulación sea muy variable, pero al final esas condiciones convergen a un grupo pequeño de reguladores cuya expresión depende del CC y mantiene una lógica de regulación similar en el CC de diferentes eucariontes.

3.2 Modelo de la regulación del ciclo celular por auxinas

Las auxinas son morfógenos vegetales involucrados en la división celular, la elongación, la dominancia apical, el desarrollo de raíces laterales y en el desarrollo de tejido vascular [1, 234]. En la punta de la raíz se distingue un flujo de auxinas con concentración máxima en el CQ y que solo llega hasta la zona de transición [235]. Esta hormona se mueve por difusión a través de las membranas, como su movimiento es limitado, requiere de proteínas integrales de membrana (PIN) para su transporte direccional a otras partes de la planta [235].

Endoreduplicación		Centro Quiescente	
AUX	🟥	**AUX**	🟩
CYCD3;1		**CYCD3;1**	[120]
SCF	[205]	**SCF**	[69, 194]
RBR	[237]	**RBR**	[172]
E2Fa	[61]	**E2Fa**	
E2Fb	[2, 117]	**E2Fb**	
E2Fc	[177]	**E2Fc**	
E2Fe	[178]	**E2Fe**	[178]
MYB77		**MYB77**	
MYB3R		**MYB3R**	
CYCB1;1	🟥	**CYCB1;1**	🟥
CDKB1;1		**CDKB1;1**	[89, 93]
CYCA2;3		**CYCA2;3**	[93]
KRP1	[181]	**KRP1**	[64, 172]
APC/C	[95, 178, 209, 210]	**APC/C**	[95]

Fig. 3.3. Atractores adicionales al del CC, esperados para el modelo de la regulación del CC por auxinas. El rojo indica que el nodo está ausente, el verde es presente y el blanco que no hay información o no es relevante para ese atractor. Dentro de las celdas se indica la(s) referencia(s).

En esta sección presentamos el avance del modelo que integra el efecto de esta hormona en la progresión del CC. Hasta ahora solo se ha incluido regulación transcripcional y degradación de proteínas, posteriormente, la regulación epigenética también se debería tomar en cuenta [236].

3.2.1 Planteamiento de las reglas lógicas

Se siguieron los mismos supuestos de la sección 2.1.2 y se agregó uno sobre la regulación transcripcional de MYB77 y auxinas: cuando las auxinas y MYB77 tenían nodos en común, se asumió que actúan como un dímero (i.e. $MYB77 \wedge AUX$). En plantas con pérdida de función del FT MYB77, la expresión de los genes de respuesta a auxinas está atenuada. MYB77 interactúa con un factor de respuesta a auxinas (ARF7) [196].

Es importante tomar en cuenta el modelo recién propuesto para la regulación del CC por los sitios de unión de los E2Fs y los AuxRE, en el cual se afirma que cuando hay muchas auxinas se degradan los Aux/IAA y SKP2A junto con E2Fc-DPb, quedando libres los sitios E2F y AuxRE para la transcripción de los genes blanco. Si los niveles de auxinas disminuyen ligeramente, los Aux/IAA se degradarían pero E2FC (y no SKP2A) se vuelve a sintetizar y por lo tanto los sitios

AuxRE quedarían activos mientras que los blancos de E2Fc estarían reprimidos, eso permite la transición S/G2 mientras se bloquea la G1/S por la falta de SCF^{SKP2A} [238]. Lor reguladores del CC que no aparecen a continuación, mantienen su regla lógica descrita en la sección 2.1.3:

1. $CYCD3; 1 = \neg SCF \wedge Aux$
   La transcripción de CYCD3;1 se induce por auxinas en células del periciclo [107].

2. $E2Fa = (Aux \vee \neg E2Fc) \wedge \neg(CDKB1; 1 \wedge CYCA2; 3)$
   El dímero LBD18/LBD33, blanco de la vía de señalización de las auxinas, regula positivamente la expresión de E2Fa [239].

3. $E2Fb = (E2Fa \wedge \neg RBR) \wedge Aux$
   La estabilidad de la proteína E2Fb es favorecida por auxinas [2].

4. $E2Fc = \neg(Aux \wedge SCF \wedge \neg KRP1 \wedge CYCD3; 1) \wedge ((E2Fa \wedge \neg RBR) \vee MYB3R1/4)$
   Al menos *in vitro*, la interacción SKP2A-DPb se ve proporcionalmente favorecida por la concentración de auxinas; DPb es la proteína con la que interactúa E2Fc para unirse al ADN [240], y SKP2A es una subunidad de la ligasa de ubiquitinas E3 SCF.

5. $CYCB1; 1 = \neg APC/C \wedge ((Aux \wedge MYB77) \vee MYB3R1/4 \vee ((\neg RBR \vee (\neg KRP1 \wedge CYCD3; 1)) \wedge E2Fb \wedge \neg E2Fc))$
   CYCB1;1 tiene dos *auxin-response elements* (AuxRE) y se ha observado la inducción de su expresión con auxinas exógenas [47].

6. $CDKB1; 1 = ((\neg RBR \vee (\neg KRP1 \wedge CYCD3; 1)) \wedge E2Fb \wedge \neg E2Fc) \vee MYB3R1/4 \vee (MYB77 \wedge Aux)$
   La expresión de CDKB1;1 es abatida cuando se transfiere a las células a un medio sin auxinas, pero ese efecto es contrarrestado cuando se sobre-expresa E2Fb, un activador transcripcional de esta cinasa [2].

7. $CYCA2; 3 = \neg APC/C \wedge (MYB3R1/4 \vee (MYB77 \wedge Aux))$
   La expresión de la ciclina CYCA2;3 disminuye cuando se bloquea la vía de la señalización de auxinas, mientras que su sobre-expresión contrarresta parcialmente el fenotipo causado por la reducción de la vía de señalización de esta hormona [241].

8. $KRP1 = (MYB77 \vee MYB3R1/4) \wedge \neg(CDKB1; 1 \wedge CYCA2; 3 \wedge SCF) \wedge \neg Aux$
   En presencia de auxinas, disminuyen los niveles de KRP2 aunque esté bajo el promotor 35S [134]. Como el modelo del CC propuesto no incluye KRP2, supusimos que esta regulación recaía sobre KRP1.

	Endoreduplicación				Ciclo Celular										
Aux	0	0	0	**Aux**	1	1	1	1	1	1	1	1	1	1	1
CYCD3	0	0	0	**CYCD3**	1	1	1	1	0	0	0	0	0	0	1
SCF	0	0	0	**SCF**	0	0	0	1	1	1	1	1	1	0	0
RBR	0	0	1	**RBR**	0	0	0	0	0	1	1	1	1	1	1
E2Fa	0	1	1	**E2Fa**	1	1	1	1	0	0	0	0	0	0	1
E2Fb	0	0	0	**E2Fb**	0	1	1	1	1	0	0	0	0	0	0
E2Fc	0	0	1	**E2Fc**	0	1	1	1	0	1	1	1	1	1	1
E2Fe	0	1	1	**E2Fe**	0	1	1	1	1	1	1	0	0	0	0
MYB77	0	0	0	**MYB77**	0	0	1	1	1	1	0	0	0	0	0
MYB3R	0	0	0	**MYB3R**	0	0	0	1	1	1	1	1	1	1	0
CYCB1	0	0	0	**CYCB1**	0	0	0	1	1	1	1	1	1	0	0
CDKB1	0	0	0	**CDKB1**	0	0	0	1	1	1	1	1	1	1	1
CYCA2	0	0	0	**CYCA2**	0	0	0	1	1	1	1	1	1	0	0
KRP1	0	0	0	**KRP1**	0	0	0	0	0	0	0	0	0	0	0
APC	1	1	1	**APC**	0	1	0	0	0	0	0	0	1	1	1
Frec.	50%			Frec.	50%										

Fig. 3.4. Atractores Obtenidos.

9. $\text{APC/C} = (\neg\text{E2Fe} \land ((\text{E2Fa} \land \neg\text{RBR}) \lor \text{MYB3R1/4} \lor \text{MYB77})) \lor \neg Aux$

Se incluyó $\lor \neg Aux$ para indicar que la falta de auxinas favorece la presencia del APC/C, efecto que sería equivalente a lo que se observa en el dominio de transición donde no hay señalización de auxinas y las citocininas inducen la expresión a CCS52A1 [210].

10. $Aux = Aux$

Las auxinas se incluyeron en el modelo como "input" o entrada.

3.2.2 Atractores esperados y obtenidos del modelo booleano de la regulación del ciclo celular por auxinas

En la Fig. 3.3 se muestran el estado esperado de los genes/proteínas para las células en endorreduplicación o en estado quiescente. La endorreduplicación también estaría caracterizada por un atractor cíclico, en donde el estado de varias proteínas puede oscilar. En este caso, los atractores están determinados por el valor del nodo Aux. Lo que no determina ese nodo es el comportamiento cíclico de los atractores.

En su estado actual, no es posible identificar con precisión las fases de la endorreduplicación en el atractor de endociclo. Además de las incosistencias comentadas, el modelo actual sugiere que los nodos o interacciones incluidas no son suficientes para recuperar un atractor de estado

quiescente. Una posibilidad sería incluir reguladores transcripcionales de la diferenciación o a las citocininas. WOX5, SCR y SHR por ejemplo, participan en el control de la progresión del CC (Sección 1.7) mientras que las citocininas son morfógenos que tienen efectos considerables en el destino celular [242]. Las auxinas y la citocininas actuan sinergísticamente en el meristemo apical de vástago pero son antagonistas en la punta de la raíz. Es interesante que las citocininas regulan la progresión del CC en diferentes puntos, tanto en la transición G1/S, por inducción de la expresión de CYCD3;1 [133], como en la G2/M por la inducción del activador del APC/C, CCS52A1. En células en cultivo de tabaco, la concentración endógena de esta hormona tiene picos alrededor de las fases S y M [107].

3.3 Patrones de comportamiento celular en la raíz de *Arabidopsis*

En el meristemo apical de la raíz de *Arabidopsis*, al igual que los NCT en organismos multicelulares, se distinguen zonas con distinta actividad celular. En un modelo propuesto por Barrio y colaboradores (ANEXO B), y en el que tuve la oportunidad de colaborar, se integró la dinámica de la proliferación celular con el transporte de auxinas y un campo de fuerzas físicas, lo que fue suficiente para recuperar la transición a proliferación o a elongación que se observan en la raíz. Este modelo se validó comparando el resultado con mediciones de células de raíces y tratamientos de auxinas.

La motivación de incluir campos físicos es porque son una fuente de información posicional [243], eso afecta el destino celular tanto en organismos vegetales como animales. En plantas, por ejemplo se sabe que las células de la cofia afectan la transición a la zona de elongación. Cuando se evita que las células de cofia mueran a tiempo y se desprendan de la punta de la raíz, las células epidérmicas y la raíz están reducidas, probablemente porque las células de la cofia dificultarían la expansión celular [244].

Al contrario, el campo físico es modificado con la propia dinámica de proliferación celular, ya que las células deben crecer antes de dividirse, por lo tanto una de las hipótesis del modelo es que hay un campo físico macroscópico a lo largo de la punta de la raíz que resulta del crecimiento y proliferación celulares así como de las células epidermales y de la cofia que rodean a la punta de la raíz. También es importante destacar que la implementación de este modelo supone que el flujo y concentración de auxinas es resultado de la síntesis, degradación y transporte que responden a ese campo elástico. Donde las células se están dividiendo o expandiendo, el campo se modifica, lo que también afectaría a la proliferación celular.

En el modelo se hicieron varias simplificaciones. Dado que estudiar la proliferación celular en sí no era la finalidad del modelo, la dinámica del CC se redujo a un comportamiento como el

que se observa en un sistema de depredador-presa Lotka-Volterra, donde sólo las cíclinas determinantes para las transiciones G1/S y G2/M se tomaron en cuenta. En este modelo, la concentración de auxinas está directamente relacionada al único parámetro de este sistema dinámico de ciclinas, cada célula se divide más rápido o más lento dependiendo de su concentración de auxinas. Experimentalmente se ha observado que la progresión del CC depende de ciertos umbrales de concentración de auxinas.

El comportamiento celular del ápice de la raíz se recuperó con este modelo, del mismo modo que las alteraciones celulares provocadas por la modificación del transporte o concentración de auxinas. Esto indica que la dinámica entre las fuerzas físicas, el gradiente de auxinas y la división celular pueden explicar la manera en que las células se dividen en la punta de la raíz. Un módulo del CC más completo facilitaría el discernimiento adecuado de la división del CQ, la cual tuvo un valor fijo en este modelo.

3.4 Coordinación entre proliferación y diferenciación celular en *Caenorhabditis elegans*

Durante el desarrollo del proyecto de la red de regulación del CC de *Arabidopsis*, se presentó la oportunidad de colaborar en otro proyecto sobre la determinación de los destinos celulares en la vulva de *Caenorhabditis elegans*. En un trabajo previo se encontró [245] que la división celular es fundamental para entender la determinación de los destinos de las células precursoras de la vulva en *Caenorhabditis elegans*, por lo que incluimos la regulación del CC como un módulo funcional acoplado a la red de diferenciación celular. El artículo referido se encuentra en el ANEXO C.

El modelo derivado nos ayuda a identificar células especificadas cuando establecemos las condiciones del medio de crecimiento en que pierden su identidad. Con el modelo también fue posible distinguir la influencia que tiene el módulo de diferenciación en la duración del CC. También se evaluó el efecto de la eliminación de interacciones, que a diferencia de la simulación de mutantes (pérdida o ganancia de función), tendría un efecto menos drástico, sería equivalente a mutar sitios de reconocimiento de FTs, o alterar ciertos dominios funcionales de las proteínas. Gracias a este análisis novedoso se detectaron cambios en la red que causan quiescencia, endorreduplicación o un CC más corto.

La regulación de los precursores de la vulva en *C. elegans* es un ejemplo concreto de la conexión entre los módulos funcionales de la diferenciación y la proliferación celular. La regulación de LIN-12[1] por complejos CDK-ciclina destaca la importancia del control temporal del

---

[1]Receptor de membrana que pertenece a la familia Notch

módulo de diferenciación, debido a la actividad de CDK-ciclina dependiente de la fase del CC. Esta regulación de la vía Notch por el CC es responsable de mantener el potencial de las células precursoras de la vulva, al permitirles mantenerse en un estado competente y ser responsivas a la concentración de LIN-3 y a señales extracelulares. Como señalamos en la sección 1.7, la regulación temporal o la duración de las fases del CC repercuten directamente en el destino celular, pese a esto, el tema a penas se empieza a explorar.

3.5 Conclusión

En este trabajo hemos reunido datos de diversas fuentes con la finalidad de explorar un tema fascinante tanto desde el punto de vista biológico como del dinámico. Recurrimos a los modelos booleanos como una herramienta teórica que complementa a la investigación experimental, y facilita la formulación y el acotamiento de hipótesis al aportar una explicación sistémica de la regulación molecular del CC de *Arabidopsis*. Las contribuciones del modelo a la regulación del CC en *Arabidopsis* son:

- **La proposición del oscilador transcripcional y la relación entre complejos que median la degradación de proteínas.** Estas interacciones no se habían investigado en plantas, pero hay observaciones que sugieren su existencia como en otros eucariontes. El oscilador transcripcional corresponde a la coordinación directa entre FTs requeridos para la transición G1/S (E2Fs) y G2/M (MYB); la relación entre complejos ligasas de ubiquitina, se refiere a la regulación negativa del SCF por parte del APC/C.

- **Una propuesta para la regulación alternativa de la transición G2/M del CC de *Arabidopsis*.** Dado que las proteínas que modulan la transición G2/M en mamíferos o levadura (Wee/Cdc25) no conservan sus funciones en esta planta, retomamos consideraciones de otros autores para fundamentar una propuesta distinta que incluye a la proteína KRP y a la cinasa CDKB específica de plantas.

- **La clarificación de la dinámica de regulación de la vía E2F-RBR.** La unión diferencial de la proteína RBR a los FTs E2Fa y E2Fb, en presencia de la ciclina CYCD3;1, permitieron expresar las reglas lógicas que explican las diferencias en la función de estos factores.

- **Una explicación del mecanismo por el que las señales fisiológicas y del desarrollo interfieren en la regulación diferencial del CC en la punta de la raíz.** La revisión del impacto que tiene el programa de desarrollo y el ambiente en los componentes del CC junto con la simulación de mutantes, revelan parcialmente la relación entre dichas señales y el comportamiento diferencial del CC en la raíz (i.e. quiescencia, proliferación

celular o endorreduplicación); un ejemplo sería la ganancia de función de la subunidad activadora del APC/C, la cual recuperó un atractor equivalente al fenotipo observado con la señalización de las citocininas al inducir la expresión de esa subunidad en la zona de endorreduplicación de la raíz.

El modelo dinámico de la regulación del CC que hemos propuesto para *Arabidopsis*, es una aproximación inicial para entender la regulación espacio-temporal de la proliferación celular durante el desarrollo de la raíz. Es posible que aspectos como la redundancia funcional tengan que ser reconsiderados, o que se tengan que agregar suposiciones adicionales. Por ejemplo, en el modelo se tomó en cuenta la CYCD3;1 porque esta ciclina de tipo D parece ser relevante para células del dominio de proliferación, sin embargo en el CQ sería la CYCD3;3 (inhibida por WOX5), o en las células iniciales la CYCD6;1 (activada por auxinas o por el heterodímero formado por SHORT-ROOT y SCARECROW; SHR-SCR), las ciclinas responsables de la re-entrada al CC. Las metodologías propuestas recientemente para analizar el papel de cada gen de una red regulatoria [246] o para encontrar los cambios en un grupo de genes que modificarían el conjunto de estados estacionarios [247] serán, sin duda, herramientas que permitan explorar el efecto de las condiciones ambientales o los morfógenos en la determinación de la quiescencia, endorreduplicación o diferencias en las tasas de proliferación celular. Identificando al conjunto de señales que inducen cambios en los atractores, ya sea en la(s) configuración(es) o en el número de atractores posibles, podríamos proponer procedimientos no genéticos para modificar el crecimiento o la morfogénesis de una planta.

El modelo de la regulación del CC de *Arabidopsis* también ayudará a esclarecer la razón de que algunas alteraciones dependan de la etapa del desarrollo del organismo, o incluso de la fase del CC en que se presentan. Por ejemplo, la sobre-expresión transitoria de E2Fa en protoplastos de hoja madura causan la transición del estado quiescente (en G1 o G0) a la fase S [117]. Adicionalmente, la desdiferenciación, la re-entrada al CC y la inducción a la rediferenciación también se pueden estudiar con el modelo propuesto. Esos procesos pueden ocurrir casi en cualquier célula vegetal diferenciada, ya que a diferencia de los animales, la mayoría de las células vegetales son totipotentes[2] [7]. Una comparación entre la dinámica del CC vegetal y el animal, ayudaría a entender por qué las células vegetales son capaces de mantener su totipotencia mientras que las animales la van perdiendo durante su desarrollo.

La topología y la dinámica de la red propuesta sugieren que el patrón cíclico de actividad o transcripción de los reguladores del CC es una propiedad que emerge a partir de las relaciones entre sus componentes. Con este trabajo comenzamos a entender la relación recíproca entre la

---

[2]Células que tienen el potencial de originar cualquier tipo de célula que conforma al organismo

regulación del CC y el desarrollo, pues este último también influye en la regulación de los componentes del CC a través de reguladores transcripcionales de la diferenciación. Con la integración de otros módulos funcionales como la regulación genética o los morfógenos vegetales, la red de la regulación del CC ayudará a entender mejor la interacción entre genotipo (nivel molecular) y fenotipo (nivel órgano/organismo) en el crecimiento y morfogénesis. Por último, el modelo será un instrumento que simplifique la obtención de conclusiones en relación a la regulación genética, degradación específica de proteínas, y evolución de la red de regulación del CC de *Arabidopsis*.

REFERENCIAS

1. Ramirez-Parra E, Desvoyes B, Gutierrez C. Balance between cell division and differentiation during plant development. Int J Dev Biol. 2005;49(5-6):467–477.

2. Magyar Z, De Veylder L, Atanassova A, Bakó L, Inzé D, Bögre L. The role of the Arabidopsis E2FB transcription factor in regulating auxin-dependent cell division. Plant Cell. 2005;17(September):2527–2541.

3. Roeder aHK, Cunha A, Ohno CK, Meyerowitz EM. Cell cycle regulates cell type in the Arabidopsis sepal. Development. 2012;139(23):4416–4427.

4. De Veylder L, Beeckman T, Beemster GTS, Krols L, Terras F, Landrieu I, et al. Functional Analysis of Cyclin-Dependent Kinase Inhibitors of Arabidopsis. Plant Cell. 2001;13(7):1653–1668.

5. Beemster GTS, Fiorani F, Inzé D. Cell cycle: the key to plant growth control? Trends Plant Sci. 2003;8(4):154–158.

6. Ingram GC, Waites R. Keeping it together: Co-ordinating plant growth. Curr Opin Plant Biol. 2006;9(1):12–20.

7. De Veylder L, Beeckman T, Inzé D. The ins and outs of the plant cell cycle. Nat Rev Mol Cell Biol. 2007;8(8):655–665.

8. Vandepoele K, Raes J, De Veylder L, Rouze P, Rombauts S, Inze D. Genome-wide analysis of core cell cycle genes in Arabidopsis. Plant Cell. 2002;14(4):903–916.

9. Dewitte W, Murray JAH. The plant cell cycle. Annu Rev Plant Biol. 2003;54:235–264.

10. Nurse P. The Wellcome Lecture, 1992. Cell cycle control. Philos Trans R Soc Lond B Biol Sci. 1993;341(1298):449–454.

11. Bedhomme M, Jouannic S, Champion A, Simanis V, Henry Y. Plants, MEN and SIN. Plant Physiol Biochem. 2008;46(1):1–10.

12. Doerner PW. Cell Cycle Regulation in Plants. Plant Physiol. 1994;106(3):823–827.

13. Robbens S, Khadaroo B, Camasses A, Derelle E, Ferraz C, Inzé D, et al. Genome-wide analysis of core cell cycle genes in the unicellular green alga Ostreococcus tauri. Mol Biol Evol. 2005;22(3):589–597.

14. Novak B, Tyson JJ. Modeling the control of DNA replication in fission yeast. Proc Natl Acad Sci U S A. 1997;94(17):9147–9152.

15. Li F, Long T, Lu Y, Ouyang Q, Tang C. The yeast cell-cycle network is robustly designed. Proc Natl Acad Sci U S A. 2004;101(14):4781–4786.

16. Chen KC, Calzone L, Csikasz-Nagy A, Cross FR, Novak B, Tyson JJ. Integrative analysis of cell cycle control in budding yeast. Mol Biol Cell. 2004;15(8):3841–62.

17. Goldbeter a. A minimal cascade model for the mitotic oscillator involving cyclin and cdc2 kinase. Proc Natl Acad Sci U S A. 1991;88(20):9107–9111.

18. Novák B, Tyson JJ. A model for restriction point control of the mammalian cell cycle. J Theor Biol. 2004;230(4 SPEC. ISS.):563–579.

19. Fauré A, Naldi A, Chaouiya C, Thieffry D. Dynamical analysis of a generic Boolean model for the control of the mammalian cell cycle. Bioinformatics. 2006;22(14):124–131.

20. Fauré A, Naldi A, Lopez F, Chaouiya C, Ciliberto A, Thieffry D. Modular logical modelling of the budding yeast cell cycle. Mol Biosyst. 2009;5(12):1787–1796.

21. Larson-Rabin Z, Li Z, Masson PH, Day CD. FZR2/CCS52A1 expression is a determinant of endoreduplication and cell expansion in Arabidopsis. Plant Physiol. 2009 feb;149(2):874–84.

22. Lee HO, Davidson JM, Duronio RJ. Endoreplication: Polyploidy with purpose. Genes Dev. 2009;23(21):2461–2477.

23. Gutierrez C. The Arabidopsis cell division cycle. In: Arabidopsis Book. vol. 7; 2009. p. e0120.

24. Dudits D, Ábrahám E, Miskolczi P, Ayaydin F, Bilgin M, Horvtáh GV. Cell-cycle control as a target for calcium, hormonal and developmental signals: The role of phosphorylation in the retinoblastoma-centred pathway. Ann Bot. 2011;107(7):1193–1202.

25. Dissmeyer N, Nowack MK, Pusch S, Stals H, Inzé D, Grini PE, et al. T-loop phosphorylation of Arabidopsis CDKA;1 is required for its function and can be partially substituted by an aspartate residue. Plant Cell. 2007;19(3):972–985.

26. Loog M, Morgan DO. Cyclin specificity in the phosphorylation of cyclin-dependent kinase substrates. Nature. 2005;434(7029):104–108.

27. Nowack MK, Harashima H, Dissmeyer N, Zhao X, Bouyer D, Weimer AK, et al. Genetic Framework of Cyclin-Dependent Kinase Function in Arabidopsis. Dev Cell. 2012;22(5):1030–1040.

28. Shen WH. The plant E2F-Rb pathway and epigenetic control. Trends Plant Sci. 2002;7(11):505–511.

29. Ito M. Conservation and diversification of three-repeat Myb transcription factors in plants. J Plant Res. 2005;118(1):61–69.

30. Zhu W, Giangrande PH, Nevins JR. E2Fs link the control of G1/S and G2/M transcription. EMBO J. 2004;23(23):4615–26.

31. Dehghan Nayeri F. Identification of transcription factors linked to cell cycle regulation in Arabidopsis. Plant Signal Behav. 2014;9(11):e972864.

32. Orlando Da, Lin CY, Bernard A, Wang JY, Socolar JES, Iversen ES, et al. Global control of cell-cycle transcription by coupled CDK and network oscillators. Nature. 2008;453(7197):944–947.

33. Sevim V, Gong X, Socolar JES. Reliability of transcriptional cycles and the yeast cell-cycle oscillator. PLoS Comput Biol. 2010;6(7):18.

34. Kovacs LaS, Orlando Da, Haase SB. Transcription network and cyclin/CDKs: The yin and yang of cell cycle oscillators. Cell Cycle. 2008;7(17):2626–2629.

35. De Jager SM, Scofield S, Huntley RP, Robinson AS, Den Boer BGW, Murray JaH. Dissecting regulatory pathways of G1/S control in Arabidopsis: Common and distinct targets of CYCD3;1, E2Fa and E2Fc. Plant Mol Biol. 2009;71(4-5):345–365.

36. De Veylder L, Joubès J, Inzé D. Plant cell cycle transitions. Curr Opin Plant Biol. 2003;6(6):536–543.

37. Ramirez-Parra E, Fründt C, Gutierrez C. A genome-wide identification of E2F-regulated genes in Arabidopsis. Plant J. 2003;33(4):801–811.

38. Sugimoto-Shirasu K, Roberts K. "Big it up": Endoreduplication and cell-size control in plants. Curr Opin Plant Biol. 2003;6(6):544–553.

39. Vandepoele K, Vlieghe K, Florquin K, Hennig L, Beemster GTS, Gruissem W, et al. Genome-wide identification of potential plant E2F target genes. Plant Physiol. 2005;139(1):316–328.

40. Inzé D, De Veylder L. Cell cycle regulation in plant development. Annu Rev Genet. 2006;40:77–105.

41. Castellano MDM, Boniotti MB, Caro E, Schnittger A, Gutierrez C. DNA Replication Licensing Affects Cell Proliferation or Endoreplication in a Cell Type – Specific Manner. Plant Cell. 2004;16(September):2380–2393.

42. Kumpf R, Thorstensen T, Rahman MA, Heyman J, Nenseth HZ, Lammens T, et al. The ASHR3 SET-domain Protein Controls Cell Division Competence of the Meristem and Quiescent Centre of the Arabidopsis thaliana Primary Root. Plant Physiol. 2014;.

43. Yao G, Lee TJ, Mori S, Nevins JR, You L. A bistable Rb-E2F switch underlies the restriction point. Nat Cell Biol. 2008;10(4):476–482.

44. De Jager SM, Menges M, Bauer UM, Murray JaH. Arabidopsis E2F1 binds a sequence present in the promoter of S-phase-regulated gene AtCDC6 and is a member of a multigene family with differential activities. Plant Mol Biol. 2001;47(4):555–568.

45. Wittenberg C, Reed SI. Cell cycle-dependent transcription in yeast: promoters, transcription factors, and transcriptomes. Oncogene. 2005;24(17):2746–2755.

46. Ito M. Factors controlling cyclin B expression. Plant Mol Biol. 2000;43(5-6):677–690.

47. Planchais S, Perennes C, Glab N, Mironov V, Inzé D, Bergounioux C. Characterization of cis-acting element involved in cell cycle phase-independent activation of Arath;CycB1;1 transcription and identification of putative regulatory proteins. Plant Mol Biol. 2002;50(1):111–127.

48. Nakata Y, Shetzline S, Sakashita C, Kalota A, Rallapalli R, Rudnick SI, et al. c-Myb contributes to G2/M cell cycle transition in human hematopoietic cells by direct regulation of cyclin B1 expression. Mol Cell Biol. 2007;27(6):2048–2058.

49. Breeden LL. Periodic transcription: A cycle within a cycle. Curr Biol. 2003;13(1):31–38.

50. Cokus S, Rose S, Haynor D, Grønbech-Jensen N, Pellegrini M. Modelling the network of cell cycle transcription factors in the yeast Saccharomyces cerevisiae. BMC Bioinformatics. 2006;7:381.

51. Doonan J. Plant growth: Roots in the cell cycle. Curr Biol. 1996;6(7):788–789.

52. Cross FR, Buchler NE, Skotheim JM. Evolution of networks and sequences in eukaryotic cell cycle control. Philos Trans R Soc B Biol Sci. 2011;366(1584):3532–3544.

53. Oakenfull EA, Riou-Khamlichi C, Murray JaH. Plant D-type cyclins and the control of G1 progression. Philos Trans R Soc Lond B Biol Sci. 2002;357(1422):749–760.

54. Planchais S, Samland AK, Murray JaH. Differential stability of Arabidopsis D-type cyclins: CYCD3;1 is a highly unstable protein degraded by a proteasome-dependent mechanism. Plant J. 2004;38(4):616–625.

55. Menges M, Samland AK, Planchais S, Murray JA. The D-Type Cyclin CYCD3;1 Is Limiting for the G1-to-S-Phase Transition in Arabidopsis. Plant Cell. 2006;18(4):893–906.

56. Berckmans B, De Veylder L. Transcriptional control of the cell cycle. Curr Opin Plant Biol. 2009 oct;12(5):599–605.

57. Durfee T, Feiler HS, Gruissem W. Retinoblastoma-related proteins in plants: homologues or orthologues of their metazoan counterparts? Plant Mol Biol. 2000;43(5-6):635–642.

58. Malumbres M, Barbacid M. Cell cycle, CDKs and cancer: a changing paradigm. Nat Rev Cancer. 2009;9(3):153–166.

59. Sanchez MDLP, Caro E, Desvoyes B, Ramirez-Parra E, Gutierrez C. Chromatin dynamics during the plant cell cycle. Semin Cell Dev Biol. 2008;19(6):537–546.

60. Gutierrez C, Ramirez-Parra E, Castellano MM, Del Pozo JC. G1 to S transition: More than a cell cycle engine switch. Curr Opin Plant Biol. 2002;5(6):480–486.

61. De Veylder L, Beeckman T, Beemster GTS, De Almeida Engler J, Ormenese S, Maes S, et al. Control of proliferation, endoreduplication and differentiation by the Arabidopsis E2Fa-DPa transcription factor. EMBO J. 2002;21(6):1360–1368.

62. Poznic M. Retinoblastoma protein: A central processing unit. J Biosci. 2009;34(2):305–312.

63. Castellano MM, del Pozo JC, Ramirez-Parra E, Brown S, Gutierrez C. Expression and stability of Arabidopsis CDC6 are associated with endoreplication. Plant Cell. 2001;13(12):2671–2686.

64. Verkest A, Weinl C, Inze D, Veylder LD, Schnittger A. Switching the Cell Cycle. Kip-Related Proteins in Plant Cell Cycle Control. Plant Physiol. 2005;139(November):1099–1106.

65. Komaki S, Sugimoto K. Control of the plant cell cycle by developmental and environmental cues. Plant Cell Physiol. 2012;53(6):953–964.

66. Vanneste S, Coppens F, Lee E, Donner TJ, Xie Z, Van Isterdael G, et al. Developmental regulation of CYCA2s contributes to tissue-specific proliferation in Arabidopsis. EMBO J. 2011;30(16):3430–3441.

67. Schnittger A, Schöbinger U, Stierhof YD, Hülskamp M. Ectopic B-type cyclin expression induces mitotic cycles in endoreduplicating Arabidopsis trichomes. Curr Biol. 2002;12(5):415–420.

68. Boudolf V, Vlieghe K, Beemster GT, Magyar Z, Torres Acosta JA, Maes S, et al. The Plant-Specific Cyclin-Dependent Kinase CDKB1;1 and Transcription Factor E2Fa-DPa Control the Balance of Mitotically Dividing and Endoreduplicating Cells in Arabidopsis. Plant Cell. 2004;16(10):2683–2692.

69. del Pozo JC, Boniotti MB, Gutierrez C. Arabidopsis E2Fc functions in cell division and is degraded by the ubiquitin-SCF(AtSKP2) pathway in response to light. Plant Cell. 2002;14(12):3057–3071.

70. Peeper DS, Parker LL, Ewen ME, Toebes M, Hall FL, Xu M, et al. A- and B-type cyclins differentially modulate substrate specificity of cyclin-cdk complexes. EMBO J. 1993;12(5):1947–1954.

71. Weingartner M, Criqui Mc, Mészáros T, Binarova P, Schmit Ac, Helfer A, et al. Expression of a nondegradable cyclin B1 affects plant development and leads to endomitosis by inhibiting the formation of a phragmoplast. Plant Cell. 2004;16(3):643–657.

72. Haga N, Kato K, Murase M, Araki S, Kubo M, Demura T, et al. R1R2R3-Myb proteins positively regulate cytokinesis through activation of KNOLLE transcription in Arabidopsis thaliana. Development. 2007;134(6):1101–1110.

73. López-Avilés S, Kapuy O, Novák B, Uhlmann F. Irreversibility of mitotic exit is the consequence of systems-level feedback. Nature. 2009;459(7246):592–595.

74. Francis D. A commentary on the G2/M transition of the plant cell cycle. Ann Bot. 2011;107(7):1065–1070.

75. Tominaga Y, Li C, Wang RH, Deng CX. Murine Wee1 plays a critical role in cell cycle regulation and pre-implantation stages of embryonic development. Int J Biol Sci. 2006;2(4):161–170.

76. De Schutter K, Joubès J, Cools T, Verkest A, Corellou F, Babiychuk E, et al. Arabidopsis WEE1 kinase controls cell cycle arrest in response to activation of the DNA integrity checkpoint. Plant Cell. 2007;19(1):211–225.

77. Shimotohno A, Ohno R, Bisova K, Sakaguchi N, Huang J, Koncz C, et al. Diverse phosphoregulatory mechanisms controlling cyclin-dependent kinase-activating kinases in Arabidopsis. Plant J. 2006;47(5):701–710.

78. Dissmeyer N, Weimer AK, Pusch S, De Schutter K, Alvim Kamei CL, Nowack MK, et al. Control of cell proliferation, organ growth, and DNA damage response operate independently of dephosphorylation of the Arabidopsis Cdk1 homolog CDKA;1. Plant Cell. 2009;21(11):3641–3654.

79. Cook GS, Grønlund AL, Siciliano I, Spadafora N, Amini M, Herbert RJ, et al. Plant WEE1 kinase is cell cycle regulated and removed at mitosis via the 26S proteasome machinery. J Exp Bot. 2013;64(7):2093–2106.

80. Dissmeyer N, Weimer AK, De Veylder L, Novak B, Schnittger A. The regulatory network of cell-cycle progression is fundamentally different in plants versus yeast or metazoans. Plant Signal Behav. 2010;5(12):1613–1618.

81. Boudolf V, Inzé D, De Veylder L. What if higher plants lack a CDC25 phosphatase? Trends Plant Sci. 2006;11(10):474–479.

82. Davidich MI, Bornholdt S. Boolean network model predicts cell cycle sequence of fission yeast. PLoS One. 2008;3(2).

83. Genschik P, Marrocco K, Bach L, Noir S, Criqui MC. Selective protein degradation: A rheostat to modulate cell-cycle phase transitions. J Exp Bot. 2014;65(10):2603–2615.

84. Francis D. The plant cell cycle–15 years on. New Phytol. 2007;174(2):261–278.

85. Kevei Z, Baloban M, da Ines O, Tiricz H, Kroll A, Regulski K, et al. Conserved CDC20 cell cycle functions are carried out by two of the five isoforms in arabidopsis thaliana. PLoS One. 2011;6(6).

86. Fülöp K, Tarayre S, Kelemen Z, Horváth G, Kevei Z, Nikovics K, et al. Arabidopsis anaphase-promoting complexes: Multiple activators and wide range of substrates might keep APC perpetually busy. Cell Cycle. 2005;4(8):1084–1092.

87. Doonan JH. The plant cell cycle: an overview. Methods Mol Biol. 2005;296:31–50.

88. Coudreuse D, Nurse P. Driving the cell cycle with a minimal CDK control network. Nature. 2010;468(7327):1074–1079.

89. Verkest A, Manes CLdO, Vercruysse S, Maes S, Van Der Schueren E, Beeckman T, et al. The cyclin-dependent kinase inhibitor KRP2 controls the onset of the endoreduplication cycle during Arabidopsis leaf development through inhibition of mitotic CDKA;1 kinase complexes. Plant Cell. 2005 jun;17(6):1723–36.

90. Beemster G, Veylder LD. Genome-wide analysis of gene expression profiles associated with cell cycle transitions in growing organs of Arabidopsis. Plant Physiol. 2005;138(June):734–743.

91. Jégu T, Latrasse D, Delarue M, Mazubert C, Bourge M, Hudik E, et al. Multiple functions of Kip-related protein5 connect endoreduplication and cell elongation. Plant Physiol. 2013;161(4):1694–705.

92. Imai KK, Ohashi Y, Tsuge T, Yoshizumi T, Matsui M, Oka A, et al. The A-type cyclin CYCA2;3 is a key regulator of ploidy levels in Arabidopsis endoreduplication. Plant Cell. 2006;18(2):382–396.

93. Boudolf V, Lammens T, Boruc J, Van Leene J, Van Den Daele H, Maes S, et al. CDKB1;1 forms a functional complex with CYCA2;3 to suppress endocycle onset. Plant Physiol. 2009;150(3):1482–1493.

94. Magyar Z, Horváth B, Khan S, Mohammed B, Henriques R, De Veylder L, et al. Arabidopsis E2FA stimulates proliferation and endocycle separately through RBR-bound and RBR-free complexes. EMBO J. 2012;31(6):1480–1493.

95. Vanstraelen M, Baloban M, Da Ines O, Cultrone A, Lammens T, Boudolf V, et al. APC/C-CCS52A complexes control meristem maintenance in the Arabidopsis root. Proc Natl Acad Sci U S A. 2009;106(28):11806–11811.

96. Berckmans B, Lammens T, Van Den Daele H, Magyar Z, Bögre L, De Veylder L. Light-dependent regulation of DEL1 is determined by the antagonistic action of E2Fb and E2Fc. Plant Physiol. 2011;157(3):1440–51.

97. Eckardt Na. Ins and Outs of E2Fs. Plant Cell. 2002;14(12):2977–2980.

98. Bramsiepe J, Wester K, Weinl C, Roodbarkelari F, Kasili R, Larkin JC, et al. Endoreplication controls cell fate maintenance. PLoS Genet. 2010;6(6):1–14.

99. Liberman LM, Sparks EE, Moreno-Risueno Ma, Petricka JJ, Benfey PN. MYB36 regulates the transition from proliferation to differentiation in the Arabidopsis root. Proc Natl Acad Sci. 2015;p. 201515576.

100. Doonan J, Hunt T. Why don't plants get cancer? Nature. 1996;380(6574):481–482.

101. Doerner P, Jorgensen JEE, You R, Steppuhn J, Lamb C. Control of root growth and development by cyclin expression. Nature. 1996;380(6574):520–523.

102. Braun AC. Plant tumors. Biochim Biophys Acta. 1978 oct;516(2):167–91.

103. Sultan SE. Phenotypic plasticity for plant development, function and life history. Trends Plant Sci. 2000;5(12):537–542.

104. Skirycz A, De Bodt S, Obata T, De Clercq I, Claeys H, De Rycke R, et al. Developmental stage specificity and the role of mitochondrial metabolism in the response of Arabidopsis leaves to prolonged mild osmotic stress. Plant Physiol. 2010;152(1):226–244.

105. Fusconi A. Regulation of root morphogenesis in arbuscular mycorrhizae: What role do fungal exudates, phosphate, sugars and hormones play in lateral root formation? Ann Bot. 2014;113(1):19–33.

106. Scheres B. Stem-cell niches: nursery rhymes across kingdoms. Nat Rev Mol Cell Biol. 2007;8(5):345–354.

107. Del Pozo JC, Lopez-Matas MA, Ramirez-Parra E, Gutierrez C. Hormonal control of the plant cell cycle. Physiol Plant. 2005;123(2):173–183.

108. Ivanov VB, Dubrovsky JG. Longitudinal zonation pattern in plant roots: Conflicts and solutions. Trends Plant Sci. 2013;18(5):237–243.

109. Ivanov VB. Relationship between cell proliferation and transition to elongation in plant roots. Int J Dev Biol. 1997;41(6):907–915.

110. Ivanov VB, Dobrochaev AE, Baskin TI. What the distribution of cell lengths in the root meristem does and does not reveal about cell division. J Plant Growth Regul. 2002;21(1):60–67.

111. Beemster GTS, De Vusser K, De Tavernier E, De Bock K, Inzé D. Variation in growth rate between Arabidopsis ecotypes is correlated with cell division and A-type cyclin-dependent kinase activity. Plant Physiol. 2002;129(2):854–864.

112. Baskin TI. On the constancy of cell division rate in the root meristem. Plant Mol Biol. 2000 aug;43(5-6):545–54.

113. Cools T, Iantcheva A, Maes S, Van Den Daele H, De Veylder L. A replication stress-induced synchronization method for Arabidopsis thaliana root meristems. Plant J. 2010;64(4):705–714.

114. Meijer M, Murray JaH. Cell cycle controls and the development of plant form. Curr Opin Plant Biol. 2001;4(1):44–49.

115. Desvoyes B, Fernández-Marcos M, Sequeira-Mendes J, Otero S, Vergara Z, Gutierrez C. Looking at plant cell cycle from the chromatin window. Front Plant Sci. 2014;5(July):369.

116. He SS, Liu J, Xie Z, O'Neill D, Dotson S. Arabidopsis E2Fa plays a bimodal role in regulating cell division and cell growth. Plant Mol Biol. 2004;56(2):171–184.

117. Sozzani R, Maggio C, Varotto S, Canova S, Bergounioux C, Albani D, et al. Interplay between Arabidopsis activating factors E2Fb and E2Fa in cell cycle progression and development. Plant Physiol. 2006;140(4):1355–1366.

118. Sozzani R, Iyer-Pascuzzi A. Postembryonic control of root meristem growth and development. Curr Opin Plant Biol. 2014;17(1):7–12.

119. Cruz-Ramírez A, Díaz-Triviño S, Blilou I, Grieneisen VA, Sozzani R, Zamioudis C, et al. A bistable circuit involving SCARECROW-RETINOBLASTOMA integrates cues to inform asymmetric stem cell division. Cell. 2012;150(5):1002–1015.

120. Forzani C, Aichinger E, Sornay E, Willemsen V, Laux T, Dewitte W, et al. WOX5 Suppresses CYCLIN D Activity to Establish Quiescence at the Center of the Root Stem Cell Niche. Curr Biol. 2014;24(16):1939–1944.

121. Wenger J, Marks MD. E2F and retinoblastoma related proteins may regulate GL1 expression in developing Arabidopsis trichomes. Plant Signal Behav. 2008;3(6):420–422.

122. Hardwick LJa, Philpott A. Nervous decision-making: To divide or differentiate. Trends Genet. 2014;30(6):254–261.

123. Vallier L. Cell Cycle Rules Pluripotency. Cell Stem Cell. 2015;17(2):131–132.

124. Gonzales KAU, Liang H, Lim YS, Chan YS, Yeo JC, Tan CP, et al. Deterministic Restriction on Pluripotent State Dissolution by Cell-Cycle Pathways. Cell. 2015 jul;162(3):564–579.

125. Ubeda-Tomás S, Beemster GTS, Bennett MJ. Hormonal regulation of root growth: Integrating local activities into global behaviour. Trends Plant Sci. 2012;17(6):326–331.

126. Moubayidin L, Di Mambro R, Sabatini S. Cytokinin-auxin crosstalk; 2009.

127. Richard C, Lescot M, Inzé D, De Veylder L. Effect of auxin, cytokinin, and sucrose on cell cycle gene expression in Arabidopsis thaliana cell suspension cultures. Plant Cell Tissue Organ Cult. 2002;69(2):167–176.

128. Takatsuka H, Umeda M. Hormonal control of cell division and elongation along differentiation trajectories in roots. J Exp Bot. 2014;65(10):2633–2643.

129. Reitz MU, Gifford ML, Schafer P. Hormone activities and the cell cycle machinery in immunity-triggered growth inhibition. J Exp Bot. 2015;66(8):2187–2197.

130. Tank JG, Pandya RV, Thaker VS. Phytohormones in regulation of the cell division and endoreduplication process in the plant cell cycle. RSC Adv. 2014;4(24):12605.

131. Hacham Y, Holland N, Butterfield C, Ubeda-Tomas S, Bennett MJ, Chory J, et al. Brassinosteroid perception in the epidermis controls root meristem size. Development. 2011;138(5):839–848.

132. González-García MP, Vilarrasa-Blasi J, Zhiponova M, Divol F, Mora-García S, Russinova E, et al. Brassinosteroids control meristem size by promoting cell cycle progression in Arabidopsis roots. Development. 2011;138(5):849–859.

133. Riou-Khamlichi C, Huntley R, Jacqmard A, Murray Ja. Cytokinin activation of Arabidopsis cell division through a D-type cyclin. Science. 1999;283(5407):1541–1544.

134. Sanz L, Dewitte W, Forzani C, Patell F, Nieuwland J, Wen B, et al. The Arabidopsis D-type cyclin CYCD2;1 and the inhibitor ICK2/KRP2 modulate auxin-induced lateral root formation. Plant Cell. 2011;23(2):641–660.

135. López-Juez E, Dillon E, Magyar Z, Khan S, Hazeldine S, de Jager SM, et al. Distinct light-initiated gene expression and cell cycle programs in the shoot apex and cotyledons of Arabidopsis. Plant Cell. 2008;20(4):947–968.

136. Ren H, Santner A, Pozo JCD, Murray JaH, Estelle M. Degradation of the cyclin-dependent kinase inhibitor KRP1 is regulated by two different ubiquitin E3 ligases. Plant J. 2008;53(5):705–716.

137. Wang H, Zhou Y, Bird Da, Fowke LC. Functions, regulation and cellular localization of plant cyclin-dependent kinase inhibitors. J Microsc. 2008;231(2):234–246.

138. Reyt G, Boudouf S, Boucherez J, Gaymard F, Briat JF. Iron- and Ferritin-Dependent Reactive Oxygen Species Distribution: Impact on Arabidopsis Root System Architecture. Mol Plant. 2015 mar;8(3):439–453.

139. Skirycz A, Claeys H, De Bodt S, Oikawa A, Shinoda S, Andriankaja M, et al. Pause-and-Stop: The Effects of Osmotic Stress on Cell Proliferation during Early Leaf Development in Arabidopsis and a Role for Ethylene Signaling in Cell Cycle Arrest. Plant Cell. 2011;23(5):1876–1888.

140. Jurado S, Triviño SD, Abraham Z, Manzano C, Gutierrez C, Del Pozo C. SKP2A protein, an F-box that regulates cell division, is degraded via the ubiquitin pathway. Plant Signal Behav. 2008;3(10):810–812.

141. Perilli S, Di Mambro R, Sabatini S. Growth and development of the root apical meristem. Curr Opin Plant Biol. 2012;15(1):17–23.

142. Hirano H, Shinmyo A, Sekine M. Arabidopsis G1 cell cycle proteins undergo proteasome-dependent degradation during sucrose starvation. Plant Physiol Biochem. 2011;49(6):687–691.

143. Hirano H, Shinmyo A, Sekine M. Both negative and positive G1 cell cycle regulators undergo proteasome-dependent degradation during sucrose starvation in Arabidopsis. Plant Signal Behav. 2011 sep;6(9):1394–6.

144. Polyn S, Willems A, De Veylder L. Cell cycle entry, maintenance, and exit during plant development. Curr Opin Plant Biol. 2015;23:1–7.

145. Peng L, Skylar A, Chang PL, Bisova K, Wu X. CYCP2;1 integrates genetic and nutritional information to promote meristem cell division in Arabidopsis. Dev Biol. 2014;393(1):160–170.

146. No Title;0.

147. Novak B, Csikasz-Nagy A, Gyorffy B, Chen K, Tyson JJ. Mathematical model of the fission yeast cell cycle with checkpoint controls at the G1/S, G2/M and metaphase/anaphase transitions. Biophys Chem. 1998;72(1-2):185–200.

148. Novak B, Pataki Z, Ciliberto A, Tyson JJ. Mathematical model of the cell division cycle of fission yeast. Chaos. 2001;11(1):277–286.

149. Tyson JJ, Csikasz-Nagy A, Novak B. The dynamics of cell cycle regulation. BioEssays. 2002;24(12):1095–1109.

150. Li B, Shao B, Yu C, Ouyang Q, Wang H. A mathematical model for cell size control in fission yeast. J Theor Biol. 2010;264(3):771–781.

151. Qu Z, MacLellan WR, Weiss JN. Dynamics of the cell cycle: checkpoints, sizers, and timers. Biophys J. 2003;85(6):3600–3611.

152. Csikász-Nagy A, Battogtokh D, Chen KC, Novák B, Tyson JJ. Analysis of a generic model of eukaryotic cell-cycle regulation. Biophys J. 2006;90(12):4361–4379.

153. Tyson JJ, Novak B. Temporal Organization of the Cell Cycle. Curr Biol. 2008;18(17):759–768.

154. Davidich MI, Bornholdt S. Boolean Network Model Predicts Knockout Mutant Phenotypes of Fission Yeast. PLoS One. 2013;8(9).

155. Irons DJ. Logical analysis of the budding yeast cell cycle. J Theor Biol. 2009;257(4):543–559.

156. Hong C, Lee M, Kim D, Kim D, Cho KH, Shin I. A checkpoints capturing timing-robust Boolean model of the budding yeast cell cycle regulatory network. BMC Syst Biol. 2012;6(1):129.

157. Singhania R, Sramkoski RM, Jacobberger JW, Tyson JJ. A hybrid model of mammalian cell cycle regulation. PLoS Comput Biol. 2011;7(2).

158. Zhao X, Harashima H, Dissmeyer N, Pusch S, Weimer AK, Bramsiepe J, et al. A General G1/S-Phase Cell-Cycle Control Module in the Flowering Plant Arabidopsis thaliana. PLoS Genet. 2012;8(8).

159. Apri M, Kromdijk J, de Visser PHB, de Gee M, Molenaar J. Modelling cell division and endoreduplication in tomato fruit pericarp. J Theor Biol. 2014 may;349:32–43.

160. Tyson JJ, Novak B. Regulation of the eukaryotic cell cycle: molecular antagonism, hysteresis, and irreversible transitions. J Theor Biol. 2001;210(2):249–263.

161. Guardavaccaro D, Pagano M. Stabilizers and Destabilizers Controlling Cell Cycle Oscillators. Mol Cell. 2006;22(1):1–4.

162. Zhang T, Schmierer B, Novak B. Cell cycle commitment in budding yeast emerges from the cooperation of multiple bistable switches. Open Biol. 2011;1(3):110009–110009.

163. Kapuy O, He E, López-Avilés S, Uhlmann F, Tyson JJ, Novák B. System-level feedbacks control cell cycle progression. FEBS Lett. 2009;583(24):3992–3998.

164. Ingolia N. Cell cycle: Bistability is needed for robust cycling. Curr Biol. 2005;15(23).

165. Ferrell JE, Tsai TYC, Yang Q. Modeling the cell cycle: Why do certain circuits oscillate? Cell. 2011;144(6):874–885.

166. Borghi L, Gutzat R, Fütterer J, Laizet Y, Hennig L, Gruissem W. Arabidopsis RETINOBLASTOMA-RELATED is required for stem cell maintenance, cell differentiation, and lateral organ production. Plant Cell. 2010;22(6):1792–1811.

167. Azpeitia E. Dynamic network-based epistasis analysis: Boolean examples. Front Plant Sci. 2011;2(December):1–12.

168. Wang RS, Saadatpour A, Albert R. Boolean modeling in systems biology: an overview of methodology and applications. Phys Biol. 2012;9(5):055001.

169. Ortiz-Gutiérrez E, García-Cruz K, Azpeitia E, Castillo A, de la Paz Sánchez M, Álvarez-Buylla ER. A Dynamic Gene Regulatory Network Model That Recovers the Cyclic Behavior of Arabidopsis thaliana Cell Cycle. PLoS Comput Biol. 2015;11(9):e1004486.

170. Adachi S, Nobusawa T, Umeda M. Quantitative and cell type-specific transcriptional regulation of A-type cyclin-dependent kinase in Arabidopsis thaliana. Dev Biol. 2009;329(2):306–314.

171. Mariconti L, Pellegrini B, Cantoni R, Stevens R, Bergounioux C, Cella R, et al. The E2F family of transcription factors from Arabidopsis thaliana. Novel and conserved components of the retinoblastoma/E2F pathway in plants. J Biol Chem. 2002;277(12):9911–9919.

172. Wildwater M, Campilho A, Perez-Perez JM, Heidstra R, Blilou I, Korthout H, et al. The RETINOBLASTOMA-RELATED gene regulates stem cell maintenance in Arabidopsis roots. Cell. 2005;123(7):1337–1349.

173. Boniotti MB, Gutierrez C. A cell-cycle-regulated kinase activity phosphorylates plant retinoblastoma protein and contains, in Arabidopsis, a CDKA/cyclin D complex. Plant J. 2001;28(3):341–350.

174. Dewitte W, Riou-Khamlichi C, Scofield S, Healy JMS, Jacqmard A, Kilby NJ, et al. Altered cell cycle distribution, hyperplasia, and inhibited differentiation in Arabidopsis caused by the D-type cyclin CYCD3. Plant Cell. 2003;15(1):79–92.

175. Marrocco K, Bergdoll M, Achard P, Criqui MC, Genschik P. Selective proteolysis sets the tempo of the cell cycle. Curr Opin Plant Biol. 2010;13(6):631–639.

176. Del Pozo JC, Diaz-Trivino S, Cisneros N, Gutierrez C. The E2FC-DPB Transcription Factor Controls Cell Division, Endoreplication and Lateral Root Formation in a SCF-Dependent Manner. Plant Signal Behav. 2007;2(4):273–274.

177. del Pozo JC, Diaz-Trivino S, Cisneros N, Gutierrez C. The balance between cell division and endoreplication depends on E2FC-DPB, transcription factors regulated by the ubiquitin-SCFSKP2A pathway in Arabidopsis. Plant Cell. 2006;18(9):2224–2235.

178. Lammens T, Boudolf V, Kheibarshekan L, Zalmas LP, Gaamouche T, Maes S, et al. Atypical E2F activity restrains APC/CCCS52A2 function obligatory for endocycle onset. Proc Natl Acad Sci U S A. 2008;105(38):14721–14726.

179. Haga N, Kobayashi K, Suzuki T, Maeo K, Kubo M, Ohtani M, et al. Mutations in MYB3R1 and MYB3R4 Cause Pleiotropic Developmental Defects and Preferential Down-Regulation of Multiple G2/M-Specific Genes in Arabidopsis. Plant Physiol. 2011;157(2):706–717.

180. Van Leene J, Hollunder J, Eeckhout D, Persiau G, Van De Slijke E, Stals H, et al. Targeted interactomics reveals a complex core cell cycle machinery in Arabidopsis thaliana. Mol Syst Biol. 2010;6(397):397.

181. Weinl C, Weinl C, Marquardt S, Kuijt SJH, Nowack MK, Jakoby MJ, et al. Novel Functions of Plant Cyclin-Dependent Kinase Inhibitors, ICK1/KRP1, Can Act Non-Cell-Autonomously and Inhibit Entry into Mitosis. Plant Cell. 2005;17(6):1704–1722.

182. Araki S, Ito M, Soyano T, Nishihama R, Machida Y. Mitotic cyclins stimulate the activity of c-Myb-like factors for transactivation of G2/M phase-specific genes in tobacco. J Biol Chem. 2004;279(31):32979–32988.

183. Wang H, Fowke LC, Crosby WL. A Plant Cyclin-dependent Kinase Inhibitor Gene. Nature. 1997;386:451–452.

184. Wang H, Qi Q, Schorr P, Cutler AJ, Crosby WL, Fowke LC. ICK1, a cyclin-dependent protein kinase inhibitor from Arabidopsis thaliana interacts with both Cdc2a and CycD3, and its expression is induced by abscisic acid. Plant J. 1998;15(4):501–510.

185. Zhang L, Wang C. F-box protein Skp2: a novel transcriptional target of E2F. Oncogene. 2006;25(18):2615–2627.

186. Rustici G, Mata J, Kivinen K, Lió P, Penkett CJ, Burns G, et al. Periodic gene expression program of the fission yeast cell cycle. Nat Genet. 2004;36(8):809–817.

187. Menges M, Hennig L, Gruissem W, Murray JaH. Cell cycle-regulated gene expression in Arabidopsis. J Biol Chem. 2002;277(44):41987–42002.

188. Menges M, Hennig L, Gruissem W, Murray JaH. Genome-wide gene expression in an Arabidopsis cell suspension. Plant Mol Biol. 2003;53(4):423–442.

189. Menges M, de Jager SM, Gruissem W, Murray JA. Global analysis of the core cell cycle regulators of Arabidopsis identifies novel genes, reveals multiple and highly specific profiles of expression and provides a coherent model for plant cell cycle control. Plant J. 2005;41(4):546–566.

190. Romero I, Fuertes A, Benito MJ, Malpica JM, Leyva A, Paz-Ares J. More than 80R2R3-MYB regulatory genes in the genome of Arabidopsis thaliana. Plant J. 1998;14(3):273–284.

191. Prouse MB, Campbell MM. The interaction between MYB proteins and their target DNA binding sites. Biochim Biophys Acta - Gene Regul Mech. 2012;1819(1):67–77.

192. Leone G, DeGregori J, Yan Z, Jakoi L, Ishida S, Williams RS, et al. E2F3 activity is regulated during the cell cycle and is required for the induction of S phase. Genes Dev. 1998;12(14):2120–2130.

193. Peters JM. SCF and APC: The yin and yang of cell cycle regulated proteolysis. Curr Opin Cell Biol. 1998;10(6):759–768.

194. Vodermaier HC. APC/C and SCF: Controlling each other and the cell cycle. Curr Biol. 2004;14(18):787–796.

195. Bashir T, Dorrello NV, Amador V, Guardavaccaro D, Pagano M. Control of the SCF(Skp2-Cks1) ubiquitin ligase by the APC/C(Cdh1) ubiquitin ligase. Nature. 2004;428(6979):190–193.

196. Shin R, Burch AY, Huppert Ka, Tiwari SB, Murphy AS, Guilfoyle TJ, et al. The Arabidopsis transcription factor MYB77 modulates auxin signal transduction. Plant Cell. 2007;19(8):2440–2453.

197. Team RC. R: A Language and Environment for Statistical Computing. 2012;.

198. Müssel C, Hopfensitz M, Kestler Ha. BoolNet-an R package for generation, reconstruction and analysis of Boolean networks. Bioinformatics. 2010;26(10):1378–1380.

199. Sánchez-Corrales YE, Álvarez-Buylla ER, Mendoza L. The Arabidopsis thaliana flower organ specification gene regulatory network determines a robust differentiation process. J Theor Biol. 2010;264(3):971–983.

200. Di Cara A, Garg A, De Micheli G, Xenarios I, Mendoza L. Dynamic simulation of regulatory networks using SQUAD. BMC Bioinformatics. 2007;8:462.

201. Mendoza L, Xenarios I. A method for the generation of standardized qualitative dynamical systems of regulatory networks. Theor Biol Med Model. 2006;3:13.

202. Rossignol P, Stevens R, Perennes C, Jasinski S, Cella R, Tremousaygue D, et al. AtE2F-a and AtDP-a, members of the E2F family of transcription factors, induce Arabidopsis leaf cells to re-enter S phase. Mol Genet Genomics. 2001;266(6):995–1003.

203. Heyman J, De Veylder L. The anaphase-promoting complex/cyclosome in control of plant development. Mol Plant. 2012;5(6):1182–1194.

204. Dewitte W, Scofield S, Alcasabas Aa, Maughan SC, Menges M, Braun N, et al. Arabidopsis CYCD3 D-type cyclins link cell proliferation and endocycles and are rate-limiting for cytokinin responses. Proc Natl Acad Sci U S A. 2007;104(36):14537–14542.

205. Jurado S, Díaz-Triviño S, Abraham Z, Manzano C, Gutierrez C, Pozo CD. SKP2A, an F-box protein that regulates cell division, is degraded via the ubiquitin pathway. Plant J. 2008;53(5):828–841.

206. Ferreira PC, Hemerly aS, Engler JD, van Montagu M, Engler G, Inzé D. Developmental expression of the arabidopsis cyclin gene cyc1At. Plant Cell. 1994;6(12):1763–1774.

207. Boudolf V, Barrôco R, Engler JDA, Verkest A, Beeckman T, Naudts M, et al. B1-type cyclin-dependent kinases are essential for the formation of stomatal complexes in Arabidopsis thaliana. Plant Cell. 2004;16(4):945–955.

208. Cheng Y, Cao L, Wang S, Li Y, Shi X, Liu H, et al. Downregulation of multiple CDK inhibitor ICK/KRP genes upregulates the E2F pathway and increases cell proliferation, and organ and seed sizes in Arabidopsis. Plant J. 2013;75(4):642–655.

209. Li Z, Larson-rabin Z, Masson PH, Day CD. FZR2/CCS52A1 mediated endoreduplication in Arabidopsis development. Plant Signal Behav. 2009;(May):451–453.

210. Takahashi N, Kajihara T, Okamura C, Kim Y, Katagiri Y, Okushima Y, et al. Cytokinins control endocycle onset by promoting the expression of an APC/C activator in arabidopsis roots. Curr Biol. 2013;23(18):1812–1817.

211. Espinosa-Soto C, Padilla-Longoria P, Alvarez-Buylla ER. A gene regulatory network model for cell-fate determination during Arabidopsis thalianal flower development that is robust and recovers experimental gene expression profiles. Plant Cell. 2004;16(11):2923–2939.

212. Benítez M, Espinosa-Soto C, Padilla-Longoria P, Alvarez-Buylla ER. Interlinked nonlinear subnetworks underlie the formation of robust cellular patterns in Arabidopsis epidermis: a dynamic spatial model. BMC Syst Biol. 2008;2:98.

213. Wittmann DM, Krumsiek J, Saez-Rodriguez J, Lauffenburger Da, Klamt S, Theis FJ. Transforming Boolean models to continuous models: methodology and application to T-cell receptor signaling. BMC Syst Biol. 2009;3:98.

214. Krumsiek J, Pölsterl S, Wittmann DM, Theis FJ. Odefy–from discrete to continuous models. BMC Bioinformatics. 2010;11:233.

215. Charvin G, Oikonomou C, Siggia ED, Cross FR. Origin of irreversibility of cell cycle start in budding yeast. PLoS Biol. 2010;8(1).

216. Menges M, Murray JaH. Synchronous Arabidopsis suspension cultures for analysis of cell-cycle gene activity. Plant J. 2002;30(2):203–212.

217. Azpeitia E, Benítez M, Vega I, Villarreal C, Alvarez-Buylla ER. Single-cell and coupled GRN models of cell patterning in the Arabidopsis thaliana root stem cell niche. BMC Syst Biol. 2010;4(1):134.

218. Barrio Ra, Romero-Arias JR, Noguez Ma, Azpeitia E, Ortiz-Gutiérrez E, Hernández-Hernández V, et al. Cell Patterns Emerge from Coupled Chemical and Physical Fields with Cell Proliferation Dynamics: The Arabidopsis thaliana Root as a Study System. PLoS Comput Biol. 2013;9(5):1–12.

219. Mu RL, Cao YR, Liu YF, Lei G, Zou HF, Liao Y, et al. An R2R3-type transcription factor gene AtMYB59 regulates root growth and cell cycle progression in Arabidopsis. Cell Res. 2009;19(11):1291–304.

220. Garduño Ochoa R. Hacia un enfoque de sistemas biológicos. México: CONACYT; 1985.

221. Pomerening JR, Sun YK, Ferrell JE. Systems-level dissection of the cell-cycle oscillator: Bypassing positive feedback produces damped oscillations. Cell. 2005;122(4):565–578.

222. Yao G, Tan C, West M, Nevins JR, You L. Origin of bistability underlying mammalian cell cycle entry. Mol Syst Biol. 2011;7(485):485.

223. Doerner P. Transcript. In: Verma DPS, Hong Z, editors. Cell Division Control in Plants. Berlin, Heidelberg: Springer Berlin Heidelberg; 2008. p. 13–32.

224. Gérard C, Goldbeter A. From simple to complex patterns of oscillatory behavior in a model for the mammalian cell cycle containing multiple oscillatory circuits. Chaos. 2010;20(4):045109.

225. Maher M, Cong F, Kindelberger D, Nasmyth K, Dalton S. Cell cycle-regulated transcription of the CLB2 gene is dependent on Mcm1 and a ternary complex factor. Mol Cell Biol. 1995;15(6):3129–3137.

226. Wittenberg C, Sugimoto K, Reed SI. G1-specific cyclins of S. cerevisiae: cell cycle periodicity, regulation by mating pheromone, and association with the p34CDC28 protein kinase. Cell. 1990;62(2):225–237.

227. Cooper K. Rb, whi it's not just for metazoans anymore. Oncogene. 2006;25(38):5228–5232.

228. Gauthier NP, Jensen LJ, Wernersson R, Brunak S, Jensen TS. Cyclebase.org: version 2.0, an updated comprehensive, multi-species repository of cell cycle experiments and derived analysis results. Nucleic Acids Res. 2010 jan;38(Database issue):D699–702.

229. Pramila T, Wu W, Miles S, Noble WS, Breeden LL. The forkhead transcription factor Hcm1 regulates chromosome segregation genes and fills the S-phase gap in the transcriptional circuitry of the cell cycle. Genes Dev. 2006;20(16):2266–2278.

230. Cooper S, Shedden K, Vu-Phan D. Invariant mRNA and mitotic protein breakdown solves the Russian Doll problem of the cell cycle. Cell Biol Int. 2009;33(1):10–18.

231. Cooper S. On a heuristic point of view concerning the expression of numerous genes during the cell cycle. IUBMB Life. 2012;64(1):10–17.

232. De Almeida Engler J, De Veylder L, De Groodt R, Rombauts S, Boudolf V, De Meyer B, et al. Systematic analysis of cell-cycle gene expression during Arabidopsis development. Plant J. 2009;59(4):645–660.

233. Jensen LJ, Jensen TS, de Lichtenberg U, Brunak S, Bork P. Co-evolution of transcriptional and post-translational cell-cycle regulation. Nature. 2006;443(7111):594–597.

234. Perrot-Rechenmann C. Cellular responses to auxin: division versus expansion. Cold Spring Harb Perspect Biol. 2010;2(5).

235. Overvoorde P, Fukaki H, Beeckman T. Auxin control of root development. Cold Spring Harb Perspect Biol. 2010;2(6):1–16.

236. Manzano C, Ramirez-Parra E, Casimiro I, Otero S, Desvoyes B, De Rybel B, et al. Auxin and Epigenetic Regulation of SKP2B, an F-Box That Represses Lateral Root Formation. Plant Physiol. 2012;160(2):749–762.

237. Perilli S, Perez-perez JM, Mambro RD, Peris L, Díaz-triviño S, Bianco MD, et al. RETINOBLASTOMA-RELATED protein stimulates cell differentiation in the Arabidopsis root meristem by interacting with cytokinin signaling. Plant Cell. 2013;25(11):4469–78.

238. Del Pozo JC, Manzano C. Auxin and the ubiquitin pathway. Two players-one target: The cell cycle in action. J Exp Bot. 2014;65(10):2617–2632.

239. Berckmans B, Vassileva V, Schmid SPC, Maes S, Parizot B, Naramoto S, et al. Auxin-Dependent Cell Cycle Reactivation through Transcriptional Regulation of Arabidopsis E2Fa by Lateral Organ Boundary Proteins. Plant Cell. 2011;23(10):3671–3683.

240. Jurado S, Abraham Z, Manzano C, López-Torrejón G, Pacios LF, Del Pozo JC. The Arabidopsis cell cycle F-box protein SKP2A binds to auxin. Plant Cell. 2010;22(12):3891–3904.

241. Ishida T, Adachi S, Yoshimura M, Shimizu K, Umeda M, Sugimoto K. Auxin modulates the transition from the mitotic cycle to the endocycle in Arabidopsis. Development. 2010;137(1):63–71.

242. Muraro D, Byrne H, King J, Voß U, Kieber J, Bennett M. The influence of cytokinin-auxin cross-regulation on cell-fate determination in Arabidopsis thaliana root development. J Theor Biol. 2011;283(1):152–167.

243. Hernández-Hernández V, Rueda D, Caballero L, Alvarez-Buylla ER, Benítez M. Mechanical forces as information: an integrated approach to plant and animal development. Front Plant Sci. 2014;5(June):265.

244. Kumpf RP, Nowack MK. The root cap: a short story of life and death. J Exp Bot. 2015;66(19):5651–5662.

245. Weinstein N, Mendoza L. A network model for the specification of vulval precursor cells and cell fusion control in Caenorhabditis elegans. Front Genet. 2013;4(JUN):1–24.

246. Davila-Velderrain J, Villarreal C, Alvarez-Buylla ER. Reshaping the epigenetic landscape during early flower development: induction of attractor transitions by relative differences in gene decay rates. BMC Syst Biol. 2015;9(1):1–14.

247. Wells DK, Kath WL, Motter AE. Control of Stochastic and Induced Switching in Biophysical Networks. Phys Rev X. 2015;5(3):031036.

ANEXO A

Artículo: Modelo del ciclo celular de *Arabidopsis*

A Dynamic Gene Regulatory Network Model That Recovers the Cyclic Behavior of *Arabidopsis thaliana* Cell Cycle

Elizabeth Ortiz-Gutiérrez[1,2], Karla García-Cruz[1], Eugenio Azpeitia[1,2¤], Aaron Castillo[1,2], María de la Paz Sánchez[1], Elena R. Álvarez-Buylla[1,2]*

1 Instituto de Ecología, Universidad Nacional Autónoma de México, 3er Circuito Exterior, Junto a Jardín Botánico Exterior, México, D.F. CP 04510, México, **2** Centro de Ciencias de la Complejidad-C3, Universidad Nacional Autónoma de México, Ciudad Universitaria, Apartado Postal 70–275, México, D.F. 04510, México

¤ INRIA project-team Virtual Plants, joint with CIRAD and INRA, UMR AGAP, Montpellier, France
* eabuylla@gmail.com

Abstract

Cell cycle control is fundamental in eukaryotic development. Several modeling efforts have been used to integrate the complex network of interacting molecular components involved in cell cycle dynamics. In this paper, we aimed at recovering the regulatory logic upstream of previously known components of cell cycle control, with the aim of understanding the mechanisms underlying the emergence of the cyclic behavior of such components. We focus on *Arabidopsis thaliana*, but given that many components of cell cycle regulation are conserved among eukaryotes, when experimental data for this system was not available, we considered experimental results from yeast and animal systems. We are proposing a Boolean gene regulatory network (GRN) that converges into only one robust limit cycle attractor that closely resembles the cyclic behavior of the key cell-cycle molecular components and other regulators considered here. We validate the model by comparing our *in silico* configurations with data from loss- and gain-of-function mutants, where the endocyclic behavior also was recovered. Additionally, we approximate a continuous model and recovered the temporal periodic expression profiles of the cell-cycle molecular components involved, thus suggesting that the single limit cycle attractor recovered with the Boolean model is not an artifact of its discrete and synchronous nature, but rather an emergent consequence of the inherent characteristics of the regulatory logic proposed here. This dynamical model, hence provides a novel theoretical framework to address cell cycle regulation in plants, and it can also be used to propose novel predictions regarding cell cycle regulation in other eukaryotes.

Author Summary

In multicellular organisms, cells undergo a cyclic behavior of DNA duplication and delivery of a copy to daughter cells during cell division. In each of the main cell-cycle (CC)

stages different sets of proteins are active and genes are expressed. Understanding how such cycling cellular behavior emerges and is robustly maintained in the face of changing developmental and environmental conditions, remains a fundamental challenge of biology. The molecular components that cycle through DNA duplication and citokinesis are interconnected in a complex regulatory network. Several models of such network have been proposed, although the regulatory network that robustly recovers a limit-cycle steady state that resembles the behavior of CC molecular components has been recovered only in a few cases, and no comprehensive model exists for plants. In this paper we used the plant *Arabidopsis thaliana*, as a study system to propose a core regulatory network to recover a cyclic attractor that mimics the oscillatory behavior of the key CC components. Our analyses show that the proposed GRN model is robust to transient alterations, and is validated with the loss- and gain-of-function mutants of the CC components. The interactions proposed for *Arabidopsis thaliana* CC can inspire predictions for further uncovering regulatory motifs in the CC of other organisms including human.

Introduction

The eukaryotic cell cycle (CC) in multicellular organisms is regulated spatio-temporally to yield normal morphogenetic patterns. In plants, organogenesis occurs over the entire lifespan, thus CC arrest, reactivation, and cell differentiation, as well as endoreduplication should be dynamically controlled at different points in time and space [1]. Endoreduplication is a variation of the CC, in which cells increase their ploidy but do not divide. Normal morphogenesis thus depends on a tight molecular coordination among cell proliferation, cell differentiation, cell death and quiescence. These biological processes share common regulators which are influenced by environmental and developmental stimuli [1–3]. It would not be parsimonious to depend on different regulatory circuits to control such interlinked cellular processes, CC behaviors and responses. Thus we postulate that a common network is deployed in all of them. Such overall conserved CC network may then connect to different regulatory networks underlying cell differentiation in contrasting tissue types or to signal transduction pathways elicited under different conditions, and thus yield the emergence of contrasting cellular behaviors in terms of cycling rate, entrance to endocycle, differentiation, etc.

Furthermore, the overall CC behaviors are widely conserved and robust among plants and animals. Hence, we aim at further investigating the collective behavior of the key upstream regulators and studied CC components to understand the mechanisms involved in the robustness of CC regulation under changing developmental stages and environmental conditions faced by plants along their life-cycles. Previous studies, that have shown the oscillatory behavior of several transcription factors, that had not been associated as direct regulators of the CC, support our proposed hypothesis [4]. We thus propose to uncovering the set of necessary and sufficient regulatory interactions underlying the core regulatory network of plant CC, including some key upstream transcriptional regulators.

Computational tools are essential to understanding the collective and dynamical behavior of these components within the regulatory networks involved. As a means of uncovering the main topological and architectural traits of such networks, we propose to use Boolean formalisms that are simple and have proven to be useful and powerful to follow changes in the activity of regulators of complex networks in different organisms and biological processes [5, 6].

Although the key CC components have been described in different organisms, the complexity and dynamic nature of the molecular interactions that are involved in CC regulation and

the emergence of the cyclic behavior of the CC molecular components are not well understood yet. The use of systemic, dynamic and mathematical or computational approaches has been useful towards this already. Previous models have focused mainly on yeast and animal systems and have been useful to analyze many traits of CC behavior such as robustness, hysteresis, irreversibility and bistability [7–11]. The latter two properties have been validated with experimental data [12–14].

We herein summarize the main traits and components of the eukaryotic CC. The molecular CC regulators have been described and they are well conserved across distantly related organisms [15, 16]. CC progression is regulated by Cyclin-Dependent Kinases (CDKs) [17] that associate with different cyclins to confer substrate specificity [18]. CDK-cyclin complexes trigger the transition from G1 (Gap 1) to synthesis phase (S phase) in where the genome is duplicated, and from G2 (Gap 2) to mitotic phase (M phase) for the delivery of the newly duplicated DNA to the two daughter cells [19] (see for a review [17, 20]). The CDK-cyclin activity also regulates the cell transit between G and S phases during the endoreduplication process [21, 22].

Two CDKs (CDKA and CDKB) are involved in CC regulation. CDKA;1-CYCDs and CDKA;1-CYCA3 complexes regulate G1/S and S phase progression [23–25]; while CDKB-CYCA2 and CDKB-CYCBs regulate G2/M phase and M progression [26–28]. Thus CDK-cyclin activity is finely-tuned by phosphorylation, interactions with CDK inhibitors such as Kip-related proteins (KRPs), and degradation of cyclins and KRPs by Skp1/Cullin/F-box (SCF), as well as by the anaphase-promoting complex/Cyclosome (APC/C) [29–31]. Besides these components, plant CC machinery has a greater number of CC regulators than other eukaryotes and some of those components such as the CDKB are plant-specific.

Several key transcriptional regulators participate in the G1/S and G2/M transitions [32]. The E2F/RBR pathway regulates G1/S transition by transcriptional modulation of many genes required for CC progression and DNA replication [33, 34]. While E2Fa and E2Fb with their dimerization partner (DP) activate transcription of a subset of S phase genes, E2Fc-DP represses transcription [35]. The function of E2Fa and E2Fb is inhibited by their interaction with RBR [36]; in G1/S transition CDKA;1-CYCD-mediated RBR hyperphosphorylation, releases E2Fa/b-DP heterodimers allowing transcriptional activation of E2Fa and E2Fb targets. Simultaneously the E2Fc-DP transcriptional inhibitor is degraded [37].

Little is known about the regulation of G2/M transition in plants, however a class of conserved transcription factors belonging to the MYB family has been described, that seem to have key roles in CC regulation. MYB transcription factors have a prominent role during G2/M transition, by regulating, for example, CYCB1;1 which is determinant in triggering mitosis [38–43]. For the mitosis exit, APC/C mediates degradation of the mitotic cyclins as CYCB1;1 and CYCA2;3, inactivating CDK-cyclin complexes. CCS52A2, an activator subunit of APC/C, is transcriptionally inhibited by E2Fe [44].

Some previous models have recovered the limit cycle attractor as well for CC components [45–48]. A pioneer model of the CC focused on mitotic CDK-cyclin heterodimer and a cyclin protease oscillatory behavior [49]. On the other hand, Novak and Tyson incorporated additional nodes and interactions to model the G1/S and G2/M transitions of the *S. pombe* CC [50, 51]. They also analyzed evolutionary roles of CC regulators [52], mutant phenotypes [53], stable steady states [7] and the role of cues such as cell size or pheromones in CC progression [54, 55]. Additionally, comprehensive CC continuous models [45] and generic modules for eukaryotic CC regulation [56, 57] have been proposed.

In addition to continuous formalisms, CC models have used discrete approaches as Boolean models for yeast and mammalian systems [46–48, 58–61], and more recently, hybrid models for mammalian cells have been published [62]. Subsequently, time-delayed variables [63] and variables defining CC events [47, 48] were incorporated. Time robustness was improved with

specifications of the temporal order with which each component is activated [60]. Recent published reports on CC dynamics use steady state probability distributions and potential landscapes, and highlight the enormous potential of CC models to characterize normal and altered regulation of mammalian CC [64, 65].

Yeast CC Boolean models with summatory thresholds [58, 59], incorporated self-degradation for proteins, but did not incorporate several negative regulators explicitly. In a later work [61], nodes were kept active when the summatory effect of their regulators was greater than the activation threshold, which implies self-degradation of the protein, when such summatory is equal to or below the threshold. Fauré and Thieffry have transformed CC Boolean models, that use threshold functions, to models with a combinatorial scheme, and they have also presented a broader discussion about these two approaches to logical frameworks [66].

Two Boolean models of budding yeast CC and another one of mammalian CC recover cyclic attractors [46–48]. The mammalian CC model [46] also recovers a fixed-point attractor corresponding to G0. In another study, Fauré and collaborators integrated three modules to yield a comprehensive model for the budding yeast CC GRN [47]. The components included variables to represent cellular growth, citokinesis, bud formation, DNA replication and the formation of the spindle. The yeast CC model by Irons also included variables of CC events (e.g. bud formation or DNA replication) as well as time delays [48]. In contrast to other eukaryotes, in *Arabidopsis thaliana* (*A. thaliana* herein) very few attempts have been made to integrate available experimental data on CC regulators using mechanistic models. Only a study that considers the G1/S transition has been proposed and contributed to show some additional conserved features of this CC control point among eukaryotes [67].

We integrated available experimental data on 29 *A. thaliana* regulatory interactions involved in CC progression into a Boolean discrete model, that recovers key properties of the observed plant CC. The regulatory network, that we put forward, also incorporates three uncovered interactions, based on animal systems (E2Fb → SCF, CDKB1;1-CYCA2;3 ⊣ E2Fa, APC/C ⊣ SCF), as well as 16 interactions based on bioinformatic analyses. Therefore, the latter proposed interactions constitute new predictions that should be tested experimentally. The use of yeast or animal data is supported by the fact that main CC components or regulatory motifs are conserved among eukaryotes [16]. In our model, we include solely molecular components and avoid artificial self-degradation loops, which have been used for recovering the limit cycle attractor. We validated the model simulating loss- and gain-of-function lines, and hence demonstrate that the Boolean network robustly implements true dynamical features of the biological CC regulatory network under wild type and genetic alterations. Possible artifacts due to the discrete dynamical nature of the model used, and of its synchronous updating scheme, were discarded by comparing the Boolean model results to those of a continuous approximation model. The continuous model indeed recovers the robust limit cycle that mimics the dynamical behavior of CC components under a wide range of parameters tested. Finally, we provide novel predictions that can be tested against biological experimental measurements in future studies. The model put forward constitutes a first mechanistic and integrative explanation to *A. thaliana* CC.

Materials and Methods

Boolean model

We proposed a Boolean approach to integrate and study the qualitative complex logic of regulation of the molecular components underlying the CC dynamics. We formalized available experimental data on logical functions and tables of truth that rule how the state of a particular component is altered as a function of the states of all the components that regulate it. In a Boolean model each node state can be 0, when the expression of a gene or other type of molecular

component or complex of such components is unexpressed or "OFF", or 1 when it is expressed, or "ON". Nodes states are updated according to the function: $X_i(t+1) = F_i(X_{i_1}(t), X_{i_2}(t), \ldots, X_{i_k}(t))$, where $X_i(t+1)$ is the state of X_i gene at time $t+1$ and $X_{i_1}(t), X_{i_2}(t), \ldots, X_{i_k}(t)$ is the set of its regulators at time t. The set of logical rules for all the network components defines the dynamics of the system. By applying the logical rules to all nodes for several iterations, the dynamics of the whole network can be followed until it reaches a steady state; a configuration or set of configurations that does not change any more or are visited in a cyclical manner, respectively. Such state is called an "attractor". Single-point attractors only have one GRN configuration, or cyclic attractors with period n, which have n configurations that are visited indefinitely in the same order. In this paper we propose a GRN model that converges to a single limit cycle attractor that recovers the CC molecular components' states of presence (network configuration) in a cyclic pattern that mimics the pattern observed for the molecular components included in the model along the different CC phase.

Model assumptions

A. thaliana CC Boolean model has the following assumptions:

1. Nodes represent mRNA, proteins or protein complexes involved in CC phase transitions. Node state "ON" is for the presence of regulator, and "OFF" is for absence; in the latter case, it may also indicate instances in which a component may be present but non-functional due to a post-translational modification.

2. The state of the RBR (RETINOBLASTOMA-RELATED) node corresponds to a 1 or "ON" when this protein is in its hypo-phosphorylated form and therefore is ready to inhibit E2F transcription factors.

3. When a particular CDK is not specified, a cyclin can form a complex with CDKA;1, a kinase that is always present because it is expressed in proliferative tissues [68] during the complete CC.

4. E2Fa, E2Fb and E2Fc need dimerization partner proteins (DPa or DPb) for its DNA-binding. Given that DP expression does not change drastically in CC [69], we assumed that the state of these heterodimers is given only by the presence of E2F factors.

5. The Boolean logical functions integrate and formalize experimental data available mainly for the *A. thaliana* root apical meristem, however some data from leaves were considered, and we assumed that these are also valid for CC regulation in the root meristem. Also, data from other systems and data obtained by sequence promoter analysis were considered as indicated in each case [27, 39, 40, 67, 70–85] (summarized in Table 1).

6. The dynamics of complex formation (such as CDK-cyclin and KRP1, or RBR and E2F factors) are specified directly in the Boolean function of their target genes. For instance, the logic rule for E2Fb is *E2Fa & !RBR*, indicating that E2Fb state is "ON" when it is transcriptionally activated by E2Fa free of RBR. All E2Fa targets also included in their logical rules RBR, as is shown in S1 Text. Then, the presence of KRP1 or RBR in a logical rule does not imply that they are regulators acting directly on the corresponding target.

7. The updating scheme for the node states was synchronous.

Periodic expression and promoter sequence analysis

Most regulatory interactions and logical rules were obtained from the *A. thaliana* data [20, 21, 25–27, 29, 30, 35, 37, 38, 40, 43, 44, 78–80, 85–103] (detailed in Table 2). *A. thaliana* CC-

Table 1. Hypothetical Interactions for the *A. thaliana* CC Network.

Regulator		Target	Data supporting the proposition of the interaction	Refs.
E2Fb	→	SCF	F-box protein Skp2 is part of the SCF complex and is transcriptionally regulated by E2F1 in humans. In *A. thaliana*, it has only been reported that E2F factors regulate FBL17, another F-box protein.	[67, 70]
E2Fb	→	MYB77	Direct regulation between E2F and MYB factors has been reported in budding yeast and mammals, but in plants it could include at least one intermediary; *A. thaliana* could have a similar regulation because its CC also presents transcriptional waves in G1/S and G2/M transitions as yeasts and mammals. After analyzing the two main families of transcription factors involved in CC regulation: TCP and MYB, we propose MYB77 as a mediator between E2F and MYB regulation. Using available microarray analyses, we found that MYB77 shows CC-dependent expression with a peak in M phase. In addition to having binding sites for E2F, with the identification of the binding site recognized by MYB77, we can hypothesize that MYB77 regulates MYB3R1/4 and other CC genes.	[39, 71–74]
MYB77	→	E2Fe, KRP1, MYB3R1/4, CYCB1;1, CYCA2;3, CDKB1;1, CCS52A2	The sequence CNGTTR identified as a consensus site recognized by MYB77 was used to find its possible targets among CC core genes. Several of them are expressed just before G2 to M phase transition.	[75–77]
MYB3R1/4	→	SCF, RBR, CDKB1;1, CYCA2;3, APC/C, E2Fc, MYB3R1/4, KRP1	The consensus site of MYB3R4 was found in SKP2A, RBR, CDKB1;1, CYCA2;3, CCS52A2, KRP1, E2Fc, MYB3R1/4 and CYCB1;1 by *in silico* analysis described in the Materials and Methods section. In tobacco, NtmybA1 and NtmybA2 genes have the MSA sequence and they can regulate themselves. MYB3R1/4 might promote the expression of KRP1, since KRP1 has a peak of expression in G2/M and has eight putative MSA elements. CYCB1;1 regulation by MYB3R1/4 also has experimental support.	[40, 78]
CDKB1;1-CYCA2;3	⊣	E2Fa	It has been hypothesized that a cause of low levels of E2Fa could be due to its high turnover rate as result of CDKB1;1 phosphorylation. This E2F factor has putative CDK-phosphorylation sites in its N-terminal end, and a high CDK activity inversely correlates with its DNA binding ability *in vitro*. This hypothesis is supported by observations in mammalian cells.	[27, 79–81]
APC/C	⊣	SCF	It was proposed that APC/C and SCF functions are mutually exclusive during CC progression, which led to the identification of the relationship amongst them. In proliferating mammal cells, levels of Skp2, a SCF subunit, oscillate under the pattern of APC/C substrates. Furthermore, the APC/C subunit Cdh1 participates in the degradation of Skp2 and the reduction of Cdh1 expression stabilizes Skp2. *A. thaliana* SCF and APC/C seem have the same roles during CC as their animal counterparts.	[82–85]

A summary of the data led us to propose interactions that have not been previously described for *A. thaliana* CC. ⊣ stands for negative regulation and → for positive regulation.

dependent expression data for validation was obtained from: [72–74]. The consensus site used for MYB77 was CNGTTR, according to: [75, 76], while that for MYB3R4 was AACGG according to: [43]. The motifs were searched in the regulatory sequences of all network nodes using Pathmatch tool (http://arabidopsis.org/cgi-bin/patmatch/nph-patmatch.pl) of TAIR. Regulatory sequences in TAIR10 Loci Upstream Sequences-1000bp and TAIR10 5' UTRs datasets were used.

Software for robustness analysis and mutant simulation

We used *BoolNet* [104] (a library of *R* language [105]) and *Atalia*(Á. Chaos; http://web.ecologia.unam.mx/achaos/Atalia/atalia.htm) to simulate the CC GRN dynamics and perform robustness, and mutant analyses. Systematic alterations in Boolean functions for robustness

Table 2. Experimental Interactions for the *A. thaliana* CC Network and their Evidence.

Regulator		Target	Description of the interaction	Refs.
CDKA;1-CYCD3;1	⊣	RBR	Studies suggest that complexes formed by CDKA;1 and D-type cyclins phosphorylate RBR.	[20, 86–89]
CDKA;1-CYCD3;1	⊣	RBR–E2Fb	E2Fb–RBR complex diminishes in CYCD3;1 overexpressor line.	[90]
CDKA;1-CYCD3;1	⊣	E2Fc	CDKA;1 bound to D-type cyclin affects formation of E2Fc-DPb complex and its binding to DNA. The recognition of E2Fc by the SCF complex depends on phosphorylation mediated by CDKA;1.	[35, 37, 91]
SCF	⊣	CYCD3;1	SCF is involved in the ubiquitination required for CYCD3;1 degradation.	[92]
SCF	⊣	KRP1	SCF ubiquitinates KRP1 to be degraded.	[85, 93]
SCF	⊣	E2Fc	E2Fc shows the accumulation in *skp2a* mutant (subunit of SCF); the overexpression of SKP2A reduces levels of E2Fc.	[35, 91]
RBR	⊣	E2Fa/b	RBR is a negative regulator of E2Fa/b transcriptional activity.	[90]
E2Fa	→	E2Fb	E2Fb transcription is induced in E2Fa overexpressor line.	[94]
E2Fa	→	E2Fc	E2Fc has binding sites for E2F and it is induced in E2Fa-DPa overexpressors.	[80, 94]
E2Fa	→	RBR	Transcriptional control of RBR is under E2Fa transcriptional activity.	[95]
E2Fa	→	APC/C	CCS52A2, a component of APC/C, is induced when RBR-free E2Fa is overexpressed.	[90]
E2Fb	→	CYCB1;1	CYCB1;1 expression is induced when RBR-free E2Fb increases; targets of E2Fb are genes needed for G2/M transition.	[79, 80, 90]
E2Fb	→	CDKB1;1	Inducible expression of E2Fb promotes CDKB1;1 expression.	[79]
E2Fb	→	E2Fe	E2Fb induces transcription of E2Fe.	[96]
E2Fc	⊣	CDKB1;1	The effect of E2Fb can be countered by E2Fc; with E2Fc destabilization increments CDKB1;1.	[96, 97]
E2Fc	⊣	CYCB1;1	CYCB1;1 expression increases when E2Fc expression is silenced; E2Fc overexpression reduces CYCB1;1 level.	[37]
E2Fc	⊣	E2Fa	E2Fa messengers increase when E2Fc expression is silenced.	[37]
E2Fc	⊣	E2Fe	E2Fc counteracts the positive effect that E2Fb has in the expression of E2Fe.	[96]
E2Fe	⊣	APC/C	Expression of CCS52A, a subunit of APC/C, is downregulated by E2Fe.	[44]
MYB3R1/4	→	CYCB1;1	MYB3R1/4 recognizes the sequence AACGG required for CYCB1;1 expression; other regulators seem to drive its G2/M-specific expression.	[38, 43]
CDKB1;1	—	CYCA2;3	CYCA2;3 interacts with CDKB1;1 to form a functional complex.	[25, 27]
CDKB1;1-CYCA2;3	⊣	KRP1	In complex with CYCA2;3, CDKB1;1 could promote KRP1 proteolysis as promotes KRP2 proteolysis; both KRPs could have similar roles in mitosis entry, since both interact with CDKA;1 and are expressed in G2/M.	[21, 27, 78]
CDKB1;1, CDKA;1	—	CYCB1;1	B-type cyclins interact with B-type and A-type CDKs.	[25, 26]
CDKA;1-CYCB1;1	→	MYB3R1/4	The overexpression of MYB3R4 enhances the 2-fold activity of its target promoters in comparison to WT, and the co-expression of MYB3R4 and CYCB1;1 enhances them 4-fold; CycB1 and other mitotic cyclins enhances the activity of NtmybA2 factors in tobacco.	[40, 98, 99]
KRP1	⊣	CYCD3;1	KRP1 is able to interact with CDKA;1 and CYCD3;1.	[29, 93, 100, 101]
KRP1	⊣	CYCB1;1	KRP1 binding to CDKA;1 inhibits the activity of CDKA–CYCB1;1.	[30, 100]
APC/C	⊣	CYCB1;1	The APC/C complex ubiquitinates CYCB1;1 to be degraded.	[102]
APC/C	⊣	CYCA2;3	CYCA2;3 is stabilized with loss-of-function mutations in APC/C subunits or with mutations in its D-box.	[27, 103]

Summary of experimental evidence supporting interactions of *A. thaliana* CC GRN. ⊣ represents negative regulation, → is for positive and — represents the formation of functional complex.

analyses were done with Atalia, while stochastic perturbations in random networks to compare attractor's robustness were done with BoolNet. For random perturbations made in transitions between network configurations or in Boolean functions, the "bitflip" method was applied. To validate the GRN model proposed here, we used BoolNet and simulated loss- and gain-of-function mutations for each node, by skipping the node's logical rule and setting the respective gene to "0" and "1", respectively.

Continuous model

For the continuous model, we followed [106, 107]. In the continuous version of the model the rate of change for each x_i node is represented by a differential equation that comprises production as well as decay rates:

$$\frac{dx_i}{dt} = \frac{-e^{0.5h} + e^{-h*(\omega_i)}}{(1 - e^{0.5h}) * (1 + e^{-h*(\omega_i - 0.5)})} - \gamma_i x_i \tag{1}$$

The parameter *h* determines the form of the curve; when *h* is very close to 0, the curve becomes a straight line, while with values close to 100, the curve approximates a step function. The parameter ω_i is the continuous form of $F_i(X_{i_1}(t), X_{i_2}(t), \ldots, X_{i_k}(t))$ used in the Boolean model, and γ_i is its degradation rate. Detailed information about the continuous model can be found in S2 Text.

Results

The regulatory network recovers a dynamical model of *A. thaliana* CC

The CC model proposed here integrates and synthesizes published data for *A. thaliana* CC components interactions, as well as some molecular data from other organisms (mammal and yeast), that we propose as predictions for *A. thaliana* CC regulation, and assume to be conserved among all eukaryotes. The whole set of interactions and nodes included in the model and detailed in Tables 1 and 2 are shown in Fig 1. Four types of molecular interactions can be distinguished: (i) transcriptional regulation, (ii) ubiquitination, (iii) phosphorylation and (iv) physical protein-protein interactions. Additionally, an *in silico* analysis of transcription factors and promoters was carried out, in order to further substantiate 16 predicted interactions in the GRN (these are: E2Fb → MYB77; MYB77 → E2Fe, MYB3R1/4, KRP1, CYCB1;1, CYCA2;3, CDKB1;1 and CCS52A2; MYB3R1/4 → SCF, RBR, CDKB1;1, CYCA2;3, APC/C, KRP1, E2Fc and MYB3R1/4). The logical rules are available in S1 Text.

Our results show that the nodes and interactions considered are sufficient to recover a single robust cyclic steady state, and thus the cyclic behavior of the components considered. Such behavior closely resembles the periodic patterns observed during actual CC progression, Fig 2. The first two columns or network configurations match a G1 state, given that during the early G1 phase, the CDKA;1-CYCD3;1 complex is absent or inactive by the presence of KRP1 [92, 93, 108]. The CDKA;1-CYCD3;1 state is given only by the presence of CYCD3;1 since CDKA;1 is always expressed in proliferative cells [68]. To facilitate understanding, in Fig 2 the complex CDKA;1-CYCD3;1 is shown instead of only CYCD3;1. The absence of mitotic cyclins (CYCA2;3 and CYCB1;1) at this stage [28, 38], as well as the APC/C presence until the early G1 phase, which is needed for the mitosis exit, also coincides with experimental observations [44, 109, 110]. The presence of the RBR protein in G1-phase implies an inactive state of the E2F, as expected [33, 111, 112]. Then, the third column resembles G1/S transition, where the presence of CDKA;1-CYCD3;1 complex would be inducing RBR phosphorylation and its inactivation [32]. In the fourth configuration, the S-phase is represented by RBR inactivation and E2Fa/b transcriptional activation [113]. In the fifth and sixth configuration, E2Fc state returns to "ON" but RBR state is kept in "OFF", which indicates that transcription driven by E2Fa and E2Fb can still happen. Indeed, the E2Fb factor appears from the fifth configuration and it is consistent with their function regulating the expression of genes needed to achieve the G2/M transition. In the sixth configuration, MYB77 is turned on, although in synchronization experiments it has been observed to be on until the beginning of mitosis [73]. During G2-phase the MYB transcription factors and KRP1 are expressed [31, 73, 93], the former would maintain
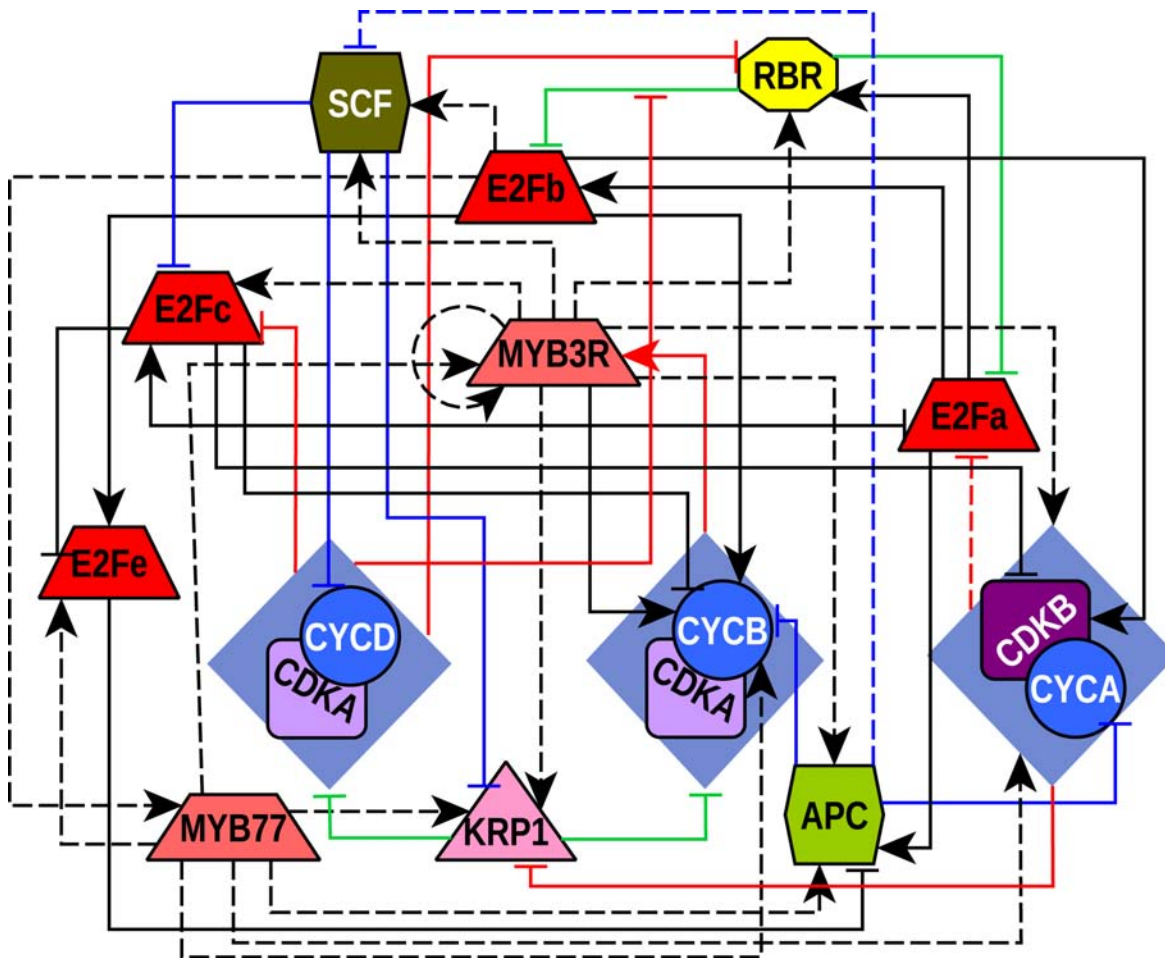
Fig 1. Regulatory network of the *A. thaliana* CC. The network topology depicts the proteins included in the model as well as the relationship among them. Nodes are proteins or complexes of proteins and edges stand for the existing types of relationships among nodes. The trapezoid nodes are transcription factors, the circles are cyclins, the squares are CDKs, the triangle represent stoichiometric CDK inhibitor, the hexagons are E3-ubiquitin ligase complexes and the octagon is a negative regulator of E2F proteins. Edges with arrow heads are positive regulations and edges with flat ends illustrate negative regulations. The red edges indicate regulation by phosphorylation while blue ones indicate ubiquitination, the green ones show physical protein-protein interactions and the black edges transcriptional regulation. Only CDK-cyclin interactions are not represented with a line. Interactions to or from rhombuses stand for interactions that involve the CDK as well as the cyclin. A solid line indicates that there is experimental evidence to support such interaction and dotted lines represent proposed interactions grounded on evidence from other organisms or *in silico* analysis.

doi:10.1371/journal.pcbi.1004486.g001

dimers of CDKA;1 and mitotic cyclins inactive; and together, this data is consistent with what is observed in the seventh configuration of the CC attractor. In the eighth column, KRP1 is lost because it was phosphorylated by CDKB1;1-CYCA2;3, which is active in the G2/M transition and the onset of mitosis [27]. The phosphorylation of KRP1 drives its degradation and posterior activation of mitotic complexes such as CDKA;1-CYCB1;1 to trigger mitosis [21, 78] (configuration 9 and 10 in Fig 2). The lack of APC/C at the onset of mitosis is determinant for the accumulation of the mitotic cyclins, but APC/C presence is necessary for the mitosis exit [110], which occurs in the eleventh configuration of the attractor (Fig 2). Thus, our CC GRN model recovers a unique attractor of eleven network configurations (Fig 2), which shows a congruent
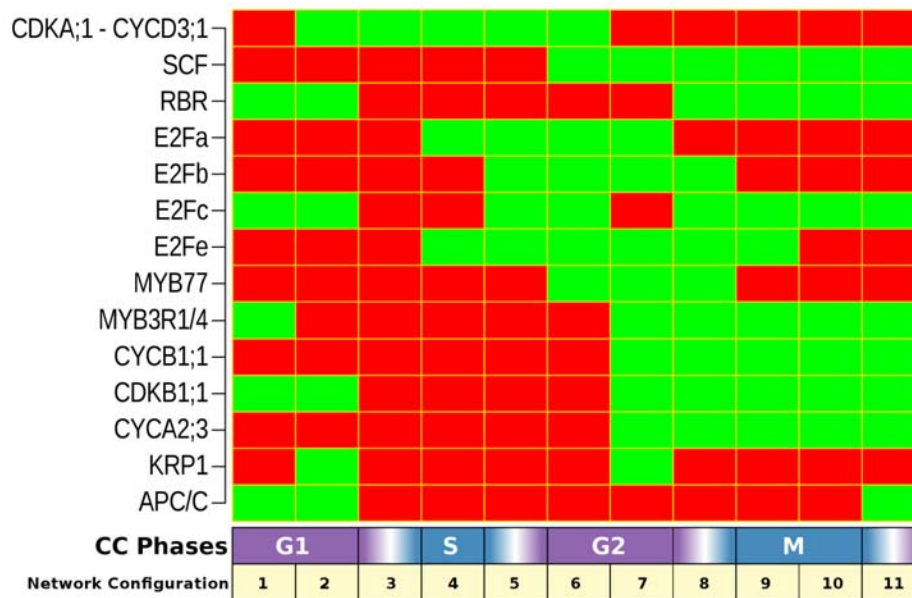
Fig 2. Attractor corresponding to a dynamic network of CC in *A. thaliana*. 100% of the whole set of network configurations converges to a unique attractor composed by 11 configurations. Each column is a network configuration (state of each network component) and the rows represent the state of each node during CC progression. The squares in green indicate components that are in an "ON" state and the ones in red are nodes in an "OFF" state.

cyclic behavior of its components with that observed experimentally. This result validates that the proposed set of restrictions converge to a single cyclic behavior, which is independent of the initial conditions. A further validation of the proposed CC model, would imply that the recovered cyclic attractor is robust to permanent alterations, as is the case for real CC behavior that is highly robust to external and internal perturbations [14, 58, 114, 115].

The CC Boolean model is robust to alterations

To provide further validation for the proposed CC regulatory network, we performed robustness analyses of the attractor to four types of alterations in the logical functions of the model. First, we altered the output of each logical rule by systematically flipping one by one, each one of their bits. We found that 87.47% of the perturbed networks recovered the original attractor, while 1.77% of the altered networks maintained the original attractor and produced new ones (see supplementary material S3 Text for details). In contrast, the remaining 10.76% of alterations reduced the number of network configurations of the original attractor. In the second robustness analysis, after calculating the transitions between one network configuration to the next one, one bit (i.e. the state of a node) of this next configuration is randomly chosen and its value changed. Then, the network is reconstructed and its attractors recovered again. This procedure was repeated 100 times, thus we found that in 88.2 ± 3.2 out of the 100 perturbations (mean ± SD) the original attractor was reached. These results suggest that the proposed GRN for *A. thaliana* CC is robust to alterations as expected and in coincidence with previous GRN models proposed for other developmental processes [116, 117].

To confirm that the robustness recovered in these two types of analyses is a specific property of the network under study, we performed robustness analyses of randomly generated

networks with similar structures (same number of input interactors for the logical functions) to the one proposed here for the *A. thaliana* CC regulatory network, and compared the above robustness analyses results to those recovered for equivalent analyses for the random networks. We generated 1000 random networks. Then, 100 copies of the random and of our network were done. In each copy we randomly flipped the value of one bit in one logical function (to confirm the first robustness analysis), or in one next configuration (for the second robustness analysis). When perturbations are made in logical functions, the *A. thaliana* CC GRN recovers its attractor in 68% of perturbations, while the median of percentage of cases in which such attractor was recovered in the random networks was only 18.55% (mean 19.12% ± 13.86 SD, Fig 3A). The difference between the 68% of this latter analysis and the 87.47% of the first robustness analysis could be due to sampling error. If transitions between network configurations are perturbed, the median of original attractors recovered in random networks is 24.2% (mean 24.6% ± 18.2 SD). In contrast, the original attractor of *A. thaliana* CC GRN was found in 88% of perturbed networks starting with that grounded on experimental data (Fig 3B). These results confirm that the CC GRN proposed here is much more robust than randomly generated networks with similar topologies and suggests that its robustness is not due to overall structural properties of the network.

Boolean models can produce cyclic dynamics as an artifact due to their discrete nature and the time delays implied. To address this issue we approximated the Boolean model to a continuous system of differential equations following [106, 107, 118, 119]. To recover steady states of such continuous system, the continuous versions of the GRN were evaluated for 1000 different randomly picked initial conditions (See S2 Text). In all cases and independently of the methodology (i.e. [106, 107] or [118, 119]), we recovered the same limit cycle steady state. In the continuous model, key cyclins for the main phase transitions, CYCD3;1 and CYCB1;1, have an oscillatory behavior that is not attenuated with time (Fig 4). Importantly, this result is robust to changes in the decay rates or alterations of the *h* parameter that affects the shape of activation function (see details in S2 Text); the limit cycle was recovered in 92.86% of the cases. The results of the continuous model corroborate that the limit cycle attractor recovered by the Boolean version, is not due to an artifact associated to the discrete and synchronous nature of the Boolean model, but is rather an emergent property of the underlying network architecture and topology. In addition, the recovery of the cyclic behavior of the continuous model constitutes a further robustness test for the Boolean model.

Previous studies have also tested asynchronous updating schemes [46]. In this study we have used a continuous form of the model to discard that the recovered cyclic attractor is due to an artifact owing to the discrete and synchronous nature of the model used. Future studies could approach analyses of asynchronous behavior of the model by devising some priority classes distinguishing fast and slow processes, and thus refining the asynchronous attractor, under a plausible updating scheme. On the other hand, biological time delays may be involved in CC progression, but they are not enough for irreversibility. The CC unidirectionality has been proposed to be a consequence of system-level regulation [120], here we hypothesize that the ordered transitions of *A. thaliana* CC are an emergent property of network architecture and dynamics.

Simulated loss- and gain-of-function mutants recover observed patterns: normal CC and endocycle

An additional validation analysis for the proposed *A. thaliana* CC model implies simulating loss- and gain-of-function mutations and comparing the recovered attractors with the expression profiles documented experimentally for each mutant tested. We simulated mutants by fixing the corresponding node to 0 or 1 in loss- and gain-of-functions mutations, respectively.
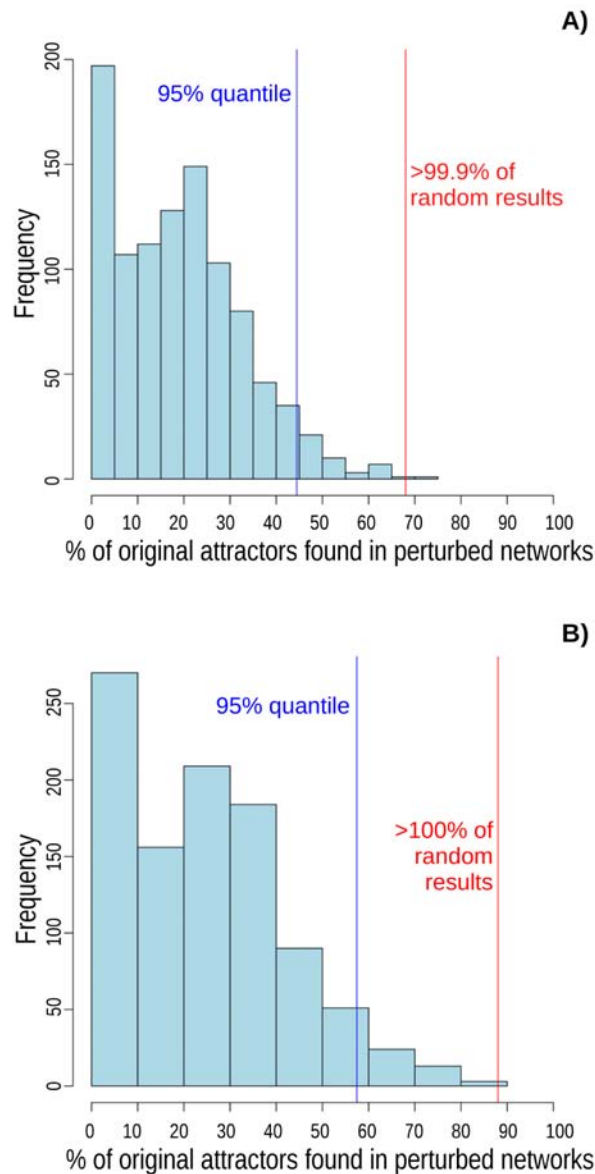
Fig 3. Attractor robustness analysis. Random networks with similar structure to *A. thaliana* CC GRN were less tolerant to perturbations than original CC GRN. The frequency of perturbations that recovered the original attractor after a perturbation in the Boolean functions, is shown in: (A), where the red line indicates that *A. thaliana* CC GRN recovers its original attractor in 68% of perturbations (the median of random networks was 18.55% and mean 19.12% ± 13.86 SD). When transitions between network configurations are perturbed (B), *A. thaliana* CC GRN recovers its original attractor in 88% (vertical red line) of perturbations, while the median of random networks that recover the original attractor was 24.2% (mean 24.6% ± 18.2 SD). Vertical blue line indicates the 95% quantile. 1000 random networks were analyzed.

doi:10.1371/journal.pcbi.1004486.g003

CDK-Cyclin activity
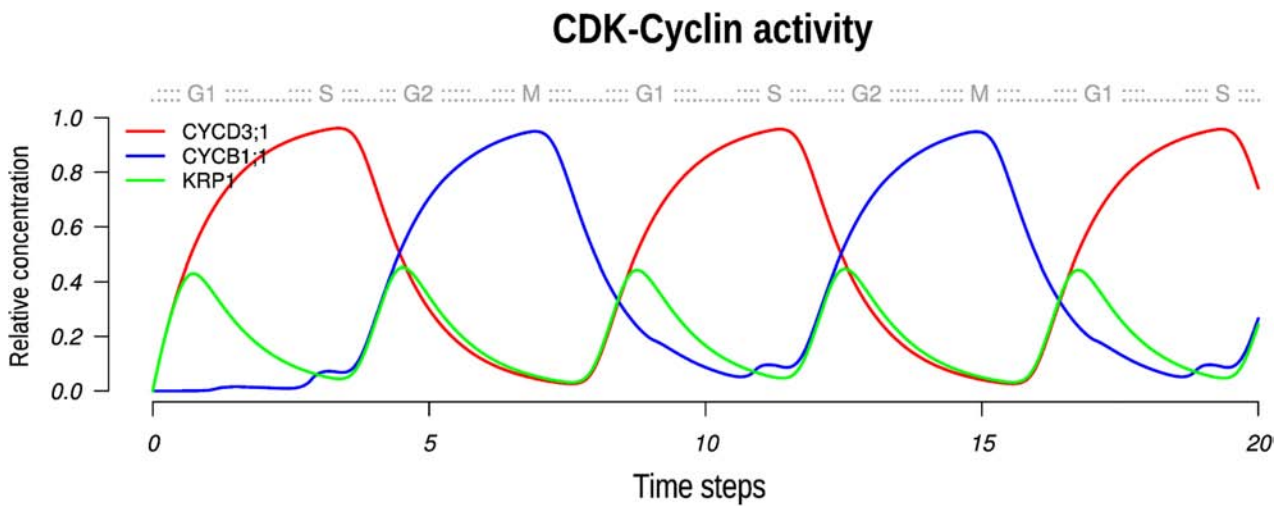
Fig 4. Continuous version of the *A. thaliana* CC Boolean model. In this graph we show the activity of the CDKA;1-CYCD3;1 and the CDKA;1-CYCB1;1 complexes as a function of the amount of cyclins, and KRP1 inhibitor. The CDK-cyclin activity is the limiting factor to pass the G1/S and the G2/M checkpoints. A little more than two complete CC are shown (upper horizontal axis) to confirm that oscillations are maintained.

The recovered altered configurations are summarized in S4 Text, and in Table 3 as well as in Table 4 for gain- and loss-of-function mutants, respectively. The simulated mutant attractors are coherent with experimental data in most cases [2, 21, 23, 30, 35, 37, 43, 44, 76, 79, 80, 88, 90–93, 103, 108, 109, 111, 113, 114, 121–129]. In Fig 5 we show a representative example of attractors recovered by simulations of CDKB1;1 and KRP1 loss-of-function and APC/C and E2Fa gain-of-function mutants. It is noteworthy that several simulated mutants, such as mitotic cyclins or B-type CDK loss-of-function, converge to a cyclic attractor that corresponds to the configuration observed under an endoreduplicative cycle (e.g. Fig 5A). In such attractors, endoreduplication inductors, such as APC/C, KRP1 and E2Fc [37, 78, 130] are present, at least in some network configurations (Fig 5A, 5C and 5D-right). Another outstanding feature of these mutant attractors is that, although mitotic CDK-cyclin complex may be present, it is inhibited by KRP1, therefore there is no CDK-cyclin activity to trigger the onset of mitosis. These data are coincident with the reported regulation during the onset of endoreduplication [21]. In the attractors where E2Fa coincides with alternating states of RBR, it suggests that DNA replication may occur (Fig 5). Likely due to plant redundancy, some mutations do not produce an obvious impaired phenotype. Such is the case of KRP1 loss-of-function, in which loss-of-function simulation, a cyclic attractor identical to the original one is recovered, as is expected (see Table 4), because such mutants do not show an evident altered CC behavior (Fig 5B) [93].

Interestingly, the simulation of a constitutively active APC/C also converges to a single cyclic attractor, which corresponds to an endoreduplication cycle, since it has Gap and S phases, but lacks an M-phase configuration. This coincides with the experimental observation that the overexpression of one of the APC/C subunits (CCS52A) promotes entry to an endo-cycle [44] (see Table 3). Another interesting example is the gain-of-function mutation of E2Fa that yields two cyclic attractors, one corresponding to the normal CC cycle and the other one

Table 3. Phenotypes of gain-of-function mutations in CC components.

Node	Phenotypes of gain of function	Recovered attractor(s)	Refs.	Model
CYCD3;1	Inhibition of CC exit, increases division zones and ectopic divisions. Decreases G1 phase duration and increases G2 duration. Delays expression of G2/M genes.	Fixed-point attractor of G2-phase.	[108, 121]	PA
SCF	SKP2A gain-of-function enhances proliferation, and increases number of cells in G2/M and ploidy levels decrease.	Oscillates between G1 and S.	[122, 123]	NR
RBR	CC arrest, cells in root apical meristem lose CYCB1;1 expression; in rice, the number of cells synthesizing DNA decrease.	Fixed-point attractor characterizing G1 arrest.	[2, 88]	A
E2Fa	Mitosis and endoreduplication are promoted.	One attractor comprising 40.48% of initial conditions that is a WT CC. The other closely resembles an endocycle but APC/C activity is lower (59.52% of configurations).	[111, 113]	A
E2Fb	Cell division is induced but endoreduplication is suppressed; CC duration and cells are shorter, and the amount of S-phase transcripts increases.	Similar to WT but with a shorter S phase.	[79, 80]	A
E2Fc	Overexpression of a non-degradable form of E2Fc leads to larger cells or a lack of division.	Fixed-point attractor where only E2Fc and CYCD3;1 are present, congruent with a CC-arrest.	[35]	PA
E2Fe	Reduces ploidy levels.	CC arrest in M phase.	[44]	PA
MYB77	Plants are stunted but there is no information about how CC could be affected.	CC arrest in a mitotic state.	[76]	-
MYB3R1/4	No available data about how it could alter cell division.	Two fixed-point attractors of CC arrest at early G1 phase, state of E2Fa varies among them.	-	-
CYCB1;1	Root growth enhanced, slightly small cells.	WT CC	[124]	A
CDKB1;1	Does not seem to affect CC behavior.	WT CC	[125]	A
CYCA2;3	Not enough to produce multicellular trichomes but the proportion of polyploid cells is less.	WT CC	[103]	A
KRP1	CC arrest and inhibition of cell proliferation, G2 phase is longer; a weak overexpression of KRP2 led to an increment in DNA ploidy.	Attractor with period 2 oscillating between G1 and G1/S transition.	[21, 30, 126]	PA
APC/C	Gain-of-function of APC/C subunit CCS52A2 enhanced endoreduplication entry; more cells with increased DNA ploidy.	Cyclic attractor pointing to endocycle.	[44]	A

Summary of mutant phenotypes and recovered attractors simulating that mutation. **A** means that the result of simulation is in Agreement with the data available in the reference(s). **PA** means it is Partially Agrees with evidence, because not all expected traits were reproduced by the attractor but this does not contradict the mutant phenotype. **NR** are attractors that do not make sense with expected behavior and therefore, the model did Not Recover the mutant phenotype.

doi:10.1371/journal.pcbi.1004486.t003

to an endocycle (Table 3). It has been shown that this gene is required for both processes [111] that are apparently exclusive, although in both processes the DNA replication occurs and among E2Fa targets there are genes required for S-phase. Thus our model suggests that the regulation of E2Fa at the end of G2 phase is decisive for CC exit and transition to endoreduplication. In this E2Fa gain-of-function simulation, we found an inconsistency with APC/C because this E3 ubiquitin ligase is decisive for endoreduplication, while in the simulated attractor is only present in one network configuration (Fig 5D-right). Such behavior observed in the endoreduplication attractor for E2Fa gain-of-function leads to unstable activity in the CDK-cyclin complex (Fig 5D), thus suggesting that the increase in APC/C is required for endoreduplication entry as well as its progression. In the attractor of the simulated APC/C gain-of-function, the states of the CYCD3;1, SCF, E2Fb, E2Fc and MYB nodes are more stable than in

Table 4. Phenotypes of loss-of-function mutations in CC components.

Node	Phenotypes of loss of function	Recovered attractor(s)	Refs.	Model
CYCD3;1	When this cyclin is depleted by sucrose starvation, cells are arrested in G1 phase; in adult leaves, triple mutant of *cycd3;1–3* led to a diminished number of cells.	Period 2 oscillating between G1 and G1/S transition.	[23, 92]	A
SCF	Plants with a diminished level of SKP2 do not show obvious affected development but KRP1 is accumulated.	Similar to a normal CC but endoreduplication would be favored by the KRP1 stabilization.	[93]	A
RBR	Proliferation is promoted and cell differentiation is impaired; downregulation of RBR in rice promotes an increase of cells in S-phase.	One attractor of a normal CC (includes 81.98% of possible configurations) and other attractor oscillates among G2-S-G2 (18.02% of configurations).	[127]	A
E2Fa	Expression of E2Fb, RBR and other CC regulators decrease; more cells in G1 and G2 with respect to WT.	Fixed-point attractor with E2Fe and CYCD3;1 present suggesting an arrest in a Gap phase.	[90]	PA
E2Fb	Without information.	Fixed-point attractor representing the G1/S transition.	-	-
E2Fc	Mitotic proteins such as CYCB1;1 have increased expression, ploidy is reduced.	Fixed-point attractor of M phase arrest.	[37, 91]	PA
E2Fe	Increased endoreduplication.	Attractor of endoreduplication (period 7).	[44]	A
MYB77	Lower density of lateral roots, inconclusive data to evaluate simulation.	CC of seven configurations.	[76]	-
MYB3R1/4	Lower levels of G2/M transcripts, incomplete cell division, some embryos only have one cell with multiple nuclei.	2 attractors, the first seems a three-configurations endocycle, and the second is a CC of seven configurations where APC/C is always absent.	[43]	A
CYCB1;1	Cyclin widely used as a marker of cell proliferation, its absence is associated with differentiated cells.	Attractor characterizing endocycle (period 8), intriguingly APC/C is never present.	[128]	-
CDKB1;1	Overexpression of a dominant negative allele leads to enhanced endoreduplication.	Attractor of endoreduplication (period 11).	[129]	A
CYCA2;3	In null mutants, cells with 2C DNA content decreases before than in WT, endocycles begin before and are faster than in WT.	Attractor which is an endocycle (period 7).	[103]	PA
KRP1	No evident phenotypic effects observed but relative kinase activity increases to 1.5 in relation to WT.	A CC without alterations.	[114]	A
APC/C	Loss of CCS52A2 function (activator subunit of APC/C) produces a decrement in the number of meristematic cells without affecting endoreduplication index; cells in quiescent center become mitotically active.	Fixed-point attractor of a CC arrest previous to conclude mitosis.	[109]	PA

Summary of mutant phenotypes and recovered attractor when that mutation was simulated. Abbreviations in Model column are as in Table 3.

endoreduplication attractors of CDKB1;1 loss-of-function or E2Fa gain-of-function, where E2Fb, E2Fc and MYB factors expression states alternate between "ON" and "OFF" (Fig 5).

We highlight APC/C gain-of-function simulations, as it provides a possible mechanism for plant hormones action over the CC machinery and, thus how such key morphogens regulate cell proliferation patterns. Recently, Takahashi and collaborators reported a direct connection between cytokinins and CC machinery in *A. thaliana* root [131]. The authors showed that ARR2, a transcriptional factor of cytokinins signaling, induces expression of APC/C activator protein CCS52A1. Our simulated APC/C gain-of-function is congruent with that observation, since it reproduces the configuration attained by a cell entering an endocycle when APC/C activity is enhanced (Fig 5C), as it happens at the elongation zone of *A. thaliana* root. Therefore, our model is able to recover the attractors of loss- and gain-of-function mutant phenotypes reported experimentally, and it thus provides a mechanistic explanation for observed patterns of expression in both normal CC and during endoreduplication cycles or endocycle.
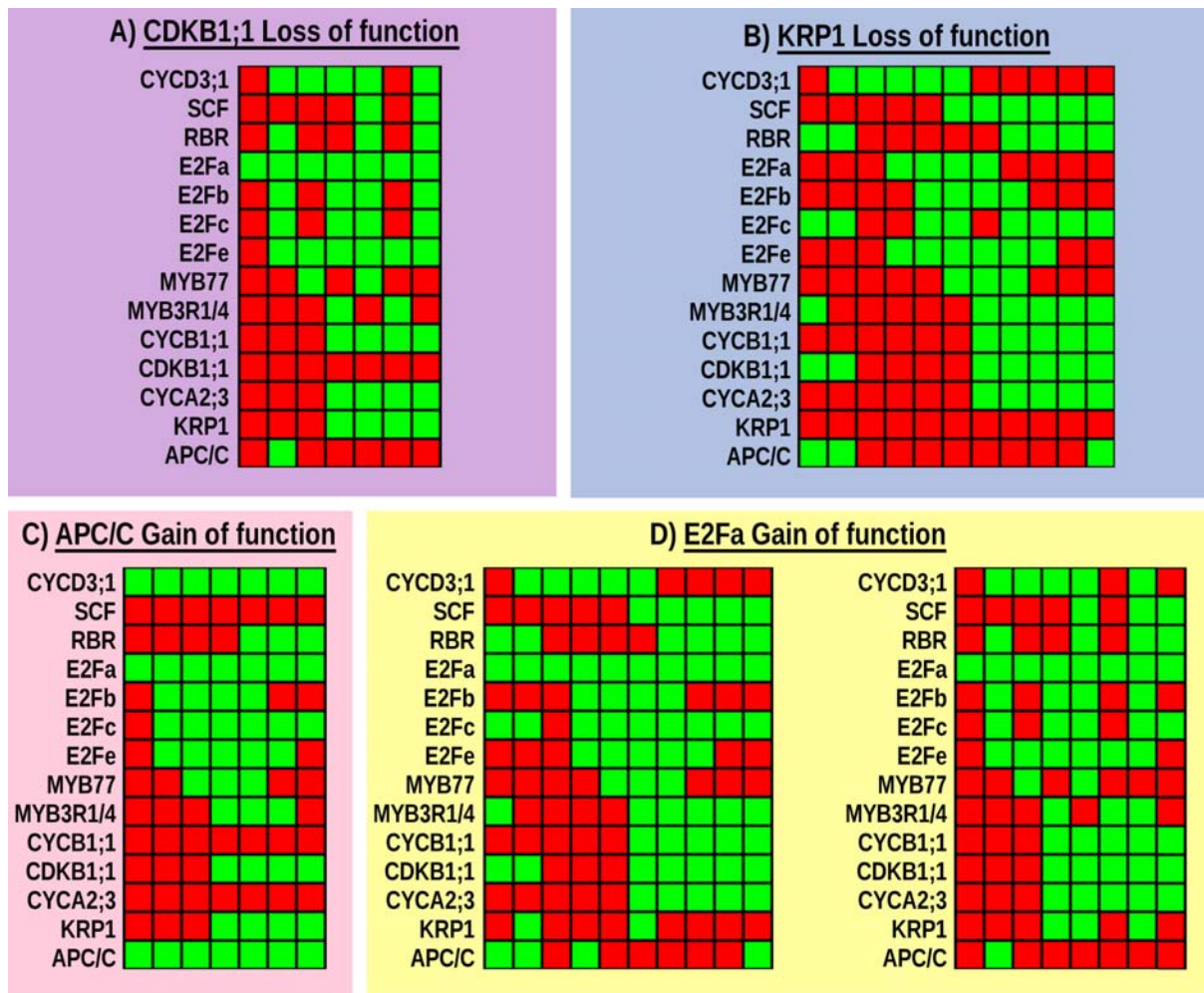
Fig 5. Attractors recovered by simulations of loss- or gain-of-function mutants of four CC components. (A) The simulation of loss of CDKB1;1 function produced only one cyclic attractor with period 7 that resembles G1 → S → G2 → G1 cycle, whereas in (B) with simulation of loss of KRP1 function, one cyclic attractor was attained, which has period 11 and comprises 100% of the initial conditions. This attractor is almost identical to WT phenotype but without KRP1. With the simulation of APC/C gain-of-function, a single attractor with period 7 was recovered, which is shown in (C) and is consistent with an endoreduplication cycle. Attractors obtained with the simulation of E2Fa overexpression are shown in (D). Two attractors were found, one of them has period 10 and the 40.48% of the initial conditions converge to that cycle that is closely similar to the WT CC attractor. The second attractor that correspond to E2Fa overexpression has period 8 and it is very similar to the endoreduplication attractor of loss of CDKB1;1 function, which comprises 59.52% of possible network configurations.

doi:10.1371/journal.pcbi.1004486.g005

Plant E2Fc and KRP1: validation of *A. thaliana* CC GRN

We test if the CC GRN recovers the periodic patterns observed in synchronization experiments of *A. thaliana* CC molecular components. Interestingly, the E2Fc repressor and KRP1 are regulators that have two short lapses of expression in the attractor recovered in the continuous model ([Fig 6](#)), and experimentally they also show two peaks of expression when synchronized with aphidicolin [74]. In such synchronization experiments, the expression of E2Fc increases
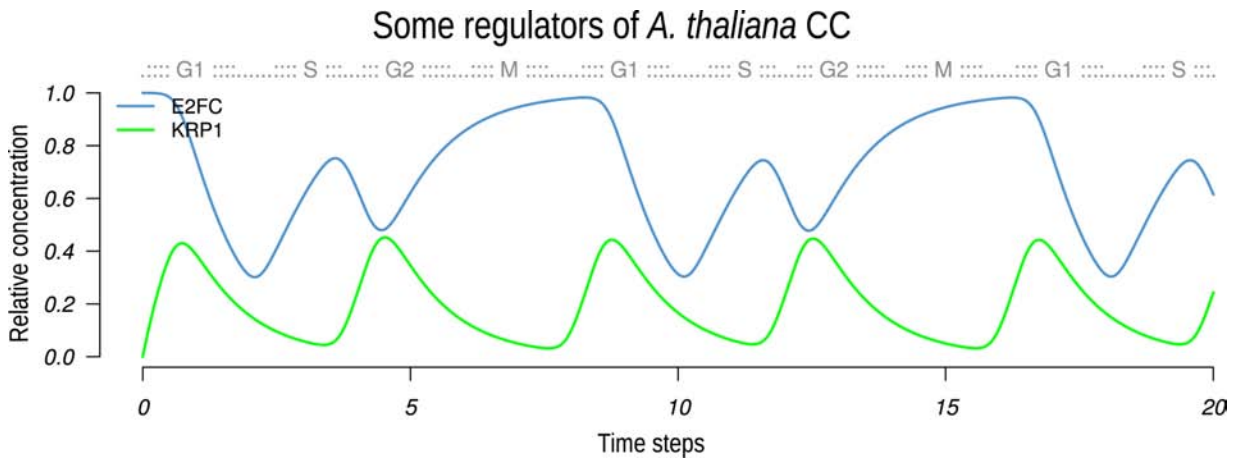
Fig 6. Dynamical behavior of E2Fc and KRP1 according to the continuous model. These nodes were chosen by their peculiar pattern of expression, which was qualitatively recovered by the Boolean and continuous models.

from late S to middle G2, but then it decreases dramatically in late G2. In the model, E2Fc appears from S to G2 phase, and then a second increment of E2Fc expression in G2/M is observed. The latter correspondence is a further validation of the CC GRN model proposed here. Furthermore, synchronization experiments using sucrose have shown that KRP1 is expressed previous to G1/S transition and before mitosis [132], in a similar way that occurs in the model. More recently it has been proposed that KRP1 has a role during G1/S and G2/M transitions [93]; the latter should be important for endoreduplication control [78]. Once again, such roles and expression profiles are consistent with the recovered active state of KRP1 in our model.

In contrast with the consistent behaviors of E2Fc and KRP1 components to recovered results with our model, E2Fe results do not coincide with previous observations. In our model this E2F factor presents only one peak from S to early M phase, but according to synchronization experiments [69], E2Fe has two peaks of expression. One of its peaks is due to regulation by other E2F family factors during S phase, while the G2/M peak could be due to MSA elements. Indeed, when the regulatory motifs for E2F binding are deleted from E2Fe, it can still be expressed although at lower levels [96], suggesting that additional transcription factors regulate its expression. Such factors could belong to the MYB family as suggested for the *A. thaliana* CC GRN proposed here.

Discussion

The canonical cyclic behavior of eukaryotic cells as they go from DNA duplication to cytokinesis suggests that a conserved underlying mechanism with shared molecular components and/ or regulatory logic should exist. While yeast and animal CC have been thoroughly studied and modelled, plant CC is less studied and no comprehensive model for it has been proposed.

In this study we put forward a Boolean model of the *A. thaliana* CC GRN. We show that this model robustly recovers a single cyclic attractor or steady state with 11 network configurations. Such configurations correspond to those observed experimentally for the CC components included here at each one of the CC stages. In addition, the canonical order of sequential transitions that is recovered also mimics the observed temporal pattern of transition from one

configuration to another one along the CC ([Fig 2](#)). The fact that the 16,384 initial conditions of the proposed system converge to this single cyclic attractor already suggests that the GRN comprises a robust module that integrates the necessary and sufficient set of components and interactions to recover molecular oscillations experimentally observed. The proposed GRN is also robust to alterations, being similarly robust to previously published models for other cell differentiation or developmental modules [116, 117, 133]. The model is validated because it recovers *A. thaliana* wild type and altered (in gain- and loss-of-function) configurations and cycling behaviors. The comparison between experimentally observed and recovered gene configurations is summarized in Tables [3](#) and [4](#).

Some cyclins such as CYCD3;1 and CYCB1;1, important components during G1/S and G2/M transitions, show a mutually exclusive regulation, as occurs in a predator-prey Lotka-Volterra dynamical system [134], even though they do not interact directly. Their mutual exclusion is achieved thanks to the coordinated expression of genes with specific proteolytic degradation capacity. Our cyclic attractor shows two transcriptional periods, one of them in S-phase regulated by E2F-RBR pathway, and the second one operating at a time previous to M-phase and regulated by MYB transcription factors. The SCF and APC/C ubiquitin ligases work during G2-to-M phases, and during mitosis exit, respectively. Therefore, the fourteen nodes and their interactions proposed in the CC GRN constitute a necessary and sufficient set of restrictions to recover the oscillations of node states characteristic of CC phases.

Two alternative possibilities could drive CC progression in actual organisms. The first would imply that transitions from one CC state to the next would require external cues, like the cell size. The alternative possibility is that CC progression and the temporal pattern of transitions among stages are both emergent consequences of an underlying complex regulatory network, and do not require external cues, or these only reinforce such temporal progression emergent from complex underlying regulatory interactions. Our CC GRN model supports the latter. This does not imply that several internal or external signals or molecules, such as hormones or other types of cues could alter the CC. Therefore, the two alternative possibilities are not exclusive but they likely complement or enhance each other. Indeed, *A. thaliana* CC is regulated by plant hormones, light, sucrose, osmotic stress [135] or oxidative stress [136]. These could now be modelled as CC modulators.

In the model proposed here we avoided redundancy. For instance, the KRP1 node represents the KRP family members that share several functions. Also the metaphase-anaphase transition could be added to the model when more data about APC/C regulation (i.e. negative feedback loop comprising CDK-cyclin complexes, or the regulation of Cdc20 homologues) becomes available in plants. Apparently, these simplifications did not disrupt the main features of the *A. thaliana* CC, since the cyclic behavior distinctive of the CC components was correctly recovered.

A mechanistic model for the *A. thaliana* CC: novel predictions

Our proposed GRN model suggests some predictions regarding the regulation of certain CC components in *A. thaliana*. Such predictions can be classified into two types. The first type pertains to those recovered by *in silico* promoter analysis. The predictions of the second type were inferred from data of other eukaryotes, because they seem to imply conserved components and some evidence from *A. thaliana* suggested that these interactions are part of the CC GRN in *A. thaliana*. Three interactions belong to the second type, E2Fb → SCF, CDKB1;1-CYCA2;3 ⊣ E2Fa and APC/C ⊣ SCF (see [Table 1](#) for a synthesis of hypothetical interactions). Although some evidence supports the idea that these interactions could exist in *A. thaliana*, they should be corroborated with additional experimental examination.

Our model provides a dynamic explanation to the cyclic behavior of certain transcription factors and predicts a novel interaction for E2F and MYB regulators; they connect waves of periodic expression that seem to be key for the robust limit cycle attractor that characterizes CC behavior. Interestingly, previous studies have shown that such periodic transcription can be maintained even in the absence of S-phase and mitotic cyclins [4], which underpin the role of a transcription factor network oscillator for the correct CC progression [137]. A regulatory interaction between E2F and MYB factors (or among the equivalent regulators) may be conserved among other eukaryotes (e.g. mammals and yeast), but there is no experimental support yet for it in *A. thaliana*. After looking for the same direct evidence in *A. thaliana* and not finding it, we thought about an alternative regulatory mechanism that consists in transcription factors acting between E2F and MYB. Hence, we decided to analyze the important transcription factor families known so far, to find out if one of their members could be mediating the regulation between E2F and MYB. The TCP (for Teosinte branched 1, Cycloidea, PCF) and the MYB family were chosen because they have been reported to be involved in CC regulation [42]. Based on their gene expression patterns and promoter sequence analysis, MYB77 was our best candidate: it is expressed at the beginning of M phase, and could be regulated by E2F and regulator of MYB (see Table 1). A second possibility might be that several tissue-specific transcription factors are involved in E2F-MYB genetic regulation (e.g. GL3, MYB88, SHR/SCR [17], MYB59 [138] or even members of the MADS box gene family could be implied). Indeed, we have recently documented that a MADS-box gene, XAL1, encodes a transcription factor that regulates several CC components (García-Cruz et al., in preparation).

A. thaliana CC in comparison to animal and yeast CC

Differences among eukaryotic CCs allow us to recognize or characterize alternative mechanisms for the regulation of CC. The first difference between GRN of *A. thaliana* CC and that of other eukaryotes, concerns the number of duplicates of some key regulators. *A. thaliana* has up to ten copies of some of the genes that encode for CC regulators (e.g. families of cyclins or CDK), while yeast, mammals or the algae *Ostreococcus tauri*, have much fewer duplicates [20, 139–141]. The only exception concerns the homologues of Retinoblastoma protein, of which there are three members in humans and mouse, and only one copy in *A. thaliana* [127]. Future models should address the explicit role of CC duplicated components in the plastic response of plant development to environmental conditions. Being sessile, such developmental adjustments, as plants grow under varying environments, are expected to be more important, complex and dynamic than in motile yeast and animals. One possibility is that different members of the same gene family are linked to different transduction pathways of signals that modulate CC dynamics.

The second difference among *A. thaliana* and other CC was regarding the transcriptional regulation throughout the GRN underlying it. For instance, *S. cerevisiae* does not have RBR or E2F homologues, but instead has Whi5, Swi4,6 and Mbp1 proteins which perform equivalent regulatory functions to the former CC components [142, 143]. *S. cerevisiae* does not have any MYB transcription factors but it presents other transcriptional regulators, such as Fkh1/2, Ndd1 and Mcm1 [142, 144, 145], which regulate the G2/M transition in a similar way to MYBs in mammals.

Contrary to the conservation in G1/S transition [15, 67], molecular components controlling G2/M transition seem to vary among different eukaryotes. It seems that molecules such as WEE1 kinase and CDC25 phosphatase are not conserved. In *A. thaliana*, CDC25-like has phosphatase and arsenate-reductase functions [146], while *A. thaliana* WEE1 phosphorylates monomeric CDKA;1 *in vitro* [147], and *Nicotiana tabacum* WEE1 inhibits CDK activity *in*

vitro [148]. However the lack of any obvious mutant phenotype of CDC25 or WEE1 loss-of-function mutants predicts that these genes are not involved in the regulation of a normal CC. Additionally, although WEE1 has a role during DNA damage [146, 149], does not seem to have a CDKA;1 recognition domain [150]. CDC25-like does not have the required sites for CDKA;1 recognition [150]. In summary, the positive regulatory feedback between CDKA;1 and CDC25-like, as well as the mutual-inhibitory feedback loop between CDKA;1 and WEE1, seem not to be conserved in *A. thaliana*.

Given all that evidence for G2/M regulation, we integrated the regulatory interactions between stoichiometric CDK inhibitor (KRP1), B-type plant specific CDK and MYB transcriptional factors. It is not surprising that there are clear differences between plant G2 phase regulation and that of other organisms, because variations in this control point could define cell fate. Although differences among the *A. thaliana* CC GRN uncovered here and that of yeasts and animals have now become clear, we think that the basic regulatory CC module reported here, will be a useful framework to incorporate and discover new components of the CC GRNs in plants and also in other eukaryotes.

Despite the fact that our CC GRN model recovers observed CC stage configurations and their canonical pattern of temporal transitions, it did not recover an alternative attractor that corresponds to the endocycle. We hypothesize that the same multi-stable GRN underlies both states, and additional components yet to be connected to the CC GRN will ensure a cyclic attractor corresponding to the complete CC, and another one with shorter period corresponding to the endocycle. In its present form, our model suggests that CYCD3;1 function, which has been associated with the proliferative state [108] and with a delay in the endocycle onset [23], is important to enter the endocycle. Besides, it also has been reported that CYCD3;1 plays a role in G1/S transition [121] and regulates RBR protein during DNA replication [89]. Furthermore, the endoreduplication attractor obtained in some of our mutant simulations (e.g. Fig 5A, 5C and 5D-right) also supports the role of CYCD3;1 in entering an endocycle.

The GRN model of *A. thaliana* CC could help to identify physiological or developmental interactions involved in the tight relationship between proliferation and differentiation observed during different stages of development [1, 88, 108, 109, 126]. Previous to cell division, the cell senses its intracellular and environmental conditions to arrest or promote CC progress. Such cues directly affect the CC machinery, which does not depend on a master or central regulator.

CC control is the result of a network formed by feedback and feedforward loops between complexes of CDK-cyclin and its regulators. It is not evident how complex dynamical processes such as CC progression emerge from simple interactions among components acting simultaneously. The proposed CC GRN will be very helpful to study how cell proliferation/differentiation decisions and balance keeps a suitable spatio-temporal control of CC during plant growth and development.

Supporting Information

S1 Text. Logical rules of *A. thaliana* CC Boolean model.
(PDF)

S2 Text. Equations, parameters, analysis of parameters and initial conditions of the continuous version of *A. thaliana* CC model.
(PDF)

S3 Text. New recovered attractors by robustness analysis. Additional attractors yielded by making alterations in each bit of logical functions.
(PDF)

S4 Text. Attractors obtained in the simulation of mutant phenotypes.
(PDF)

Author Contributions

Analyzed the data: AC EA EOG ERAB MPS KGC. Wrote the paper: EOG ERAB MPS. Conceived and coordinated the study and established the overall logic and core questions to be addressed: ERAB Conceived and planned the modeling approaches and specific analyses to be done: EOG ERAB Recovered all the information from the literature: AC EA EOG MPS KGC Established the logical functions: EA EOG Programmed and ran all the modeling and analyses: EA EOG.

References

1. Ramirez-Parra E, Desvoyes B, Gutierrez C. Balance between cell division and differentiation during plant development. Int J Dev Biol. 2005; 49:467–77. doi: 10.1387/ijdb.052001er PMID: 16096957

2. Dudits D, Abrahám E, Miskolczi P, Ayaydin F, Bilgin M, Horváth GV. Cell-cycle control as a target for calcium, hormonal and developmental signals: the role of phosphorylation in the retinoblastoma-centred pathway. Ann Bot. 2011 5; 107(7):1193–202. doi: 10.1093/aob/mcr038 PMID: 21441245

3. Ubeda-Tomas S, Beemster GT, Bennett MJ. Hormonal regulation of root growth: integrating local activities into global behaviour. Trends Plant Sci. 2012;.

4. Orlando DA, Lin CY, Bernard A, Wang JY, Socolar JES, Iversen ES, et al. Global control of cell-cycle transcription by coupled CDK and network oscillators. Nature. 2008 6; 453(7197):944–7. doi: 10.1038/nature06955 PMID: 18463633

5. Azpeitia E, Benítez M, Padilla-Longoria P, Espinosa-Soto C, Alvarez-Buylla ER. Dynamic network-based epistasis analysis: Boolean examples. Front Plant Sci. 2011; 2(92). doi: 10.3389/fpls.2011.00092 PMID: 22645556

6. Wang RS, Saadatpour A, Albert R. Boolean modeling in systems biology: an overview of methodology and applications. Phys Biol. 2012 10; 9(5):055001. doi: 10.1088/1478-3975/9/5/055001 PMID: 23011283

7. Tyson JJ, Novak B. Regulation of the eukaryotic cell cycle: molecular antagonism, hysteresis, and irreversible transitions. J Theor Biol. 2001; 210(2):249–63. doi: 10.1006/jtbi.2001.2293 PMID: 11371178

8. Guardavaccaro D, Pagano M. Stabilizers and destabilizers controlling cell cycle oscillators. Mol Cell. 2006; 22(1):1–4. doi: 10.1016/j.molcel.2006.03.017 PMID: 16600864

9. Zhang T, Schmierer B, Novak B. Cell cycle commitment in budding yeast emerges from the cooperation of multiple bistable switches. Open Biol. 2011; 1(3). doi: 10.1098/rsob.110009 PMID: 22645649

10. Kapuy O, He E, Lopez-Aviles S, Uhlmann F, Tyson JJ, Novak B. System-level feedbacks control cell cycle progression. FEBS Lett. 2009; 583(24):3992–8. doi: 10.1016/j.febslet.2009.08.023 PMID: 19703449

11. Ingolia N. Cell cycle: bistability is needed for robust cycling. Curr Biol. 2005 12; 15(23):R961–3. doi: 10.1016/j.cub.2005.11.012 PMID: 16332526

12. Pomerening JR, Kim SY, Ferrell JE. Systems-level dissection of the cell-cycle oscillator: bypassing positive feedback produces damped oscillations. Cell. 2005 8; 122(4):565–78. doi: 10.1016/j.cell.2005.06.016 PMID: 16122424

13. Charvin G, Oikonomou C, Siggia ED, Cross FR. Origin of irreversibility of cell cycle start in budding yeast. PLoS Biol. 2010 1; 8(1):e1000284. doi: 10.1371/journal.pbio.1000284 PMID: 20087409

14. Yao G, Tan C, West M, Nevins JR, You L. Origin of bistability underlying mammalian cell cycle entry. Mol Syst Biol. 2011; 7:485. doi: 10.1038/msb.2011.19 PMID: 21525871

15. Cross FR, Buchler NE, Skotheim JM. Evolution of networks and sequences in eukaryotic cell cycle control. Philos Trans R Soc Lond B Biol Sci. 2011; 366(1584):3532–44. doi: 10.1098/rstb.2011.0078 PMID: 22084380

16. Jensen LJ, Jensen TS, de Lichtenberg U, Brunak S, Bork P. Co-evolution of transcriptional and post-translational cell-cycle regulation. Nature. 2006 10; 443(7111):594–7. PMID: 17006448

17. Komaki S, Sugimoto K. Control of the plant cell cycle by developmental and environmental cues. Plant Cell Physiol. 2012 6; 53(6):953–64. doi: 10.1093/pcp/pcs070 PMID: 22555815

18. Peeper DS, Parker LL, Ewen ME, Toebes M, Hall FL, Xu M, et al. A- and B-type cyclins differentially modulate substrate specificity of cyclin-cdk complexes. EMBO J. 1993 5; 12(5):1947–54. PMID: 8491188

19. Nieuwland J, Scofield S, Murray JAH. Control of division and differentiation of plant stem cells and their derivatives. Semin Cell Dev Biol. 2009 12; 20(9):1134–42. doi: 10.1016/j.semcdb.2009.09.011 PMID: 19770062

20. Inzé D, De Veylder L. Cell cycle regulation in plant development. Annu Rev Genet. 2006; 40:77–105. doi: 10.1146/annurev.genet.40.110405.090431 PMID: 17094738

21. Verkest A, Manes CL, Vercruysse S, Maes S, Van Der Schueren E, Beeckman T, et al. The cyclin-dependent kinase inhibitor KRP2 controls the onset of the endoreduplication cycle during Arabidopsis leaf development through inhibition of mitotic CDKA;1 kinase complexes. Plant Cell. 2005; 17 (6):1723–36. doi: 10.1105/tpc.105.032383 PMID: 15863515

22. Beemster GT, De Veylder L, Vercruysse S, West G, Rombaut D, Van Hummelen P, et al. Genome-wide analysis of gene expression profiles associated with cell cycle transitions in growing organs of Arabidopsis. Plant Physiol. 2005 6; 138(2):734–43. doi: 10.1104/pp.104.053884 PMID: 15863702

23. Dewitte W, Scofield S, Alcasabas AA, Maughan SC, Menges M, Braun N, et al. Arabidopsis CYCD3 D-type cyclins link cell proliferation and endocycles and are rate-limiting for cytokinin responses. Proc Natl Acad Sci U S A. 2007; 104(36):14537–42. doi: 10.1073/pnas.0704166104 PMID: 17726100

24. Boruc J, Inze D, Russinova E. A high-throughput bimolecular fluorescence complementation protein-protein interaction screen identifies functional Arabidopsis CDKA/B-CYCD4/5 complexes. Plant Signal Behav. 2010; 5(10):1276–81. doi: 10.4161/psb.5.10.13037 PMID: 20861687

25. Van Leene J, Hollunder J, Eeckhout D, Persiau G, Van De Slijke E, Stals H, et al. Targeted interactomics reveals a complex core cell cycle machinery in Arabidopsis thaliana. Mol Syst Biol. 2010; 6:397. doi: 10.1038/msb.2010.53 PMID: 20706207

26. Weingartner M, Criqui MC, Meszaros T, Binarova P, Schmit AC, Helfer A, et al. Expression of a non-degradable cyclin B1 affects plant development and leads to endomitosis by inhibiting the formation of a phragmoplast. Plant Cell. 2004; 16(3):643–57. doi: 10.1105/tpc.020057 PMID: 15004270

27. Boudolf V, Lammens T, Boruc J, Van Leene J, Van Den Daele H, Maes S, et al. CDKB1;1 forms a functional complex with CYCA2;3 to suppress endocycle onset. Plant Physiol. 2009; 150(3):1482–93. doi: 10.1104/pp.109.140269 PMID: 19458112

28. Vanneste S, Coppens F, Lee E, Donner TJ, Xie Z, Isterdael GV, et al. Developmental regulation of CYCA2s contributes to tissue-specific proliferation in Arabidopsis. EMBO J. 2011 8; 30(16):3430–41. doi: 10.1038/emboj.2011.240 PMID: 21772250

29. De Veylder L, Beeckman T, Beemster GT, Krols L, Terras F, Landrieu I, et al. Functional analysis of cyclin-dependent kinase inhibitors of Arabidopsis. Plant Cell. 2001 7; 13(7):1653–68. doi: 10.1105/TPC.010087 PMID: 11449057

30. Wang H, Zhou Y, Bird DA, Fowke LC. Functions, regulation and cellular localization of plant cyclin-dependent kinase inhibitors. J Microsc. 2008 8; 231(2):234–46. doi: 10.1111/j.1365-2818.2008.02039.x PMID: 18778421

31. Verkest A, Weinl C, Inze D, De Veylder L, Schnittger A. Switching the cell cycle. Kip-related proteins in plant cell cycle control. Plant Physiol. 2005; 139(3):1099–106. doi: 10.1104/pp.105.069906 PMID: 16286449

32. De Veylder L, Joubes J, Inze D. Plant cell cycle transitions. Curr Opin Plant Biol. 2003; 6(6):536–43. doi: 10.1016/j.pbi.2003.09.001 PMID: 14611951

33. Gutierrez C, Ramirez-Parra E, Castellano MM, del Pozo JC. G1 to S transition: more than a cell cycle engine switch. Curr Opin Plant Biol. 2002; 5(6):480–6. doi: 10.1016/S1369-5266(02)00301-1 PMID: 12393009

34. de Jager SM, Menges M, Bauer UM, Murra JA. Arabidopsis E2F1 binds a sequence present in the promoter of S-phase-regulated gene AtCDC6 and is a member of a multigene family with differential activities. Plant Mol Biol. 2001 11; 47(4):555–68. doi: 10.1023/A:1011848528377 PMID: 11669580

35. del Pozo JC, Boniotti MB, Gutierrez C. Arabidopsis E2Fc functions in cell division and is degraded by the ubiquitin-SCF(AtSKP2) pathway in response to light. Plant Cell. 2002; 14(12):3057–71. doi: 10.1105/tpc.006791 PMID: 12468727

36. Henley SA, Dick FA. The retinoblastoma family of proteins and their regulatory functions in the mammalian cell division cycle. Cell Div. 2012; 7(1):10. doi: 10.1186/1747-1028-7-10 PMID: 22417103

37. del Pozo JC, Diaz-Trivino S, Cisneros N, Gutierrez C. The balance between cell division and endoreplication depends on E2FC-DPB, transcription factors regulated by the ubiquitin-SCFSKP2A pathway in Arabidopsis. Plant Cell. 2006; 18(9):2224–35. doi: 10.1105/tpc.105.039651 PMID: 16920782

38. Planchais S, Perennes C, Glab N, Mironov V, Inze D, Bergounioux C. Characterization of cis-acting element involved in cell cycle phase-independent activation of Arath;CycB1;1 transcription and identification of putative regulatory proteins. Plant Mol Biol. 2002; 50(1):111–27. doi: 10.1023/A:1016018711532 PMID: 12139003

39. Zhu W, Giangrande PH, Nevins JR. E2Fs link the control of G1/S and G2/M transcription. EMBO J. 2004 11; 23(23):4615–26. doi: 10.1038/sj.emboj.7600459 PMID: 15510213

40. Ito M. Conservation and diversification of three-repeat Myb transcription factors in plants. J Plant Res. 2005; 118(1):61–9. doi: 10.1007/s10265-005-0192-8 PMID: 15703854

41. Nakata Y, Shetzline S, Sakashita C, Kalota A, Rallapalli R, Rudnick SI, et al. c-Myb contributes to G2/M cell cycle transition in human hematopoietic cells by direct regulation of cyclin B1 expression. Mol Cell Biol. 2007; 27(6):2048–58. doi: 10.1128/MCB.01100-06 PMID: 17242210

42. Berckmans B, De Veylder L. Transcriptional control of the cell cycle. Curr Opin Plant Biol. 2009 10; 12 (5):599–605. doi: 10.1016/j.pbi.2009.07.005 PMID: 19700366

43. Haga N, Kobayashi K, Suzuki T, Maeo K, Kubo M, Ohtani M, et al. Mutations in MYB3R1 and MYB3R4 cause pleiotropic developmental defects and preferential down-regulation of multiple G2/M-specific genes in Arabidopsis. Plant Physiol. 2011 10; 157(2):706–17. doi: 10.1104/pp.111.180836 PMID: 21862669

44. Lammens T, Boudolf V, Kheibarshekan L, Zalmas LP, Gaamouche T, Maes S, et al. Atypical E2F activity restrains APC/CCCS52A2 function obligatory for endocycle onset. Proc Natl Acad Sci U S A. 2008 9; 105(38):14721–6. doi: 10.1073/pnas.0806510105 PMID: 18787127

45. Chen KC, Calzone L, Csikasz-Nagy A, Cross FR, Novak B, Tyson JJ. Integrative analysis of cell cycle control in budding yeast. Mol Biol Cell. 2004 8; 15(8):3841–62. doi: 10.1091/mbc.E03-11-0794 PMID: 15169868

46. Fauré A, Naldi A, Chaouiya C, Thieffry D. Dynamical analysis of a generic Boolean model for the control of the mammalian cell cycle. Bioinformatics. 2006; 22(14):e124–31. doi: 10.1093/bioinformatics/btl210 PMID: 16873462

47. Fauré A, Naldi A, Lopez F, Chaouiya C, Ciliberto A, Thieffry D. Modular logical modelling of the budding yeast cell cycle. Mol Biosyst. 2009 12; 5(12):1787–96. doi: 10.1039/b910101m PMID: 19763337

48. Irons DJ. Logical analysis of the budding yeast cell cycle. J Theor Biol. 2009 4; 257(4):543–59. doi: 10.1016/j.jtbi.2008.12.028 PMID: 19185585

49. Goldbeter A. A minimal cascade model for the mitotic oscillator involving cyclin and cdc2 kinase. Proc Natl Acad Sci U S A. 1991 10; 88(20):9107–11. doi: 10.1073/pnas.88.20.9107 PMID: 1833774

50. Novak B, Tyson JJ. Modeling the control of DNA replication in fission yeast. Proc Natl Acad Sci U S A. 1997 8; 94(17):9147–52. doi: 10.1073/pnas.94.17.9147 PMID: 9256450

51. Novak B, Csikasz-Nagy A, Gyorffy B, Chen K, Tyson JJ. Mathematical model of the fission yeast cell cycle with checkpoint controls at the G1/S, G2/M and metaphase/anaphase transitions. Biophys Chem. 1998; 72:185–200. doi: 10.1016/S0301-4622(98)00133-1 PMID: 9652094

52. Novak B, Csikasz-Nagy A, Gyorffy B, Nasmyth K, Tyson JJ. Model scenarios for evolution of the eukaryotic cell cycle. Philos Trans R Soc Lond B Biol Sci. 1998; 353(1378):2063–76. doi: 10.1098/rstb.1998.0352 PMID: 10098216

53. Novak B, Pataki Z, Ciliberto A, Tyson JJ. Mathematical model of the cell division cycle of fission yeast. Chaos. 2001; 11(1):277–286. doi: 10.1063/1.1345725 PMID: 12779461

54. Tyson JJ, Csikasz-Nagy A, Novak B. The dynamics of cell cycle regulation. Bioessays. 2002; 24 (12):1095–109. doi: 10.1002/bies.10191 PMID: 12447975

55. Li B, Shao B, Yu C, Ouyang Q, Wang H. A mathematical model for cell size control in fission yeast. J Theor Biol. 2010 6; 264(3):771–81. doi: 10.1016/j.jtbi.2010.03.023 PMID: 20303984

56. Qu Z, MacLellan WR, Weiss JN. Dynamics of the cell cycle: checkpoints, sizers, and timers. Biophys J. 2003 12; 85(6):3600–11. doi: 10.1016/S0006-3495(03)74778-X PMID: 14645053

57. Csikász-Nagy A, Battogtokh D, Chen KC, Novák B, Tyson JJ. Analysis of a generic model of eukaryotic cell-cycle regulation. Biophys J. 2006 6; 90(12):4361–79. doi: 10.1529/biophysj.106.081240 PMID: 16581849

58. Li F, Long T, Lu Y, Ouyang Q, Tang C. The yeast cell-cycle network is robustly designed. Proc Natl Acad Sci U S A. 2004; 101(14):4781–6. doi: 10.1073/pnas.0305937101 PMID: 15037758

59. Davidich MI, Bornholdt S. Boolean network model predicts cell cycle sequence of fission yeast. PLoS One. 2008; 3(2):e1672. doi: 10.1371/journal.pone.0001672 PMID: 18301750

60. Hong C, Lee M, Kim D, Kim D, Cho KH, Shin I. A checkpoints capturing timing-robust Boolean model of the budding yeast cell cycle regulatory network. BMC Syst Biol. 2012; 6:129. doi: 10.1186/1752-0509-6-129 PMID: 23017186

61. Davidich MI, Bornholdt S. Boolean network model predicts knockout mutant phenotypes of fission yeast. PLoS One. 2013; 8(9):e71786. doi: 10.1371/journal.pone.0071786 PMID: 24069138

62. Singhania R, Sramkoski RM, Jacobberger JW, Tyson JJ. A hybrid model of mammalian cell cycle regulation. PLoS Comput Biol. 2011; 7(2):e1001077. doi: 10.1371/journal.pcbi.1001077 PMID: 21347318

63. Srividhya J, Gopinathan MS. A simple time delay model for eukaryotic cell cycle. J Theor Biol. 2006 8; 241(3):617–27. doi: 10.1016/j.jtbi.2005.12.020 PMID: 16473373

64. Li C, Wang J. Landscape and flux reveal a new global view and physical quantification of mammalian cell cycle. Proc Natl Acad Sci U S A. 2014 9; 111(39):14130–5. doi: 10.1073/pnas.1408628111 PMID: 25228772

65. Li C, Wang J. Quantifying the underlying landscape and paths of cancer. J R Soc Interface. 2014 11; 11(100):20140774. doi: 10.1098/rsif.2014.0774 PMID: 25232051

66. Fauré A, Thieffry D. Logical modelling of cell cycle control in eukaryotes: a comparative study. Mol Biosyst. 2009 12; 5(12):1569–81. doi: 10.1039/b907562n PMID: 19763341

67. Zhao X, Harashima H, Dissmeyer N, Pusch S, Weimer AK, Bramsiepe J, et al. A General G1/S-Phase Cell-Cycle Control Module in the Flowering Plant Arabidopsis thaliana. PLoS Genetics. 2012 8; 8(8): e1002847. doi: 10.1371/journal.pgen.1002847 PMID: 22879821

68. Adachi S, Nobusawa T, Umeda M. Quantitative and cell type-specific transcriptional regulation of A-type cyclin-dependent kinase in Arabidopsis thaliana. Dev Biol. 2009; 329(2):306–14. doi: 10.1016/j.ydbio.2009.03.002 PMID: 19285489

69. Mariconti L, Pellegrini B, Cantoni R, Stevens R, Bergounioux C, Cella R, et al. The E2F family of transcription factors from Arabidopsis thaliana. Novel and conserved components of the retinoblastoma/E2F pathway in plants. J Biol Chem. 2002 3; 277(12):9911–9. doi: 10.1074/jbc.M110616200 PMID: 11786543

70. Zhang L, Wang C. F-box protein Skp2: a novel transcriptional target of E2F. Oncogene. 2006 4; 25 (18):2615–27. doi: 10.1038/sj.onc.1209286 PMID: 16331253

71. Rustici G, Mata J, Kivinen K, Lio P, Penkett CJ, Burns G, et al. Periodic gene expression program of the fission yeast cell cycle. Nat Genet. 2004; 36(8):809–17. doi: 10.1038/ng1377 PMID: 15195092

72. Menges M, Hennig L, Gruissem W, Murray JAH. Cell cycle-regulated gene expression in Arabidopsis. J Biol Chem. 2002 11; 277(44):41987–2002. doi: 10.1074/jbc.M207570200 PMID: 12169696

73. Menges M, Hennig L, Gruissem W, Murray JAH. Genome-wide gene expression in an Arabidopsis cell suspension. Plant Mol Biol. 2003 11; 53(4):423–42. doi: 10.1023/B:PLAN.0000019059.56489.ca PMID: 15010610

74. Menges M, de Jager SM, Gruissem W, Murray JA. Global analysis of the core cell cycle regulators of Arabidopsis identifies novel genes, reveals multiple and highly specific profiles of expression and provides a coherent model for plant cell cycle control. Plant J. 2005; 41(4):546–66. doi: 10.1111/j.1365-313X.2004.02319.x PMID: 15686519

75. Romero I, Fuertes A, Benito MJ, Malpica JM, Leyva A, Paz-Ares J. More than 80R2R3-MYB regulatory genes in the genome of Arabidopsis thaliana. Plant J. 1998 5; 14(3):273–84. doi: 10.1046/j.1365-313X.1998.00113.x PMID: 9628022

76. Shin R, Burch AY, Huppert KA, Tiwari SB, Murphy AS, Guilfoyle TJ, et al. The Arabidopsis transcription factor MYB77 modulates auxin signal transduction. Plant Cell. 2007 8; 19(8):2440–53. doi: 10.1105/tpc.107.050963 PMID: 17675404

77. Prouse MB, Campbell MM. The interaction between MYB proteins and their target DNA binding sites. Biochim Biophys Acta. 2012 1; 1819(1):67–77. doi: 10.1016/j.bbagrm.2011.10.010 PMID: 22067744

78. Weinl C, Marquardt S, Kuijt SJH, Nowack MK, Jakoby MJ, Hülskamp M, et al. Novel functions of plant cyclin-dependent kinase inhibitors, ICK1/KRP1, can act non-cell-autonomously and inhibit entry into mitosis. Plant Cell. 2005 6; 17(6):1704–22. doi: 10.1105/tpc.104.030486 PMID: 15749764

79. Magyar Z, De Veylder L, Atanassova A, Bakó L, Inzé D, Bögre L. The role of the Arabidopsis E2FB transcription factor in regulating auxin-dependent cell division. Plant Cell. 2005 9; 17(9):2527–41. doi: 10.1105/tpc.105.033761 PMID: 16055635

80. Sozzani R, Maggio C, Varotto S, Canova S, Bergounioux C, Albani D, et al. Interplay between Arabidopsis activating factors E2Fb and E2Fa in cell cycle progression and development. Plant Physiol. 2006 4; 140(4):1355–66. doi: 10.1104/pp.106.077990 PMID: 16514015

81. Leone G, DeGregori J, Yan Z, Jakoi L, Ishida S, Williams RS, et al. E2F3 activity is regulated during the cell cycle and is required for the induction of S phase. Genes Dev. 1998 7; 12(14):2120–30. doi: 10.1101/gad.12.14.2120 PMID: 9679057

82. Peters JM. SCF and APC: the Yin and Yang of cell cycle regulated proteolysis. Curr Opin Cell Biol. 1998; 10(6):759–68. doi: 10.1016/S0955-0674(98)80119-1 PMID: 9914180

83. Vodermaier HC. APC/C and SCF: controlling each other and the cell cycle. Curr Biol. 2004 9; 14(18): R787–96. doi: 10.1016/j.cub.2004.09.020 PMID: 15380093

84. Bashir T, Dorrello NV, Amador V, Guardavaccaro D, Pagano M. Control of the SCF(Skp2-Cks1) ubiquitin ligase by the APC/C(Cdh1) ubiquitin ligase. Nature. 2004 3; 428(6979):190–3. doi: 10.1038/nature02330 PMID: 15014502

85. Marrocco K, Bergdoll M, Achard P, Criqui MC, Genschik P. Selective proteolysis sets the tempo of the cell cycle. Curr Opin Plant Biol. 2010; 13(6):631–9. doi: 10.1016/j.pbi.2010.07.004 PMID: 20810305

86. Boniotti MB, Gutierrez C. A cell-cycle-regulated kinase activity phosphorylates plant retinoblastoma protein and contains, in Arabidopsis, a CDKA/cyclin D complex. Plant J. 2001 11; 28(3):341–50. doi: 10.1046/j.1365-313X.2001.01160.x PMID: 11722776

87. Dewitte W, Murray JA. The plant cell cycle. Annu Rev Plant Biol. 2003; 54:235–64. doi: 10.1146/annurev.arplant.54.031902.134836 PMID: 14502991

88. Wildwater M, Campilho A, Perez-Perez JM, Heidstra R, Blilou I, Korthout H, et al. The RETINOBLASTOMA-RELATED gene regulates stem cell maintenance in Arabidopsis roots. Cell. 2005 12; 123 (7):1337–49. doi: 10.1016/j.cell.2005.09.042 PMID: 16377572

89. Nowack MK, Harashima H, Dissmeyer N, Zhao X, Bouyer D, Weimer AK, et al. Genetic framework of cyclin-dependent kinase function in Arabidopsis. Dev Cell. 2012 5; 22(5):1030–40. doi: 10.1016/j.devcel.2012.02.015 PMID: 22595674

90. Magyar Z, Horvath B, Khan S, Mohammed B, Henriques R, De Veylder L, et al. Arabidopsis E2FA stimulates proliferation and endocycle separately through RBR-bound and RBR-free complexes. EMBO J. 2012; 31(6):1480–93. doi: 10.1038/emboj.2012.13 PMID: 22307083

91. Del Pozo JC, Diaz-Trivino S, Cisneros N, Gutierrez C. The E2FC-DPB Transcription Factor Controls Cell Division, Endoreplication and Lateral Root Formation in a SCF-Dependent Manner. Plant Signal Behav. 2007; 2(4):273–4. doi: 10.4161/psb.2.4.3897 PMID: 19704635

92. Planchais S, Samland AK, Murray JA. Differential stability of Arabidopsis D-type cyclins: CYCD3;1 is a highly unstable protein degraded by a proteasome-dependent mechanism. Plant J. 2004; 38 (4):616–25. doi: 10.1111/j.0960-7412.2004.02071.x PMID: 15125768

93. Ren H, Santner A, del Pozo JC, Murray JA, Estelle M. Degradation of the cyclin-dependent kinase inhibitor KRP1 is regulated by two different ubiquitin E3 ligases. Plant J. 2008; 53(5):705–16. doi: 10.1111/j.1365-313X.2007.03370.x PMID: 18005227

94. Vandepoele K, Vlieghe K, Florquin K, Hennig L, Beemster GT, Gruissem W, et al. Genome-wide identification of potential plant E2F target genes. Plant Physiol. 2005; 139(1):316–28. doi: 10.1104/pp.105.066290 PMID: 16126853

95. He SS, Liu J, Xie Z, O'Neill D, Dotson S. Arabidopsis E2Fa plays a bimodal role in regulating cell division and cell growth. Plant Mol Biol. 2004; 56(2):171–84. doi: 10.1007/s11103-004-2748-8 PMID: 15604736

96. Berckmans B, Lammens T, Van Den Daele H, Magyar Z, Bögre L, De Veylder L. Light-dependent regulation of DEL1 is determined by the antagonistic action of E2Fb and E2Fc. Plant Physiol. 2011 11; 157(3):1440–51. doi: 10.1104/pp.111.183384 PMID: 21908689

97. López-Juez E, Dillon E, Magyar Z, Khan S, Hazeldine S, de Jager SM, et al. Distinct light-initiated gene expression and cell cycle programs in the shoot apex and cotyledons of Arabidopsis. Plant Cell. 2008 4; 20(4):947–68. doi: 10.1105/tpc.107.057075 PMID: 18424613

98. Haga N, Kato K, Murase M, Araki S, Kubo M, Demura T, et al. R1R2R3-Myb proteins positively regulate cytokinesis through activation of KNOLLE transcription in Arabidopsis thaliana. Development. 2007 3; 134(6):1101–10. doi: 10.1242/dev.02801 PMID: 17287251

99.   Araki S, Ito M, Soyano T, Nishihama R, Machida Y. Mitotic cyclins stimulate the activity of c-Myb-like factors for transactivation of G2/M phase-specific genes in tobacco. J Biol Chem. 2004 7; 279 (31):32979–88. doi: 10.1074/jbc.M403171200 PMID: 15175336

100. Wang H, Fowke LC, Crosby WL. A plant cyclin-dependent kinase inhibitor gene. Nature. 1997 4; 386 (6624):451–2. doi: 10.1038/386451a0 PMID: 9087400

101. Wang H, Qi Q, Schorr P, Cutler AJ, Crosby WL, Fowke LC. ICK1, a cyclin-dependent protein kinase inhibitor from Arabidopsis thaliana interacts with both Cdc2a and CycD3, and its expression is induced by abscisic acid. Plant J. 1998 8; 15(4):501–10. doi: 10.1046/j.1365-313X.1998.00231.x PMID: 9753775

102. Fulop K, Tarayre S, Kelemen Z, Horvath G, Kevei Z, Nikovics K, et al. Arabidopsis anaphase-promoting complexes: multiple activators and wide range of substrates might keep APC perpetually busy. Cell Cycle. 2005; 4(8):1084–92. doi: 10.4161/cc.4.8.1856 PMID: 15970679

103. Imai KK, Ohashi Y, Tsuge T, Yoshizumi T, Matsui M, Oka A, et al. The A-type cyclin CYCA2;3 is a key regulator of ploidy levels in Arabidopsis endoreduplication. Plant Cell. 2006 2; 18(2):382–96. doi: 10.1105/tpc.105.037309 PMID: 16415207

104. Müssel C, Hopfensitz M, Kestler HA. BoolNet–an R package for generation, reconstruction and analysis of Boolean networks. Bioinformatics. 2010 5; 26(10):1378–80. doi: 10.1093/bioinformatics/btq124 PMID: 20378558

105. Team RC; R Foundation for Statistical Computing. R: A Language and Environment for Statistical Computing. 2012;.

106. Sánchez-Corrales YE, Alvarez-Buylla ER, Mendoza L. The Arabidopsis thaliana flower organ specification gene regulatory network determines a robust differentiation process. J Theor Biol. 2010 6; 264 (3):971–83. doi: 10.1016/j.jtbi.2010.03.006 PMID: 20303988

107. Di Cara A, Garg A, De Micheli G, Xenarios I, Mendoza L. Dynamic simulation of regulatory networks using SQUAD. BMC Bioinformatics. 2007; 8:462. doi: 10.1186/1471-2105-8-462 PMID: 18039375

108. Dewitte W, Riou-Khamlichi C, Scofield S, Healy JMS, Jacqmard A, Kilby NJ, et al. Altered cell cycle distribution, hyperplasia, and inhibited differentiation in Arabidopsis caused by the D-type cyclin CYCD3. Plant Cell. 2003 1; 15(1):79–92. doi: 10.1105/tpc.004838 PMID: 12509523

109. Vanstraelen M, Baloban M, Da Ines O, Cultrone A, Lammens T, Boudolf V, et al. APC/C-CCS52A complexes control meristem maintenance in the Arabidopsis root. Proc Natl Acad Sci U S A. 2009; 106(28):11806–11. doi: 10.1073/pnas.0901193106 PMID: 19553203

110. Heyman J, De Veylder L. The anaphase-promoting complex/cyclosome in control of plant development. Mol Plant. 2012 11; 5(6):1182–94. doi: 10.1093/mp/sss094 PMID: 23034505

111. De Veylder L, Beeckman T, Beemster GT, de Almeida Engler J, Ormenese S, Maes S, et al. Control of proliferation, endoreduplication and differentiation by the Arabidopsis E2Fa-DPa transcription factor. EMBO J. 2002 3; 21(6):1360–8. doi: 10.1093/emboj/21.6.1360 PMID: 11889041

112. Poznic M. Retinoblastoma protein: a central processing unit. J Biosci. 2009 6; 34(2):305–12. doi: 10.1007/s12038-009-0034-2 PMID: 19550046

113. Rossignol P, Stevens R, Perennes C, Jasinski S, Cella R, Tremousaygue D, et al. AtE2F-a and AtDP-a, members of the E2F family of transcription factors, induce Arabidopsis leaf cells to re-enter S phase. Mol Genet Genomics. 2002 2; 266(6):995–1003. doi: 10.1007/s00438-001-0624-7 PMID: 11862494

114. Cheng Y, Cao L, Wang S, Li Y, Shi X, Liu H, et al. Downregulation of multiple CDK inhibitor ICK/KRP genes upregulates the E2F pathway and increases cell proliferation, and organ and seed sizes in Arabidopsis. Plant J. 2013 8; 75(4):642–55. doi: 10.1111/tpj.12228 PMID: 23647236

115. Cruz-Ramírez A, Díaz-Triviño S, Blilou I, Grieneisen VA, Sozzani R, Zamioudis C, et al. A Bistable Circuit Involving SCARECROW-RETINOBLASTOMA Integrates Cues to Inform Asymmetric Stem Cell Division. Cell. 2012 8;.

116. Espinosa-Soto C, Padilla-Longoria P, Alvarez-Buylla ER. A gene regulatory network model for cell-fate determination during Arabidopsis thaliana flower development that is robust and recovers experimental gene expression profiles. Plant Cell. 2004; 16(11):2923–39. doi: 10.1105/tpc.104.021725 PMID: 15486106

117. Benítez M, Espinosa-Soto C, Padilla-Longoria P, Alvarez-Buylla ER. Interlinked nonlinear subnetworks underlie the formation of robust cellular patterns in Arabidopsis epidermis: a dynamic spatial model. BMC Syst Biol. 2008; 2:98. doi: 10.1186/1752-0509-2-98 PMID: 19014692

118. Wittmann DM, Krumsiek J, Saez-Rodriguez J, Lauffenburger DA, Klamt S, Theis FJ. Transforming Boolean models to continuous models: methodology and application to T-cell receptor signaling. BMC Syst Biol. 2009; 3:98. doi: 10.1186/1752-0509-3-98 PMID: 19785753

119. Krumsiek J, Pölsterl S, Wittmann DM, Theis FJ. Odefy–from discrete to continuous models. BMC Bioinformatics. 2010; 11:233. doi: 10.1186/1471-2105-11-233 PMID: 20459647

120. López-Avilés S, Kapuy O, Novák B, Uhlmann F. Irreversibility of mitotic exit is the consequence of systems-level feedback. Nature. 2009 5; 459(7246):592–5. doi: 10.1038/nature07984 PMID: 19387440

121. Menges M, Samland AK, Planchais S, Murray JA. The D-type cyclin CYCD3;1 is limiting for the G1-to-S-phase transition in Arabidopsis. Plant Cell. 2006; 18(4):893–906. doi: 10.1105/tpc.105.039636 PMID: 16517759

122. Jurado S, Diaz-Trivino S, Abraham Z, Manzano C, Gutierrez C, del Pozo C. SKP2A, an F-box protein that regulates cell division, is degraded via the ubiquitin pathway. Plant J. 2008; 53(5):828–41. doi: 10.1111/j.1365-313X.2007.03378.x PMID: 18036202

123. Jurado S, Trivino SD, Abraham Z, Manzano C, Gutierrez C, Del Pozo C. SKP2A protein, an F-box that regulates cell division, is degraded via the ubiquitin pathway. Plant Signal Behav. 2008; 3 (10):810–2. doi: 10.4161/psb.3.10.5888 PMID: 19704565

124. Doerner P, Jorgensen JE, You R, Steppuhn J, Lamb C. Control of root growth and development by cyclin expression. Nature. 1996; 380(6574):520–3. doi: 10.1038/380520a0 PMID: 8606769

125. Boudolf V, Barrôco R, de Almeida Engler J, Verkest A, Beeckman T, Naudts M, et al. B1-type cyclin-dependent kinases are essential for the formation of stomatal complexes in Arabidopsis thaliana. Plant Cell. 2004 4; 16(4):945–55. doi: 10.1105/tpc.021774 PMID: 15031414

126. Roeder AHK, Cunha A, Ohno CK, Meyerowitz EM. Cell cycle regulates cell type in the Arabidopsis sepal. Development. 2012 10;.

127. Borghi L, Gutzat R, Fütterer J, Laizet Y, Hennig L, Gruissem W. Arabidopsis RETINOBLASTOMA-RELATED is required for stem cell maintenance, cell differentiation, and lateral organ production. Plant Cell. 2010 6; 22(6):1792–811. doi: 10.1105/tpc.110.074591 PMID: 20525851

128. Ferreira PC, Hemerly AS, Engler JD, van Montagu M, Engler G, Inzé D. Developmental expression of the arabidopsis cyclin gene cyc1At. Plant Cell. 1994 12; 6(12):1763–74. doi: 10.1105/tpc.6.12.1763 PMID: 7866022

129. Boudolf V, Vlieghe K, Beemster GT, Magyar Z, Torres Acosta JA, Maes S, et al. The plant-specific cyclin-dependent kinase CDKB1;1 and transcription factor E2Fa-DPa control the balance of mitotically dividing and endoreduplicating cells in Arabidopsis. Plant Cell. 2004; 16(10):2683–92. doi: 10.1105/tpc.104.024398 PMID: 15377755

130. Li Z, Larson-Rabin Z, Masson PH, Day CD. FZR2/CCS52A1 mediated endoreduplication in Arabidopsis development. Plant Signal Behav. 2009 5; 4(5):451–3. doi: 10.4161/psb.4.5.8480 PMID: 19816101

131. Takahashi N, Kajihara T, Okamura C, Kim Y, Katagiri Y, Okushima Y, et al. Cytokinins Control Endocycle Onset by Promoting the Expression of an APC/C Activator in Arabidopsis Roots. Curr Biol. 2013 September; 23(18):1812–1817. doi: 10.1016/j.cub.2013.07.051 PMID: 24035544

132. Menges M, Murray JAH. Synchronous Arabidopsis suspension cultures for analysis of cell-cycle gene activity. Plant J. 2002 4; 30(2):203–12. doi: 10.1046/j.1365-313X.2002.01274.x PMID: 12000456

133. Azpeitia E, Benítez M, Vega I, Villarreal C, Alvarez-Buylla ER. Single-cell and coupled GRN models of cell patterning in the Arabidopsis thaliana root stem cell niche. BMC Syst Biol. 2010; 4:134. doi: 10.1186/1752-0509-4-134 PMID: 20920363

134. Barrio RA, Romero-Arias JR, Noguez MA, Azpeitia E, Ortiz-Gutiérrez E, Hernández-Hernández V, et al. Cell patterns emerge from coupled chemical and physical fields with cell proliferation dynamics: the Arabidopsis thaliana root as a study system. PLoS Comput Biol. 2013 5; 9(5):e1003026. doi: 10.1371/journal.pcbi.1003026 PMID: 23658505

135. Skirycz A, Claeys H, De Bodt S, Oikawa A, Shinoda S, Andriankaja M, et al. Pause-and-stop: the effects of osmotic stress on cell proliferation during early leaf development in Arabidopsis and a role for ethylene signaling in cell cycle arrest. Plant Cell. 2011; 23(5):1876–88. doi: 10.1105/tpc.111.084160 PMID: 21558544

136. Reyt G, Boudouf S, Boucherez J, Gaymard F, Briat JF. Iron- and Ferritin-Dependent Reactive Oxygen Species Distribution: Impact on Arabidopsis Root System Architecture. Mol Plant. 2015; 8(3):439–453. doi: 10.1016/j.molp.2014.11.014 PMID: 25624148

137. Sevim V, Gong X, Socolar JES. Reliability of transcriptional cycles and the yeast cell-cycle oscillator. PLoS Comput Biol. 2010; 6(7):e1000842. doi: 10.1371/journal.pcbi.1000842 PMID: 20628620

138. Mu RL, Cao YR, Liu YF, Lei G, Zou HF, Liao Y, et al. An R2R3-type transcription factor gene AtMYB59 regulates root growth and cell cycle progression in Arabidopsis. Cell Res. 2009 11; 19 (11):1291–304. doi: 10.1038/cr.2009.83 PMID: 19581938

139. Vandepoele K, Raes J, De Veylder L, Rouze P, Rombauts S, Inze D. Genome-wide analysis of core cell cycle genes in Arabidopsis. Plant Cell. 2002; 14(4):903–16. doi: 10.1105/tpc.010445 PMID: 11971144

140. Gutierrez C. The Arabidopsis cell division cycle. Arabidopsis Book. 2009; 7:e0120. doi: 10.1199/tab.0120 PMID: 22303246

141. Malumbres M, Barbacid M. Cell cycle, CDKs and cancer: a changing paradigm. Nat Rev Cancer. 2009; 9(3):153–66. doi: 10.1038/nrc2602 PMID: 19238148

142. Wittenberg C, Reed SI. Cell cycle-dependent transcription in yeast: promoters, transcription factors, and transcriptomes. Oncogene. 2005 4; 24(17):2746–55. doi: 10.1038/sj.onc.1208606 PMID: 15838511

143. Bertoli C, Skotheim JM, de Bruin RAM. Control of cell cycle transcription during G1 and S phases. Nat Rev Mol Cell Biol. 2013 8; 14(8):518–28. doi: 10.1038/nrm3629 PMID: 23877564

144. Breeden LL. Periodic transcription: a cycle within a cycle. Curr Biol. 2003 1; 13(1):R31–8. doi: 10.1016/S0960-9822(02)01386-6 PMID: 12526763

145. Cokus S, Rose S, Haynor D, Grønbech-Jensen N, Pellegrini M. Modelling the network of cell cycle transcription factors in the yeast Saccharomyces cerevisiae. BMC Bioinformatics. 2006; 7:381. doi: 10.1186/1471-2105-7-381 PMID: 16914048

146. Francis D. A commentary on the G2/M transition of the plant cell cycle. Ann Bot. 2011 5; 107(7):1065–70. doi: 10.1093/aob/mcr055 PMID: 21558458

147. Shimotohno A, Ohno R, Bisova K, Sakaguchi N, Huang J, Koncz C, et al. Diverse phosphoregulatory mechanisms controlling cyclin-dependent kinase-activating kinases in Arabidopsis. Plant J. 2006; 47 (5):701–10. doi: 10.1111/j.1365-313X.2006.02820.x PMID: 16856985

148. Cook GS, Grønlund AL, Siciliano I, Spadafora N, Amini M, Herbert RJ, et al. Plant WEE1 kinase is cell cycle regulated and removed at mitosis via the 26S proteasome machinery. J Exp Bot. 2013; 64 (7):2093–2106. doi: 10.1093/jxb/ert066 PMID: 23536609

149. Dissmeyer N, Weimer AK, Pusch S, De Schutter K, Alvim Kamei CL, Nowack MK, et al. Control of cell proliferation, organ growth, and DNA damage response operate independently of dephosphorylation of the Arabidopsis Cdk1 homolog CDKA;1. Plant Cell. 2009; 21(11):3641–54. doi: 10.1105/tpc.109.070417 PMID: 19948791

150. Dissmeyer N, Weimer AK, De Veylder L, Novak B, Schnittger A. The regulatory network of cell-cycle progression is fundamentally different in plants versus yeast or metazoans. Plant Signal Behav. 2010; 5(12):1613–8. doi: 10.4161/psb.5.12.13969 PMID: 21139435

ANEXO B

Artículo: Campos físicos y químicos acoplados a la dinámica de proliferación

Cell Patterns Emerge from Coupled Chemical and Physical Fields with Cell Proliferation Dynamics: The *Arabidopsis thaliana* Root as a Study System

Rafael A. Barrio[1]*, José Roberto Romero-Arias[1], Marco A. Noguez[2], Eugenio Azpeitia[3,4], Elizabeth Ortiz-Gutiérrez[3,4], Valeria Hernández-Hernández[3,4], Yuriria Cortes-Poza[4], Elena R. Álvarez-Buylla[3,4]*

1 Instituto de Física, Universidad Nacional Autónoma de México (UNAM), México, Distrito Federal, México, 2 Universidad Autónoma de la Ciudad de México, Mexico, Distrito Federal, México, 3 Instituto de Ecología, Universidad Nacional Autónoma de México, México, Distrito Federal, México, 4 Centro de Ciencias de la Complejidad-C3, Universidad Nacional Autónoma de México, Distrito Federal, México

Abstract

A central issue in developmental biology is to uncover the mechanisms by which stem cells maintain their capacity to regenerate, yet at the same time produce daughter cells that differentiate and attain their ultimate fate as a functional part of a tissue or an organ. In this paper we propose that, during development, cells within growing organs obtain positional information from a macroscopic physical field that is produced in space while cells are proliferating. This dynamical interaction triggers and responds to chemical and genetic processes that are specific to each biological system. We chose the root apical meristem of *Arabidopsis thaliana* to develop our dynamical model because this system is well studied at the molecular, genetic and cellular levels and has the key traits of multicellular stem-cell niches. We built a dynamical model that couples fundamental molecular mechanisms of the cell cycle to a tension physical field and to auxin dynamics, both of which are known to play a role in root development. We perform extensive numerical calculations that allow for quantitative comparison with experimental measurements that consider the cellular patterns at the root tip. Our model recovers, as an emergent pattern, the transition from proliferative to transition and elongation domains, characteristic of stem-cell niches in multicellular organisms. In addition, we successfully predict altered cellular patterns that are expected under various applied auxin treatments or modified physical growth conditions. Our modeling platform may be extended to explicitly consider gene regulatory networks or to treat other developmental systems.

Introduction

The study of stem-cell niche patterns, and specifically how stem cells can maintain their totipotent state while simultaneously giving rise to daughter cells that obtain distinct fates to form differentiated tissues and organs, is fundamental to understanding the development of multicellular organisms [1]. Although plants and animals have key differences in their development (e.g. lack of cell migration in plant development), the cellular organization of stem-cell niches in both lineages reveals striking similarities [1,2]. In both plants and animals, stem-cell niches are formed by an organizer group of cells with low rates of division, surrounded by stem cells with slightly higher division rates. Moving distally from the organizer and stem cells, cells proliferate at high rates. This proliferation domain (also called amplification domain) is bordered by the elongation and then the differentiation domains where proliferation stops and expansion and differentiation, respectively, take place [1,3].

Gene interactions within intracellular complex regulatory networks (GRN) [4,5] or from morphogen dynamics at supracellular scales (see [6,7]) are fundamental for proper growth and development. Indeed organ and tissue development, as well as stem cell maintenance relies to a great extent on complex transcriptional regulatory networks and chemical fields. However, these are not the only components of pattern formation. It is now recognized that physical fields are also critical to explain developmental patterns, as they may provide positional information that modifies cell behavior and differentiation (see [6,7]). At the cellular level, the simplest physical constraint is space. Cell expansion is driven by turgidity, which is an important force acting on the cell wall [8]. The cell wall is a network of rigid cellulose microfibrils cross-linked by polysaccharides and proteins, that confer stiffness to the wall and allows it to resist turgidity [9]. Expansion of the cell is opposed by the rigidity of the cell wall, producing a real stress field. Recent evidence shows that these kind of mechanical cues are transmitted to the nucleus and, directly or indirectly, regulate transcription factors (see for instance [10] and references therein).

Given the complexity of the processes involved in the coupling of developmental restrictions, mathematical and computational tools have become indispensable in our efforts to understand the network of interactions involved in cellular differentiation and

Author Summary

The emergence of tumors results from altered cell differentiation and proliferation during organ and tissue development. Understanding how such altered or normal patterns are established is still a challenge. Molecular genetic approaches to understanding pattern formation have searched for key central genetic controllers. However, biological patterns emerge as a consequence of coupled complex genetic and non-genetic sub-systems operating at various spatial and temporal scales and levels of organization. We present a two-dimensional model and simulation benchmark that considers the integrated dynamics of physical and chemical fields that result from cell proliferation. We aim at understanding how the cellular patterns of stem-cell niches emerge. In these, organizer cells with very low rates of proliferation are surrounded by stem cells with slightly higher proliferation rates that transit to a domain of active proliferation and then of elongation and differentiation. We quantified such cellular patterns in the *Arabidopsis thaliana* root to test our theoretical propositions. The results of our simulations closely mimic observed root cellular patterns, thus providing a proof of principle that coupled physical fields and chemical processes under active cell proliferation give rise to stem-cell patterns. Our framework may be extended to other developmental systems and to consider gene regulatory networks.

organ development. Previously [11] we demonstrated that a simplified version of the originally proposed GRN [12,13] involved in floral development, could be coupled with a mesoscopic physical field. This provides positional information to cells in the floral meristem which is required to produce the overall spatial pattern of cells observed during early flower development. This and other similar studies [14] suggest that robust morphogenetic patterns in multicellular organisms emerge from complex interconnected dynamical processes, acting at different levels of organization and spatio-temporal scales. However, models that include such dynamical processes into the dynamics of pattern formation in multicellular organs are in their infancy [15,16]. Here we use the *Arabidopsis thaliana* (*A. thaliana*) root apical meristem as a study system to propose a model that couples cell proliferation and growth with chemical-physical dynamical processes to predict the emergence of patterns in a multicellular and multi-scale system.

The *A. thaliana* root has become an important experimental model for understanding the molecular, cellular and biophysical basis of morphogenesis in complex organs. This is due to its relatively simple cellular structure and its indeterminate growth, which gives rise to a multicellular structure with distinct cell proliferation and elongation domains. Importantly, the root apical meristem exhibits the typical cellular organization of stem cells described above (see Fig. 1). At the tip of roots stem cells are located surrounding the quiescent centre cells or the organizer cells (green cells in Fig. 1); together, they constitute the stem-cell niche (SCN) of the Arabidopsis root. Towards the base of the plant, the stem cells transit to a cell proliferation domain (CPD) where cells have high rates of cell division (also called proximal meristem by some authors, for example: [17]), then they enter a transition domain (TD), where cells have low or no probability of dividing, but they have not started to elongate [18]. The SCN, the CPD and the TD comprise the root apical meristem (RAM). More distally from the organizer center, cells cease to proliferate and start to grow in the elongation domain (EZ). Upon expanding to
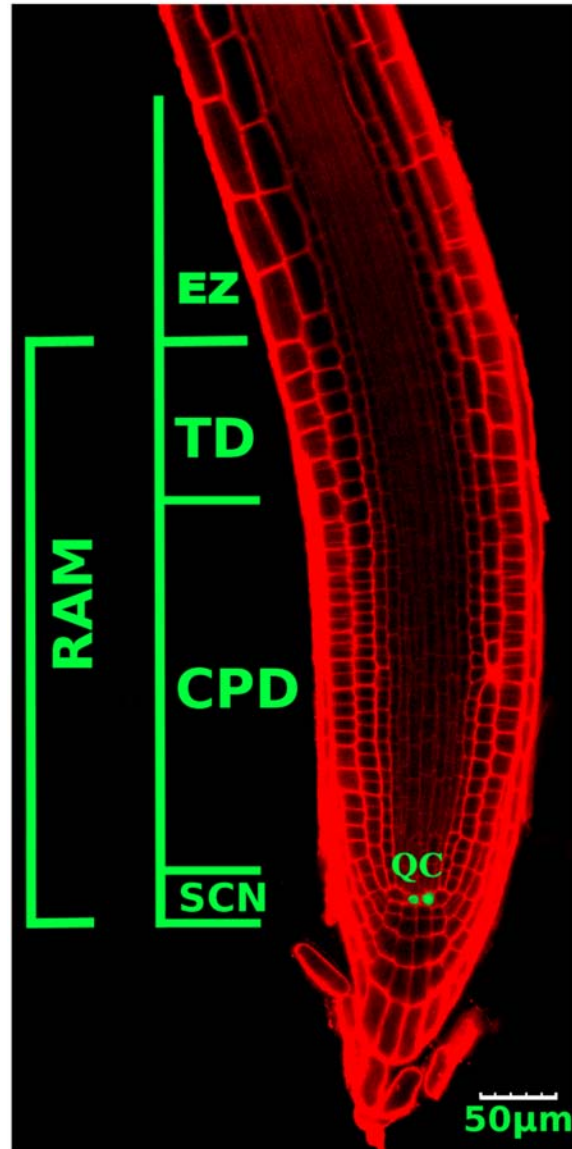
Figure 1. Confocal microscopy image of the *A. thaliana* root tip. The stem-cell niche (SCN) with the quiescent cells (QC, in green) and surrounding stem cells, the cell proliferation domain (CPD) with actively proliferating cells, the transition domain (TD) and the elongation zone (EZ), where cells do not proliferate, are indicated. The SCN, CPD and TD comprise the RAM.
doi:10.1371/journal.pcbi.1003026.g001

their maximum length, cells attain their final fate in the differentiation domain and produce the different tissues of the root.

Key experimental data on cell cycle regulation and auxin behavior in the root are used to develop our model. Patterns of cell proliferation along the root longitudinal (apical-basal) axis are greatly affected by the dynamics of the cell cycle itself and by the concentration of several plant hormones, including auxin [19–23]. Cells in the root proliferation domain of the RAM undergo several

rounds of division before starting to elongate in the elongation domain. A complex network of regulatory interactions controls the cell cycle, in which cyclin proteins are key regulators. As their name suggests, the expression of cyclins oscillates during each cell cycle. At the beginning of each cell cycle, D-type cyclins (CYCD) induce the expression of the RETINOBLASTOMA-RELATED (RBR) gene through E2F-RBR pathway. RBR is a negative regulator of E2F transcription factors, which activate the transcription of mitotic cyclin CYCB. Later, CYCB cyclins are degraded by the Anaphase-promoting complex/cyclosome, thus completing the cycle and returning to the beginning of the cell cycle (see reviews in: [24,25]). For the present study, the oscillatory and time differential expressions of CYCD and CYCB are sufficient to represent the cell cycle dynamics. The cell cycle phases and main regulators are illustrated in Fig. 2.

Auxin is a phytohormone involved in almost every aspect of plant development (see [26–32]). Auxin is a key regulator of cell proliferation and cell elongation, and also modulates cell cycle progression and cyclins [33–35]. Auxin has been shown to upregulate mitotic cyclin (CYCA and CYCB) expression, and the over-expression of CYCA can partially recover the phenotype caused by low auxin levels, thus suggesting that auxin promotes cell cycle progression [35]. It is also well-documented that auxin gradients correlate with apical-basal patterns of cell proliferation and elongation along the root (see [35–41]). There is an auxin concentration gradient along the longitudinal axis of the root, with the maximum concentration detected at the stem-cell niche, specifically in the quiescent center [41,42]. While other hormones are important in root growth and development, we exclusively consider auxin due to its clear role in regulating cell cycle dynamics and its measurable concentration gradient that correlates with root developmental patterning [26].

Theoretical and experimental studies suggest that such auxin gradients depend critically on the polar localization of the auxin efflux transporter proteins, belonging to the *PINFORMED* gene family (*PIN*) (see [43–47]). Five *PIN* members are expressed throughout the root, namely *PIN1, 2, 3, 4* and *7*. The proteins PIN1, 3, 4, and 7 maintain a continuous auxin flow from the base to the apex along the central tissues of the root. At the most apical zone, below the QC, auxin is laterally redistributed to the peripheral tissues by PIN3, 4, and 7. Finally, PIN2 directs flow from the root apex to the base in addition to lateral auxin flow in
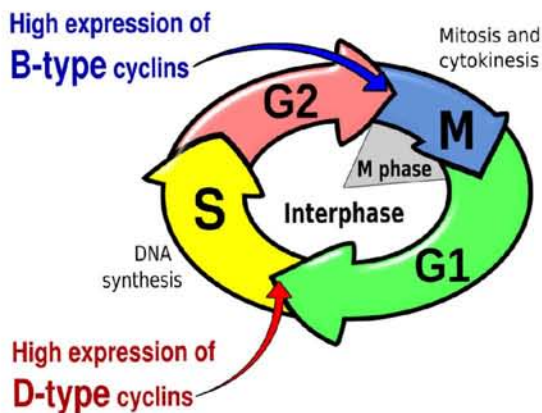
peripheral tissues. In conjunction, all PIN proteins create a reverse fountain mechanism that maintains an auxin gradient along the root [43,46,48].

Physical signals have been shown to affect auxin distribution, for instance auxin gradients can be modified by mechanically-induced root bending [49,50], or by changes in gravitational fields [51,52]. Polar auxin transport and microtubule orientation also respond to mechanical forces in the shoot apical meristem [53,54]. Such evidence suggests that auxin transport is affected by and tightly coupled to physical forces. Furthermore, there is increasing evidence that mechanical stress is extremely important for plant morphogenesis; for instance, experiments show that differentiation of mesenchymal cells is influenced by the rigidity of the intracellular matrix [55].

In this paper we propose a simple model to study the interaction between cell proliferation dynamics, local auxin concentration (that in turn depends on the polar localization of PIN transporters in the cell membranes), and an elastic physical field arising from the inherent growth dynamics of the root. Our model provides a formal tool that can be used to understand and predict the emergence of the cellular patterns in the root tip. This type of model can be extended to explore similarities in stem-cell niche organization and subsequent cellular behaviors (proliferation, elongation and differentiation) of plants and animals, and to predict if such cellular organization might be explained by the coupling of generic non-linear physical and chemical fields relevant to cell proliferation dynamics. Our model is validated with experimental measurements on cell size and proliferation patterns along *A. thaliana* root, and sets the stage for developing similar approaches in other systems.

Model

Roots are three-dimensional structures. However, the root tip presents a consistent cylindrical symmetry that allows one to ignore changes in the transverse plane of the root when considering growth models. It is therefore possible to use a two-dimensional domain consisting of undifferentiated cells to represent the shape of the root tip. This approximation allows for numerical analysis of the model in 2D space. The model can be validated by comparing the patterns obtained with those observed experimentally in longitudinal histological or optical sections as the ones readily used in experimental assays done with *A. thaliana* roots. In some cases we have also compared our results obtained from 3D roots.

Based on the shape and spatial arrangement of the root, we conclude that cell reproduction in the early stages of root development involves mainly three chained dynamics of cell proliferation and resulting elastic field, and of the pattern of auxin concentration, whose co-occurrence provides the spatial information necessary to regulate the proliferation rate of each cell and to ultimately determine its future fate during differentiation (see Fig. 3 for a schematic summary of the processes to be modeled and the region of the root in which they take place).

Our first hypothesis is that a macroscopic physical field along the root tip results from cell growth and proliferation within this tissue in addition to constrained conditions imposed by the root cap and the epidermal cells surrounding the root. We propose that this field is elastic in nature and can be characterized by point functions of stress, pressure, or local mechanical forces that stem from the symplastic nature of plant tissues that are formed by interconnected cells surrounded by cellulose cell walls. Perfect equilibrium represents a state in which there are no mechanical forces acting anywhere in the system. In practice, this equilibrium

Figure 2. Simplified scheme of the cell cycle. The four main phases and the expression of two key cyclins are indicated.
doi:10.1371/journal.pcbi.1003026.g002
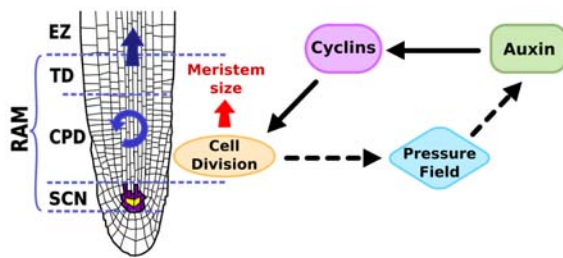
Figure 3. Histological drawing of the *A. thaliana* root tip. Here we show the SCN and the same domains as shown in Fig. 1 are indicated along the root apical-basal axis, as well as an schematic representation of the processes that are included in the cellular model and their interactions.
doi:10.1371/journal.pcbi.1003026.g003

cannot be completely achieved because of the geometric hindrances that impede the macroscopic system to reach a global minimum in the energy landscape, trapping it in a local minimum. In this situation there are remnant forces, and consequently the field is not uniform. Our model considers this lack of uniformity as a source of spatial information.

Our second hypothesis is that the synthesis, degradation and transportation of auxin respond to the local elastic field in a direct way, producing a dynamic pattern of auxin concentration along the longitudinal axis of the root tip. This is important, since the dynamical behavior of the formation of an auxin gradient should be very different from the relaxation dynamics of the elastic field, and it should occur at a different spatio-temporal scale.

Our third hypothesis proposes a direct relationship between auxin concentration and cell cycle regulation that determines cell proliferation rate. In the locations where cells divide and expand, the elastic field is greatly modified and, in fact, it is reinforced locally. This, in turn, affects the cell proliferation dynamics.

In short, we propose that the interaction among three different coupled dynamics (the relaxation of the physical field, the transport and concentration gradient of auxins and the oscillations of the cell cycle regulators, i.e., the cyclins) capture the key aspects underlying the overall emergent patterns of cell proliferation/ elongation, as well as the macroscopic appearance and overall shape of the root. Our model includes the three dynamical processes (cell proliferation, auxin spatio-temporal concentration patterns and the elastic field) and their couplings in a two-dimensional domain that represents a longitudinal section of the root.

Cell dynamics and physical fields

We start by modeling the space occupied by a cell. Expansion of the cell volume, whether by turgidity or growth, is opposed by the rigidity of the cell wall producing a real stress field [9,56]. This field is also present at the larger scale of a group of cells, such as within the root apical meristem, since the increase in volume required by cell growth and division is opposed by the surface forces exerted by the root cap and epidermal cells surrounding it [57]. From this perspective, it is logical to assume that this stress field is self-regulated, that is, the accumulation of local stress (or pressure) triggers mechanisms that prevent (or enhance) cell division and growth. This assumption of self-regulation has been incorporated into previous models of cellular interactions: Dupuy and collaborators [58] used a rigidity matrix to model the relationship between cell displacement and implied forces. A form of potential energy has likewise been proposed as a way of

describing the equilibrium between turgor and cell wall resistance [59]. Finally, in a recent paper investigating the floral meristem of *A. thaliana*, potential energy was proposed as the means of regulating auxin transport [15].

In our model for the root apex, we define a spatial domain in which a potential function acts. The spatial derivatives of this function render the mechanical force as a function of time and space. Taking advantage of the radial symmetry of the region of the root tip, we consider a two-dimensional space and divide it into cells. We simulate cells by a Voronoi diagram obtained from a collection of generating points that represent the position assigned to each cell.

Voronoi diagrams

A Voronoi diagram, or tessellation, associated with a collection of points assigns to each point a limited region of space in the form of a convex polygon (polyhedron in three dimensions). Voronoi cells are used nowadays in many fields of science, however it was Honda [60] who first proposed the use of 2D Voronoi to model cells in a biological context.

Our domain is defined as follows: 1) We construct a regular shape with points on a rectangle and a parabolic tip. The exterior points are fixed and represent the epidermal cells surrounding the ground tissue of the root (See Videos S1 and S2). 2) These points in the border cannot define a convex polygon, so the corresponding cells have a point at infinity. 3) We create N points with random coordinates in the interior of this domain and perform a Voronoi tessellation using a Delaunay triangulation algorithm.

A typical configuration is shown in Fig. 4. Observe that the areas of the cells (A_i) vary in size and shape, and that the generating points shown in the figure ($\vec{r}_i$) do not correspond, in general, to the centre of mass of the cells ($\vec{r}_{0_i}$).

The average $\bar{A}_0 = \sum_{i=1}^{N} A_i/N$ is the space that each cell would occupy in a regular hexagonal lattice. Analogously, the distance is $d_i = |\vec{r}_i - \vec{r}_{0_i}| = 0 \forall i$ in the regular array. In two dimensions the array of cells with minimal surface energy is the hexagonal lattice, and we use this fact to define a potential function around this equilibrium configuration.

Elastic fields

Previous studies have used springs to simulate the interactions among cells [61], and the elements of the cellular walls [62,63]. In our case the equilibrium area $\bar{A}_0$ could be used to fix the size of mature cells, so deviations from this value would represent immature cells. If the cells in the tissue tend to be isotropic in shape, then a value of d_i different from zero would represent cells with the wrong shape and, consequently, largely stressed.

Regardless of the actual functional form of the energy potential, it is possible to make a Taylor expansion around the equilibrium state retaining only the first non-zero terms, provided one considers small deviations from equilibrium. The first non-trivial contributions correspond to a quadratic form, whose coefficients can be interpreted as force constants.

Therefore, we propose a harmonic potential acting on each cell i

$$V(x_i, y_i, t) = \frac{K_v}{2}(A_i(t) - \bar{A}_0(t))^2 + \frac{K_c}{2}(\vec{r}_i(t) - \vec{r}_{0_i}(t))^2 \qquad (1)$$

where the first term tends to uniformize the size, and the second term is related with the shape of the cells. K_v and K_c are elastic constants.
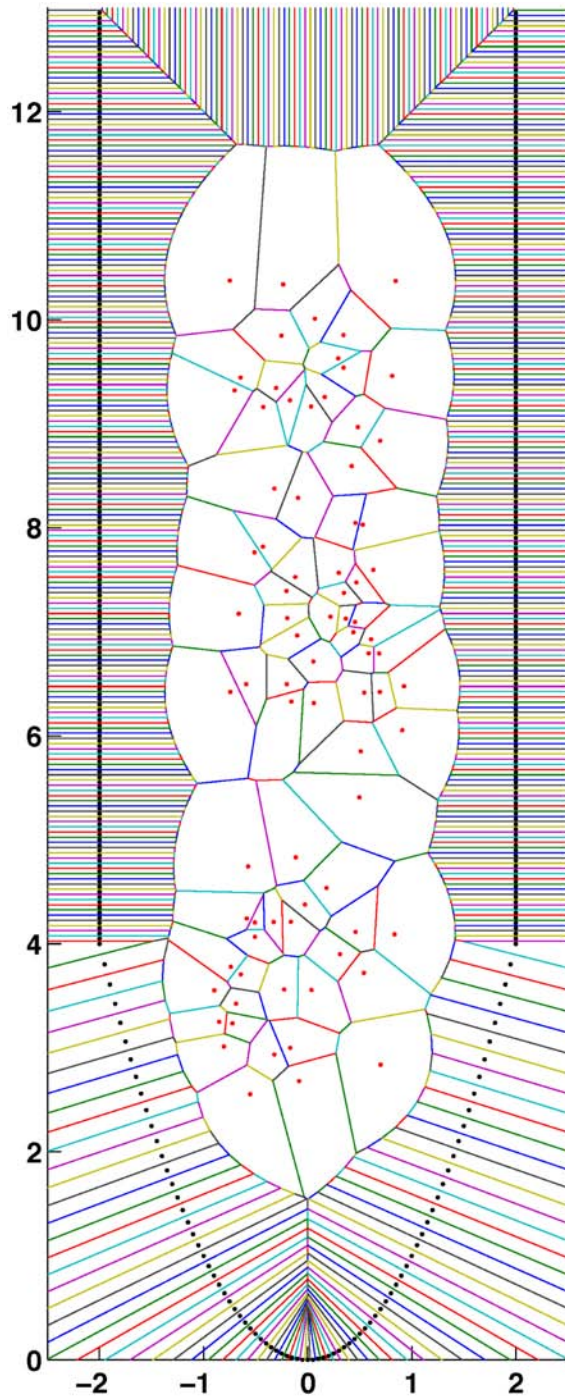
The expressions for the components of the force are:

$$F_x(x_i, t) = -\frac{K_v}{2} \left[\frac{1}{2} \sum_{m=1}^{M} \frac{(x_i - x_m) \cdot l_{i,m}}{|\vec{r}_i - \vec{r}_m|} \{A_i - \tilde{A}_0\} \right]$$
$$- K_c(x_i - x_{0_i})$$
$$\qquad\qquad (2)$$
$$F_y(y_i, t) = -\frac{K_v}{2} \left[\frac{1}{2} \sum_{m=1}^{M} \frac{(y_i - y_m) \cdot l_{i,m}}{|\vec{r}_i - \vec{r}_m|} \{A_i - \tilde{A}_0\} \right]$$
$$- K_c(y_i - y_{0_i})$$

where $l_{i,m}$ is the length of the edge shared between neighboring cells, and we have omitted the time dependence of the variables on the right hand side. All quantities in Eqs. 1 and 2 can be readily calculated with the algorithm used to define the Voronoi diagram.

Since this is a conservative system, and there is no reason to assume conservation in the root system, we include dissipation in the form of friction that simulates losses due to the inability of cells to make drastic elastic changes of shape or size. Therefore, the total force should be:

$$\vec{F}_T(x_i, y_i, t) = -\nabla V(x_i, y_i, t) - k\vec{v}(x_i, y_i, t) \qquad (3)$$

where $\vec{v}$ is the velocity and k is a friction coefficient. The N coupled dynamical equations of this newtonian system

$$\frac{\partial \vec{v}}{\partial t} = \vec{F}_T$$
$$\qquad\qquad (4)$$
$$\frac{\partial \vec{r}}{\partial t} = \vec{v}$$

can be integrated numerically by using a simple Euler method, imposing fixed boundary conditions on the fixed surface points.

As an example of the relaxation process with this scheme, in Fig. 5 we show the configuration of points in Fig. 4 after 2000 time iterations. The numerical calculation was stopped when the relative changes of the positions and velocities was less than 10^{-10}. The magnitude of the constants K_c, K_v and k sets the units of the time variations of the dynamical behavior of the system, and should be adjusted to physical units when modeling the growth of the RAM. One should consider the number of cell divisions per unit time (2.6 events/hr), the cell production rate (between 0 and 6 cells $\times$ mm^{-1}hr^{-1}) and the cell proliferation rate distribution (between 0 and 50 μm/hr) in the RAM [64]. The final form of the relaxed field suggests that it could be used to transfer positional information to the cells in the meristem. In order to achieve the latter, the auxin concentration must be coupled to the local value of the potential.

We introduced the process of cell division and proliferation into the simulation by defining two points inside a cell when it undergoes mitosis. The resulting Voronoi cells then locally alter the field, and the extra space needed for the two daughter cells is obtained by moving the upper border of the domain a proper distance to provide the exact extra space required. We show details of this process below.

Auxin transport

It is assumed that the field V is involved in the processes of auxin transport. In any transport equation there are basically two aspects to be considered: the hydrodynamic forces compelling a fluid to move, and the diffusion phenomena. Both are important for the case of auxins. Furthermore, the process of auxin transport

Figure 4. Typical initial configuration of cells after the Voronoi tessellation of random generating points.
doi:10.1371/journal.pcbi.1003026.g004
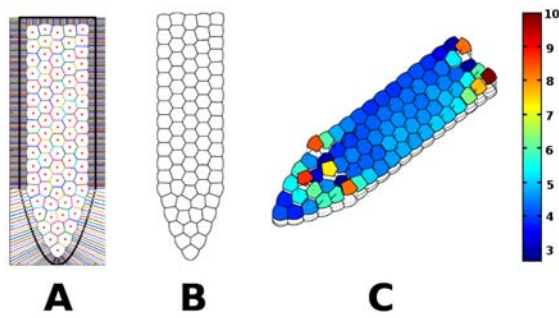
Figure 5. Configuration of cells after 2000 time iterations. (A) The points in Fig. 4 once they have attained equilibrium using the potential (See Video S3). (B) Final configuration of the cells in the RAM. Observe the regularity of the shapes and sizes of the cells. (C) 2D profile of the field after relaxation. Observe that it is not constant, but there are three well defined sections (See Video S4).
doi:10.1371/journal.pcbi.1003026.g005

is recognized to be active, meaning that the transfer of matter through the cell membranes could go against the concentration gradient of auxin molecules due to the action of PIN proteins. We propose that the amount of matter Q transported per unit time from cell i to a neighbor cell m is proportional to the gradient of the field V:

$$Q_{i,m} = -P_{i,m} \cdot A_{i,m} \cdot |V_i - V_m|, \tag{5}$$

where $P_{i,m}$ represents the permeability of the membrane and $A_{i,m}$ is the contact surface between the cells i and m (the line $l_{i,m}$ in 2D).

Observe that if the values of the $P_{i,m}$'s were constant, this equation would reduce to the well known Darcy's Law in hydraulics, which is analogous to Fourier's law in heat conduction, or Ohm's law in electrical networks. However this is not the case, because of the action of the PIN proteins which are critical. Therefore, the permeability is:

$$P_{i,m} = \alpha(c_i - c_m)\mathcal{F}_{i,m}, \tag{6}$$

where α is a constant related with the time scale of the dynamics, and the direction of the flux with respect to the concentration gradient $(c_i - c_m)$ (diffusion term) is given by the logical function $\mathcal{F}_{i,m}$. This latter function mimics the action of the PIN molecules, which attach to the membrane according to orientation and position in the domain.

We can simplify this action by considering "gates", which could be opened (1) or closed (0) according to specified simple rules. Let $\mathcal{S}$ be the set of cells at the surface, i.e. in contact with the immobile epidermal cells. We have set the following rules: All gates are closed, except

1. when $i,m \in \mathcal{S}$ and i is above m,
2. or if $i,m \notin \mathcal{S}$ and i is below m,
3. or if $i \notin \mathcal{S}$ and $m \in \mathcal{S}$ and i is above m.

The dynamical equation for the concentration of auxins in cell i is then:

$$\frac{1}{\alpha}\frac{\partial c_i}{\partial t} = \sum_{m=1}^{M} l_{im}(c_i - c_m)|V_i - V_m|, \tag{7}$$

where the sum is over all neighboring cells. This expression can be

readily integrated numerically in parallel with Eq. 4, once the parameter α has been properly adjusted.

In Fig. 6 we show the effect of the logical rules on the formation of auxin gradients. On the left we show a calculation without these rules, that is, maintaining all the membranes permeable. In (B) we incorporate the PIN action into the model. Observe that the distribution of the concentration of auxins (normalized with its maximum value) is similar to the one observed in real roots [42].

Cell division cycle

We shall assume that the period of the cell division cycle is regulated by the local concentration of auxins c_i. We are aware that this is an oversimplification of the complex hormonal regulation of the cell cycle in plants, but auxin has been shown to be an important component of such regulation [65]. We therefore need a model for the oscillations of cyclin concentrations. The robustness of these oscillations suggests that a non-linear oscillator would be a good model. We consider a two-component system for simplicity, considering CYCD and CYCB as the two key players. Since both undergo regular out-of phase oscillations with maxima related to the transitions between the G1-S and G2-M phases, respectively (See Fig. 2), we choose a simple Lotka-Volterra non-linear system with two components, generally used in ecology to model the predator-prey dynamics. This system presents all characteristics required for the observed time behavior of the concentration of cyclins [66]. The adimensional activator-inhibitor dynamical equations are:

$$\begin{aligned} \frac{\partial u}{\partial \tau} &= u(1-v) \\ \frac{\partial v}{\partial \tau} &= \beta v(u-1), \end{aligned} \tag{8}$$

where u and v represent CYCD and CYCB, respectively. This system presents an oscillatory behavior, provided β is within a certain range, whose period (T) and wave shape depend only on β and on the boundary conditions. It is easily shown that the period is:

$$T = \frac{2\pi}{\sqrt{\beta}}, \tag{9}$$
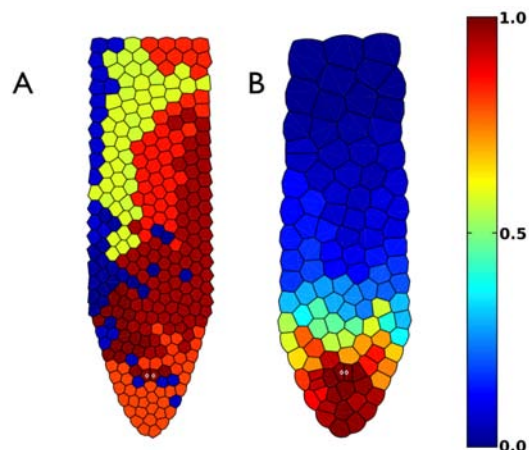
Figure 6. Typical numerical integration of Eq. 7 showing the formation of auxin gradients. (A) All gates are open (no PIN action). (B) Including the logical rules to open the gates to model the PIN action.
doi:10.1371/journal.pcbi.1003026.g006
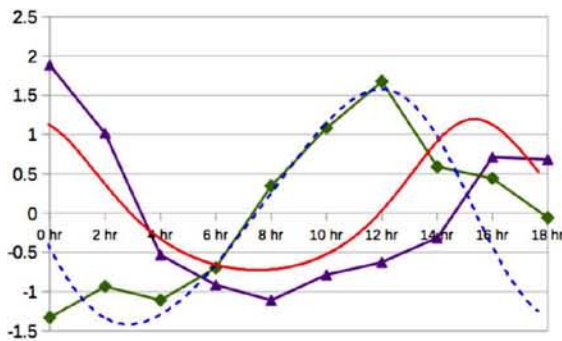
Figure 7. Variation of two-type cyclins concentrations and typical oscillations from the Lotka-Volterra model. Relative expression data of D-type cyclins (purple triangles) and B-type cyclins (green rhombuses) were taken from analysis of gene expression profiles using aphidicolin synchronization on Ref. [76], and are available on GENEVESTIGATOR web page. The oscillations from the Lotka-Volterra model of the inhibitor (blue dashed line) and the activator (red line) are also shown.
doi:10.1371/journal.pcbi.1003026.g007

which is inversely proportional to the square root of the ratio of the linear growth rate of the "prey" (u) to the death rate of the "predator" (v). In Fig. 7 we illustrate the oscillations of both variables.

Experimental data has shown that the cell cycle is arrested if the auxin concentration is below or above certain threshold values, and that the cycle period increases with auxin concentration [65]. Therefore, we simply assume that the auxin concentration is linearly related to the only parameter of this dynamical system: $\beta = \gamma c(i)$. Hence, each cell has its individual clock, which runs faster or slower depending on the auxin concentration in the model under consideration. We couple this dynamical feature into the numerical calculation of the model by performing a division of cell i when $t = \delta(n\Delta t - T_i[\tau])$ (where the $\delta-$function is one when the number of iterations $n\Delta t$, used in the Euler integration, surpasses the period). Therefore, γ is another constant that relates the time scale of reproduction (τ) to the time step used for relaxation dynamics. Parameters α and γ should be fitted according to the observed time scales for each of the three dynamics. Time step Δt (in seconds) should be obtained as well.

In practice, the act of cellular division is performed in the following manner:

1. At each time step, advance the internal clock of all cells according to the value of the local auxin concentration given by the cell life-cycle model.

2. Detect the cells in which the internal clock completes one period (a single division event occurs every cycle), and set the clock of these cells to zero.

3. In each one of these cells, $\vec{r}_i$ is substituted by two points, oriented at random and at equal distances of $\vec{r}_i$. This distance is typically of the order of a quarter of the radius of the cell.

4. The kinetic energy ($v_i^2/2$) of the mother cell is equally divided between mother and daughter cells.

5. The upper boundary of the domain is shifted upwards to increase the area by the exact amount required by these new cells to grow eventually to adult size.

The changes in the domain size and the size of the new cells produce a rearrangement of all cells, and this changes the local

value of the elastic field, which, at the same time, drives the auxin concentration that, in turn, regulates the division rate of all cells. We hypothesize that coupling among such three dynamics at different time scales is sufficient to produce the growth of the root with cellular patterns that mimic those of real systems in a wide region of the parameter space. We verified that the process is extremely robust against changes of initial conditions.

Results

In Fig. 8 we show the dynamical loop that integrates the dynamical equations with an Euler method. The program is initiated by choosing the values of the number of cells (N), the position of each cell (r_i), their proliferation rate (v_i), the gates given by the PIN action between two cells ($\mathcal{F}_{i,m}$) and the concentration of auxins (c_i) at time $t = 0$.

It is important to note that we normalize the auxin concentration function c with its maximum value at every time step. This allows our model to take into account the role of possible sources and sinks of auxin, since c is not a conserved quantity. The final distribution of auxin is insensitive to the initial conditions, but we start with a random distribution of auxin with a maximum at the quiescent centre in accordance with experimental observations. We recovered the same results if auxin concentrations were random at initial conditions (data not shown). The cycle clocks of each cell are set to zero at $t = 0$ and reset after a successful cell division.

The shape and color of the boxes (Fig. 8) represent the action of the different dynamics as described in experimental systems (see Fig. 3). The red square indicates a subroutine that includes the logical rules $\mathcal{F}_{i,m}$ of the PIN action and the red circles represent points of logical decisions at appropriate times. Black arrows represent the direction of flux of the simulation and the black-dash arrow indicates a decision related to the time condition for the dynamics of the cyclins. Eq. 4 is implemented in the blue diamond
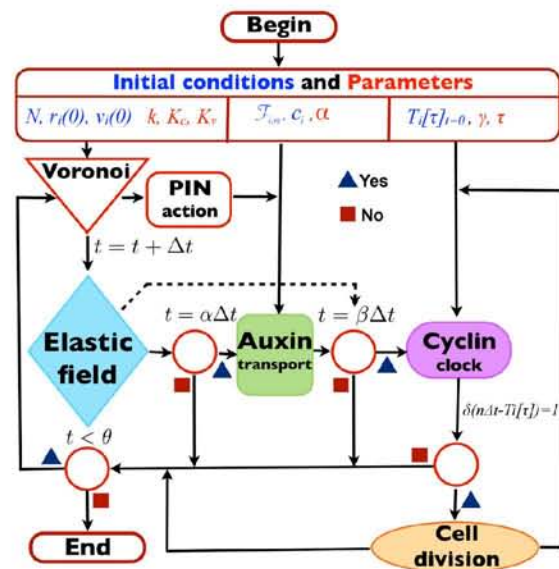
Figure 8. Flow-chart diagram of the program used for the numerical simulations. We show the parameters in red and the initial conditions in blue at the top of the diagram.
doi:10.1371/journal.pcbi.1003026.g008

block that represents the elastic field with time scale Δt. The loop is performed while the time t is less than the final time θ. Eq. 7 is implemented in the green block. The cyclin period is calculated for each cell at the violet block using Eqs. 8 and 9 and the threshold $\beta = \gamma c(i)$. Cellular divisions are performed as a subroutine represented by the orange block, and cell proliferation alters the conditions of all three dynamics.

The first step is to estimate the values of the parameters of the system. The adjustable parameters are the quantities indicated in red in Fig. 8. We start with the kinematical parameters. The constant K_c is related to the elastic modulus E of the cells. This quantity is measured when studying the mechanics of walls, cells, and tissues and is of the order of $E \sim 10 \text{MPa}$, as reported in [67].

For simplicity let us consider hexagonal cells in equilibrium. The magnitude of the elastic force is $|F_E| = ES_0\Delta L/L_0$, where S_0 is the contact area between two cells, $\Delta L = |A - A_0|^{1/2}$ is the change in length just after division, where $A_0 = \sqrt{3}L_0^2$ is the area of the hexagon, if L_0 is the distance between centroids of two contiguous cells. This should be equal to the corresponding force magnitude in our model $|F_{K_c}| = K_c|\vec{r}_i - \vec{r}_{0_i}|$. Just after a cell division, $A = A_0/2$, thus $\Delta L = \sqrt{\sqrt{3}L_0^2/2}$, $|\vec{r}_i - \vec{r}_{0_i}| \simeq L_0/2$ and $S_0 = A_0/6$. Equating the two forces we obtain

$$K_c \simeq \frac{L_0}{\sqrt{2\sqrt{3}}}E.$$

Taking the average diameter of a mature cell as $L_0 = 15$ μm [64] and the experimental value $E = 10$ MPa we obtain $K_c \sim 80$ Pa $-$ m.

At this stage, K_v should be related to the properties of the cell membrane, the metabolism of cell growth and the turgor pressure. It is difficult to associate the action of the first term of Eq.(1) to a single biological property. However, the dynamics of this term should produce a restoring force of the same order of magnitude as the second term, if the form and geometry of the domain are to be maintained during the growth dynamics. Therefore, if we use a value of $K_v = 80$ Pa/m the system should relax to a set of cells with roughly the same size and shape, as shown in the calculation of Fig. 5B. We found numerically that this produces results for the dynamics of growth that are comparable to the experimental quantities measured.

Parameter k is related to the viscous damping of the cell motion. The dynamical friction constant k can be estimated by observing that the amplitude of the oscillatory motion $e^{-i\omega t}$, caused by the harmonic forces should be reduced, to avoid oscillations, by a factor of $1/e$ in a lapse of at most one period $T = 2\pi/\omega$, that is $k \geq m/T$. Note that in Eq. (4) the mass of the cell (m) is considered to be one. This gives $\omega = 2\sqrt{K_c/m} \approx 18 \text{ sec}^{-1}$, and $k = m\omega/2\pi = 2.84$ Pa $-$ m $-$ sec.

The values used in the calculations are $K_c = 80$, $K_v = 80$ and $k = 3$. With these values we obtain the real time scale of an iteration step Δt in the numerical calculations, by finding the number of iterations needed to obtain the experimental number of cell divisions in that lapse. In seven days, our observations showed (see Fig. 1) that the number of cells in the meristem is about 350. In averaged calculations we reproduce this number in 3400 iterations by using $\gamma = 100$ and $\alpha = 8$. This means that the lapse representing one iteration is the number of minutes in 7 days over the number of iterations, that is $\Delta t = (7 \times 24 \times 60)/3400 = 3$ min. Considering that the average auxin concentration is $\langle c \rangle = 0.5$, the value of β is ≈ 50 in units of τ, which is about 100 times Δt. These values produce a single cell cycle period on the order of 12 hr, as shown in Fig. 7 [66].

In Fig. 9 (and Video S5) we provide an example of the growth of the system. We start with eight points at random in the parabolic tip of the domain, and fix the position of two additional points that represent the quiescent cells in the centre of the domain, marked with a white symbol. These cells reproduce at a rate ten times lower than the others; they divide after ten divisions per cell on average (in the right panel of the figure these quiescent cells have just divided). The auxin concentration in these cells is set to the maximum initially, and this is represented by a dark red color in the figure. The cell's position, shape, and proliferation rate are calculated every time step and the auxin is transported between cells. After 400 time steps the cells are attaining a uniform shape and size (Fig. 9), and the auxin gradient is already formed. This gradient will dictate the time in which a complete cell proliferation cycle is accomplished locally, followed by a cell division event that produces a sudden increase of the local potential that, in turn, governs auxin transport.

Despite these complicated dynamical interactions, the auxin gradient is preserved throughout and the process of growth and cell patterning is by no means random. This can be seen in Fig. 10. The overall pattern that emerges after some cycles of coupled dynamics is very similar to the apical-basal pattern of cell proliferation and elongation observed in RAM and along the length of the root tip. Such dynamics and emergent pattern are robust to initial conditions.

It is interesting to note that the region around the quiescent center in the stem-cell niche shows the greatest concentration of auxin, and a maximum in the potential. Also, the cell division cycle is minimum at this location. An intermediate region in which the auxin concentration diminishes and the potential is very small, but the cell proliferation rate is roughly constant, surrounds the quiescent cells. Finally, the most distal part from the tip (towards the base of the plant) is characterized by a very small concentration of auxin, causing the cell proliferation rate to be very small, and the potential to increase enormously. The combination of these effects results in the arrest of cell proliferation and in the formation of the elongation zone at a defined distance from the root tip. The emergent patterns recovered in the model are similar to those observed for the distribution of auxin as reported in Ref. [68], and the pattern of cell proliferation along the root longitudinal axis reported in Ref. [69]. Our results are also in agreement with the qualitative patterns of cell proliferation and elongation that are observed along the apical-basal, longitudinal axis of the growing A. thaliana root.
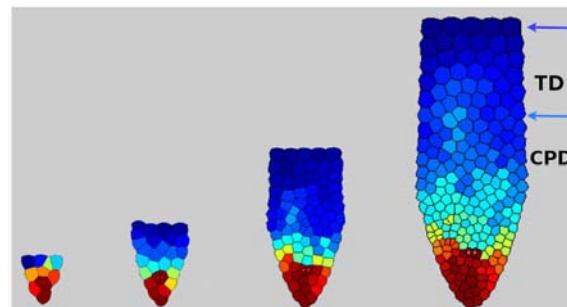
Figure 9. Typical calculation of the dynamical growth of the root using the model described. We show four snapshots of the configuration at 400, 1400, 2400 and 3400 time steps. The color code represents the concentration of auxins, red for the maximum and blue for the minimum. See Video S5.
doi:10.1371/journal.pcbi.1003026.g009
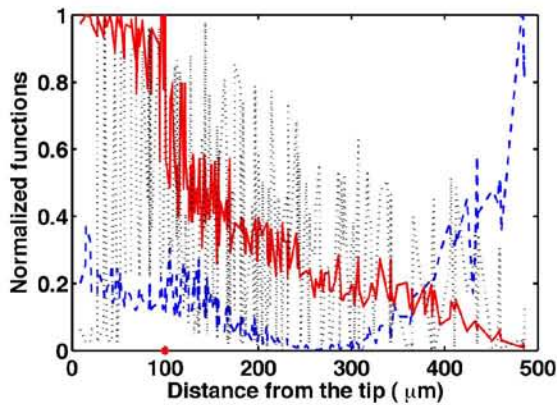
Figure 10. Plots of local potential, auxin concentration and cell cycle, after coupling dynamics. The normalized local potential (dashed-blue), the auxin concentration (red) and the advance of the cycle clock (dotted-black) as functions of the distance from the tip (μm), at $t = 3400$ time steps, corresponding to seven days.
doi:10.1371/journal.pcbi.1003026.g010

We can use this model to predict what patterns are expected under different growth conditions. In Fig. 11 we show a histogram of the number of cell divisions occurring at a given distance from tip, as obtained from an example calculation in which we fixed the parameter $\alpha = 8$. Interestingly, we observe that the length of the RAM does not surpass a certain value, which depends on α, because the modeled coupled dynamics prevents cells far from the tip to divide. Such types of coupled dynamics could explain the emergence of the transition from proliferation to the elongation cellular states in real roots, as well as the limited ranges or domain sizes of actively proliferating cells in stem-cell niches of plants and animals [1,3].

Hence, our model can be used to generate novel predictions concerning the role of the parameters considered in the model, and in determining RAM size and cell proliferation and elongation patterns along the root apical-basal axis for *A. thaliana* under different environmental or growth conditions. Our general model
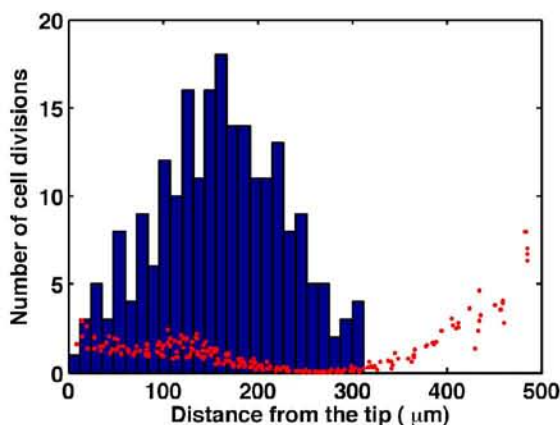
could eventually be adjusted to model stem-cell niches in other plants and animal systems, as well as modeling growth and differentiation in communities of unicellular organisms if similar physical fields can be postulated in such latter cases.

In order to examine the quantitative behavior of the model and validate it with published experimental data, we compared our model's predictions to measurements of the proliferation rates along the axis of the *A. thaliana* root as a function of the distance from the quiescent centre [64]. We ran numerous iterations of the model in order to obtain a reasonable statistical sample. We show a typical result from the simulations run to the experimental data in Fig. 12. Panel (A) shows the available experimental results for cell proliferation rates along the apical-basal axis of the root reported in Ref. [64] as a continuous red curve. The numerical results from our model are shown in blue. These results were obtained using the estimated parameter values that give the time in hours and the sizes in μm. We shifted the origin to account for the fact that all quantities in our calculations were measured from the tip of the domain and not from the quiescent centre. Notice that the simulated and experimentally generated curves are very similar.

In Fig. 12(B) we show an histogram of the frequency distribution of cell size. This histogram varies with different iterations because of the stochastic nature of cell proliferation and growth dynamics [70]. However, all calculations share the same qualitative characteristics; namely an unimodal distribution between ~ 10 and ~ 35 μm, with a maximum around 15 μm. This result was already recovered by Verbelen and collaborators Ref. [71]. The red curve was obtained by measuring the cell size in an Arabidopsis root Fig. 1. Similar curves have been obtained for many different plant species, including wheat [70].
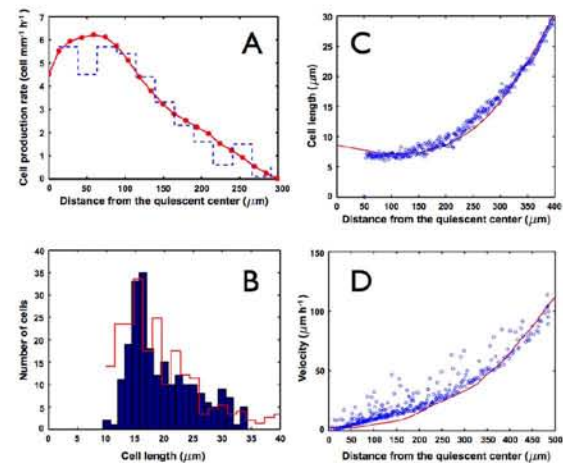
Figure 12. Comparisons between results obtained with the model and experimental data. (A) Cell proliferation rate as a function of the distance from the quiescent centre; calculation from Fig. 9 after six days of growth. The red line and dots are the experimental points reported in Ref. [64]. (B) Frequency distribution for cell length. Experimental data were taken from our laser microscope image of Fig. 1. (C) Average cell length as a function of the distance from the quiescent centre; calculation from Fig. 9 after six days of growth. The red line is the experimental result reported in Ref. [64]. (D) Average cell proliferation velocity as a function of the distance from the quiescent centre; calculation from Fig. 9 after six days of growth. The red line is the experimental result reported in Ref. [64].
doi:10.1371/journal.pcbi.1003026.g012

Figure 11. Histogram of the number of cell divisions obtained along the root when $\alpha = 8$**.** The potential profile is shown as red dots. Observe that there are no cell divisions beyond ~ 300 μm, meaning that the meristem has attained a stationary length.
doi:10.1371/journal.pcbi.1003026.g011

In Fig. 12(C) we show the variation of cell length along the longitudinal axis of the root. The red curve is the experimental result from Ref. [64]. It should be pointed out that the experiment was obtained by measuring the cell flux in a fixed point and by counting along the axis of the root in two dimensions, which is very convenient when comparing with our two-dimensional model. In order to mimic the experimental procedures, our numerical results were obtained by spotting the centroids of the Voronoi cells in the final time, which corresponds to six days. We calculated the length (l) by assigning an area of $A_i = \pi(l/2)^2$ to each cell. Again, a shift of 10 μm in the horizontal axis was needed to account for the difference in the origin, and the results for each cell are displayed as blue dots in the figure. Once again, the agreement between our simulated results and the experimental data are clear.

Finally, in Fig. 12(D) we show the average cell proliferation velocity, as defined in Ref. [64], as a function of the distance from the quiescent centre (red line), and compare it with our results (blue dots). In the experiment, Beemster and collaborators measured the difference in position of each cell for two subsequent times, averaged over time. In our calculation we measured the difference in position of each cell with respect to the apex of the root, which is itself being displaced every time a cell division takes place. By changing the frame of reference, we can compare the reported experiment with our results. The agreement is also remarkable when one compares the simulation results recovered with our model and the experimental data. This is more significant than the previous validations, since this result reflects the totality of the dynamical behavior in time and not only in a frozen snapshot, as in the previous cases.

Discussion

We present a dynamical model that couples auxin concentration gradients, cell proliferation and a physical tension field in a two-dimensional spatial domain that mimics the *A. thaliana* root tip. We have validated our model with both static and dynamic cellular empirical data, and have shown that our model recovers the pattern of rates of cell proliferation observed in the apical-basal axis of roots. The model also recovers the discrete transition from the proliferative to the elongation domains. Thus, our model puts forward a novel theoretical framework to test hypothesis concerning the coupled roles of auxin, cell proliferation, and physical fields dynamics in the emergence of the cellular pattern observed along the *A. thaliana* root tip. Ultimately, we have postulated a complex system in which the main emergent property of the coupled dynamics is at the appropriate spatial and cellular structure for the intracellular genetic networks to express differentially along the root. However, the explicit consideration of complex gene regulatory networks is out of the scope of this paper.

Our model and analysis suggest that the size of the RAM depends on the value of the parameter α (Fig. 13) in a rather defined manner. This parameter represents the ratio between the time scales of the potential relaxation and the auxin transport mechanisms. The length of the RAM decreases as the auxin transport parameter α increases as a power law. Therefore, this quantitative prediction can be verified experimentally, as auxin concentrations and transport along the root can be modified by manipulating the conditions of root growth (e.g. adding NPA to the growth medium to block auxin transport). Previous experimental work has suggested that the size of the RAM varies depending on growth conditions and is altered with external supplementation of auxin [39].

Given that plant growth is influenced by the mechanical behavior of the cell wall, measurements of the mechanical
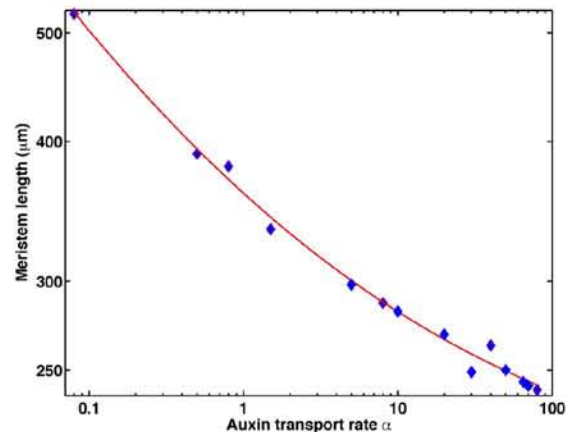
Figure 13. Log-log plot of the maximum RAM as a function of the parameter α. Numerical results are blue rhombuses, and the red line is the best fit with a function of the form $f(x) = 1.7x^{-0.26} + 1.88$ with $R^2 = .993$.

doi:10.1371/journal.pcbi.1003026.g013

properties of living cell walls are important to fully understand how cellular organization is achieved. Like most biological materials, material properties of cell walls change as a function of age, the magnitude of forces they are subjected to, and immediate physiological conditions [67,72]. This confers spatial and temporal heterogeneity on cell wall constituents, complicating measurements of the mechanical properties of plant living walls even with present-day instrumentation. Furthermore, a single modulus of elasticity is not sufficient because of the structural anisotropy of the cell wall [67]. Therefore, comparisons between the predicted values of Kv and Kc of our model and the values reported for the modulus of elasticity of real cell walls are far from being straightforward. However, the fact that we reproduced the root tip pattern with the selected values suggests that they are likely to be biologically meaningful.

More generally, our work reinforces conclusions from recent studies that experimentally demonstrate the importance of physical forces in the regulation of root apical-basal patterning [49,53], such as the mechanical induction of lateral roots or the coordination between auxin concentration and microtubule orientation [49,53,54]. It is remarkable that simple arguments concerning uniform size, shape and geometry of cell disposition is sufficient to produce a non-uniform field that provides sufficient spatial information to recover the overall dynamical growth pattern observed along the root. It is thus predicted that modification of physical forces would change the size and the pattern of these zones, an issue that could in principle be further explored theoretically and experimentally.

Auxin response is modulated not only by auxin concentration, but also by the auxin signaling pathway, which includes many components of different gene families, and which interact through several feedback loops, creating non-linear behaviors. Consequently, auxin concentration at any location does not necessarily coincide with auxin response. Even if this is not the case in the root [68], it could be important to include an explicit model of the auxin signaling pathway in future extensions of our model. In addition, in our model we considered the polar PIN configuration as fixed, as in Ref. [46]. However, in reality a more robust dynamic auxin transport is observed when the PIN expression is regulated by auxin [73].

In our model we fixed the position and number of the quiescent cells. We are aware that the root stem-cell niches are regulated by a complex regulatory network [74]. WUSCHEL RELATED HOMEOBOX5 (WOX5) is a Quiescent Center identity gene indispensable for the maintenance of the undifferentiated state of stem cells and niche size regulation, and it is part of the proposed root stem-cell niche regulatory network [74,75]. Recent theoretical and experimental work has suggested that WOX5 regulates and is regulated by auxin [36,74]. In our calculations we input several initial conditions for auxin concentration, and demonstrated that the model is fairly robust to these changes. However, as shown in Fig. 6, neglecting the action of PIN polarization destroys the auxin gradient along the root. Including these and other regulatory interactions in a future model would enable us to explicitly consider intracellular complex gene regulatory networks, which are likely coupled among cells by physical and hormone fields.

The complex network underlying the cell cycle was also reduced to consider two basic components, because for our purposes, only the phases of the oscillations of the concentrations matter. Since CYCA and CYCB oscillate in phase, we consider them as a single variable; and because CYCD oscillates in anti phase, we take this to mean that there is an activator-inhibitor interaction between these two groups of proteins. In our model we stressed the importance of the relationship between auxin concentration and the regulation of cell proliferation, and we neglected the details of the known regulatory processes of the cell cycle, which although important, do not directly affect the overall results of our simulation. Nonetheless, such details of the gene regulatory network underlying the cell cycle, cell differentiation and auxin dynamics should be incorporated in future developments of the model.

In conclusion, we have put forward a minimal mathematical model that considers the essential dynamical coupling of cell proliferation with a physical field and chemical (hormone) gradients, in order to explore if such processes are sufficient to obtain the emergence of cellular organization during stem-cell niche patterning and organ growth. We have used the *A. thaliana* root as our study system.

Despite the simplification of many biological details, our model is able to recover patterns that greatly resemble those observed in stem-cell niches of plants and animals, and particularly those in the *A. thaliana* root tip. The remarkable coincidence between the

simulated cellular characteristics along the model root apical-basal axis (shown in Fig. 12), with those that have been observed and quantified in actual roots, validates the qualitative features and utility of our model for understanding the emergence of cellular patterns in such a multicellular organ. Furthermore, the cellular patterns of stem-cells among multicellular plants and animals have generic traits. Our model provides a formal tool to explore if such traits may be explained by the generic non-linear coupling of relevant physical and chemical fields to discover emergent properties of cell proliferation dynamics across biological systems.

Supporting Information

Video S1 Dynamical growth and proliferation of cells and boundary.
(MP4)

Video S2 Dynamical behavior of stem cells only.
(MP4)

Video S3 Relaxation process for a fixed number of cells.
(MP4)

Video S4 Dynamical changes of the local cell potential.
(MP4)

Video S5 Dynamical development of auxin concentration.
(MP4)

Author Contributions

Conceived and designed the experiments: RAB EA EOG ERAB. Performed the experiments: RAB JRRA MAN YCP. Analyzed the data: RAB JRRA MAN EA EOG VHH YCP ERAB. Contributed reagents/materials/analysis tools: RAB JRRA MAN EA YCP ERAB. Wrote the paper: RAB JRRA MAN EA EOG ERAB.

References

1. Scheres B (2007) Stem-cell niches: nursery rhymes across kingdoms. Nat Rev Mol Cell Biol 8: 345–54.
2. Sablowski R (2004) Plant and animal stem cells: conceptually similar, molecularly distinct? Trends Cell Biol 14: 605–11.
3. Li L, Xie T (2005) Stem cell niche: structure and function. Annu Rev Cell Dev Biol 21: 605–31.
4. Huang S (2012) The molecular and mathematical basis of Waddington's epigenetic landscape: A framework for post-Darwinian biology? Bio Essays 34: 149–157.
5. Álvarez-Buylla E, Chaos A, Aldana M, Benítez M, Cortes-Poza Y, et al. (2008) Floral morphogenesis: Stochastic explorations of a gene network epigenetic landscape. PLoS ONE 3: e3626.
6. Newman S, Bhat R (2008) Dynamical patterning modules: physico-genetic determinants of morphological development and evolution. Phys Biol 5: 015008.
7. Newman S, Bhat R (2009) Dynamical patterning modules: a "pattern language" for development and evolution of multicellular form. Int J Dev Biol 53: 693–705.
8. Fernandes AN, Chen X, Scotchford CA, Walker J, Wells DM, et al. (2012) Mechanical properties of epidermal cells of whole living roots of Arabidopsis thaliana : An atomic force microscopy study. Phys Rev E Stat Nonlin Soft Matter Phys 85: 021916.
9. Hamant O, Traas J, Boudaoud A (2010) Regulation of shape and patterning in plant development. Curr Opin Genet Dev 20: 454–9.
10. Mammoto A, Mammoto T, Ingber DE (2012) Mechanosensitive mechanisms in transcriptional regulation. J Cell Sci 125: 3061–73.
11. Barrio RA, Hernández-Machado A, Varea C, Romero-Arias JR, Álvarez-Buylla E (2010) Flower development as an interplay between dynamical physical fields and genetic networks. PLoS ONE 5: e13523.
12. Espinosa-Soto C, Padilla-Longoria P, Alvarez-Buylla ER (2004) A gene regulatory network model for cell-fate determination during Arabodopsis thaliana ower development that is robust and recovers experimental gene expression profiles. Plant Cell 16: 2923–2939.
13. Alvarez-Buylla ER, Azpeitia E, Barrio R, Benitez M, Padilla-Longoria P (2010) From ABC genes to regulatory networks, epigenetic landscapes and ower morphogenesis: Making biological sense of theoretical approaches. Semin Cell Dev Biology 21: 108–117.
14. Kwiatkowska D (2008) Flowering and apical meristem growth dynamics. J Exp Bot 59: 187–201.
15. van Mourik S, Kaufmann K, van Dijk ADJ, Angenent GC, Merks RMH, et al. (2012) Simulation of organ patterning on the oral meristem using a polar auxin transport model. PLoS ONE 7: e28762.
16. Hester S, Belmonte J, Gens JS, Clendenon SG, Glazier J (2011) A multi-cell, multi-scale model of vertebrate segmentation and somite formation. PLoS Comput Biol 7: e1002155, doi:10.1371/journal.pcbi.1002155.
17. Perilli S, Mambro RD, Sabatini S (2012) Growth and development of the root apical meristem. Curr Opin Plant Biol 15: 17–23.
18. Ivanov VB, Dubrovsky JG (2012) Longitudinal zonation pattern in plant roots: conics and solutions. Trends Plant Sci 00219-1: S1360–1385.
19. Benková E, Hejátko J (2009) Hormone interactions at the root apical meristem. Plant Mol Biol 69: 383–96.

20. Garay-Arroyo A, De La Paz Sánchez M, García-Ponce B, Azpeitia E, Álvarez Buylla ER (2012) Hormone symphony during root growth and development. Dev Dyn 241: 1867–1885.

21. Sanz L, Murray JA, Dewitte W (2012) To divide and to rule; regulating cell division in roots during post-embryonic growth. In: Lüttge U, Beyschlag W, Büdel B, Francis D, editors. Progress in Botany. Volume 73. Berlin Heidelberg: Springer. pp. 57–80.

22. Moubayidin L, Perilli S, Ioio RD, Mambro RD, Costantino P, et al. (2010) The rate of cell differentiation controls the Arabidopsis root meristem growth phase. Curr Biol 20: 1138–43.

23. Ivanov VB (1997) Relationship between cell proliferation and transition to elongation in plant roots. Int J Dev Biol 41: 907–15.

24. Inzé D, De Veylder L (2006) Cell cycle regulation in plant development. Annu Rev Genet 40: 77–105.

25. De Veylder L, Beeckman T, Inzé D (2007) The ins and outs of the plant cell cycle. Nat Rev Mol Cell Biol 8: 655–65.

26. Overvoorde P, Fukaki H, Beeckman T (2010) Auxin control of root development. Cold Spring Harb Perspect Biol 2: a001537.

27. Woodward A, Bartel B (2005) Auxin: regulation, action, and interaction. Ann Bot 95: 707–735.

28. Guilfoyle T, Hagen G (2007) Auxin response factors. Curr Opin Plant Biol 10: 453–460.

29. Kleine-Vehn J, Friml J (2008) Polar targeting and endocytic recycling in auxin-dependent plant development. Annu Rev Cell Dev Biol 24: 447–473.

30. Mockaitis K, Estelle M (2008) Auxin receptors and plant development: a new signaling paradigm. Annu Rev Cell Dev Biol 24: 55–80.

31. Lau S, Jürgens G, De Smet I (2008) The evolving complexity of the auxin pathway. Plant Cell 20: 1738–1746.

32. Vanneste S, Friml J (2009) Auxin: a trigger for change in plant development. Cell 136: 1005–1016.

33. Himanen K, Boucheron E, Vanneste S, de Almeida Engler J, Inzé D, et al. (2002) Auxin-mediated cell cycle activation during early lateral root initiation. Plant cell 14: 2339–51.

34. Oakenfull EA, Riou-Khamlichi C, Murray JAH (2002) Plant D-type cyclins and the control of G1 progression. Philos Trans R Soc Lond B Biol Sci 357: 749–60.

35. Ishida T, Adachi S, Yoshimura M, Shimizu K, Umeda M, et al. (2010) Auxin modulates the transition from the mitotic cycle to the endocycle in Arabodopsis. Development 137: 63–71.

36. Ding Z, Friml JL (2010) Auxin regulates distal stem cell differentiation in Arabodopsis roots. Proc Natl Acad Sci U S A 107: 12046–51.

37. Jurado S, Abraham Z, Manzano C, López-Torrejón G, Pacios L, et al. (2010) The Arabidopsis cell cycle F-box protein SKP2A binds to auxin. Plant Cell 22: 3891–904.

38. Tromas A, Braun N, Muller P, Khodus T, Paponov IA, et al. (2009) The AUXIN BINDING PROTEIN 1 is required for differential auxin responses mediating root growth. PLoS ONE 4: e6648.

39. Ioio RD, Nakamura K, Moubayidin L, Perilli S, Taniguchi M, et al. (2008) A genetic framework for the control of cell division and differentiation in the root meristem. Science 322: 1380–1384.

40. Friml J, Benková E, Blilou I, Wisniewska J, Hamann T, et al. (2002) AtPIN4 mediates sink-driven auxin gradients and root patterning in Arabidopsis. Cell 108: 661–673.

41. Sabatini S, Beis D, Wolkenfelt H, Murfett J, Guilfoyle T, et al. (1999) An auxin-dependent distal organizer of pattern and polarity in the Arabodopsis root. Cell 99: 463–472.

42. Petersson S, Johansson A, Kowalczyk M, Makoveychuk A, Wang J, et al. (2009) An auxin gradient and maximum in the Arabodopsis root apex shown by high-resolution cell-specific analysis of IAA distribution and synthesis. Plant Cell 21: 1659–1668.

43. Blilou I, Xu J, Wildwater M, Willemsen V, Paponov I, et al. (2005) The PIN auxin efflux facilitator network controls growth and patterning in Arabidopsis roots. Nature 433: 39–44.

44. Vieten A, Vanneste S, Wisniewska J, Benková E, Benjamins R, et al. (2005) Functional redundancy of PIN proteins is accompanied by auxin-dependent cross-regulation of PIN expression. Development 132: 4521–4531.

45. Petrásek J, Mravec J, Bouchard R, Blakeslee J, Abas M, et al. (2006) PIN proteins perform a rate-limiting function in cellular auxin efflux. Science 312: 914–918.

46. Grieneisen V, Xu J, Marée P AFand Hogeweg, Scheres B (2007) Auxin transport is sufficient to generate a maximum and gradient guiding root growth. Nature 449: 1008–1013.

47. Mironova V, Omelyanchuk N, Yosiphon G, Fadeev S, Kolchanov N, et al. (2010) A plausible mechanism for auxin patterning along the developing root. BMC Syst Biol 4: 98.

48. Swarup R, Bennett M (2003) Auxin transport: the fountain of life in plants? Dev Cell 5: 824–826.

49. Ditengou FA, Teale WD, Kochersperger P, Flittner KA, Kneuper I, et al. (2008) Mechanical induction of lateral root initiation in Arabidopsis thaliana. Proc Natl Acad Sci U S A 105: 18818–18823.

50. Laskowski M, Grieneisen V, Hofhuis H, Hove C, Hogeweg P, et al. (2008) Root system architecture from coupling cell shape to auxin transport. PLoS Biol 16: e307.

51. Kleine-Vehn J, Ding Z, Jones A, Tasaka M, Morita M, et al. (2010) Gravity-induced PIN transcytosis for polarization of auxin uxes in gravity-sensing root cells. Proc Natl Acad Sci U S A 107: 22344–22349.

52. Palme K, Dovzhenko A, Ditengou F (2006) Auxin transport and gravitational research: perspectives. Protoplasma 229: 175–181.

53. Heisler M, Hamant O, Krupinski P, Uyttewaal M, Ohno C, et al. (2010) Alignment between PIN1 polarity and microtubule orientation in the shoot apical meristem reveals a tight coupling between morphogenesis and auxin transport. PLoS Biol 8: e1000516.

54. Nakayama N, Smith RS, Mandel T, Robinson S, Kimura S, et al. (2012) Mechanical regulation of auxin-mediated growth. Curr Biol 22: 1468–76.

55. Engler AJ, Sen S, Sweeney HL, Disher DE (2006) Matrix elasticity directs stem cell lineage specification. Cell 126: 677–689.

56. Hamant O, Heisler MG, Jonsson H, Krupinski P, Uyttewaal M, et al. (2008) Developmental patterning by mechanical signals in Arabidopsis. Science 322: 1650–1655.

57. Kutschera U, Niklas KJ (2007) The epidermal-growth-control theory of stem elongation: an old and a new perspective. J Plant Physiol 164: 1395–409.

58. Dupuy L, Mackenzie J, Haseloff J (2010) Coordination of plant cell division and expansion in a simple morphogentetic system. Proc Natl Acad Sci U S A 107: 2711–2716.

59. Merks RM, Guravage M, Inzé D, Beemster GT (2011) VirtualLeaf: An open-source framework for cell-based modeling of plant tissue growth and development. Plant Physiol 155: 656–666.

60. Honda H (1978) Description of cellular patterns by Dirichlet domains: the two-dimensional case. J Theor Biol 72: 523–543.

61. Prusinkiewicz P, Lindenmayer A (1990) The algorithmic beauty of plants. New York: Springer-Verlag.

62. Jönsson H, Heisler MG, Shapiro BE, Meyerowitz EM, Mjolsness E (2006) An auxin-driven polarized transport model por phyllotaxis. Proc Natl Acad Sci U S A 103: 1633–1638.

63. Rudge T, Haseloff J (2005) A computational model of cellular morphogenesis in plants. Lect Notes Comput Sci 3630: 78–87.

64. Beemster GT, Baskin TI (1998) Analysis of cell division and elongation underlying the developmental acceleration of root growth in Arabidopsis thaliana. Plant Physiol 116: 1515–1526.

65. Perrot-Rechenmann C (2010) Cellular responses to auxin: division versus expansion. Cold Spring Harb Perspect Biol 2: a001446.

66. Menges M, De Jager SM, Gruissem W, Murray JA (2005) Global analysis of the core cell cycle regulators of Arabidopsis identifies novel genes, reveals multiple and highly specific profiles of expression and provides a coherent model for plant cell cycle control. Plant Cell 41: 546–566.

67. Mirabet V, Das P, Boudaoud A, Hamant O (2011) The role of mechanical forces in plant morphogenesis. Annu Rev Plant Biol 62: 365–85.

68. Brunoud G, Wells D, Oliva M, Larrieu A, Mirabet V, et al. (2012) A novel sensor to map auxin response and distribution at high spatio-temporal resolution. Nature 482: 103–106.

69. Baskin TI (2000) On the constancy of cell division rate in the root meristem. Plant Mol Biol 43: 545–554.

70. Ivanov VB, Dobrochaev AE, Baskin TI (2002) What the distribution of cell lengths in the root meristem does and does not reveal about cell division. J Plant Growth Regul 21: 60–67.

71. Verbelen JP, Cnodder TD, Le J, Vissenberg K, Baluska F (2006) The root apex of Arabidopsis thaliana consists of four distinct zones of growth activites. Plant Signal Behav 1: 296–304.

72. Niklas K, Spatz H (2012) Plant physics. Chicago: University of Chicago Press. 447 pp.

73. Mironova V, Omelyanchuk N, Novoselova E, Doroshkov A, Kazantsev F, et al. (2012) Combined in silico/in vivo analysis of mechanisms providing for root apical meristem self-organization and maintenance. Ann Bot 110:349–360.

74. Azpeitia E, Benitez M, Vega I, Villarreal C, Alvarez-Buylla E (2010) Single-cell and coupled GRN models of cell patterning in the Arabidopsis thaliana root stem cell niche. BMC Syst Biol 4: 134.

75. Sarkar A, Luijten M, Miyashima S, Lenhard M, Hashimoto T, et al. (2007) Conserved factors regulate signalling in Arabidopsis thaliana shoot and root stem cell organizers. Nature 446: 811–814.

76. Menges M, Hennig L, Gruissem W, Murray JAH (2003) Genome-wide gene expression in an Arabidopsis cell suspension. Plant molecular biology 53: 423–442.

ANEXO C

Artículo: Modelo del ciclo celular y la diferenciación en *C. elegans*

BMC
Bioinformatics

RESEARCH ARTICLE

Open Access

A model of the regulatory network involved in the control of the cell cycle and cell differentiation in the *Caenorhabditis elegans* vulva

Nathan Weinstein[1,2,5], Elizabeth Ortiz-Gutiérrez[1,3,5], Stalin Muñoz[4], David A Rosenblueth[4,5], Elena R Álvarez-Buylla[3,5] and Luis Mendoza[2,5*]

Abstract

Background: There are recent experimental reports on the cross-regulation between molecules involved in the control of the cell cycle and the differentiation of the vulval precursor cells (VPCs) of *Caenorhabditis elegans*. Such discoveries provide novel clues on how the molecular mechanisms involved in the cell cycle and cell differentiation processes are coordinated during vulval development. Dynamic computational models are helpful to understand the integrated regulatory mechanisms affecting these cellular processes.

Results: Here we propose a simplified model of the regulatory network that includes sufficient molecules involved in the control of both the cell cycle and cell differentiation in the *C. elegans* vulva to recover their dynamic behavior. We first infer both the topology and the update rules of the cell cycle module from an expected time series. Next, we use a symbolic algorithmic approach to find which interactions must be included in the regulatory network. Finally, we use a continuous-time version of the update rules for the cell cycle module to validate the cyclic behavior of the network, as well as to rule out the presence of potential artifacts due to the synchronous updating of the discrete model. We analyze the dynamical behavior of the model for the wild type and several mutants, finding that most of the results are consistent with published experimental results.

Conclusions: Our model shows that the regulation of Notch signaling by the cell cycle preserves the potential of the VPCs and the three vulval fates to differentiate and de-differentiate, allowing them to remain completely responsive to the concentration of LIN-3 and lateral signal in the extracellular microenvironment.

Keywords: *C. elegans*, Vulva, Fate determination, Cell cycle

Background

The nematode *Caenorhabditis elegans* has been extensively used as a model organism in research areas such as genetics, genomics, cellular signaling cascades, neuroscience, aging, developmental biology, and cell differentiation [1-4]. *C. elegans* is specially suitable for the study of cell differentiation because its cell lineage map is both fully

characterized and almost invariant [5,6]. In particular, the vulva of *C. elegans* has been used as an experimental model for the study of organ formation, cellular fusion, and intracellular signaling [7-11].

The vulva has two main biological functions, namely, copulation and egg laying. This organ is formed by seven epithelial rings connecting the uterus with the ventral hypodermis, forming a path from the interior of the uterus to the external environment. This path is closed to keep pathogens out of the worm, except when the vulval muscles open it to perform its functions. Each ring of the vulva is formed by cells of a different kind, namely (in ventral-to-dorsal order): vulA, vulB1, vulB2,

*Correspondence: lmendoza@biomedicas.unam.mx
[2]Instituto de Investigaciones Biomédicas, Universidad Nacional Autónoma de México, México DF, México
[5]Centro de Ciencias de la Complejidad, Universidad Nacional Autónoma de México, México DF, México
Full list of author information is available at the end of the article

vulC, vulD, vulE, and vulF, containing a total of 22 nuclei (Figure 1). In the adult, most of these rings are formed by a single tetranucleated syncytium, the exceptions being

Figure 1 Formation and specialization of the vulval cells during the first hours of development of *C. elegans*. Larval phase L1: 0 h) After eclosion, the worm has two rows of P cells in the middle ventral region. 10 h) The rows merge. Larval phase L2: 12 h) The cells P1-P12 undergo a longitudinal division, the anchor cell forms (brown oval), and P3.p-P8.p become vulval precursor cells (VPCs). 25 h) P6.p responds to LIN-3/EGF secreted by the AC and acquires the primary fate (red), this cell secrets the DSL ligands that constitute the lateral signal. 28 h) P5.p and P7.p respond to the lateral signal of P6.p, thus acquiring the secondary fate (yellow). The rest of the VPCs acquire the tertiary fate forming the pattern $3^{rd}3^{rd}2^{nd}1^{st}2^{nd}3^{rd}$. Larval phase L3: 30 h) Cells P3.p to P8.p divide longitudinally, and the daughters of the secondary fate cells are polarized. 32 h) The descendants of the tertiary fate cells fuse with hyp7 and the rest divide longitudinally once more, and the most proximal granddaughters of P6.p are induced again by the anchor cell (AC). Larval phase L4: 36 h) Formation of the adult vulval cells: some descendants of the VPCs divide a third time with the pattern LLTN TTTT NTLL. L stands for a lateral division, forming anterior and posterior daughters. T is a transverse division, forming left and right daughters. N stands for no division. Cells are classified, in proximal to distal order as vulF (red), vulE (orange red), vulD (orange), vulC (yellow), vulB2 and vulB1 (green yellow), and vulA (green).

the binucleated syncytium ring vulD, as well as the vulB1 and vulB2 rings that contain two half-ring binucleated syncytia each [6].

The cellular and molecular mechanisms controlling the development of the vulva have been experimentally studied for more than three decades by means of cell ablations [12-14], mutations causing some specific vulval phenotypes [15-18], or mutations that rescue vulval phenotypes [19-24]. Furthermore, the roles of the Ras/MAPK, Fgf, Notch, and Wnt signaling cascades during the formation of the vulva have been extensively studied [11,25-27].

The first stage of vulval development is the formation of the vulval competence group. The nematode is born with two rows of P cells containing six cells each (Figure 1, 0h); these cells migrate towards the ventral mid-line forming one row (Figure 1, 10 h). The P cells then undergo a longitudinal division; the anterior daughter cells acquire neuronal fates, while the posterior daughter cells acquire hypodermal fates. Six of the posterior daughters, namely P3.p, P4.p, P5.p, P6.p, P7.p, and P8.p (Figure 1, 12 h), are induced by Wnt and Ras signaling to become the vulval competence group [28-30].

The second stage of the process is defined by the differentiation and proliferation, instead of the formation of vulval cells. It is known that the fate of VPCs (Figure 1, 25 h and 28 h) is determined by the induction from the anchor cell (AC, a gonadal cell located dorsally with respect to the cell P6.p), the lateral signaling among the VPCs, and the concentration of Wnt ligands secreted by the AC as well as cells near the tail. The VPCs may acquire one of three fates, P6.p acquires the primary fate that is characterized by the expression of *egl-17, lin-39, apx-1,* and *dsl-1* as well as the transverse division of its granddaughters. P5.p and P7.p acquire the secondary fate that is characterized by the expression of *lin-11* and *lip-1* and the diverse planes of division of its granddaughters. Specifically, the most proximal granddaughters do not divide, the next most proximal granddaughters divide transversely, and the two most distal granddaughters divide longitudinally. P3.p, P4.p, and P8.p acquire the tertiary fate, tertiary fate VPCs divide longitudinally once, and their daughters fuse with hyp7. Then, the VPCs divide longitudinally once and the cells that acquired the tertiary fate fuse with the ventral hypoderm. Also, the daughters of the secondary fate cells are polarized by Wnt signaling (Figure 1, 30 h). At this point the six remaining VPC daughters undergo a second longitudinal division (Figure 1, 32 h). Finally, most of the granddaughters of the VPCs divide a third time, except for the most proximal descendants of the secondary fate cells.

The third stage of the process is morphogenesis and determination of the final fates of vulval cells. The vulval cells migrate towards the AC, and then they fuse
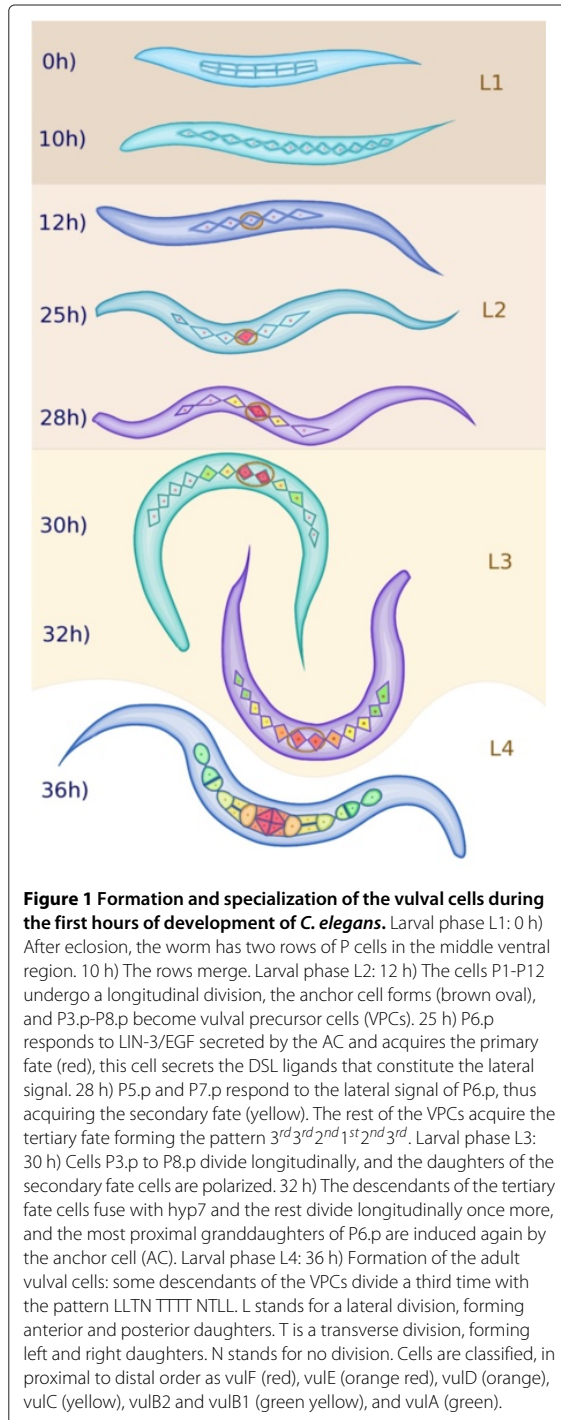
forming the seven rings that give the adult vulva its final shape. During this stage the AC breaks the membrane that separates the gonad from the epidermis, connecting both tissues and opening the vulval channel. The developing vulva directs the growth and attachment of the vulval muscles [6-8,11], and the adult fates of the vulval cells are determined. Remarkably, there is scarce information regarding the molecular network that controls this third stage of the cell differentiation in the vulva [11,31].

The cell cycle and fate determination in *C. elegans* are synchronized due to the interconnection of the molecular mechanisms controlling both processes, which is described in detail as part of the molecular basis of the regulatory network. Additionally, the heterochronic genes *lin-4*, *lin-14*, and *lin-28* are important for the control of developmental timing. In the vulva, LIN-14 activity is required during L1, LIN-28 activity is necessary during L2 and early L3 to prevent premature vulval cell divisions, and *lin-4* activity is required during L3 for the cellular divisions that occur during this stage, and the proper determination of the secondary fate [11,32,33].

There are several models describing the process of cell specialization in the vulva of *C. elegans* [34]. The first models were diagrammatic and static [14,35], describing how the inductive and lateral signals interact to determine the fates of the VPCs. Later models emphasized the importance of the concentration of the inductive and lateral signals, producing bi-dimensional fate maps [36-38], and epigenetic landscapes [39]. Some models were developed with a focus on the importance of the order in the sequence of signals [40-42], others incorporated an evolutionary perspective [37,38], and still others were built to test new methodologies or tools for the simulation of molecular network models [43-47]. Recently, we proposed a dynamic regulatory network model to include the molecules that are involved in the control of cell fusion and cell polarization during the first stages of vulva development. Such a model included the Wnt, Ras, and Notch signaling pathways, as well as the interactions among them, and the relevant Hox genes [30].

The cell cycle has been extensively studied in several species, and as a result there is a large number of mathematical and computational models for eukaryotes in general [48-51], mammals [52,53], and also for several specific model systems, including fission yeast [54-58], budding yeast [59-61], amphibian embryos [62,63], *A. thaliana* ([64], Ortiz-Gutiérrez *et al.* in preparation), and notably the embryonic cell cycle of *C. elegans* [65]. Many discrete and continuous dynamical models have been used to find the molecular interactions that are necessary and sufficient to recover the observed cyclic behavior of several cell cycle regulators. Some models have focused on the cell cycle checkpoints [54,55,62], or have analyzed the role of cell mass during cell cycle progression [55,58,59]. While most of the previous models were built with the use of ordinary differential equations [48,49,53,56,58], there are also examples of hybrid [52] and discrete models [60,61,65,66].

Despite the abundance of models developed for VPC fate determination and cell cycle dynamics in other organisms and the *C. elegans* embryo, the effect of coordination of the cell cycle and cell differentiation during vulval development has not been fully explored. Hereby we present the first model to include the molecular mechanism involved in the control of the postembryonic cell cycle of *C. elegans*. Dynamical models are important to understand how the molecular components involved in these cellular processes are integrated to coordinate the differentiation and proliferation during VPC fate specification. Such an integrative model is the focus of this paper. Our main findings are that the regulation of Notch signaling by the cell cycle preserves the potential of the VPCs and the three vulval fates to differentiate and dedifferentiate, and that sequential control does not eliminate the sensitivity of the VPCs to inductive or lateral signaling during VPC fate determination.

Results and discussion
The regulatory network
The regulatory network consists of 14 nodes and 37 regulatory interactions (Figure 2). The network incorporates regulatory interactions experimentally substantiated in *C. elegans*, five interactions documented in other organisms, and six interactions that constitute novel predictions from the present study. All such predictions, with the exception of the inhibition of CDK-1/CYB-3 by CKI-1, are necessary to recover the observed attractors. The exhaustive analysis of the dynamical behavior of the network as a discrete dynamical system revealed the existence of eight periodic attractors that cycle through the same stages of the cell cycle (Figure 3), partitioning evenly the state space (Figure 4).

The eight attractors can be interpreted as the patterns of molecular activation of the three vulval fates that cycle through the cell cycle (Figures 3 and 4). Attractors A, B, and C represent the primary fate, which is characterized by a high level (2 in our model) of LIN-39 and MPK-1 activity. Attractors D, E, F and G correspond to the secondary vulval fate which is characterized by LIN-12i activity. Notably, in all these attractors, LIN-12i is inactive during the first and last states of the cycle, due to the inhibitory effect of CDK-1/CYB-3. Finally, the tertiary fate is represented exclusively by attractor H, which is characterized by a low level of activity of LIN-39, and no LIN-12i, LIN-3, or lateral signal (LS) activity. This pattern of expression is observed in the VPCs during L2.

Figure 2 The network of molecules involved in the control of VPC fate determination and the cell cycle in *C. elegans*. Pointed arrows are positive regulatory interactions, and blunt arrows are negative regulatory interactions. Purple arrows are interactions reported in other organisms, and green arrows are predictions of our model. Orange nodes are part of the Notch pathway, and blue nodes are part of the Ras/MAPK pathway or its targets (LIN-39). Green nodes are CDK/Cyclin complexes, yellow nodes are CDK inhibitors, EFL-1, a transcription factor in white, and protein degradation complexes in gray. The external signals are represented as elongated hexagons, the known transcription factors as ellipses, and other proteins as rounded rectangles.

Dynamics of the cell cycle module

Figure 3 shows the dynamical behavior of the regulatory network. The model recovers eight cyclic attractors, corresponding to the observed patterns of expression in actual cells. For example, Figure 3H shows the cyclic attractor that corresponds to tertiary fate cells and VPCs. At the beginning (G1-1), the inhibitors of the cell cycle, CKI-1, LIN-35, and the APC complex, are active. Then, APC is turned off, which leads to CKI-1 inactivation (G1-3), and thus allowing the CDK-4/CYD-1 complex to become active (G1-4), which is a marker for G1 progression. Next, the LIN-35 activity is inhibited (G1-5), leading to EFL-1 activation (G1-6) first, and then the CDK-2/CYE-1 complex, a marker of the S phase (S1). Later, the SCF turns on (S2), leading to the G2 phase where only EFL-1 and SCF are active (G2). Further on, LIN-35, and the CDK-1/CYB-3 complex, which is a marker for the M phase, are activated (M1). Leading to the EFL-1 inhibition and APC activation (M2). Finally, the activity of CDK-1/CYB-3 is inhibited, leading back to the beginning of G1 (G1-1).

Figures 3E, 3F and 3G show attractors that describe the behavior of most secondary fate cells, the cell cycle in secondary fate cells is one step shorter because the G1 phase lasts for only 5 time steps. Figure 3D, which describes the cyclic behavior of a secondary fate cell in a microenvironment with a high level of LIN-3 (2 in our model), as well as Figures 3A-C that describe the cyclic behavior of primary fate cells, share the same cyclic behavior as secondary and

tertiary fate cells, except for the fact that their G1 phase lasts for only 4 steps.

By modeling the cell cycle module on its own, it is possible to observe that the cyclic behavior described above covers its entire state space (Figure 5A). Observe that the cyclic behavior of this module is maintained when it is modeled as a continuous dynamic system (Figure 5B), thus reducing the possibility of the cyclic behavior being an artifact of the modeling framework.

The differentiation process

To study the process of fate determination in our model, we followed the dynamics of the system starting from the initial patterns of expression that represent the different cell fates under different extracellular microenvironments (Figures 4 and 6). First, we followed the determination of the primary fate, which occurs when the concentration of LIN-3 is very high (3 in our model), with (Figure 7-3) or without (Figure 7-2) an active LS, or when the concentration of LIN-3 is moderately high (2 in our model) and the concentration of LS is lower than the threshold (0 in our model) (Figure 7-1). We also followed the network with an initial state representing a secondary fate cell under a microenvironment which induces a VPC to acquire the primary fate. In this case the network reaches a cyclic pattern of molecular activation that corresponds to the primary fate (Figure 7-4). Then, we followed the determination of the secondary fate, which may occur when a VPC or a primary fate cell is in the following

A)

Phase	G1-1	G1-2	G1-3	G1-4	S1	S2	G2	M1	M2
LIN-3	3	3	3	3	3	3	3	3	3
MPK-1	2	2	2	2	2	2	2	2	2
LIN-39	2	2	2	2	2	2	2	2	2
LS	1	1	1	1	1	1	1	1	1
LIN-12m	0	0	1	1	1	1	1	0	0
LIN-12i	0	0	0	1	1	1	1	1	0
CKI-1	0	0	0	0	0	0	0	0	0
EFL-1	0	0	0	1	1	1	1	1	0
LIN-35	1	1	0	0	0	0	0	1	1
SCF	0	0	0	0	0	1	1	0	0
APC	1	0	0	0	0	0	0	0	1
CDK-4/CYD-1	0	1	1	1	1	1	0	0	0
CDK-2/CYE-1	0	0	0	0	1	1	0	0	0
CDK-1/CYB-3	0	0	0	0	0	0	0	1	1

B)

Phase	G1-1	G1-2	G1-3	G1-4	S1	S2	G2	M1	M2
LIN-3	3	3	3	3	3	3	3	3	3
MPK-1	2	2	2	2	2	2	2	2	2
LIN-39	2	2	2	2	2	2	2	2	2
LS	0	0	0	0	0	0	0	0	0
LIN-12m	0	0	1	1	1	1	1	0	0
LIN-12i	0	0	0	0	0	0	0	0	0
CKI-1	0	0	0	0	0	0	0	0	0
EFL-1	0	0	0	1	1	1	1	1	0
LIN-35	1	1	0	0	0	0	0	1	1
SCF	0	0	0	0	0	1	1	0	0
APC	1	0	0	0	0	0	0	0	1
CDK-4/CYD-1	0	1	1	1	1	1	0	0	0
CDK-2/CYE-1	0	0	0	0	1	1	0	0	0
CDK-1/CYB-3	0	0	0	0	0	0	0	1	1

C)

Phase	G1-1	G1-2	G1-3	G1-4	S1	S2	G2	M1	M2
LIN-3	2	2	2	2	2	2	2	2	2
MPK-1	2	2	2	2	2	2	2	2	2
LIN-39	2	2	2	2	2	2	2	2	2
LS	0	0	0	0	0	0	0	0	0
LIN-12m	0	0	1	1	1	1	1	0	0
LIN-12i	0	0	0	0	0	0	0	0	0
CKI-1	0	0	0	0	0	0	0	0	0
EFL-1	0	0	0	1	1	1	1	1	0
LIN-35	1	1	0	0	0	0	0	1	1
SCF	0	0	0	0	0	1	1	0	0
APC	1	0	0	0	0	0	0	0	1
CDK-4/CYD-1	0	1	1	1	1	1	0	0	0
CDK-2/CYE-1	0	0	0	0	1	1	0	0	0
CDK-1/CYB-3	0	0	0	0	0	0	0	1	1

D)

Phase	G1-1	G1-2	G1-3	G1-4	S1	S2	G2	M1	M2
LIN-3	2	2	2	2	2	2	2	2	2
MPK-1	2	2	1	1	1	1	1	1	1
LIN-39	1	2	2	1	1	1	1	1	1
LS	1	1	1	1	1	1	1	1	1
LIN-12m	1	0	1	1	1	1	1	1	1
LIN-12i	0	1	1	1	1	1	1	1	0
CKI-1	0	0	0	0	0	0	0	0	0
EFL-1	0	0	0	1	1	1	1	1	0
LIN-35	1	1	0	0	0	0	0	1	1
SCF	0	0	0	0	0	1	1	0	0
APC	1	0	0	0	0	0	0	0	1
CDK-4/CYD-1	0	1	1	1	1	1	0	0	0
CDK-2/CYE-1	0	0	0	0	1	1	0	0	0
CDK-1/CYB-3	0	0	0	0	0	0	0	1	1

E)

Phase	G1-1	G1-2	G1-3	G1-4	G1-5	S1	S2	G2	M1	M2
LIN-3	1	1	1	1	1	1	1	1	1	1
MPK-1	1	1	0	0	0	0	0	0	0	0
LIN-39	1	1	1	1	1	1	1	1	1	1
LS	1	1	1	1	1	1	1	1	1	1
LIN-12m	1	1	1	1	1	1	1	1	1	1
LIN-12i	0	1	1	1	1	1	1	1	1	0
CKI-1	1	0	0	0	0	0	0	0	0	1
EFL-1	0	0	0	0	1	1	1	1	1	0
LIN-35	1	1	1	0	0	0	0	0	1	1
SCF	0	0	0	0	0	1	1	0	0	0
APC	1	0	0	0	0	0	0	0	0	1
CDK-4/CYD-1	0	0	1	1	1	1	1	0	0	0
CDK-2/CYE-1	0	0	0	0	0	1	1	0	0	0
CDK-1/CYB-3	0	0	0	0	0	0	0	0	1	1

F)

Phase	G1-1	G1-2	G1-3	G1-4	G1-5	S1	S2	G2	M1	M2
LIN-3	1	1	1	1	1	1	1	1	1	1
MPK-1	1	1	0	0	0	0	0	0	0	0
LIN-39	1	1	1	1	1	1	1	1	1	1
LS	0	0	0	0	0	0	0	0	0	0
LIN-12m	1	1	1	1	1	1	1	1	1	1
LIN-12i	0	1	1	1	1	1	1	1	1	0
CKI-1	1	0	0	0	0	0	0	0	0	1
EFL-1	0	0	0	0	1	1	1	1	1	0
LIN-35	1	1	1	0	0	0	0	0	1	1
SCF	0	0	0	0	0	1	1	0	0	0
APC	1	0	0	0	0	0	0	0	0	1
CDK-4/CYD-1	0	0	1	1	1	1	1	0	0	0
CDK-2/CYE-1	0	0	0	0	0	1	1	0	0	0
CDK-1/CYB-3	0	0	0	0	0	0	0	0	1	1

G)

Phase	G1-1	G1-2	G1-3	G1-4	G1-5	G1-6	S1	S2	G2	M1	M2
LIN-3	0	0	0	0	0	0	0	0	0	0	0
MPK-1	0	0	0	0	0	0	0	0	0	0	0
LIN-39	1	1	1	1	1	1	1	1	1	1	1
LS	1	1	1	1	1	1	1	1	1	1	1
LIN-12m	1	1	1	1	1	1	1	1	1	1	1
LIN-12i	0	1	1	1	1	1	1	1	1	1	0
CKI-1	1	1	0	0	0	0	0	0	0	0	1
EFL-1	0	0	0	0	0	1	1	1	1	1	0
LIN-35	1	1	1	1	0	0	0	0	0	1	1
SCF	0	0	0	0	0	0	0	1	1	0	0
APC	1	0	0	0	0	0	0	0	0	0	1
CDK-4/CYD-1	0	0	0	1	1	1	1	1	0	0	0
CDK-2/CYE-1	0	0	0	0	0	0	1	1	0	0	0
CDK-1/CYB-3	0	0	0	0	0	0	0	0	0	1	1

H)

Phase	G1-1	G1-2	G1-3	G1-4	G1-5	G1-6	S1	S2	G2	M1	M2
LIN-3	0	0	0	0	0	0	0	0	0	0	0
MPK-1	0	0	0	0	0	0	0	0	0	0	0
LIN-39	1	1	1	1	1	1	1	1	1	1	1
LS	0	0	0	0	0	0	0	0	0	0	0
LIN-12m	1	1	1	1	1	1	1	1	1	1	1
LIN-12i	0	0	0	0	0	0	0	0	0	0	0
CKI-1	1	1	0	0	0	0	0	0	0	0	1
EFL-1	0	0	0	0	0	1	1	1	1	1	0
LIN-35	1	1	1	1	0	0	0	0	0	1	1
SCF	0	0	0	0	0	0	0	1	1	0	0
APC	1	0	0	0	0	0	0	0	0	0	1
CDK-4/CYD-1	0	0	0	1	1	1	1	1	0	0	0
CDK-2/CYE-1	0	0	0	0	0	0	1	1	0	0	0
CDK-1/CYB-3	0	0	0	0	0	0	0	0	0	1	1

Figure 3 The attractors of our model. There is a total of eight cyclic attractors, with time running from left to right. Activity of LIN-12i, in orange, is a marker of the secondary fate (Attractors **D**, **E**, **F** and **G**). A high level of activity (2 in our model) of LIN-39, in dark blue, is a marker for the primary fate (Attractors **A**, **B**, and **C**). The tertiary fate is represented exclusively by attractor **H**, which is characterized by a low level of activity of LIN-39, and no LIN-12i, LIN-3, or lateral signal (LS) activity (This pattern of expression is observed in the VPCs during L2). CDK-4/CYD-1, shown in pale green, is activated before the S phase. CDK-2/CYE-1, shown in green, is a marker of the S phase. CDK-1/CYB-3, in dark green, is a marker for the M phase.

Basin	1	2	3	4	5	6	7	8	9*
LIN-3	3	3	2	2	1	1	0	0	0
MPK-1	*	*	*	*	*	*	*	*	*
LIN-39	*	*	*	*	*	*	*	*	*
LS	1	0	0	1	1	0	1	0	0
LIN-12m	*	*	*	*	*	*	*	*	*
LIN-12i	*	*	*	*	*	*	*	*	*
CKI-1	*	*	*	*	*	*	*	*	*
EFL-1	*	*	*	*	*	*	*	*	*
LIN-35	*	*	*	*	*	*	*	*	*
SCF	*	*	*	*	*	*	*	*	*
APC	*	*	*	*	*	*	*	*	*
CDK-4/CYD-1	*	*	*	*	*	*	*	*	*
CDK-2/CYE-1	*	*	*	*	*	*	*	*	*
CDK-1/CYB-3	*	*	*	*	*	*	*	*	*
WNT*	1	1	1	1	1	1	1	1	0
Symbol	I	H	G	F	E	D	C	B	A

Figure 4 Summary of the basins of attraction. The stars in each basin represent all possible activity levels for the molecule. The primary fate basins are colored in blue, the secondary fate basins in orange, the tertiary fate basin in green and the fusion fate basin in gray. Loss of WNT activity was simulated by changing the basal state of LIN-39 from 1 to 0.

microenvironments: LS and no LIN-3 activity (0 in our model)(Figure 8-1), low LIN-3 (1 in our model) with no LS (Figure 8-2), LS and low LIN-3 (Figure 8-3), or LS and medium high LIN-3 (Figure 8-4 and 8-5). Last, we followed the determination of the tertiary fate which may occur when a VPC/Tertiary-fate cell (Figure 9-1), a secondary fate cell (Figure 9-2) or a primary fate cell(Figure 9-3), is in a microenvironment with no LS and no LIN-3 (0 in our model).

Our model shows that the cell fates remain stable if the extracellular microenvironment remains stable, but the cells keep the potential to acquire any other fate if the microenvironment changes. Specifically, a primary or secondary fate cell has the potential to de-differentiate in a microenvironment without both LIN-3 and LS, a primary fate cell may trans-differentiate into a secondary fate cell in a microenvironment with low LIN-3 or LS and a secondary fate cell may also trans-differentiate into a primary fate cell in a microenvironment with moderately high LIN-3 and no LS or very high LIN-3 (Figures 4 and 6). Both de-differentiation and trans-differentiation have been observed experimentally [67].

Finally, it is important to note that the influence of the differentiation process over the cell cycle module has an effect on the length of the periodic behavior (Figure 3). Specifically, G1 lasts 4 time steps for the primary fate, 4

to 6 time steps for the secondary fate, and 6 time steps for the tertiary fate. This behavior arises because the Ras signaling shortens the duration of the cell cycle by inhibiting CKI-1. Specifically, when Ras signaling is moderate (Figure 3E-F), the cell cycle lasts ten time steps. But when the level of Ras signaling is high (Figure 3A-D), CKI-1 is not activated and thus the cell cycle lasts 9 time steps. The duration of the cell cycle may determine the number of times the VPCs divide, because the period of time when the VPCs may divide is limited.

Simulation of mutants
One way to validate the type of regulatory network model presented here, is to test if altered expression states of the model components lead to altered attractors that mimic the observed patterns of expression and/or phenotypes described for loss and gain of function mutants. We simulated the effect of all 32 possible single loss- and gain-of-function mutations by setting the expression level of the corresponding node to zero, one, two, or three. We obtained the attractors of all these mutant models and compared them against the available experimental data (Additional file 1: Table S1, Additional file 2). Notably, 16 of the 18 phenotypes reported in the literature (88.9%) are recovered by these simulations. The simulated phenotypes caused by 24 mutations can be

Figure 5 Dynamics of the cell cycle. A) State space of our Boolean module. Color-coded transition diagram of the cell cycle: the red component represents the activity of CKI-1, EFL-1 and LIN-35, the green component represents the activity of SCF and APC, and the blue component represents the activity of CDK-4/CYD-1, CDK-2/CYE-1 and CDK-1/CYB-3. **B)** Dynamics of our continuous model of the cell cycle. The initial state for the numerical integration starts at the first stage of G1.

considered novel predictions of our model; of those 24 simulated mutations the effect of 14 has not been reported at all in the literature, and the other 10 cause additional effects in specific extracellular microenvironments that have not been observed experimentally. Specifically, our model predicts that *a*) a constitutively active lateral signal will prevent the determination of the tertiary fate, *b*) *mpk-1(1)* will cause the loss of the primary fate, *c*) *mpk-1(2)* will cause the loss of the secondary fate, *d*) five mutations will cause the VPCs to exit the cell cycle, *e*) two mutations will cause endoreplication, *f*) 15 mutations will allow the determination of the secondary fate in an extracellular microenvironment with a medium level of LIN-3 and no LS, *g*) nine mutations will allow the determination of the primary fate in an extracellular microenvironment

with a medium level of LIN-3 and LS, *h*) 15 mutations will allow the determination of the secondary fate in an extracellular microenvironment with no LIN-3 and no LS, *i*) two mutations allow the determination of the tertiary fate in an extracellular microenvironment with LS and no LIN-3, *j*) according to our model, *lin-39(2)* represents a high concentration of constitutively phosphorylated LIN-39 and the result of its simulation is a Muv phenotype where all VPCs acquire the primary fate. Experimentally, the expression of heat shock-inducible *lin-39* after the ablation of the anchor cell during L2 was not enough to allow the VPCs to divide, and a high level of LIN-39 protein does not cause a Muv phenotype. But that might be because LIN-39 needs to be phosphorylated by MPK-1 in order to be activated [68], in order to prove or refute

Figure 6 The process of the cell differentiation. Colored triangles represent the different cellular fates. The different signals that are able to move the model from one fate to another are specified on the table at the bottom of the figure, and the primary fate basins are colored in blue, the secondary fate basins in orange, the tertiary fate basin in green and the fusion fate basin in gray.

our prediction, the same experiment would need to be repeated, but with a constitutively phosphorylated LIN-39, *k*) according to our model, *lin-12i(0)* represents the loss of the transcription factor function of *lin-12* locally in the VPCs that causes the loss of secondary fate VPCs, but not necessarily the Muv phenotype reported in the literature where *lin-12(lf)* causes two anchor cells to form, causing a Muv and Egl phenotype where most VPCs acquire the primary fate [35], in order to verify this prediction the extra AC needs to be ablated in a *lin-12(lf)* and *lip-1::GFP* background to verify that the secondary fate is lost but the VPCs may still acquire the primary and tertiary fates, *l*) According to our model, *lin-12m(0)* represents the loss of LIN-12 protein in the membrane that produces a wild type phenotype, because we assume that Notch may still be activated internally by weak Ras signaling [27]. We remark that two of our simulated mutants, namely *efl-1(0), and SCF(0)*, do not have a clear correspondence with the experimental results.

The loss of *efl-1* function has been reported to cause a phenotype that resembles the phenotype caused by *lin-35(lf)*, suggesting that it is a G1/S inhibitor. Conversely,

its co-factor *dpl-1* has been reported to both activate and inhibit the G1/S transition [69]. However, according to our model, EFL-1/DPL-1 functions as a transcriptional activator, as reported for the yeast and mammalian cell cycles [70], while *efl-1(0)* causes the cell cycle to stop between G1 and S.

Finally, according to our model, *SCF(0)* causes the cell cycle to stop at the S phase. However, the function of SCF is necessary for the cell cycle exit. *cul-1* is one of the main components of SCF, and *cul-1(lf)* causes very strong hyperplasia in the vulva, and more than 80 vulval cells are formed in those mutants [71]. SCF complexes have many diverse functions and only a few are well characterized. Specifically, SCF is necessary for CDC-25.1 degradation, which may be necessary for cell cycle quiescence [72]. Furthermore, negative regulation of CDK/Cyclin complexes is an important component even in minimal cell cycle oscillators [63]. Due to the simplified nature of our model, the function of SCF as a G1/S CDK/Cyclin regulator is crucial for cell cycle progression, but in the real system other complexes such as APC may act redundantly with SCF.

Figure 7 Primary fate determination. 1) A VPC differentiating into a primary fate cell in an extracellular microenvironment with a moderately high concentration of LIN-3 (2 in our model), **2)** A VPC differentiating into a primary fate cell in an extracellular microenvironment with a high concentration of LIN-3 (3 in our model), **3)** A VPC differentiating into a primary fate cell in an extracellular microenvironment with lateral signal and a high concentration of LIN-3 (3 in our model), **4)** A secondary fate cell transdifferentiating into a primary fate cell in an extracellular microenvironment with a high concentration of LIN-3 (3 in our model).

Removal of regulatory interactions

We systematically eliminated all of the 38 regulatory interactions, one at the time, and evaluated the effect on the attractors attained by the model (Additional file 3: Table S2, Additional file 4). Notice that the removal of 12 interactions had no effect on the dynamics of the network, thus showing the structural robustness of the model.

1) VPC to Second LS

LIN-3	0	0	0	0	0	0	0	0	0	0	0
MPK-1	0	0	0	0	0	0	0	0	0	0	0
LIN-39	1	1	1	1	1	1	1	1	1	1	1
LS	1	1	1	1	1	1	1	1	1	1	1
LIN-12m	1	1	1	1	1	1	1	1	1	1	1
LIN-12i	0	1	1	1	1	1	1	1	1	1	0
CKI-1	1	1	0	0	0	0	0	0	0	0	1
EFL-1	0	0	0	0	0	1	1	1	1	1	0
LIN-35	1	1	1	1	0	0	0	0	0	1	1
SCF	0	0	0	0	0	0	0	1	1	0	0
APC	1	0	0	0	0	0	0	0	0	0	1
CDK-4/CYD-1	0	0	0	1	1	1	1	1	0	0	0
CDK-2/CYE-1	0	0	0	0	0	0	1	1	0	0	0
CDK-1/CYB-3	0	0	0	0	0	0	0	0	0	1	1
Attractor G											

2) VPC to Second LIN3(1)

LIN-3	1	1	1	1	1	1	1	1	1	1	1	1	1
MPK-1	0	1	0	0	0	0	0	0	0	0	0	1	1
LIN-39	1	1	1	1	1	1	1	1	1	1	1	1	1
LS	0	0	0	0	0	0	0	0	0	0	0	0	0
LIN-12m	1	1	1	1	1	1	1	1	1	1	1	0	1
LIN-12i	0	1	1	1	1	1	1	1	1	1	0	0	1
CKI-1	1	1	0	0	0	0	0	0	0	0	1	1	0
EFL-1	0	0	0	0	0	1	1	1	1	1	0	0	0
LIN-35	1	1	1	1	0	0	0	0	0	1	1	1	1
SCF	0	0	0	0	0	0	0	1	1	0	0	0	0
APC	1	0	0	0	0	0	0	0	0	0	1	1	0
CDK-4/CYD-1	0	0	0	1	1	1	1	1	0	0	0	0	0
CDK-2/CYE-1	0	0	0	0	0	0	1	1	0	0	0	0	0
CDK-1/CYB-3	0	0	0	0	0	0	0	0	0	1	1	0	0
Attractor F													

3) VPC to Second LS + LIN-3(1)

LIN-3	1	1	1	1	1	1	1	1	1	1	1	1	1
MPK-1	0	1	0	0	0	0	0	0	0	0	0	1	1
LIN-39	1	1	1	1	1	1	1	1	1	1	1	1	1
LS	1	1	1	1	1	1	1	1	1	1	1	1	1
LIN-12m	1	1	1	1	1	1	1	1	1	1	1	1	1
LIN-12i	0	1	1	1	1	1	1	1	1	1	0	0	1
CKI-1	1	1	0	0	0	0	0	0	0	0	1	1	0
EFL-1	0	0	0	0	0	1	1	1	1	1	0	0	0
LIN-35	1	1	1	1	0	0	0	0	0	1	1	1	1
SCF	0	0	0	0	0	0	0	1	1	0	0	0	0
APC	1	0	0	0	0	0	0	0	0	0	1	1	0
CDK-4/CYD-1	0	0	0	1	1	1	1	1	0	0	0	0	0
CDK-2/CYE-1	0	0	0	0	0	0	1	1	0	0	0	0	0
CDK-1/CYB-3	0	0	0	0	0	0	0	0	0	1	1	0	0
Attractor E													

4) VPC to Second LS + LIN-3(2)

LIN-3	2	2	2	2	2	2	2	2	2	2	2	2	2	2
MPK-1	0	1	1	1	1	1	1	1	1	1	1	2	2	1
LIN-39	1	1	1	1	1	1	1	1	1	1	1	1	2	2
LS	1	1	1	1	1	1	1	1	1	1	1	1	1	1
LIN-12m	1	1	1	1	1	1	1	1	1	1	1	1	0	1
LIN-12i	0	1	1	1	1	1	1	1	1	1	0	0	1	1
CKI-1	1	1	0	0	0	0	0	0	0	0	0	0	0	0
EFL-1	0	0	0	0	0	1	1	1	1	1	0	0	0	0
LIN-35	1	1	1	1	0	0	0	0	0	1	1	1	1	0
SCF	0	0	0	0	0	0	0	1	1	0	0	0	0	0
APC	1	0	0	0	0	0	0	0	0	0	1	1	0	0
CDK-4/CYD-1	0	0	0	1	1	1	1	1	0	0	0	0	1	1
CDK-2/CYE-1	0	0	0	0	0	0	1	1	0	0	0	0	0	0
CDK-1/CYB-3	0	0	0	0	0	0	0	0	0	1	1	0	0	0
Attractor D														

5) First to Second

LIN-3	2	2	2	2	2	2	2	2	2	2	2	2	2	2
MPK-1	2	2	2	2	2	1	1	1	1	1	2	2	1	1
LIN-39	2	2	2	2	2	2	1	1	1	1	1	2	2	1
LS	1	1	1	1	1	1	1	1	1	1	1	1	1	1
LIN-12m	0	0	0	1	1	1	1	1	1	1	1	0	1	1
LIN-12i	0	0	0	0	1	1	1	1	1	0	0	1	1	1
CKI-1	1	0	0	0	0	0	0	0	0	0	0	0	0	0
EFL-1	0	0	0	0	1	1	1	1	1	0	0	0	0	1
LIN-35	1	1	1	0	0	0	0	0	1	1	1	1	0	0
SCF	0	0	0	0	0	0	1	1	0	0	0	0	0	0
APC	1	0	0	0	0	0	0	0	0	1	1	0	0	0
CDK-4/CYD-1	0	0	1	1	1	1	1	0	0	0	0	1	1	1
CDK-2/CYE-1	0	0	0	0	0	1	1	0	0	0	0	0	0	0
CDK-1/CYB-3	0	0	0	0	0	0	0	0	1	1	0	0	0	0
Attractor D														

Figure 8 Secondary fate determination. 1) A VPC differentiating into a secondary fate cell in an extracellular microenvironment with lateral signal, **2)** A VPC differentiating into a secondary fate cell in an extracellular microenvironment with a low concentration of LIN-3 (1 in our model), **3)** A VPC differentiating into a secondary fate cell in an extracellular microenvironment with lateral signal and a low concentration of LIN-3, **4)** A VPC differentiating into a secondary fate cell in an extracellular microenvironment with lateral signal and a moderately high (2 in our model) concentration of LIN-3, **5)** A primary fate cell transdifferentiating into a secondary fate cell in an extracellular microenvironment with a moderately high concentration of LIN-3 (2 in our model) and lateral signal.

There is a discrepancy between our model and the reported experimental results regarding the removal of the activation of LIN-12i by CDK-2/CYE-1. In the model, the elimination of this interaction has no effect on the dynamics of the network. Experimentally, however, the elimination of the aforementioned interaction causes a

1) Third fate

LIN-3	0	0	0	0	0	0	0	0	0	0	0
MPK-1	0	0	0	0	0	0	0	0	0	0	0
LIN-39	1	1	1	1	1	1	1	1	1	1	1
LS	0	0	0	0	0	0	0	0	0	0	0
LIN-12m	1	1	1	1	1	1	1	1	1	1	1
LIN-12i	0	0	0	0	0	0	0	0	0	0	0
CKI-1	1	1	0	0	0	0	0	0	0	0	1
EFL-1	0	0	0	0	0	1	1	1	1	1	0
LIN-35	1	1	1	1	0	0	0	0	0	1	1
SCF	0	0	0	0	0	0	0	1	1	0	0
APC	1	0	0	0	0	0	0	0	0	0	1
CDK-4/CYD-1	0	0	0	1	1	1	1	1	0	0	0
CDK-2/CYE-1	0	0	0	0	0	0	1	1	0	0	0
CDK-1/CYB-3	0	0	0	0	0	0	0	0	0	1	1

Attractor H

2) Second to Third

LIN-3	0	0	0	0	0	0	0	0	0	0	0	0	0	0	0	0	0	0	0	0
MPK-1	1	0	0	0	0	0	0	0	0	0	0	0	0	0	0	0	0	0	0	0
LIN-39	1	1	1	1	1	1	1	1	1	1	1	1	1	1	1	1	1	1	1	1
LS	0	0	0	0	0	0	0	0	0	0	0	0	0	0	0	0	0	0	0	0
LIN-12m	1	1	1	1	1	1	1	1	1	1	1	1	1	1	1	1	1	1	1	1
LIN-12i	1	1	1	1	1	1	1	1	1	0	0	0	0	0	0	0	0	0	0	0
CKI-1	1	0	0	0	0	0	0	0	0	1	1	1	0	0	0	0	0	0	0	0
EFL-1	0	0	0	0	1	1	1	1	1	0	0	0	0	0	0	1	1	1	1	1
LIN-35	1	1	1	0	0	0	0	0	1	1	1	1	1	1	0	0	0	0	0	1
SCF	0	0	0	0	0	0	1	1	0	0	0	0	0	0	0	0	0	1	1	0
APC	1	0	0	0	0	0	0	0	0	1	1	0	0	0	0	0	0	0	0	0
CDK-4/CYD-1	0	0	1	1	1	1	1	0	0	0	0	0	0	1	1	1	1	1	0	0
CDK-2/CYE-1	0	0	0	0	0	1	1	0	0	0	0	0	0	0	0	0	1	1	0	0
CDK-1/CYB-3	0	0	0	0	0	0	0	0	1	1	0	0	0	0	0	0	0	0	0	1

Attractor H

3) First to Third

LIN-3	0	0	0	0	0	0	0	0	0	0	0	0	0
MPK-1	2	1	0	0	0	0	0	0	0	0	0	0	0
LIN-39	2	2	1	1	1	1	1	1	1	1	1	1	1
LS	0	0	0	0	0	0	0	0	0	0	0	0	0
LIN-12m	0	0	1	1	1	1	1	1	1	1	1	1	1
LIN-12i	0	0	0	0	0	0	0	0	0	0	0	0	0
CKI-1	1	0	0	0	0	0	0	0	0	1	1	1	0
EFL-1	0	0	0	0	1	1	1	1	1	0	0	0	0
LIN-35	1	1	1	0	0	0	0	0	1	1	1	1	1
SCF	0	0	0	0	0	0	1	1	0	0	0	0	0
APC	1	0	0	0	0	0	0	0	0	1	1	0	0
CDK-4/CYD-1	0	0	1	1	1	1	1	0	0	0	0	0	0
CDK-2/CYE-1	0	0	0	0	0	1	1	0	0	0	0	0	0
CDK-1/CYB-3	0	0	0	0	0	0	0	0	1	1	0	0	0

Attractor H

Figure 9 Tertiary fate determination. 1) The tertiary fate is stable in an extracellular microenvironment without LS or LIN-3, **2)** A secondary fate cell dedifferentiating into a third fate cell in an extracellular microenvironment without LS or LIN-3, **3)** A primary fate cell dedifferentiating into a third fate cell in an extracellular microenvironment without LS or LIN-3.

diminished concentration of LIN-12i in secondary fate cells [42]. Given the Boolean nature of the variable representing LIN-12i, the model cannot represent a partial reduction on its activation. Future versions on our model will, by necessity, incorporate more levels of activation to describe LIN-12i.

We predict the effect of removing 28 interactions that are not reported in the literature. Specifically, our model predicts that *a*) removing one of eight interactions would not affect the behavior of the system, *b*) removing the ability of MPK-1 to phosphorylate LIN-39 will cause the loss of the primary fate, *c*) removing one of four interactions would inhibit VPC divisions, *d*) removing one of two interactions, will lead to an endoreplication cell cycle, *e*) removing one of four interactions would cause a longer cell cycle, *f*) removing one of eight interactions causes a shorter cell cycle, *g*) removing one of seven interactions will allow the determination of the secondary fate

in an extracellular microenvironment with no LIN-3 and no LS, *h*) removing one of ten interactions will allow the determination of the secondary fate in an extracellular microenvironment with a medium level of LIN-3 and no LS, and *j*) removing one of four interactions will allow the determination of the primary fate in an extracellular microenvironment with a medium level of LIN-3 and LS.

We then searched for the interactions that are necessary for the existence of the cyclic attractor. The update rules of our model of the cell cycle module (Equations 7-14) are not ambiguous. Without allowing ambiguity in the update rules, we found with *Griffin* [a] [73] 120 functional network topologies of the cell cycle module that allow the existence of the cyclic attractor. All such topologies include the following 14 interactions: *a*) the inhibition of EFL-1 by LIN-35, *b*) the activation of APC by CDK-1/CYB-3, *c*) the inhibition of LIN-35 by CDK-4/CYD-1, *d*) the activation of SCF by CDK-2/CYE-1, *e*) the inhibition of CDK-2/CYE-1 by SCF, *f*) the inhibition of CDK-4/CYD-1 by SCF, *g*) the inhibition of CDK-2/CYE-1 by LIN-35, *h*) the activation of CDK-1/CYB-3 by EFL-1, *i*) the inhibition of CDK-4/CYD-1 by CKI-1, *j*) the activation of CKI-1 by APC, *k*) the activation of CKI-1 by CDK-1/CYB-3, *l*) the inhibition of CDK-1/CYB-3 by CDK-4/CYD-1, *m*) the inhibition of CDK-4/CYD-1 by CDK-1/CYB-3, and *n*) the activation of CDK-2/CYE-1 by EFL-1.

We performed an additional test to check which interaction signs may be ambiguous by including all the interactions of our original model. Allowing ambiguity resulted in 2740 functional network topologies. However, in order for the cyclic attractor to exist, the following eight interaction signs must *not* be ambiguous: *a*) the inhibition of EFL-1 by LIN-35, *b*) the inhibition of CKI-1 by CDK-4/CYD-1, *c*) the inhibition of APC by SCF, *d*) the inhibition of SCF by APC, *e*) the activation of SCF by CDK-2/CYE-1, *f*) the activation of APC by CDK-1/CYB-3, *g*) the inhibition of LIN-35 by CDK-4/CYD-1, and *h*) the inhibition of LIN-35 by CDK-2/CYE-1.

Circuits
Circuits or feedback loops are circular chains of interactions. The present model contains 60 positive feedback loops, and 51 negative feedback loops (Tables 1 and 2). The work of Thomas and collaborators has demonstrated the central role of feedback loops in the determination of the dynamic behavior of a regulatory network [74]. Specifically, functional positive feedback loops are necessary for the existence of multistationarity, while negative feedback loops are necessary to obtain oscillations [75].

According to our model, there is large redundancy among circuits, and thus no single circuit can be considered essential for the determination vulval fates. By contrast, the specific combination of input signals determines the number of attractors attained by the system.

Table 1 Positive feedback loops in the network of Figure 2

1	CDK-1/CYB-3 →
2	LIN-12i →
3	LIN-39 →
4	CDK-4/CYD-1 ⊣ CKI-1 ⊣
5	CDK-2/CYE-1 ⊣ LIN-35 ⊣
6	LIN-12i → LIN-12m →
7	CDK-4/CYD-1 ⊣ CDK-1/CYB-3 ⊣
8	SCF ⊣ APC ⊣
9	CDK-2/CYE-1 ⊣ LIN-35 ⊣ EFL-1 →
10	LIN-12i ⊣ MPK-1 ⊣ LIN-12m →
11	CDK-4/CYD-1 ⊣ CDK-1/CYB-3 → CKI-1 ⊣
12	CDK-4/CYD-1 ⊣ CDK-1/CYB-3 → APC → CKI-1 ⊣
13	SCF ⊣ APC → CKI-1 ⊣ CDK-2/CYE-1 →
14	CKI-1 ⊣ CDK-2/CYE-1 → LIN-12i ⊣ MPK-1 ⊣
15	CKI-1 ⊣ CDK-1/CYB-3 ⊣ LIN-12i ⊣ MPK-1 ⊣
16	SCF ⊣ CDK-4/CYD-1 ⊣ CKI-1 ⊣ CDK-1/CYB-3 → APC ⊣
17	SCF ⊣ CDK-2/CYE-1 → LIN-12i ⊣ MPK-1 → LIN-39 →
18	SCF ⊣ CDK-4/CYD-1 ⊣ LIN-35 ⊣ EFL-1 → CDK-1/CYB-3 → APC ⊣
19	SCF ⊣ CDK-4/CYD-1 → LIN-12m → LIN-12i ⊣ MPK-1 → LIN-39 →
20	SCF ⊣ CDK-4/CYD-1 ⊣ CDK-1/CYB-3 ⊣ LIN-12i ⊣ MPK-1 → LIN-39 →
21	SCF ⊣ APC → CKI-1 ⊣ CDK-4/CYD-1 ⊣ LIN-35 ⊣ CDK-2/CYE-1 →
22	SCF ⊣ APC ⊣ CDK-1/CYB-3 ⊣ LIN-12i ⊣ MPK-1 → LIN-39 →
23	SCF ⊣ CDK-2/CYE-1 ⊣ LIN-35 ⊣ EFL-1 → CDK-1/CYB-3 → APC ⊣
24	CKI-1 ⊣ CDK-1/CYB-3 ⊣ CDK-4/CYD-1 → LIN-12m → LIN-12i ⊣ MPK-1 ⊣
25	CKI-1 ⊣ CDK-4/CYD-1 ⊣ LIN-35 → CDK-2/CYE-1 → LIN-12i ⊣ MPK-1 ⊣
26	SCF ⊣ CDK-4/CYD-1 ⊣ CDK-1/CYB-3 ⊣ LIN-12i ⊣ MPK-1 ⊣ CKI-1 ⊣ CDK-2/CYE-1 →
27	SCF ⊣ CDK-4/CYD-1 ⊣ CKI-1 ⊣ CDK-2/CYE-1 → LIN-12i ⊣ MPK-1 → LIN-39 →
28	SCF ⊣ CDK-4/CYD-1 ⊣ LIN-35 ⊣ CDK-2/CYE-1 → LIN-12i ⊣ MPK-1 → LIN-39 →
29	SCF ⊣ CDK-4/CYD-1 ⊣ LIN-35 ⊣ EFL-1 → CDK-1/CYB-3 → CKI-1 ⊣ CDK-2/CYE-1 →
30	SCF ⊣ APC → CKI-1 ⊣ CDK-4/CYD-1 ⊣ LIN-35 ⊣ EFL-1 → CDK-2/CYE-1 →
31	SCF ⊣ APC → CKI-1 ⊣ CDK-1/CYB-3 ⊣ LIN-12i ⊣ MPK-1 → LIN-39 →
32	SCF ⊣ CDK-4/CYD-1 → LIN-12m → LIN-12i ⊣ MPK-1 ⊣ CKI-1 ⊣ CDK-2/CYE-1 →
33	SCF ⊣ APC ⊣ CDK-1/CYB-3 ⊣ LIN-12i ⊣ MPK-1 ⊣ CKI-1 ⊣ CDK-2/CYE-1 →
34	CKI-1 ⊣ CDK-2/CYE-1 ⊣ LIN-35 ⊣ EFL-1 → CDK-1/CYB-3 ⊣ LIN-12i ⊣ MPK-1 ⊣
35	CKI-1 ⊣ CDK-4/CYD-1 ⊣ LIN-35 ⊣ EFL-1 → CDK-1/CYB-3 ⊣ LIN-12i ⊣ MPK-1 ⊣

Table 1 Positive feedback loops in the network of Figure 2
(Continued)

36 SCF ⊣ CDK-4/CYD-1 ⊣ CKI-1 ⊣ CDK-2/CYE-1 ⊣ LIN-35 ⊣ EFL-1 → CDK-1/CYB-3 → APC ⊣

37 SCF ⊣ CDK-4/CYD-1 ⊣ LIN-35 ⊣ EFL-1 → CDK-2/CYE-1 → LIN-12i ⊣ MPK-1 → LIN-39 →

38 SCF ⊣ CDK-4/CYD-1 ⊣ LIN-35 ⊣ EFL-1 → CDK-1/CYB-3 → APC → CKI-1 ⊣ CDK-2/CYE-1 →

39 SCF ⊣ CDK-4/CYD-1 ⊣ CDK-1/CYB-3 → CKI-1 ⊣ CDK-2/CYE-1 → LIN-12i ⊣ MPK-1 → LIN-39 →

40 SCF ⊣ APC ⊣ CDK-1/CYB-3 ⊣ CDK-4/CYD-1 → LIN-12m → LIN-12i ⊣ MPK-1 → LIN-39 →

41 SCF ⊣ APC ⊣ CDK-1/CYB-3 → CKI-1 ⊣ CDK-2/CYE-1 → LIN-12i ⊣ MPK-1 → LIN-39 →

42 CKI-1 ⊣ CDK-1/CYB-3 ⊣ CDK-4/CYD-1 ⊣ LIN-35 ⊣ EFL-1 → CDK-2/CYE-1 → LIN-12i ⊣ MPK-1 ⊣

43 SCF ⊣ CDK-2/CYE-1 → LIN-12i ⊣ MPK-1 ⊣ CKI-1 ⊣ CDK-4/CYD-1 ⊣ CDK-1/CYB-3 → APC ⊣

44 SCF ⊣ CDK-4/CYD-1 ⊣ CDK-1/CYB-3 → APC → CKI-1 ⊣ CDK-2/CYE-1 → LIN-12i ⊣ MPK-1 → LIN-39 →

45 CKI-1 ⊣ CDK-2/CYE-1 ⊣ LIN-35 ⊣ EFL-1 → CDK-1/CYB-3 ⊣ CDK-4/CYD-1 → LIN-12m → LIN-12i ⊣ MPK-1 ⊣

46 SCF ⊣ APC → CKI-1 ⊣ CDK-1/CYB-3 ⊣ CDK-4/CYD-1 → LIN-12m → LIN-12i ⊣ MPK-1 → LIN-39 →

47 SCF ⊣ APC ⊣ CDK-1/CYB-3 ⊣ CDK-4/CYD-1 → LIN-12m → LIN-12i ⊣ MPK-1 ⊣ CKI-1 ⊣ CDK-2/CYE-1 →

48 SCF ⊣ CDK-4/CYD-1 ⊣ LIN-35 → CDK-2/CYE-1 → LIN-12i ⊣ MPK-1 ⊣ CKI-1 ⊣ CDK-1/CYB-3 → APC ⊣

49 SCF ⊣ APC ⊣ CDK-1/CYB-3 ⊣ CDK-4/CYD-1 ⊣ CKI-1 ⊣ CDK-2/CYE-1 → LIN-12i ⊣ MPK-1 → LIN-39 →

50 SCF ⊣ APC ⊣ CDK-1/CYB-3 ⊣ CDK-4/CYD-1 ⊣ LIN-35 ⊣ CDK-2/CYE-1 → LIN-12i ⊣ MPK-1 → LIN-39 →

51 SCF ⊣ APC ⊣ CDK-1/CYB-3 → CKI-1 ⊣ CDK-4/CYD-1 → LIN-12m → LIN-12i ⊣ MPK-1 → LIN-39 →

52 SCF ⊣ APC ⊣ CDK-1/CYB-3 ⊣ LIN-12i ⊣ MPK-1 ⊣ CKI-1 ⊣ CDK-4/CYD-1 ⊣ LIN-35 ⊣ EFL-1 → CDK-2/CYE-1 →

53 SCF ⊣ APC → CKI-1 ⊣ CDK-4/CYD-1 ⊣ LIN-35 ⊣ EFL-1 → CDK-1/CYB-3 ⊣ LIN-12i ⊣ MPK-1 → LIN-39 →

54 SCF ⊣ APC → CKI-1 ⊣ CDK-2/CYE-1 ⊣ LIN-35 ⊣ EFL-1 → CDK-1/CYB-3 ⊣ LIN-12i ⊣ MPK-1 → LIN-39 →

55 SCF ⊣ APC → CKI-1 ⊣ CDK-1/CYB-3 ⊣ CDK-4/CYD-1 ⊣ LIN-35 ⊣ CDK-2/CYE-1 → LIN-12i ⊣ MPK-1 → LIN-39 →

56 SCF ⊣ APC ⊣ CDK-1/CYB-3 ⊣ CDK-4/CYD-1 ⊣ LIN-35 ⊣ EFL-1 → CDK-2/CYE-1 → LIN-12i ⊣ MPK-1 → LIN-39 →

57 SCF ⊣ APC ⊣ CDK-1/CYB-3 → CKI-1 ⊣ CDK-4/CYD-1 ⊣ LIN-35 ⊣ CDK-2/CYE-1 → LIN-12i ⊣ MPK-1 → LIN-39 →

58 SCF ⊣ APC → CKI-1 ⊣ CDK-1/CYB-3 ⊣ CDK-4/CYD-1 ⊣ LIN-35 ⊣ EFL-1 → CDK-2/CYE-1 → LIN-12i ⊣ MPK-1 → LIN-39 →

59 SCF ⊣ APC ⊣ CDK-1/CYB-3 → CKI-1 ⊣ CDK-4/CYD-1 ⊣ LIN-35 ⊣ EFL-1 → CDK-2/CYE-1 → LIN-12i ⊣ MPK-1 → LIN-39 →

60 SCF ⊣ APC → CKI-1 ⊣ CDK-2/CYE-1 ⊣ LIN-35 ⊣ EFL-1 → CDK-1/CYB-3 ⊣ CDK-4/CYD-1 → LIN-12m → LIN-12i ⊣ MPK-1 → LIN-39 →

Table 2 Negative feedback loops in the network of Figure 2

1 CDK-1/CYB-3 → APC ⊣

2 CKI-1 ⊣ CDK-1/CYB-3 →

3 SCF ⊣ CDK-2/CYE-1 →

4 CDK-4/CYD-1 ⊣ CKI-1 ⊣ CDK-1/CYB-3 ⊣

5 CKI-1 ⊣ CDK-1/CYB-3 → APC →

6 SCF ⊣ CDK-4/CYD-1 ⊣ CKI-1 ⊣ CDK-2/CYE-1 →

7 LIN-12i ⊣ MPK-1 → LIN-39 → LIN-12m →

8 SCF ⊣ CDK-4/CYD-1 ⊣ LIN-35 ⊣ CDK-2/CYE-1 →

9 CDK-4/CYD-1 ⊣ LIN-35 ⊣ EFL-1 → CDK-1/CYB-3 ⊣

10 SCF ⊣ CDK-4/CYD-1 ⊣ CDK-1/CYB-3 → APC ⊣

11 CKI-1 ⊣ CDK-2/CYE-1 ⊣ LIN-35 ⊣ EFL-1 → CDK-1/CYB-3 →

12 SCF ⊣ CDK-4/CYD-1 ⊣ LIN-35 ⊣ EFL-1 → CDK-2/CYE-1 →

13 CDK-4/CYD-1 ⊣ LIN-35 ⊣ EFL-1 → CDK-1/CYB-3 → CKI-1 ⊣

14 SCF ⊣ CDK-4/CYD-1 ⊣ CDK-1/CYB-3 → CKI-1 ⊣ CDK-2/CYE-1 →

15 SCF ⊣ APC ⊣ CDK-1/CYB-3 → CKI-1 ⊣ CDK-2/CYE-1 →

16 CKI-1 ⊣ CDK-4/CYD-1 → LIN-12m → LIN-12i ⊣ MPK-1 ⊣

17 CKI-1 ⊣ CDK-4/CYD-1 ⊣ CDK-1/CYB-3 ⊣ LIN-12i ⊣ MPK-1 ⊣

18 CDK-4/CYD-1 ⊣ CKI-1 ⊣ CDK-2/CYE-1 ⊣ LIN-35 ⊣ EFL-1 → CDK-1/CYB-3 ⊣

19 CKI-1 ⊣ CDK-2/CYE-1 ⊣ LIN-35 ⊣ EFL-1 → CDK-1/CYB-3 → APC →

20 CDK-4/CYD-1 ⊣ LIN-35 ⊣ EFL-1 → CDK-1/CYB-3 → APC → CKI-1 ⊣

21 SCF ⊣ CDK-4/CYD-1 ⊣ CDK-1/CYB-3 → APC → CKI-1 ⊣ CDK-2/CYE-1 →

22 SCF ⊣ APC ⊣ CDK-1/CYB-3 ⊣ CDK-4/CYD-1 ⊣ CKI-1 ⊣ CDK-2/CYE-1 →

23 SCF ⊣ APC ⊣ CDK-1/CYB-3 ⊣ CDK-4/CYD-1 ⊣ LIN-35 ⊣ CDK-2/CYE-1 →

24 CKI-1 ⊣ CDK-1/CYB-3 ⊣ CDK-4/CYD-1 ⊣ LIN-35 → CDK-2/CYE-1 → LIN-12i ⊣ MPK-1 ⊣

25 CKI-1 ⊣ CDK-4/CYD-1 ⊣ LIN-35 ⊣ EFL-1 → CDK-2/CYE-1 → LIN-12i ⊣ MPK-1 ⊣

26 SCF ⊣ CDK-2/CYE-1 → LIN-12i ⊣ MPK-1 ⊣ CKI-1 ⊣ CDK-1/CYB-3 → APC ⊣

27 SCF ⊣ CDK-4/CYD-1 ⊣ CKI-1 ⊣ CDK-1/CYB-3 ⊣ LIN-12i ⊣ MPK-1 → LIN-39 →

28 SCF ⊣ APC → CKI-1 ⊣ CDK-2/CYE-1 → LIN-12i ⊣ MPK-1 → LIN-39 →

29 SCF ⊣ APC → CKI-1 ⊣ CDK-1/CYB-3 ⊣ CDK-4/CYD-1 ⊣ LIN-35 ⊣ CDK-2/CYE-1 →

30 SCF ⊣ APC ⊣ CDK-1/CYB-3 ⊣ CDK-4/CYD-1 ⊣ LIN-35 ⊣ EFL-1 → CDK-2/CYE-1 →

31 SCF ⊣ APC ⊣ CDK-1/CYB-3 → CKI-1 ⊣ CDK-4/CYD-1 ⊣ LIN-35 ⊣ CDK-2/CYE-1 →

32 SCF ⊣ CDK-4/CYD-1 ⊣ LIN-35 ⊣ EFL-1 → CDK-1/CYB-3 ⊣ LIN-12i ⊣ MPK-1 → LIN-39 →

33 SCF ⊣ APC → CKI-1 ⊣ CDK-4/CYD-1 → LIN-12m → LIN-12i ⊣ MPK-1 → LIN-39 →

34 SCF ⊣ APC → CKI-1 ⊣ CDK-4/CYD-1 ⊣ CDK-1/CYB-3 ⊣ LIN-12i ⊣ MPK-1 → LIN-39 →

Table 2 Negative feedback loops in the network of Figure 2

35	SCF ⊣ APC → CKI-1 ⊣ CDK-1/CYB-3 ⊣ CDK-4/CYD-1 ⊣ LIN-35 ⊣ EFL-1 → CDK-2/CYE-1 →
36	SCF ⊣ APC ⊣ CDK-1/CYB-3 → CKI-1 ⊣ CDK-4/CYD-1 ⊣ LIN-35 ⊣ EFL-1 → CDK-2/CYE-1 →
37	SCF ⊣ CDK-2/CYE-1 ⊣ LIN-35 ⊣ EFL-1 → CDK-1/CYB-3 ⊣ LIN-12i ⊣ MPK-1 → LIN-39 →
38	SCF ⊣ CDK-4/CYD-1 → LIN-12m → LIN-12i ⊣ MPK-1 ⊣ CKI-1 ⊣ CDK-1/CYB-3 → APC ⊣
39	SCF ⊣ APC → CKI-1 ⊣ CDK-4/CYD-1 ⊣ LIN-35 ⊣ CDK-2/CYE-1 → LIN-12i ⊣ MPK-1 → LIN-39 →
40	SCF ⊣ APC ⊣ CDK-1/CYB-3 ⊣ LIN-12i ⊣ MPK-1 ⊣ CKI-1 ⊣ CDK-4/CYD-1 ⊣ LIN-35 → CDK-2/CYE-1 →
41	SCF ⊣ CDK-4/CYD-1 ⊣ LIN-35 ⊣ EFL-1 → CDK-1/CYB-3 ⊣ LIN-12i ⊣ MPK-1 ⊣ CKI-1 ⊣ CDK-2/CYE-1 →
42	SCF ⊣ CDK-2/CYE-1 → LIN-12i ⊣ MPK-1 ⊣ CKI-1 ⊣ CDK-4/CYD-1 ⊣ LIN-35 ⊣ EFL-1 → CDK-1/CYB-3 → APC ⊣
43	SCF ⊣ CDK-4/CYD-1 ⊣ CKI-1 ⊣ CDK-2/CYE-1 ⊣ LIN-35 ⊣ EFL-1 → CDK-1/CYB-3 ⊣ LIN-12i ⊣ MPK-1 → LIN-39 →
44	SCF ⊣ CDK-4/CYD-1 ⊣ LIN-35 ⊣ EFL-1 → CDK-2/CYE-1 → LIN-12i ⊣ MPK-1 ⊣ CKI-1 ⊣ CDK-1/CYB-3 → APC ⊣
45	SCF ⊣ CDK-4/CYD-1 ⊣ LIN-35 ⊣ EFL-1 → CDK-1/CYB-3 → CKI-1 ⊣ CDK-2/CYE-1 → LIN-12i ⊣ MPK-1 → LIN-39 →
46	SCF ⊣ APC → CKI-1 ⊣ CDK-4/CYD-1 ⊣ LIN-35 ⊣ EFL-1 → CDK-2/CYE-1 → LIN-12i ⊣ MPK-1 → LIN-39 →
47	SCF ⊣ CDK-2/CYE-1 ⊣ LIN-35 ⊣ EFL-1 → CDK-1/CYB-3 ⊣ CDK-4/CYD-1 → LIN-12m → LIN-12i ⊣ MPK-1 → LIN-39 →
48	SCF ⊣ CDK-4/CYD-1 → LIN-12m → LIN-12i ⊣ MPK-1 ⊣ CKI-1 ⊣ CDK-2/CYE-1 ⊣ LIN-35 ⊣ EFL-1 → CDK-1/CYB-3 → APC ⊣
49	SCF ⊣ CDK-4/CYD-1 ⊣ LIN-35 ⊣ EFL-1 → CDK-1/CYB-3 → APC → CKI-1 ⊣ CDK-2/CYE-1 → LIN-12i ⊣ MPK-1 → LIN-39 →
50	SCF ⊣ CDK-2/CYE-1 ⊣ LIN-35 ⊣ EFL-1 → CDK-1/CYB-3 → CKI-1 ⊣ CDK-4/CYD-1 → LIN-12m → LIN-12i ⊣ MPK-1 → LIN-39 →
51	SCF ⊣ CDK-2/CYE-1 ⊣ LIN-35 ⊣ EFL-1 → CDK-1/CYB-3 → APC → CKI-1 ⊣ CDK-4/CYD-1 → LIN-12m → LIN-12i ⊣ MPK-1 → LIN-39 →

Redundancy among feedback circuits is emerging as a generic trait of regulatory networks. Furthermore, feedback circuit redundancy could play an important role in network robustness to mutations and noise [76].

Conclusions

Our model recovers the stable patterns of activation of the considered molecular components under wild type and mutant conditions, replicating those patterns encountered on actual cells during vulval development in *C. elegans*. To the best of our knowledge, the present model is the first that explores the dynamic effect of the mechanism for the cross-regulation between the cell cycle and the cell fate determination of vulval cells, mechanism that was proposed by [42] and [77]. Our model provides a suitable approach to understand the coordinated regulation

of cell-cycle progression and differentiation during this process.

The cross-regulation between cell differentiation and cell-cycle progression in vulval cells of *C. elegans* is mediated by the activation of SCF by LIN-39, the inhibition of CKI-1 by MPK-1, the inhibition of LIN-12i by CDK-1/CYB-3, the activation of LIN-12i by CDK-2/CYE-1, and the activation of LIN-12m by CDK-4/CYD-1. The type of regulatory interactions that grant such dynamic coordination might be conserved in other biological systems [78,79], and may also constitute a useful framework to address such coordination in other systems.

Our modeling effort resulted in the following predictions for the system under study: *a*) the activation of SCF by LIN-39, removing this interaction causes cell cycle quiescence in our model. *b*) the activation of CDK-1/CYB-3 by EFL-1, removing this interaction causes an endoreplication-like cell cycle. *c*) the inhibition of CDK-4/CYD-1 by CKI-1, removing this interaction causes a short cell cycle. *d*) the inhibition of CDK-1/CYB-3 by CKI-1, removing this interaction does not change the dynamic behavior of our model, *e*) the inhibition of CDK-1/CYB-3 by CDK-4/CYD-1, removing this interaction causes a modified cell cycle. *f*) the inhibition of CDK-4/CYD-1 by CDK-1/CYB-3, removing this interaction causes a short cell cycle.

Given the importance of the Notch signaling pathway for different developmental processes, it is fundamental to understand how it interacts with other signaling pathways. Here, we highlight the temporal regulation of LIN-12 by different CDK/cyclin complexes, which leads to precise spatio-temporal regulation of Notch signaling during vulva development and opens a wide range of possibilities in the comprehension of how cell fates are established under a specific combination of intracellular and extracellular signals. Our model shows that regulation of Notch signaling by the cell cycle preserves the potential of the VPCs and the three fates to differentiate and de-differentiate, allowing them to remain completely responsive to the concentration of LIN-3 and LS in the extracellular micro-environment.

Another important contribution of our model is that the need for a sequential control of fate determination disappears completely. Without the cell cycle effect, in a microenvironment with a moderately high level of LIN-3 and LS, a VPC would acquire either the primary or the secondary fate, depending on which inductive signal affected the cell first. In our model, however, the VPC will always acquire the secondary fate. Dynamical analysis such as ours are needed to achieve an adequate understanding of molecular regulation during the development of multicellular organisms.

Certain mutations can dramatically affect the behavior of a regulatory network, even if they do not cause the loss

of all the functions of a protein. Simulating the removal of certain interactions, we were able to propose some changes to specific regions of certain proteins that could lead to abnormal vulval development in *C. elegans*.

Despite the broad agreement between our model and the experimental data, there is ample room for improvement. Specifically, we will try to incorporate in future versions the molecular mechanism involved when the cell cycle is activated or inactivated by a combination of CKI-1 activation by LIN-29 during L4 and SCF mediated degradation of CDC-25.1, as well as the molecules involved in the transitions between mitosis, meiosis, endoreplication and the embryonic cell cycle.

Methods
Molecular basis of the regulatory network
We built a simplified model of the molecular network involved in the fate determination of the VPCs and the control of the cell cycle by connecting two functional modules, that is, sets of biological molecules that are involved in accomplishing a specific biological function in the cell. Specifically, we used one module for the network of molecules involved in cell cycle control and a second module for the network of molecules involved in the control of vulval fate determination. We built the two functional modules by including only the molecules with very penetrant mutant phenotypes reported in the literature. For the fate determination module, we included only the ligands and the effectors of the Ras and Notch signaling cascades, and MPK-1, necessary to represent the mutual inhibition between them. For the cell cycle module, we included only the three main CDK/Cyclin complexes and their main regulators. Most interactions in the model are supported by experimental evidence in *C. elegans*, as summarized below. These interactions can be classified as activations or inhibitions [80], defined as follows: Given two genes *i* and *j*, *i activates j* if there exists a configuration (*i.e.* a pattern of molecular activation) $x = (x_1, \ldots, x_n)$ and values *a* and *b*, with $a > b$, such that:

$$f_j(x_1, \ldots, x_{i-1}, a, x_{i+1}, \ldots, x_n) - f_j(x_1, \ldots, x_{i-1}, b, x_{i+1}, \ldots, x_n) > 0$$

Conversely, *i inhibits j* if there exists a configuration $x = (x_1, \ldots, x_n)$ and values *a* and *b*, with $a > b$, such that:

$$f_j(x_1, \ldots, x_{i-1}, a, x_{i+1}, \ldots, x_n) - f_j(x_1, \ldots, x_{i-1}, b, x_{i+1}, \ldots, x_n) < 0$$

According to this definition, it is possible for gene *i* to both activate and inhibit gene *j*. In this case, we say that the rule or interaction is *ambiguous*. The only ambiguous update rule in our model is in LIN-12i (Equation 6). The model also contains interactions reported in other organisms, namely, the mutual inhibition between APC and SCF in mammals, the activation of CKI-1 by APC

in humans, the activation of CKI-1 by CDK-1/CYB-3 in yeast, and the inhibition of LIN-35 by CDK-2/CYE-1 in mammals. Finally, the model also includes interactions that are predictions of our model, namely, the mutual inhibition between CDK-1/CYB-3 and CDK-4/CYD-1, the activation of CDK-1/CYB-3 by EFL-1, the inhibition of CDK-4/CYD-1 and CDK-1/CYB-3 by CKI-1, and the activation of SCF by LIN-39.

Molecules involved in VPC fate determination:
The Ras/MAPK signaling cascade is represented by three nodes, LIN-3, MPK-1, and LIN-39. LIN-3 is an EGF ortholog, and functions as an external signal that is used as a parameter that does not change during each simulation. LIN-3 activates the Ras/MAPK signaling [16,29,81,82], whose main effector is MPK-1 [83,84], an ERK ortholog. MPK-1 phosphorylates many important transcription factors, such as LIN-39, LIN-1, LIN-31 and some components of the mediator complex like LIN-25 and SUR-2, that bind to the promoters of *lin-39*, activating its transcription. The LIN-39 product, is a HOM-C protein homologous to Deformed and Sex combs reduced. Importantly, phosphorylated LIN-39 activates its own expression [68,83-85].

To represent the Notch signaling cascade we included in the simplified model the lateral signal as well as the ortholog of Notch *lin-12*. The lateral signal (LS) functions as a parameter of the model, and it comprises DSL-1 and LAG-2 or APX-1. DSL-1 originates from P6.p and forms a gradient, while LAG-2 and APX-1 are membrane proteins that are also expressed by P6.p, whose effect is on the neighbor cells that are in direct physical contact, that is, P5.p and P7.p [86]. LIN-12 is represented by two nodes in our model. On the one hand, LIN-12i represents the fragment of LIN-12 that travels to the nucleus and forms part of the LIN-12intra/LAG-1/SEL-8 complex. This complex activates the transcription of the lateral signal targets, such as *lin-11*, *lip-1* and *lin-12* [87], and stabilizes the membrane localization of LIN-12 through *mir-61* and VAV-1 [88]. On the other hand, LIN-12m represents the protein localized in the membrane, functioning as a receptor for the lateral signal [89,90]. Finally, it is known that LIN-39 activates the transcription of *lin-12* [91].

We included the interactions that allow for a mutual inhibition of the Ras and Notch pathways. MPK-1 activates the mediator complex, increasing the rate at which LIN-12 is removed from the membrane and marked for degradation [92,93]. Now, LIP-1 inactivates MPK-1 [94], and ARK-1 inhibits LET-23 in a SEM-5-dependent mechanism [95]. Both LIP-1 and ARK-1 are lateral signal targets, and are activated by LIN-12i. Thus, there is a net negative effect from LIN-12i to MPK-1.

Molecules involved in the control of the cell cycle and their interactions:

In general, the molecular mechanism for the control of the cell cycle is based on the activity of a cyclin-dependent kinase (CDK), which is required to advance from one stage of the cell cycle to the next.

Each CDK binds to certain cyclins when they are available; specifically those that have a high enough binding affinity with the CDK. CDK-inhibitory proteins (CKIs) associate with Cyclin/CDK complexes to keep them inactive, and phosphorylation by Wee1/Myt1 kinases also inhibits their activity. Cyclin/CDK activation requires phosphorylation, ubiquitination and proteolysis of the CKI, phosphorylation of the CDK by a CDK-activating kinase (CAK), as well as the removal of the inhibitory phosphates by a Cdc25 phosphatase. Cyclin destruction leads to inactivation. Ubiquitination and proteolysis of cell cycle regulators in late G1 and S requires cullin-based E3 ligases such as Skp1-Cul1-F box (SCF), while in M phase and early G1 the activity of the anaphase-promoting complex (APC) –which is an E3 RING ubiquitin ligase– is needed [69].

In *C. elegans*, the regulatory function of three CDK/Cyclin complexes during the cell cycle is known: CDK-4/CYD-1 is the first complex involved in the control of the G1 to S transition, and the expression of *cdk-4* and *cyd-1* is sufficient to activate the expression the S phase marker rnr::GFP [96]. CYD-1 is likely to be degraded by SCF [97], and CDK-4/CYD-1 may be a target of CKI-1 inhibition because CKI-1 binds CYD-1 [98]. CDK-2/CYE-1 is the second complex involved in the control of the G1 to S transition, CDK-2 binds to CYE-1 and CKI-1 may inhibit CYE-1 function [69,98]. When CKI-1 is ubiquitinated, it dissociates from CDK-2/CYE-1, then CDK-2/CYE-1 activity allows the progression from G1 to S [69]. The promoter of *cye-1* contains potential EFL-1/DPL-1 binding sites [99]. CUL-1 (part of SCF) may inhibit CYE-1, and CDK-1/CYB-3 is involved in the G2 to M transition but not G1 to S [69]. CDK-1 binds to CYB-1 and CYB-3 *in vitro*, and APC-11 inhibits CYB-1 [100]. CDK-1/CYB-3 activates CDC-25.1 and it inhibits WEE-1.3 [63,69,101], thus forming two positive self regulation cycles that we include in our model without explicitly incorporating the nodes for simplicity.

Two CKIs exist in *C. elegans*, namely, *cki-1* and *cki-2*. Both are known to regulate the cell cycle, but we only included *cki-1* in the model for simplicity, and because many of the most penetrant phenotypes are the result of mutations affecting both genes [102]. The gene *cki-1* is orthologous to the mammalian cyclin-dependent kinase inhibitor p27/KIP1 and *cki-1* is required to stop the cell cycle and to stay at the G0/G1 phase. The protein CKI-1 is one of the main regulators of the postembryonic cell cycle in *C. elegans* [103]. In humans, the ortholog of FZR-1, which is a regulatory subunit of APC indirectly promotes the accumulation of the ortholog of CKI-1 [65,69]. Additionally, in yeast the ortholog of CDK-1/CYB-3 activates the ortholog of CDC-14 [65,66], then CDC-14 upregulates the accumulation of CKI-1 [65,104]. Finally, CKI-1 is negatively regulated by CDK-4/CYD-1; the evidence supporting this interaction is that CKI-1 binds to CDK-4/CYD-1 and loss of *cki-1/2* function rescues multiple aspects of the *cyd-1* loss of function (lf) and *cdk-4(lf)* mutant phenotypes [100].

The protein EFL-1 is a homolog of mammalian E2F, which inhibits the G1-to-S transition. In mammals, Rb binds to E2F, inhibiting its function as an activating transcription factor. It is worth noting that EFL-1 may need DPL-1 as a co-factor [69]. The protein LIN-35 is orthologous to Rb, CDK-4/CYD-1 negatively regulates LIN-35 activity [100,105], and in mammals, the orthologs of CDK-2 and CYE-1 are needed to fully inhibit the Rb function [105,106].

In *C. elegans*, the components of the SCF complex include the Skp1-like proteins SKR-1 and SKR-2 [97], LIN-23 (F-box), and CUL-1 [71,107,108]. The components of APC include MAT-1, MAT-2, MAT-3, CDC-26, APC-2, APC-10, APC-11, APC-17, EMB-1(APC16), EMB-27, EMB-30, and FZR-1 [97,109]. Furthermore, mammalian Cdk1 activates APC/C [110], while APC and SCF inhibit each other [110-112].

CDK-7 is a CAK ortholog, which likely associates with the cyclin CYH-1 [100], but the function of these molecules in the regulation of the cell cycle in *C. elegans* is not known because most *cdk-7* mutations are lethal. *C. elegans*, has two WEE-1 homologues, namely, *wee-1.1* and *wee-1.3*, which are active in the germ line [101,113]. There are also four CDC-25 homologues: *cdc-25.1*, *cdc-25.2*, *cdc-25.3*, and *cdc-25.4*. Of these four, only the function of CDC-25.1 as a cell cycle regulator is known [101].

Interactions between the molecules involved in the control of the cell cycle and the molecules involved in the control of VPC fate determination:

LIN-3/EGF activates Ras signaling. Now, LIN-1 and LIN-31—effectors of Ras—as well as the Mediator complex are necessary for cell cycle quiescence. Specifically, when Ras is active, LIN-1 and LIN-31 do not activate the transcription of CKI-1, and we included this regulation as an inhibition of CKI-1 by MPK-1 [77]. Moreover, LIN-1, LIN-31 and the Mediator complex activate *lin-39* transcription [68,85] and LIN-39 is required for the divisions of the VPCs [114]. Additionally, the three CDK/Cyclin complexes that regulate the cell cycle also regulate Notch signaling. In particular, the CDK-4/CYD-1 complex stabilizes the location of LIN-12 (NOTCH) on the cell membrane; the CDK-2/CYE-1 complex inhibits the proteolysis of the fragment of LIN-12 that functions as a transcription

factor in the nucleus; and the CDK-1/CYB-3 complex activates the expulsion from the nucleus and the degradation of the LIN-12 fragment [42].

The regulatory network as a dynamical system

We first reconstructed the cell cycle functional module from an expected time series with the use of *BoolNet* [115]. *BoolNet* produced a probabilistic Boolean network with several possible update rules for each node. We chose for each node the rule that best reflected the biological knowledge, and made a few modifications. Specifically, we included the mutual inhibition between APC and SCF, which does not change the dynamic of the wild type model, but changes the simulated effect of several mutations.

Next, we developed a deterministic discrete dynamical model by building the VPC fate determination module, and then connecting it with the cell cycle module. In our model there is one node with four possible levels of activation—LIN-3—. This characteristic is necessary because *a*) the VPCs P3.p, P8.p and P9.p, which acquire the tertiary fate, have no Ras activity (*i.e.* a level of 0), *b*) the VPCs P5.p and P7.p usually have a moderate level of Ras signaling which is sufficient to determine the secondary fate (*i.e.* a level of 1), *c*) P6.p is characterized by a high level of Ras signaling (*i.e.* a level of 2), which is sufficient to determine the primary fate, but only in the absence of negative regulation, and *d*) in some experiments with worms that have two or more anchor cells, the level of Ras signaling is high enough to overcome the effects of the negative regulators (*i.e.* a level of 3).

Two nodes of the network needed to be modeled as components with three levels of activation—MPK-1 and LIN-39—, which are at the end of the Ras signaling cascade, or downstream from it. They have no inhibitors to overcome, and hence only the levels 0, 1, and 2 are considered.

The rest of the nodes in the network were considered as Boolean, since the experimental evidence report either a full gain or total loss of function. Therefore, the rules determining the state of activation of each node as a function of their regulatory inputs are as follows:

$$\text{LIN-3}(t+1) = \text{LIN-3}(t) \tag{1}$$

$$\text{MPK-1}(t+1) = \begin{cases} 2 & \text{if } (\text{LIN-3}(t) = 3 \text{ and MPK-1}(t) > 0) \text{ or} \\ & (\text{LIN-3}(t) = 2 \text{ and LIN-12i}(t) = 0 \text{ and} \\ & \text{MPK-1}(t) > 0) \\ 0 & \text{if MPK-1}(t) < 2 \text{ and} \\ & ((\text{LIN-3}(t) = 1 \text{ and LIN-12i}(t) = 1) \text{or} \\ & (\text{LIN-3}(t) = 0)) \\ 1 & \text{otherwise} \end{cases} \tag{2}$$

$$\text{LIN-39}(t+1) = \begin{cases} 2 & \text{if MPK-1}(t) = 2 \text{ and LIN-39}(t) > 0 \\ 0 & \text{When simulating } \textit{lin-39} \text{ loss of function} \\ 1 & \text{otherwise} \end{cases} \tag{3}$$

$$\text{LS}(t+1) = \text{LS}(t) \tag{4}$$

$$\text{LIN-12m}(t+1) = \begin{cases} 1 & \text{if } (\text{LIN-39}(t) > 0 \text{ or LIN-12i}(t) = 1) \text{ and} \\ & (\text{MPK-1}(t) \le 1 \text{ or CDK-4/CYD-1}(t) = 1) \\ 0 & \text{otherwise} \end{cases} \tag{5}$$

$$\text{LIN-12i}(t+1) = \begin{cases} 1 & \text{if } (\text{LS}(t) = 1 \text{ and LIN-12m}(t) = 1) \text{ or} \\ & ((\text{LIN-12i}(t) = 1\text{or LIN-3}(t) = 1) \text{ and} \\ & (\text{CDK-2/CYE-1}(t) = 1 \text{ or} \\ & \text{CDK-1/CYB-3}(t) = 0)) \\ 0 & \text{otherwise} \end{cases} \tag{6}$$

$$\text{CKI-1}(t+1) = \begin{cases} 1 & \text{if } (\text{MPK-1}(t) = 0) \text{ and} \\ & (\text{CDK-4/CYD-1}(t) = 0 \text{ and APC}(t) = 1 \\ & \text{or CDK-1/CYB-3}(t) = 1)) \\ 0 & \text{otherwise} \end{cases} \tag{7}$$

$$\text{EFL-1}(t+1) = \begin{cases} 1 & \text{if LIN-35}(t) = 0 \\ 0 & \text{otherwise} \end{cases} \tag{8}$$

$$\text{LIN-35}(t+1) = \begin{cases} 1 & \text{if CDK-4/CYD-1}(t) = 0 \text{ and} \\ & \text{CDK-2/CYE-1}(t) = 0 \\ 0 & \text{otherwise} \end{cases} \tag{9}$$

$$\text{SCF}(t+1) = \begin{cases} 1 & \text{if LIN-39}(t) > 0 \text{ and APC}(t) = 0 \\ & \text{and CDK-2/CYE-1}(t) = 1 \\ 0 & \text{otherwise} \end{cases} \tag{10}$$

$$\text{APC}(t+1) = \begin{cases} 1 & \text{if SCF}(t) = 0 \text{ and CDK-1/CYB-3}(t) = 1 \\ 0 & \text{otherwise} \end{cases} \tag{11}$$

$$\text{CDK-4/CYD-1}(t+1) = \begin{cases} 1 & \text{if CKI-1}(t) = 0 \text{ and SCF}(t) = 0 \\ & \text{and CDK-1/CYB-3}(t) = 0 \\ 0 & \text{otherwise} \end{cases} \tag{12}$$

$$\text{CDK-2/CYE-1}(t+1) = \begin{cases} 1 & \text{if EFL-1}(t) = 1 \text{ and LIN-35}(t) = 0 \\ & \text{and CKI-1}(t) = 0 \text{ and SCF}(t) = 0 \\ 0 & \text{otherwise} \end{cases} \tag{13}$$

$$\text{CDK-1/CYB-3}(t+1) = \begin{cases} 1 & \text{if CKI-1}(t) = 0 \text{ and APC}(t) = 0 \\ & \text{and EFL-1}(t) = 1 \\ & \text{and (CDK-4/CYD-1}(t) = 0 \\ & \text{or CDK-1/CYB-3}(t) = 1) \\ 0 & \text{otherwise} \end{cases}$$

$$(14)$$

Subsequently, we used the software package *Griffin* [73], to find the interactions that are necessary to recover a cyclic attractor that visits the configurations characteristic of each cell-cycle phase in the temporal sequence that is observed in actual cells. Additionally, we specified that all the interaction signs must be unambiguous.

Finally, we used the SQUAD methodology [116] to build a deterministic continuous version of the cell cycle module, based on the Boolean update rules that we obtained based on an expected time series with the use of *Bool-Net*. We used the continuous version of the module to verify that the cyclic behavior of the network is not an artifact of the synchronous updating of the discrete model [63]. The differential equations describing the continuous model are as follows:

$$squad(X_i, \omega_i) = \frac{-e^{0.5h} + e^{-h(\omega_i - 0.5)}}{(1 - e^{0.5h})(1 + e^{h(\omega_i - 0.5)})} - \gamma_i X_i \quad (15)$$

$$h = 10 \quad (16)$$

$$\gamma_i = 0.95 \quad (17)$$

$$\omega_{CKI-1} = \min((1 - \text{CDK-4/CYD-1}), \max(\text{APC}, \text{CDK-1/CYB-3})) \quad (18)$$

$$\frac{d(\text{CKI-1})}{dt} = squad(\text{CKI-1}, \omega_{CKI-1}) \quad (19)$$

$$\omega_{EFL-1} = 1 - \text{LIN-35} \quad (20)$$

$$\frac{d(\text{EFL-1})}{dt} = squad(\text{EFL-1}, \omega_{EFL-1}) \quad (21)$$

$$\omega_{LIN-35} = \min(1 - \text{CDK-4/CYD-1}, 1 - \text{CDK-2/CYE-1})) \quad (22)$$

$$\frac{d(\text{LIN-35})}{dt} = squad(\text{LIN-35}, \omega_{LIN-35}) \quad (23)$$

$$\omega_{SCF} = \min(1 - \text{APC}, \text{CDK-2/CYE-1})) \quad (24)$$

$$\frac{d(\text{SCF})}{dt} = squad(\text{SCF}, \omega_{SCF}) \quad (25)$$

$$\omega_{APC} = \min(1 - \text{SCF}, \text{CDK-1/CYB-3})) \quad (26)$$

$$\frac{d(\text{APC})}{dt} = squad(\text{APC}, \omega_{APC}) \quad (27)$$

$$\omega_{CDK-4/CYD-1} = \min(1 - \text{CKI-1}, 1 - \text{SCF}, 1 - \text{CDK-1/CYB-3}) \quad (28)$$

$$\frac{d(\text{CDK-4/CYD-1})}{dt} = squad(\text{CDK-4/CYD-1}, \omega_{CDK-4/CYD-1}) \quad (29)$$

$$\omega_{CDK-2/CYE-1} = \min(\text{EFL-1}, 1 - \text{LIN-35}, 1 - \text{CKI-1}, 1 - \text{SCF}) \quad (30)$$

$$\frac{d(\text{CDK-2/CYE-1})}{dt} = squad(\text{CDK-2/CYE-1}, \omega_{CDK-2/CYE-1}) \quad (31)$$

$$\omega_{CDK-1/CYB-3} = \min(1 - \text{CKI-1}, 1 - \text{APC}, \text{EFL-1}, \max(1 - \text{CDK-4/CYD-1}, \text{CDK-1/CYB-3})) \quad (32)$$

$$\frac{d(\text{CDK-1/CYB-3})}{dt} = squad(\text{CDK-1/CYB-3}, \omega_{CDK-1/CYB-3}) \quad (33)$$

Endnote

[a] *Griffin* is a symbolic computational tool under development that uses a SAT solver to find Boolean networks satisfying certain constraints, for example, the existence of known or hypothetical interactions.

Additional files

Additional file 1: Table S1. Simulation of mutants and their phenotypic effect [8,35,71,86,100,103,114,117-121].

Additional file 2: Mutations. This file contains the attractors produced by the simulation of each mutation.

Additional file 3: Table S2. The simulated phenotypic effect caused by removing each interaction [25,27,38,42,68,85,86,88,91-94,117,119,122,123].

Additional file 4: Interactions. This file contains the attractors produced by the simulation of each interaction removal.

Author details
[1]Programa de Doctorado en Ciencias Biomédicas, Universidad Nacional Autónoma de, México DF, México. [2]Instituto de Investigaciones Biomédicas, Universidad Nacional Autónoma de México, México DF, México. [3]Instituto de Ecología, Universidad Nacional Autónoma de México, México DF, México. [4]Instituto de Investigaciones en Matemáticas Aplicadas y en Sistemas, Universidad, Nacional Autónoma de México, México DF, México. [5]Centro de Ciencias de la Complejidad, Universidad Nacional Autónoma de México, México DF, México.

References

1. Hodgkin J. Introduction to genetics and genomics. September 6, 2005 *WormBook*, ed. The *C. elegans* Research Community, WormBook, doi/10.1895/wormbook.1.7.1, http://www.wormbook.org
2. Herman MA. Hermaphrodite cell-fate specification. January 09, 2006. *WormBook*, ed. The *C. elegans* Research Community, WormBook, doi/10.1895/wormbook.1.7.1, http://www.wormbook.org
3. Golden TR, Melov S. Gene expression changes associated with aging in *C. elegans*. February 12, 2007. *WormBook*, ed. The *C. elegans* Research Community, WormBook, doi/10.1895/wormbook.1.7.1, http://www.wormbook.org
4. Hobert O. Neurogenesis in the nematode *Caenorhabditis elegans*. October 4, 2010. *WormBook*, ed. The *C. elegans* Research Community, WormBook, doi/10.1895/wormbook.1.7.1, http://www.wormbook.org
5. Sulston JE, Horvitz HR. Post-embryonic cell lineages of the nematode, *Caenorhabditis elegans*. Dev Biol. 1977;56:110–56.
6. Lints R, Hall DH. 2009. Reproductive system, egglaying apparatus. doi:10.3908/wormatlas.1.24.
7. Sharma-Kishore R, White JG, Southgate E, Podbilewicz B. Formation of the vulva in *Caenorhabditis elegans*: a paradigm for organogenesis. Development. 1999;126:691–9.
8. Sternberg PW. Vulval development. June 25, 2005. *WormBook*, ed. The *C. elegans* Research Community, WormBook, doi:10.1895/wormbook.1.7.1, http://www.wormbook.org
9. Green JL, Inoue T, Sternberg PW. Opposing Wnt pathways orient cell polarity during organogenesis. Cell. 2008;134(4):646–56.
10. Félix M-A. *Caenorhabditis elegans* vulval cell fate patterning. Phys Biol. 2012;9(4):045001.
11. Schindler AJ, Sherwood DR. Morphogenesis of the *Caenorhabditis elegans* vulva. WIREs Dev Biol. 2013;2:75–95.
12. Sulston JE, White JG. Regulation and cell autonomy during postembryonic development of *Caenorhabditis elegans*. Dev Biol. 1980;78(2):577–97.
13. Kimble J. Alterations in cell lineage following laser ablation of cells in the somatic gonad of *Caenorhabditis elegans*. Dev Biol. 1981;87(2):286–300.
14. Sternberg PW, Horvitz HR. Pattern formation during vulval development in *C. elegans*. Cell. 1986;44(5):761–72.
15. Horvitz HR, Sulston JE. Isolation and genetic characterization of cell-lineage mutants of the nematode *Caenorhabditis elegans*. Genetics. 1980;96(2):435–54.
16. Ferguson EL, Horvitz HR. Identification and characterization of 22 genes that affect the vulval cell lineages of the nematode *Caenorhabditis Elegans*. Genetics. 1985;110:17–72.
17. Seydoux G, Salvage C, Greenwald I. Isolation and Characterization of Mutations Causing Abnormal Eversion of the Vulva in *Caenorhabditis Elegans*. Dev Biol. 1993;157(2):423–36.
18. Eisenmann DM, Kim SK. Protruding vulva mutants identify novel loci and wnt signaling factors that function during *Caenorhabditis elegans* vulva development. Genetics. 2000;153(3):1097–116.
19. Beitel GJ, Clark SG, Horvitz HR. *Caenorhabditis elegans* ras gene *let-60* acts as a switch in the pathway of vulval induction. Nature. 1990;348:503–9.
20. Han M, Aroian RV, Sternberg PW. The *let-60* locus controls the switch between vulval and nonvulval cell Fates in *Caenorhabditis elegans*. Genetics. 1990;126:899–913.
21. Aroian RV, Sternberg PW. Multiple Functions of *let-23*, a *Caenorhabditis elegans* receptor tyrosine Kinase gene required for vulval induction. Genetics. 1991;128:251–67.
22. Clark SG, Stern MJ, Horvitz HR. *C. elegans* cell-signalling gene *sem-5* encodes a protein with SH2 and SH3 domains. Nature. 1992;356:340–4.
23. Clark SG, Chisholm AD, Horvitz HR. Control of Cell Fates in the Central Body Region of *C. elegans* by the Homebox Gene *lin-39*. Cell. 1993;74: 43–55.
24. Han M, Golden A, Han Y, Sternberg PW. *C. elegans lin-45* raf gene participates in *let-60 ras*-stimulated vulval differentiation. Nature. 1993;363:133–40.
25. Yoo AS, Bais C, Greenwald I. Crosstalk Between the EGFR and LIN-12/Notch Pathways in *C. elegans* Vulval Development. Science. 2004;303(5658):663–6.
26. Sundaram MV. The love–hate relationship between Ras and Notch. Genes Dev. 2005;19:1825–39.
27. Zand TP, Reiner DJ, Der CJ. Ras Effector Switching Promotes Divergent Cell Fates in *C, elegans Vulval Patterning*. Dev Cell. 2011;20(1):84–96.
28. Eisenmann DM, Maloof JN, Simske JS, Kenyon C, Kim SK. The /*beta*-catenin homolog BAR-1 and LET-60 Ras coordinately regulate the Hox gene *lin-39* during *Caenorhabditis elegans* vulval development. Development. 1998;125:3667–680.
29. Myers TR, Greenwald I. Wnt signal from multiple tissues and *lin-3/EGF* signal from the gonad maintain vulval precursor cell competence in *Caenorhabditis elegans*. Proc Nat Acad Sci USA. 2007;104(51):20368–73.
30. Weinstein N, Mendoza L. A network model for the specification of vulval precursor cells and cell fusion control in *Caenorhabditis elegans*,. Front Genet. 2013;4(112):1–24.
31. Gupta BP, Hanna-Rose W, Sternberg PW. Morphogenesis of the vulva and the vulval-uterine connection. November 30, 2012. *WormBook*, ed. The *C. elegans* Research Community, WormBook, doi:10.1895/wormbook.1.7.1, http://www.wormbook.org
32. Moss EG, Lee RC, Ambros V. The Cold Shock Domain Protein LIN-28 Controls Developmental Timing in *C. elegans and Is Regulated by the lin-4 RNA*. Cell. 1997;88:637–46.
33. Li J, Greenwald I. LIN-14 inhibition of LIN-12 contributes to precision and timing of *C. elegans* vulval fate patterning. Curr Biol. 2010;20(20):1875–9.
34. Félix M-A, Barkoulas M. Robustness and flexibility in nematode vulva development. Trends Genet. 2012;28(4):185–95.
35. Sternberg PW, Horvitz HR. The combined action of two intercellular signaling pathways specifies three cell fates during vulval induction in *C. elegans*. Cell. 1989;58(4):679–93.
36. Giurumescu CA, Sternberg PW, Asthagiri AR. Intercellular coupling amplifies fate segregation during *Caenorhabditis elegans* vulval development. Proc Nat Acad Sci USA. 2006;103(5):1331–6.
37. Giurumescu CA, Sternberg PW, Asthagiri AR. Predicting Phenotypic Diversity and the Underlying Quantitative Molecular Transitions. PLoS Comput Biol. 2009;5(4):1000354.
38. Hoyos E, Kim K, Milloz J, Barkoulas M, Pénigault J-B, Munro E, et al. Quantitative variation in autocrine signaling and pathway crosstalk in the *Caenorhabditis* vulva network. Curr Biol. 2011;21(7):527–38.
39. Corson F, Siggia ED. Geometry, epistasis, and developmental patterning. Proc Nat Acad Sci USA. 2012;109(15):5568–75.
40. Fisher J, Piterman N, Hubbard EJA, Stern MJ, Harel D. Computational insights into *Caenorhabditis elegans* vulval development. Proc Nat Acad Sci USA. 2005;102(6):1951–6.
41. Fisher J, Piterman N, Hajnal A, Henzinger TA. Predictive modeling of signaling crosstalk during *C. elegans vulval development*. PLoS Comput Biol. 2007;3(5):92.
42. Nusser-Stein S, Beyer A, Rimann I, Adamczyk M, Piterman N, Hajnal A, Fisher J. Cell-cycle regulation of NOTCH signaling during *C. elegans* vulval development. Mol Syst Biol. 2012;8(618):1–14.
43. Kam N, Hare D, Kugler H, Marelly R, Pnueli A, Hubbard EJA, et al. Formal Modeling of *C. elegans Development: A Scenario-Based Approach*. Lect Notes Comput Sci. 2003;2602:4–20.
44. Kam N, Kugler H, Marelly R, Appleby L, Fisher J, Pnueli A, et al. A scenario-based approach to modeling development: A prototype model of *C. elegans* vulval fate specification. Dev Biol. 2008;323(1):1–5.
45. Sun X, Hong P. Computational modeling of *Caenorhabditis elegans* vulval induction. Bioinformatics. 2007;23(13):499–507.
46. Li C, Nagasaki M, Ueno K, Miyano S. Simulation-based model checking approach to cell fate specification during *Caenorhabditis elegans* vulval development by hybrid functional Petri net with extension. BMC Syst Biol. 2009;3:42.

47. Fertig EJ, Danilova LV, Favorov AV, Ochs MF. Hybrid modeling of cell signaling and transcriptional reprogramming and its application in *C. elegans* development. Front Genet. 2011;2(77):1–9.

48. Tyson JJ, Novak B. Regulation of the eukaryotic cell cycle: molecular antagonism, hysteresis, and irreversible transitions. J Theor Biol. 2001;210(2):249–63.

49. Qu Z, MacLellan WR, Weiss JN. Dynamics of the Cell Cycle: Checkpoints, Sizers, and Timers. Biophys J. 2003;85(6):3600–11.

50. Csikász-Nagy A, Battogtokh D, Chen KC, Novák B, Tyson JJ. Analysis of a generic model of eukaryotic cell-cycle regulation. Biophys J. 2006;90(12): 4361–79.

51. Tyson JJ, Novak B. Temporal organization of the cell cycle. Curr Biol. 2008;18(17):759–68.

52. Singhania R, Sramkoski RM, Jacobberger JW, Tyson JJ. A hybrid model of mammalian cell cycle regulation. PLoS Comput Biol. 2011;7(2):1001077.

53. Gérard C, Goldbeter A. From quiescence to proliferation: Cdk oscillations drive the mammalian cell cycle. Front Physiol. 2012;3(413):1–18.

54. Novak B, Tyson JJ. Modeling the Control of DNA Replication in Fission Yeast. Proc Nat Acad Sci USA. 1997;94(17):9147–52.

55. Novak B, Csikasz-Nagy A, Gyorffy B, Chen K, Tyson JJ. Mathematical model of the fission yeast cell cycle with checkpoint controls at the G1/S, G2/M and metaphase/anaphase transitions. Biophys Chem. 1998;72(1–2): 185–200.

56. Novak B, Pataki Z, Ciliberto A, Tyson JJ. Mathematical model of the cell division cycle of fission yeast. Chaos. 2001;11(1):277–86. Chaos. 2001 Mar;11(1):277–286.

57. Tyson JJ, Csikasz-Nagy A, Novak B. The dynamics of cell cycle regulation. Bioessays. 2002;24(12):1095–109.

58. Li B, Shao B, Yu C, Ouyang Q, Wang H. A mathematical model for cell size control in fission yeast. J Theor Biol. 2010;264(3):771–81.

59. Chen KC, Calzone L, Csikasz-Nagy A, Cross FR, Novak B, Tyson JJ. Integrative analysis of cell cycle control in budding yeast. Mol Biol Cell. 2004;15(8):3841–62.

60. Fauré A, Naldi A, Lopez F, Chaouiya C, Ciliberto A, Thieffry D. Modular logical modelling of the budding yeast cell cycle. Mol BioSyst. 2009;5(12): 1787–96.

61. Irons DJ. Logical analysis of the budding yeast cell cycle. J Theor Biol. 2009;257(4):543–59.

62. Goldbeter A. A minimal cascade model for the mitotic oscillator involving cyclin and Cdc2 kinase. Proc Nat Acad Sci USA. 1991;88(20):9107–11.

63. Ferrell JE, Tsai TY-C, Yang Q. Modeling the cell cycle: why do certain circuits oscillate?. Cell. 2011;144:874–85.

64. Zhao X, Nico Dissmeyer HH, Pusch S, Weimer AK, Bramsiepe J, Bouyer D, et al. A General G1/S-Phase Cell-Cycle Control Module in the Flowering Plant *Arabidopsis thaliana*,. PLoS Genet. 2012;8(8):1002847.

65. Huang X, Chen L, Chim H, Chan LLH, Zhao Z, Yan H. Boolean genetic network model for the control of *C. elegans* early embryonic cell cycles. BioMed Eng OnLine. 2013;12(Suppl 1):1.

66. Li F, Long T, Lu Y, Ouyang Q, Tang C. The yeast cell-cycle network is robustly designed. Proc Nat Acad Sci USA. 2004;101(14):4781–6.

67. Wang M, Sternberg PW. Competence and Commitment of *Caenorhabditis elegans Vulval Precursor cells*. Dev Biol. 1999;212(1):12–24.

68. Wagmaister JA, Gleason JE, Eisenmann DM. Transcriptional upregulation of the *C. elegans* Hox gene *lin-39* during vulval cell fate specification. Mech Dev. 2006;123(2):135–50.

69. van den Heuvel S. Cell-cycle regulation. September 21, 2005. *WormBook*, ed. The *C. elegans* Research Community, WormBook, doi/10.1895/wormbook.1.7.1, http://www.wormbook.org

70. Cross FR, Buchler NE, Skotheim JM. Evolution of networks and sequences in eukaryotic cell cycle control. Phil Trans R Soc B. 2011;366:3532–44.

71. Kipreos ET, Lander LE, Wing JP, He WW, Hedgecock EM. *cul-1* is Required for Cell Cycle Exit in *C. elegans* and Identifies a Novel Gene Family. Cell. 1996;85:829–39.

72. Hebeisen M, Roy R. CDC-25.1 stability is regulated by distinct domains to restrict cell division during embryogenesis in *C. elegans*. Development. 2008;135:1259–69.

73. Rosenblueth DA, Muñoz S, Carrillo M, Azpeitia E. Inference of Boolean Networks from Gene Interaction Graphs using a SAT Solver In: Dediu A-H, Martín-Vide C, Truthe B, editors. 1st International Conference on Algorithms for Computational Biology (AlCoB 2014). Gewerbestrasse 11, CH-6330 Cham (ZG), Switzerland: Springer International Publishing; 2014. p. 235–46.

74. D'Ari R, Thomas R. Biological feedback. Boca Raton, Florida, USA: CRC Press; 1990.

75. Comet J-P, Noual M, Richard A, Aracena J, Calzone L, Demongeot J, et al. On circuit functionality in boolean networks. Bull Math Biol. 2013;75(6): 906–19.

76. Beníteza M, Alvarez-Buylla ER. Dynamic-module redundancy confers robustness to the gene regulatory network involved in hair patterning of *Arabidopsis epidermis*. BioSystems. 2010;102:11–5.

77. Clayton JE, van den Heuvel SJL, Saito RM. Transcriptional control of cell-cycle quiescence during *C. elegans development*. Dev Biol. 2008;313(2):603–13.

78. Caro E, Castellano MM, Gutierrez C. GEM, a novel factor in the coordination of cell division to cell fate decisions in the arabidopsis epidermis. Plant Signal Behav. 2007;2(6):494–5.

79. Dawes LJ, Sugiyama Y, Lovicu FJ, Harris CG, Shelley EJ, McAvoy JW. Interactions between lens epithelial and fiber cells reveal an intrinsic self-assembly mechanism. Dev Biol. 2014;385(2):291–303.

80. Richard A, Rossignol G, Comet1 J-P, Bernot G, Guespin-Michel J, Merieau A. Boolean models of biosurfactants production in pseudomonas fluorescens. PLoS ONE. 2012;7(1):24651.

81. Hill RJ, Sternberg PW. The gene *lin-3* encodes an inductive signal for vulval development in *C. elegans*. Nature. 1992;358:470–6.

82. Katz WS, Hill RJ, Clandinin TR, Sternberg PW. Different levels of the *C. elegans* growth factor LIN-3 promote distinct vulval precursor fates. Cell. 1995;82(2):297–307.

83. Tan PB, Lackner MR, Kim SK. MAP kinase signaling specificity mediated by the LIN-1 Ets/LIN-31 WH transcription factor complex during *C. elegans vulval induction*. Cell. 1998;93(4):569–80.

84. Sundaram MV. Canonical RTK-Ras-ERK signaling and related alternative pathways. July 1, 2013. *WormBook*, ed. The *C. elegans* Research Community, WormBook, doi/10.1895/wormbook.1.7.1, http://www. wormbook.org

85. Wagmaister JA, Miley GR, Morris CA, Gleason JE, Miller LM, Kornfeld K, et al. Identification of cis-regulatory elements from the *C. elegans* Hox gene *lin-39* required for embryonic expression and for regulation by the transcription factors LIN-1, LIN-31 and LIN-39. Dev Biol. 2006;297(2): 550–65.

86. Chen N, Greenwald I. The lateral signal for LIN-12/notch in *C. elegans vulval development comprises redundant secreted and transmembrane DSL proteins*. Dev Cell. 2004;6(2):183–92.

87. Christensen S, Kodoyianni V, Bosenberg M, Friedman L, Kimble J. lag-1, a gene required for lin-12 and glp-1 signaling in Caenorhabditis elegans, is homologous to human CBF1 and Drosophila Su(H). Development. 1996;122:1373–83.

88. Yoo AS, Greenwald I. LIN-12/Notch Activation Leads to MicroRNA-Mediated Down-Regulation of Vav in *C. elegans*. Science. 2005;310(5752):1330–3.

89. Greenwald IS, Sternberg PW, Horvitz HR. The *lin-12* locus specifies cell fates in caenorhabditis elegans. Cell. 1983;34(2):435–44.

90. Greenwald I, Kovall R. Notch signaling: genetics and structure. January 17, 2013. *WormBook*, ed. The *C. elegans* Research Community, WormBook, doi/10.1895/wormbook.1.7.1, http://www.wormbook.org

91. Takács-Vellai K, Vellai T, Chenc EB, Zhang Y, Guerry F, Stern MJ, et al. Transcriptional control of Notch signaling by a HOX and a PBX/EXD protein during vulval development in *C. elegans*. Dev Biol. 2007;302(2): 661–9.

92. Shaye DD, Greenwald I. Endocytosis-mediated downregulation of LIN-12/Notch upon Ras activation in *Caenorhabditis elegans*. Nature. 2002;420:689–90.

93. Shaye DD, Greenwald I. LIN-12/Notch trafficking and regulation of DSL ligand activity during vulval induction in *Caenorhabditis elegans*. Development. 2005;132:5081–92.

94. Berset T, Hoier EF, Battu G, Canevascini S, Hajnal A. Notch inhibition of RAS signaling through MAP Kinase phosphatase LIP-1 during *C. elegans* vulval development. Science. 2001;291(5506):1055–8.

95. Hopper NA, Lee J, Sternberg PW. ARK-1 Inhibits EGFR Signaling in *C. elegans*. Mol Cell. 2000;6(1):65–75.

96. Park M, Krause MW. Regulation of postembryonic G1 cell cycle progression in *Caenorhabditis elegans* by a cyclin D/CDK-like complex. Development. 1999;126:4849–60.

97. Kipreos ET. Ubiquitin-mediated pathways in *C. elegans*. December 01, 2005. *WormBook*, ed. The *C. elegans* Research Community, WormBook, doi/10.1895/wormbook.1.7.1, http://www.wormbook.org

98. Boxem M, van den Heuvel S. *lin-35* Rb and *cki-1* Cip/Kip cooperate in developmental regulation of G1 progression in *C. elegans*. Development. 2001;128:4349–59.

99. Brodigan TM, Liu J, Park M, Kipreos ET, Krause M. Cyclin Eexpression during development in *Caenorhabditis elegans*. Dev Biol. 2003;254:102–15.

100. Boxem M. Cyclin-dependent kinases in *C. elegans*. Cell Division. 2006;1(6):1–12.

101. Yoon S, Kawasaki I, Shim Y-H. CDC-25.1 controls the rate of germline mitotic cell cycle by counteracting WEE-1.3 and by positively regulating CDK-1 in *Caenorhabditis elegans*. Cell Cycle. 2012;11(7):1354.

102. Buck SH, Chiu D, Saito RM. The cyclin-dependent kinase inhibitors, *cki-1* and *cki-2*, act in overlapping but distinct pathways to control cell cycle quiescence during *C. elegans* development. Cell Cycle. 2009;8(16): 2613–20.

103. Hong Y, Roy R, Ambros V. Developmental regulation of a cyclin-dependent kinase inhibitor controls postembryonic cell cycle progression in *Caenorhabditis elegans*. Development. 1998;125:3585–97.

104. Koreth J, van den Heuvel S. Cell-cycle control in *Caenorhabditis elegans*: how the worm moves from G1 to S. Nature. 2005;24:2756–64.

105. Lundberg AS, Weinberg RA. Functional Inactivation of the Retinoblastoma Protein Requires Sequential Modification by at Least Two Distinct Cyclin-cdk Complexes. Mol Cell Biol. 1998;18(2):753–61.

106. Ouellet J, Roy R. The lin-35/Rb and RNAi pathways cooperate to regulate a key cell cycle transition in *C. elegans*. BMC Dev Biol. 2007;7(38):1–16.

107. Kipreos ET, Pagano M. The F-box protein family. Genome Biol. 2000;1(5): 3002.1–3002.7.

108. Yamanaka A, Yada M, Imaki H, Koga M, Ohshima Y, Nakayama K-I. Multiple Skp1-Related Proteins in *Caenorhabditis elegans*: Diverse Patterns of Interaction with Cullins and F-Box Proteins. Curr Biol. 2002;12(4):267–75.

109. Yeong FM. Anaphase-Promoting Complex in *Caenorhabditis elegans*. Mol Cell Biol. 2004;24(6):2215–25.

110. Vodermaier HC. APC/c and SCF: Controlling Each Other and the Cell Cycle. Curr Biol. 2004;14:787–96.

111. Peters J-M. SCF and APC: the Yin and Yang of cell cycle regulated proteolysis. Curr Opin Cell Biol. 1998;10(6):759–68.

112. Fukushima H, Ogura K, Wan L, Lu Y, Li V, Gao D, et al. SCF-Mediated Cdh1 Degradation Defines a Negative Feedback System that Coordinates Cell-Cycle Progression. Cell Rep. 2013;4(4):803–816.

113. Lamitina ST, L'Hernault SW. Dominant mutations in the *Caenorhabditis elegans* myt1 ortholog *wee-1.3* reveal a novel domain that controls M-phase entry during spermatogenesis. Development. 2002;129:5009–18.

114. Shemer G, Podbilewicz B. LIN-39/Hox triggers cell division and represses EFF-1/fusogen-dependent vulval cell fusion. Genes Dev. 2002;16:3136–41.

115. Müssel C, Hopfensitz M, Kestler HA. BoolNet—an R package for generation, reconstruction and analysis of Boolean networks. Bioinformatics. 2010;26(10):1378–80.

116. Weinstein N, Mendoza L. Building qualitative models of plant regulatory networks with SQUAD. Front Plant Sci. 2012;3(72):1–3.

117. Francis R, McGrath G, Zhang J, Ruddy DA, Sym M, Apfeld J, et al. *aph-1* and *pen-2* Are Required for Notch Pathway Signaling, γ-Secretase Cleavage of βAPP, and Presenilin Protein Accumulation. Dev Cell. 2002;3: 85–97.

118. Lackner MR, Kim SK. Genetic analysis of the *Caenorhabditis elegans* MAP Kinase Gene *mpk-1*. Genetics. 1998;150:103–17.

119. Maloof JN, Kenyon C. The Hox gene *lin-39* is required during C. elegans vulval induction to select the outcome of Ras signaling. Development. 1998;125:181–90.

120. Fay DS, Yochem J. The SynMuv genes of *Caenorhabditis elegans* in vulval development and beyond. Dev Biol. 2007;306:1–9.

121. Fay DS, Han M. Mutations in cye-1, a *Caenorhabditis elegans* cyclin E homolog, reveal coordination between cell-cycle control and vulval development. Development. 2000;127:4049–60.

122. Wilkinson HA, Fitzgerald K, Greenwald I. Reciprocal changes in expression of the receptor *lin-12* and its ligand *lag-2* prior to commitment in a *C. elegans* cell fate decision. Cell. 1994;79(7):1187–98.

123. Hsu V, Zobel CL, Lambie EJ, Schedl T, Kornfeld K. *Caenorhabditis elegans lin-45 raf* Is Essential for Larval Viability, Fertility and the Induction of Vulval Cell Fates. Genetics. 2002;160:481–92.